THESIS
M 1915n
1984
c.2

Geotechnical
Information Center

NEWKIRK FIELD: THE GEOLOGY OF A SHALLOW STEAMFLOOD PROJECT IN GUADALUPE COUNTY, NEW MEXICO

N.M.I.M.T.
LIBRARY
SOCORRO, N.M.

by

Curtis McKallip Jr.

Geotechnical
Information Center

Submitted in Partial Fulfillment
of the Requirements for the Degree of
Master of Science in Geology

New Mexico Institute of Mining and Technology

Socorro, New Mexico

December, 1984

Geotechnical
Information Center

JUL 17 1985

12272439

ABSTRACT

The Triassic upper Santa Rosa Sandstone is the reservoir sand of Newkirk field and contains approximately 30 million barrels of heavy oil. The sandstone is a medium- to fine-grained quartzose sandstone deposited by braided streams subject to seasonal flooding. Markov analysis of lithofacies identified in cores from the field show the sands were deposited under conditions similar to those found today at Bijou Creek, Colorado and Lake Eyre, Australia. An anticlinal fold over basement relief is the principal trapping mechanism. Overlying mudstones of the Chinle Formation provide a seal for the trap. Slumping in the sandstone caused by solution of underlying evaporites affects oil saturations and oil-water contacts. Petrographic and geochemical studies indicate that oil migrated into the trap in Jurassic or Cretaceous time from deeper Permian, Pennsylvanian, or Mississippian source beds. A magnetic study and evidence from one well indicates that a basaltic igneous intrusion underlies part of the area.

TABLE OF CONTENTS

LIST OF FIGURES

LIST OF TABLES

LIST OF PLATES (in pocket)

ACKNOWLEDGEMENTS

I wish to thank George Scott for funding this project and providing logs and cores. George Forster of the SOLV-EX corporation and Dr. Jan Wolski of the New Mexico Institute of Mining and Technology Mining Department provided valuable information concerning the Santa Rosa Tar Sands project north of Santa Rosa. My advisors, Dr. John MacMillan, Ron Broadhead, and Dave Martin provided guidance and important input into the final product.

Joe Triana, Zeke Sherman, and Doug Wilson at the New Mexico Petroleum Recovery Research Center were instrumental in setting up the permeability tests. Stefan Miska of the N.M.I.M.T. Petroleum Department gave an account of his experience in Poland with steam flood operations. Many thanks are due the Petroleum Department for providing facilities to conduct tests. The Petroleum Recovery Research Center graciously provided office space and a fertile atmosphere for this research. Jim Rice and Bob Colpitts helped with questions about the geophysical logs and regional stratigraphy. Jack Garwon of Trans-Pecos Resources graciously granted permission to use geochemical data from nearby wells. Jeff Garlough answered many questions regarding the steamflood operations at Newkirk Field.

INTRODUCTION

The purpose of this study is to enhance understanding of the depositional environment of the upper Santa Rosa Sandstone in the vicinity of two accumulations of heavy oil in the O'Connell Ranch field and the T-4 Ranch field (grouped together as the "Newkirk" field) in northeastern Guadalupe County, New Mexico (Fig. 1). Steamflooding of the field and proposed development of the field has underscored the need for a more detailed understanding of the depositional controls on the porosity and permeability of the reservoir sand. This report will concentrate on the upper Santa Rosa Sandstone and utilizes cores, geophysical logs, and sample logs from the Newkirk field. Some clues to depositional features also occur in the Santa Rosa Lake area approximately 20 miles west.

Gorman and Robeck (1946), Foster et al. (1972), Miller (1966), McGowen et al. (1979), Broadhead (1984) and others have discussed the regional stratigraphy, petrography, and structure of the Santa Rosa Sandstone. The scope of this study is local rather than regional, although the constraints and implications of the regional aspects of the formation are incorporated in conclusions drawn from study of local data. This study also incorporates and extends a local study done by the Solv-Ex Corporation at the Santa Rosa tar sand deposit 7 miles north of Santa Rosa and approximately 20 miles west of Newkirk field (Wolski and Kozushko, 1983). That report included core data from 50 drill holes. The cores were not

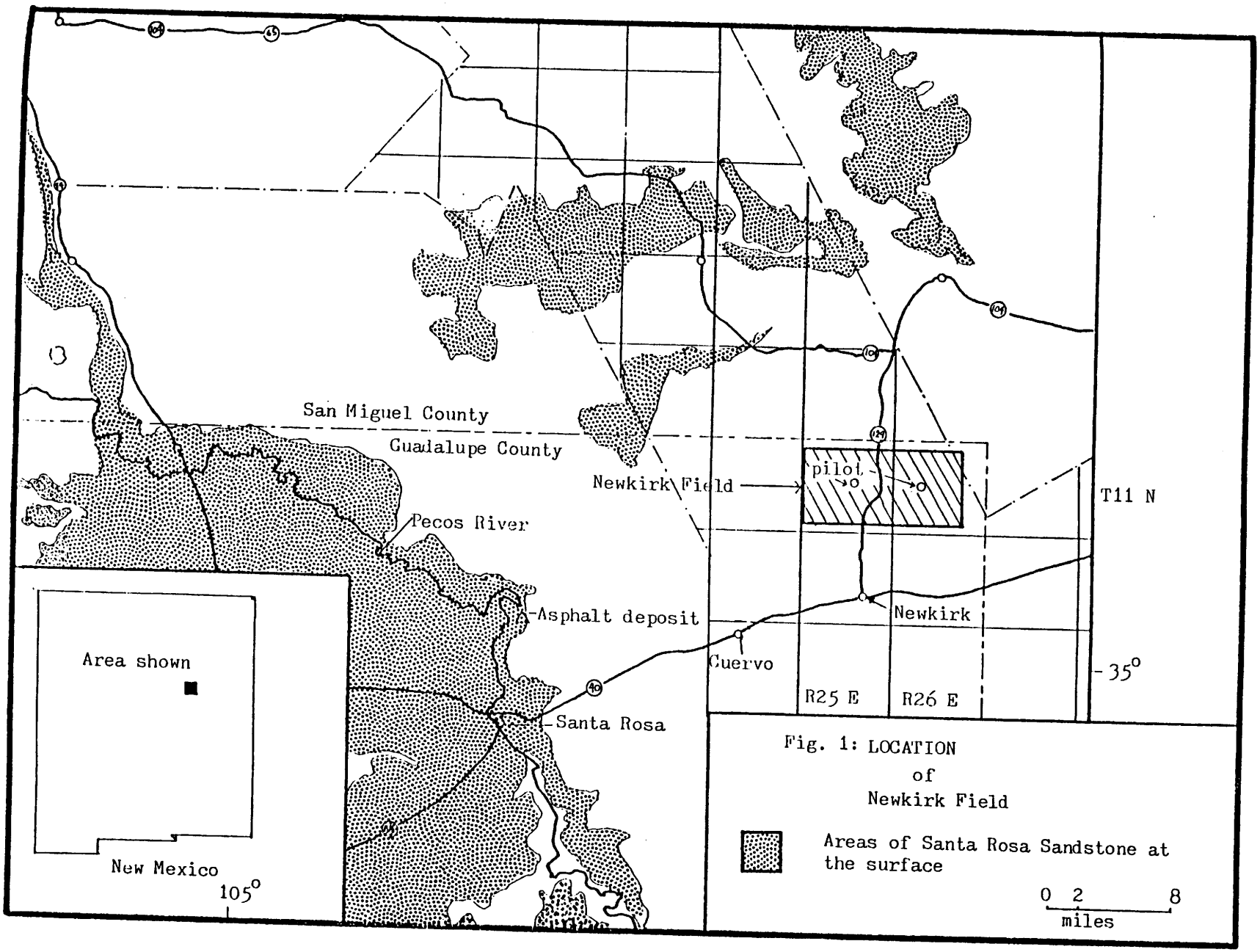

Fig. 1: LOCATION of Newkirk Field

logged with respect to important depositional features such as sedimentary structures. Other aspects of the field such as source and migration of the oil, timing of migration, tectonic history, nature of oil degradation, diagenesis, sandstone petrography, local geophysics, and other important topics are touched on briefly here and deserve a more in depth treatment elsewhere.

Methods of Investigation

Cores from approximately 32 wells in the Newkirk field have been taken. Of those, about 14 were available for study (the remainder were in Midland, Texas for testing at the time of the study). Detailed core descriptions were made of these cores with special emphasis on sedimentary structures. The Public Lands Exploration Company (P.L.E.I.) Barbara No. 1 and Samedan State No. 1 cores were slabbed and photographed.

Petrographic studies were made from 23 thin sections taken from the cores and from outcrops 20 miles west of the field. Blue epoxy was used to show effective porosity. One half of each slide was stained with Alizarin Red S to show calcite cementation more clearly. Slides were examined with a Nikon Binocular microscope (8 to 40 power) with polarizers. Photomicrographs were taken with a Nikon polarizing microscope (100 - 400 power). Drill cuttings were available but not used due to the superior information available from the cores.

Gamma ray and compensated neutron logs were the most common logging suite available for the 50 to 60 wells in the

field area. A few spontaneous potential and resistivity logs were available. Most of the cores and logs terminated in the middle mudstone unit just below the upper Santa Rosa Sandstone. Sample logs were available for the cored wells. Porosity and permeability tests at one foot intervals of the cores were done by Core Labs and the results are incorporated in this report. Two core samples were tested and compared with the results Core Labs obtained. The procedure and results are described in Appendix A. Additional clues to permeability patterns are provided by temperature response in the production wells of the pilot steamflood sites.

A magnetic survey was performed using a hand-held field magnetometer (Geometrics Portable Proton Magnetometer Model G-816) to investigate the nature of an igneous body encountered at about 1000 feet depth in the State No. 16 well and to lend clues to the nature of structure in faulted Precambrian basement rocks. The data were corrected for diurnal variation and a contour map was made. Some preliminary sections and structure maps were available from George Scott Jr. and these provided a valuable starting point for this investigation. Outcrops of the Santa Rosa at the Santa Rosa Lake dam and spillway were visited and photographed for sedimentary structures. Aerial photographs of the area were studied using a stereoscopic viewer.

East-to-west and north-to-south cross sections were drawn across the field in areas of greatest well density. As much of the available information as possible is incorporated in these

sections. The purpose of these sections is to demonstrate the complexity of the deposits and to display the core data obtained by logging the sedimentary structures. One north-to-south regional cross section was drawn to show the Precambrian through Permian sediments beneath the field area.

A structure contour map of the top of the upper sand was made and isopach maps of two prominent stringers of the upper sand were drawn. These maps involved interpretation of geophysical logs of wells not included in the cross sections and are therefore more likely to be affected by errors in correlating the two stringers.

Fence diagrams of the east and west side steamflood pilot projects were prepared to illustrate the reservoir in those important areas. One detailed drawing comparing log response to core properties was made for the Barbara No.1 well.

Interpretations of lithofacies types and corresponding depositional environment were made from the core logs These interpretations were then analyzed using Markov chain analysis after the method of Miall (1973) to investigate the cyclical nature of the sediments.

Paleocurrent directions were taken on the Cuervo member of the Chinle Formation, present at the surface in the field area, and of the upper Santa Rosa sandstone at the Santa Rosa lake dam area. Previous work (Broadhead, 1984) indicates that paleodrainage patterns of the Cuervo and the Santa Rosa are similar in the field area. Measurements of strike and dip

directions were made of faults and joints in the field area in order to delineate permeability pathways that might affect the steamflood operation. These are included in Appendix A.

CHAPTER ONE

Regional Geology

Newkirk field lies about 20 miles north of the town of Newkirk, which is approximately midway between Santa Rosa and Tucumcari in east-central New Mexico. The topography of the area is characterized by mesas and intermittent streams.

A generalized stratigraphic column of the area is shown in Fig. 2. The strata have a low regional dip to the southeast of approximately 1 to 2 degrees. The Upper Triassic Santa Rosa Sandstone is the reservoir rock in the Newkirk field. Overlying red and brown mudstones of the Chinle Formation form the seal for the reservoir. Stable carbon isotope data suggest a Permian or Pennsylvanian origin for the oil (Budding, 1979) which migrated from underlying Permian or Pennsylvanian source beds along fractures into the trap. The trapping mechanism is an anticlinal fold trending east-west with about 200 feet of closure (Scott, 1979) combined with stratigraphic pinchouts and porosity variations induced by diagenesis. Stratigraphic correlation of the reservoir sand is complicated by depositional variations and post-depositional slumping.

Stratigraphy

Precambrian rocks of the Torrance metamorphic group underly the Newkirk Field area (Foster et al, 1972) at depths ranging from approximately 4000 to 7000 feet. Carbonates and minor shales and

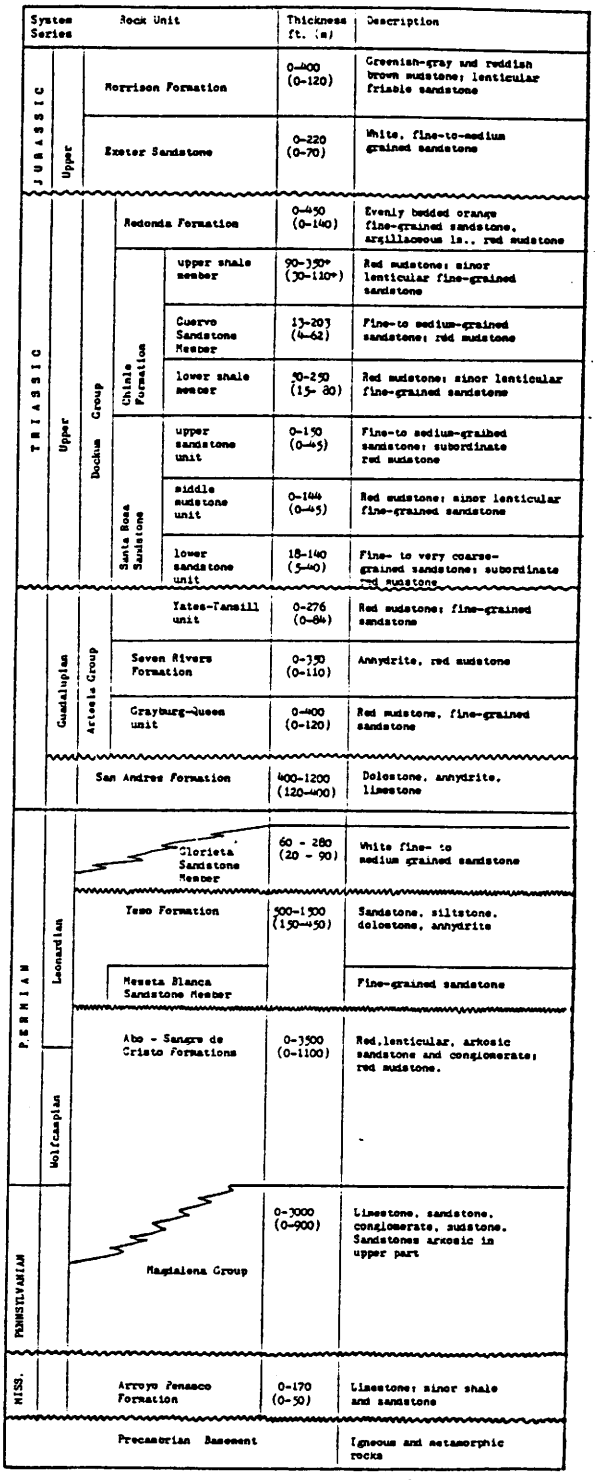

Fig. 2: Regional Stratigraphy

(Broadhead, 1984)

sandstones of Mississippian and possibly Devonian age unconformably overlie the Precambrian and range in thickness from 0 to 170 feet (Foster et al, 1972). During Pennsylvanian time, approximately 2500 feet of interbedded arkosic conglomerates and black shales were deposited. Directly beneath Newkirk field most of these have been removed by erosion (Fig. 3). These sediments grade laterally into shallow water marine carbonates elsewhere in the county. A red-bed sequence of mudstones, sandstones, and arkoses was deposited during the Permian period. These rocks constitute the Sangre de Cristo and Abo formation and are approximately 1500 feet thick in the area. Overlying the Abo Formation are approximately 1000 feet of orange sandstones, siltstones, and shales of the Permian Yeso Formation. The San Andres Formation overlies the Yeso and contains about 700 feet of interbedded limestone, dolostone, anhydrite, salt, mudstone, and a basal sandstone unit, the Glorieta Sandstone. The Artesia Group unconformably overlies the San Andres Formation and has been subdivided by Kelley (1972) into 3 parts: the basal Grayburg-Queen unit which consists of red mudstone and fine-grained sandstone, the Seven Rivers Formation which consists of anhydrite and red mudstone, and the uppermost Yates-Tansill unit which consists of red mudstone and fine-grained sandstone (Broadhead, 1984). The Artesia Group is approximately 300 feet thick in the area. Broadhead (1984) noted that the Grayburg, Queen, and Seven Rivers Formations are equivalent to the Bernal Formation. The paleotopography of the erosional surface on top of

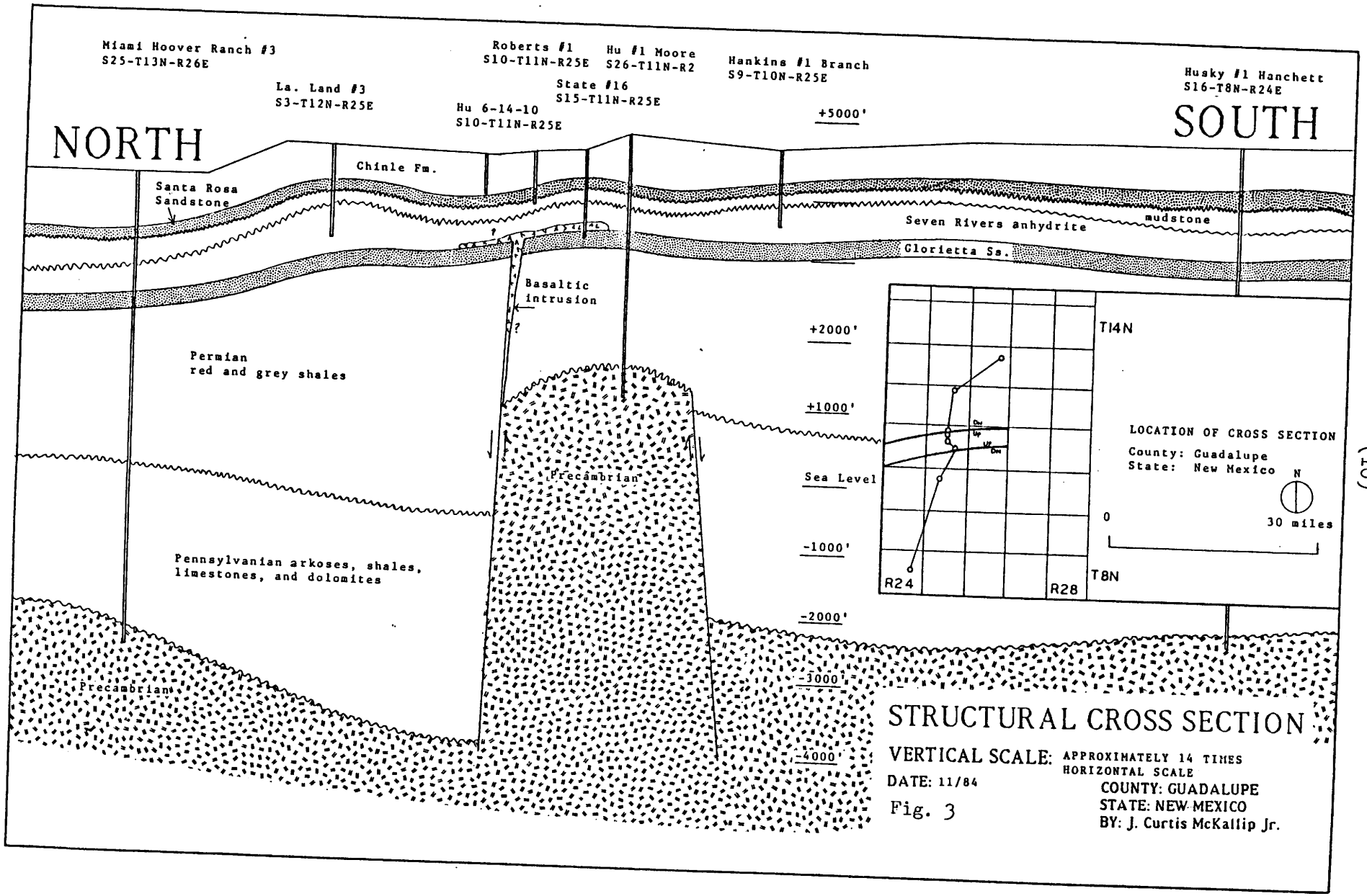
Miami Hoover Ranch #3
S25-T13N-R26E
La. Land #3
S3-T12N-R25E
Roberts #1
S10-T11N-R25E
Hu 6-14-10
S10-T11N-R25E
Hu #1 Moore
S26-T11N-R2
State #16
S15-T11N-R25E
Hankins #1 Branch
S9-T10N-R25E
Husky #1 Hanchett
S16-T8N-R24E
NORTH
SOUTH
+5000'
Chinle Fm.
Santa Rosa Sandstone
Seven Rivers anhydrite
mudstone
Glorietta Ss.
Basaltic intrusion
+2000'
+1000'
Sea Level
-1000'
-2000'
-3000'
-4000'
Permian
red and grey shales
Precambrian
Pennsylvanian arkoses, shales, limestones, and dolomites
Precambrian
T14N
T8N
R24
R28
LOCATION OF CROSS SECTION
County: Guadalupe
State: New Mexico
N
0
30 miles
STRUCTURAL CROSS SECTION
VERTICAL SCALE: APPROXIMATELY 14 TIMES HORIZONTAL SCALE
DATE: 11/84
COUNTY: GUADALUPE
STATE: NEW MEXICO
BY: J. Curtis McKallip Jr.

Fig. 3

the Artesia Group strongly influenced the depositional character of the overlying Santa Rosa Sandstone.

N.H. Darton (1921, p. 183) applied the name Santa Rosa Sandstone to a prominent sandstone-shale sequence, about 350 feet thick, near the base of the Dockum Group in the mesas of Guadalupe County near Santa Rosa, New Mexico. On the basis of vertebrate fossils and position beneath the Chinle Shale, the Santa Rosa is considered to be Upper Triassic and equivalent to the Shinarump Conglomerate farther northwest (Colbert and Gregory, 1957; Miller, 1966). The Santa Rosa Sandstone consists of intertonguing non-marine sandstones and mudstones of probable fluvial, alluvial, deltaic and lacustrine origin (Lazarus et al, 1983; McDowell et al, 1983).

Karst topography is present to the southwest in the area around Santa Rosa (Gorman and Robeck, 1946) The karst is the result of large scale subsidence and slumping caused by the leaching of soluble carbonates and sulfates in the underlying Permian units. Paleodissolution of salt in basins to the east of the study area became very active beginning in the Late Cretaceous epoch and may have begun after deposition of the Santa Rosa (Gustavson et al., 1980). The mechanism postulated by Gustavson et al. (1980) requires fresh water input at topographically high points. The water percolated downwards through relatively impermeable Dockum Group shales by migrating along fractures. Collapse over areas of dissolution would further accentuate fracturing and thus increase the potential for

groundwater movement. The depth to the top of the salt near the Texas border is generally less than 800 feet. Waters carrying the dissolved salt move laterally to emerge at the surface as salt springs, seeps, or pans in a major stream valley. Vertical thickness of salt dissolution ranges up to 600 feet and has caused vertical subsidence of the High Plains surface of about 250 feet on a regional scale. Complex folding and brecciation of overlying Permian sediments, chimneys filled with collapse breccias, and ancient and modern sinkholes are structural features associated with this dissolution.

In the study area, the northward expansion of the Pecos drainage appears to have been encouraged by solution of evaporites along its path (Lee, 1923; Morgan, 1941). Structure contours on the base of the Ogallala Formation show that the Canadian River is underlain by a series of solution troughs and basins. Logs which penetrate through the Permian section in the Newkirk field show a sequence of anhydrites and shales approximately 150 feet thick in the Seven Rivers Formation.

During one collapse event which occurred in southwestern Kansas in 1878 a sinkhole approximately 175 feet in diameter and 60 feet deep filled immediately with a brine at 159 degrees F. This brine is believed to be formation fluid forced upwards through fractures when collapse occurred. If similar fractures are present in the Santa Rosa sandstone beneath the Newkirk field, they could form pathways for preferential migration of the steam out of the reservoir.

The Santa Rosa Sandstone is overlain by brown and red siltstones, mudstones, and shales of the Chinle Formation. Together the Santa Rosa and the Chinle comprise the Dockum Group and Redonda Formation which extends over a wide area of west Texas and eastern New Mexico. The Dockum Group consists of deposits of braided and meandering streams, alluvial fans, fan deltas, highly-constructive elongate deltas, lacustrine and valley-fill deposits with rare beach and shoreline deposits (McGowen et al, 1983). The Cuervo Sandstone member of the Chinle is exposed at the surface near the Newkirk field (Kelley, 1972) and consists of tan, crossbedded medium-grained sandstones and interbedded red mudstones approximately 100 feet thick.

Dikes of basaltic composition are exposed in the area of the Santa Rosa tar sands deposit about 7 miles north of the town of Santa Rosa. A 60 foot thick intrusion of probably similar composition was encountered in the State No. 16 well on the west side of the Newkirk field at 1000 ft. depth between the competent Glorieta Sandstone below and the less competent San Andres anhydrites above (Fig. 3). The magnetic anomaly map (Plate 1 in pocket) shows a magnetic high over the general area where the intrusion is shown migrating vertically along a fault plane in cross section EE' (Fig. 3). The intensity and lateral distribution of the anomaly is similar to an anomaly mapped by Hahn (1971) in the Eifel Mountains of Germany. Basaltic pipes outcropping at the surface in that area showed magnetic anomalies of 50 - 150 gammas over areas approximately 3 miles in diameter.

These anomalies were superimposed on an anomaly of 261 gammas which extended over an area approximately 35 miles in diameter. This large anomaly is thought to be the result of a large basic pluton buried in the subsurface.

Roberts (1970) gives two distinct interpretations of the mechanics of sill intrusion. The first considers sill intrusion to occur when ascending magma encounters sedimentary rocks of equal or lesser density than itself. An underlying assumption of this hypothesis is that magmatic pressure is just sufficient to raise the magma to a certain level and no further. This assumption appears to be unlikely in many cases. The second interpretation considers sill intrusion to be the result of horizontal compression. This compression may be regional or the result of collapse. In some cases intrusion may occur due to both of these factors and possibly others. In the case of Newkirk field, intrusion may be due to both causes.

Structure

Recent work on the Precambrian (Scott, 1984) has indicated a complexly faulted basement with vertical displacements of as much as 4000 ft.. Foster et al (1972) postulated northeast and northwest trending high angle faults in the Precambrian basement. These faults are typically 20 to 70 miles long and have displacements of up to 5000 feet. Mildly folded anticlines in the area trend generally northeast. The Newkirk anticline may be a drape-fold of sediments over a horst in the Precambrian that was mapped by Scott (1984). The section in Fig. 3 was drawn using

Scott's map and well logs and shows the horst may have risen during Late Pennsylvanian and Early Permian epochs because the Pennsylvanian section was eroded from the top of the horst before deposition of the bulk of the Permian sediments. The timing of this rise would then coincide with the rise of the ancestral Rocky Mountains as described by Kluth and Coney (1981). In their model, Late Pennsylvanian suturing of the South and North American cratons in the Marathon region of west Texas produced intraplate deformations as far from the plate margin as Colorado. The Late Cretaceous Epoch marked the beginning of Laramide compressive stresses in the area. The Bonita fault near Tucumcari has been related to Laramide stresses (Stearns, 1972). Extension replaced compression as the Rio Grande Rift began to open in the Late Oligocene and Early Miocene. Extensive basalt flows 50 - 100 miles north of Newkirk have been dated at 1 - 5 million years old. Petrographic and age data for the basaltic dikes of Santa Rosa and the basaltic igneous body encountered in the State No. 16 well at the Newkirk field were not available but they are probably related to the extrusives to the north in age and composition.

History of the Newkirk Oil Field

Shows of live oil were encountered by the Humble (Exxon) No. 1 Moore well which was drilled to 3915 ft. on a surface and gravity anomaly in 1963. The shows were from the Permian Artesia Group and the Triassic Santa Rosa Sandstone. Further drilling by Humble and later by Samedan Oil company, and Public Lands

Exploration Company (renamed Corona Oil Company and now Rio Petro) expanded and delineated the extent of the field. Humble initially estimated 23 million barrels of oil in place based on an average porosity of 17.7 % and an average pay thickness of 32 feet (Scott, 1979). These estimates were revised by Scott based on later drilling, to 62 million barrels of oil in place based on an average porosity of 15%, an average water saturation of 40%, an average net pay thickness of 41 ft and a total area of 2155 acres. The field was split into two areas, Newkirk East and Newkirk West based on net pay maps. Keplinger and Associates (1980) estimated the total original oil in place at approximately 37 million barrels and initial mobile oil at about 30 million barrels.

Production by conventional means is inhibited because of the low gravity (17 degrees API) and high viscosity (1400 cp. at 71 degrees F.) of the oil. A pilot steamflood project was begun in August of 1981 in an attempt to produce economic quantities of oil. Steam at approximately 320 degrees Farenheit and 260 psi was injected in pilot injection wells on both the Newkirk East and Newkirk West prospects (Wash, 1982). Total production from April 1982 to December of 1982 was approximately 57 barrels of oil (Martin, 1983).

Permeability measurements were performed on two unextracted cores from the Newkirk field (Appendix A). A core representing the average reservoir sand (selected visually by the amount of oil saturation) gave a permeability to water of approximately 4

millidarcies at residual oil saturation and the medium-grained uncemented sand beneath the reservoir gave a permeability of 675 millidarcies. Core Labs (1980) reported water permeability after a hot water flood (at residual oil saturation) ranged between 8 - 30 millidarcies in cores from the State No. 1 well (Appendix C).

Joints were measured in the Cuervo Sandstone overlying the area and strike northwest (Appendix A). Their effects on producing wells is difficult to predict because the producing wells are placed along north-south and east-west lines from the injection wells in the pilot projects.

CHAPTER TWO

Petrography

Thin sections taken from cores in the Newkirk field were used to examine detrital grains, cement, and porosity. Scanning electron photomicrography and X-ray diffraction methods were used to determine the composition of clays in samples taken from the cores. Results are compared to studies of other authors in Table 1. A photomicrograph of sandstone from the Barbara No. 1 well at a depth of 749 feet is shown in Fig. 4. It shows muscovite flakes forming a lamination between quartz grains in the reservoir sand. Pore spaces between the quartz grains contain dead oil, kaolinite, and some calcite cement.

All of the studies showed a predominance of subhedral monocrystalline quartz grains. Feldspars comprised less than 12% of the rock and most of the plagioclase was sericitized. Rock fragments included volcanics and micritic limestones. The limestone clasts were rounded and composed of fractured and whole fragments of micritic limestone cemented together by blocky calcite cement. Pyrite was present in most of the studies in trace amounts. Calcite cement, unabraded quartz overgrowths, and vermicular kaolinite were the most common diagenetic minerals present. Porosity estimates averaged 10% in thin sections. Core Labs tests indicate total porosity average 20% in the Newkirk field reservoir which means that some of the porosity

must be present as microporosity (probably between clay packets and quartz grains) and not easily visible in thin section.

Provenance

In some areas the Santa Rosa consists of roughly 10-15% metamorphic rock fragments (Miller, 1966). The presence of sedimentary rock fragments, and plutonic quartz suggests that the Santa Rosa was derived from a combination of reworked older sediments, metamorphic rocks, and plutonic rocks. Limestone intraclasts found in coarser layers probably originated in local fresh water lakes. Flugel (1982) described carbonates formed in shallow lakes in arid and semi-arid settings. Evaporation raises the concentration of carbonate and precipitates limestones. Clays, dolomite, and evaporite minerals are usually associated with the limestones. No fossils were found in the limestone clasts.

Diagenesis

An erosional scour in the core of the O'Connell No. 1 well at a depth of 416 ft. (Plate 5 in pocket) gives important clues to the sequence of diagenetic events. Laminations truncated by slightly finer grained material are filled with oil. The pore space surrounding the laminations is well cemented with calcite. The laminations show slightly coarser grained material and a large amount of uncemented effective porosity (represented by blue epoxy in thin section). This suggests that oil migrated into the coarser laminae before the onset of calcite cementation. Predominantly point contacts between grains indicate that early cementation by calcite prevented compaction (Broadhead, 1984)

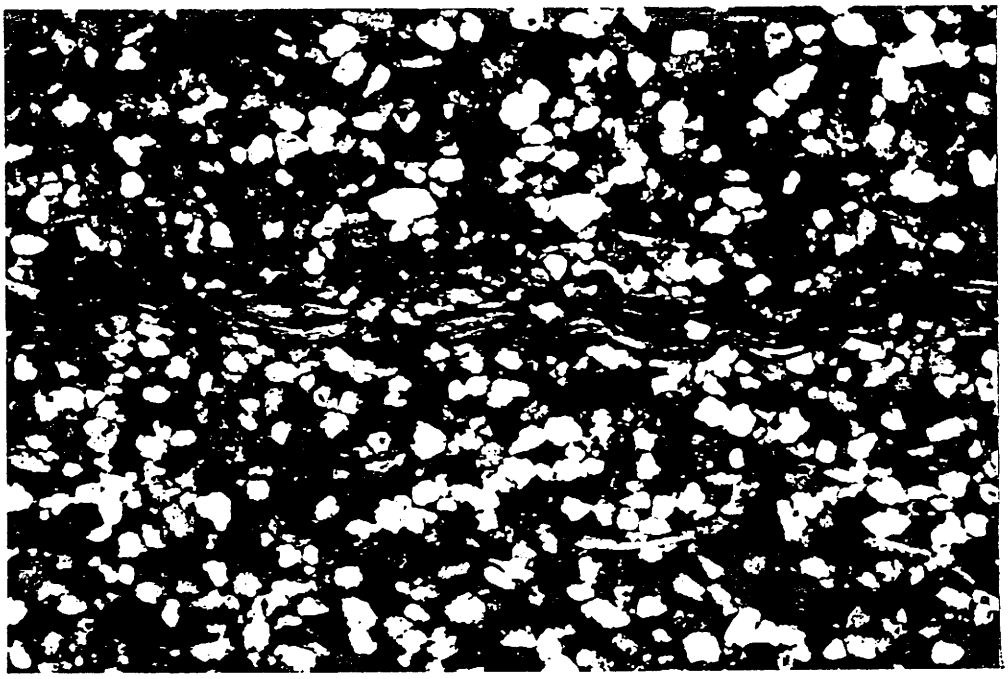

Fig. 4: Photomicrograph of the upper Santa Rosa Sandstone in thin section taken from core of the P.L.E.I. Barbara No. 1

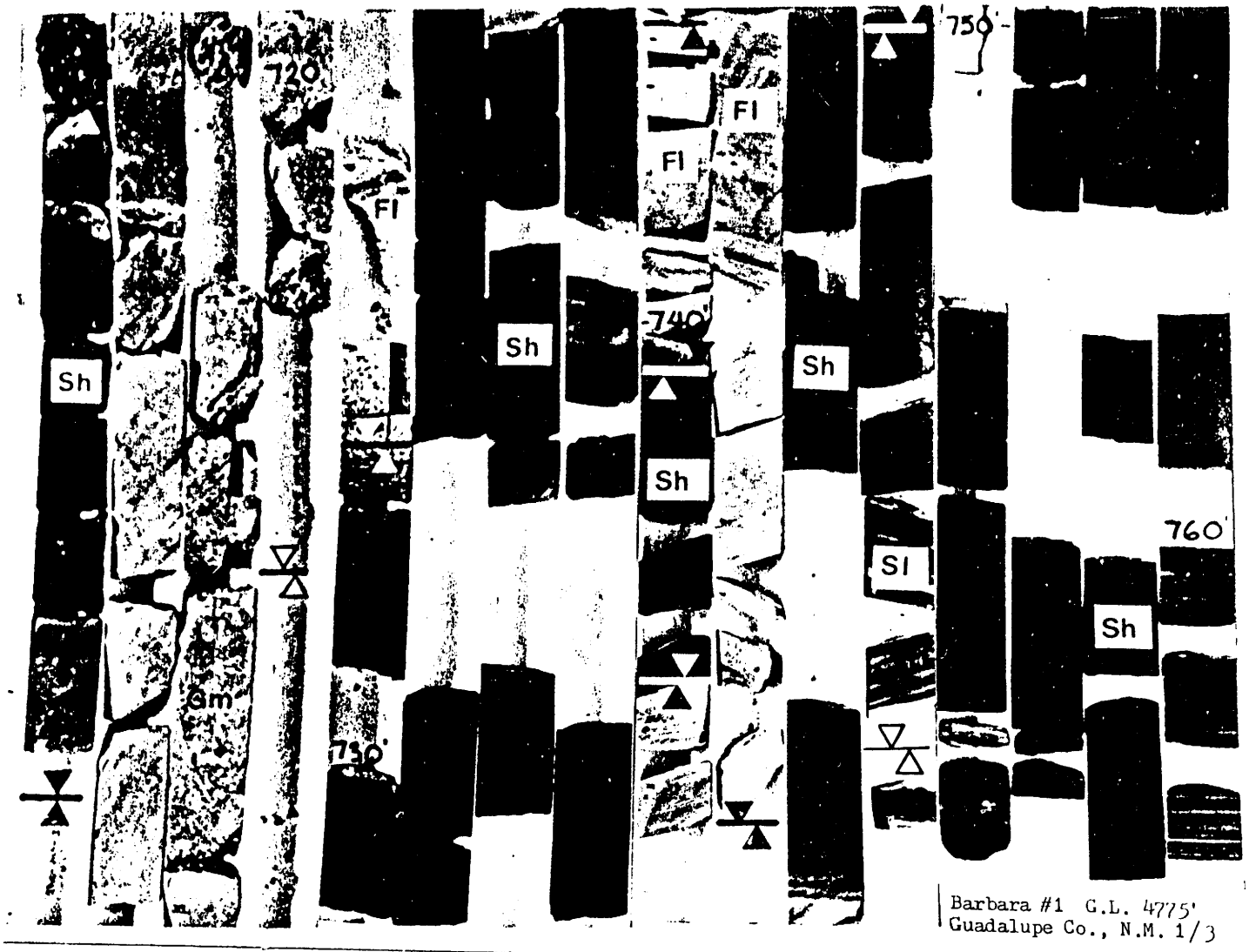

Fig. 5a: Core photographs and lithofacies: P.L.E.I. Barbara No. 1

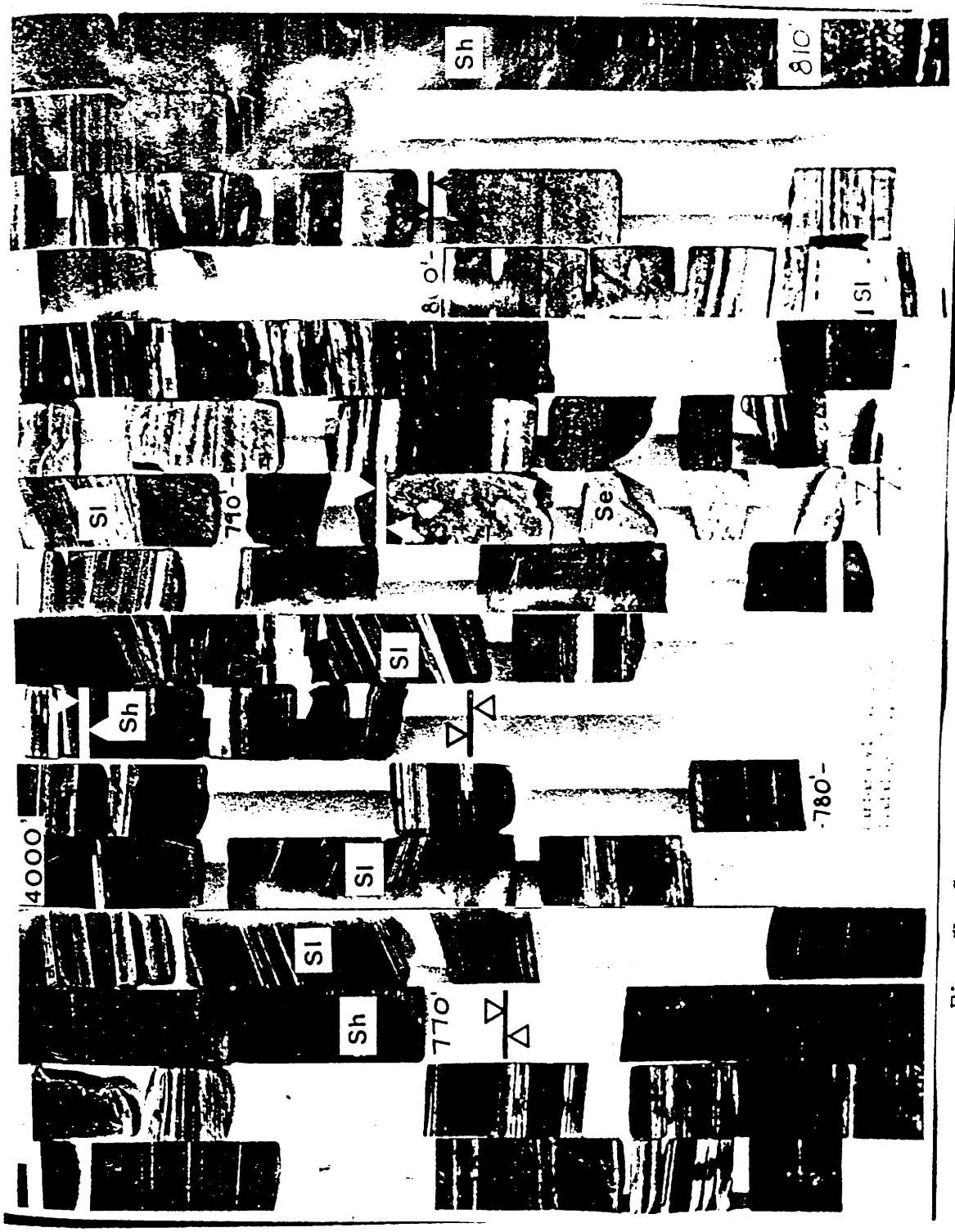

Fig. 5b: Core photographs and lithofacies: P.L.E.I. Barbara No. 1

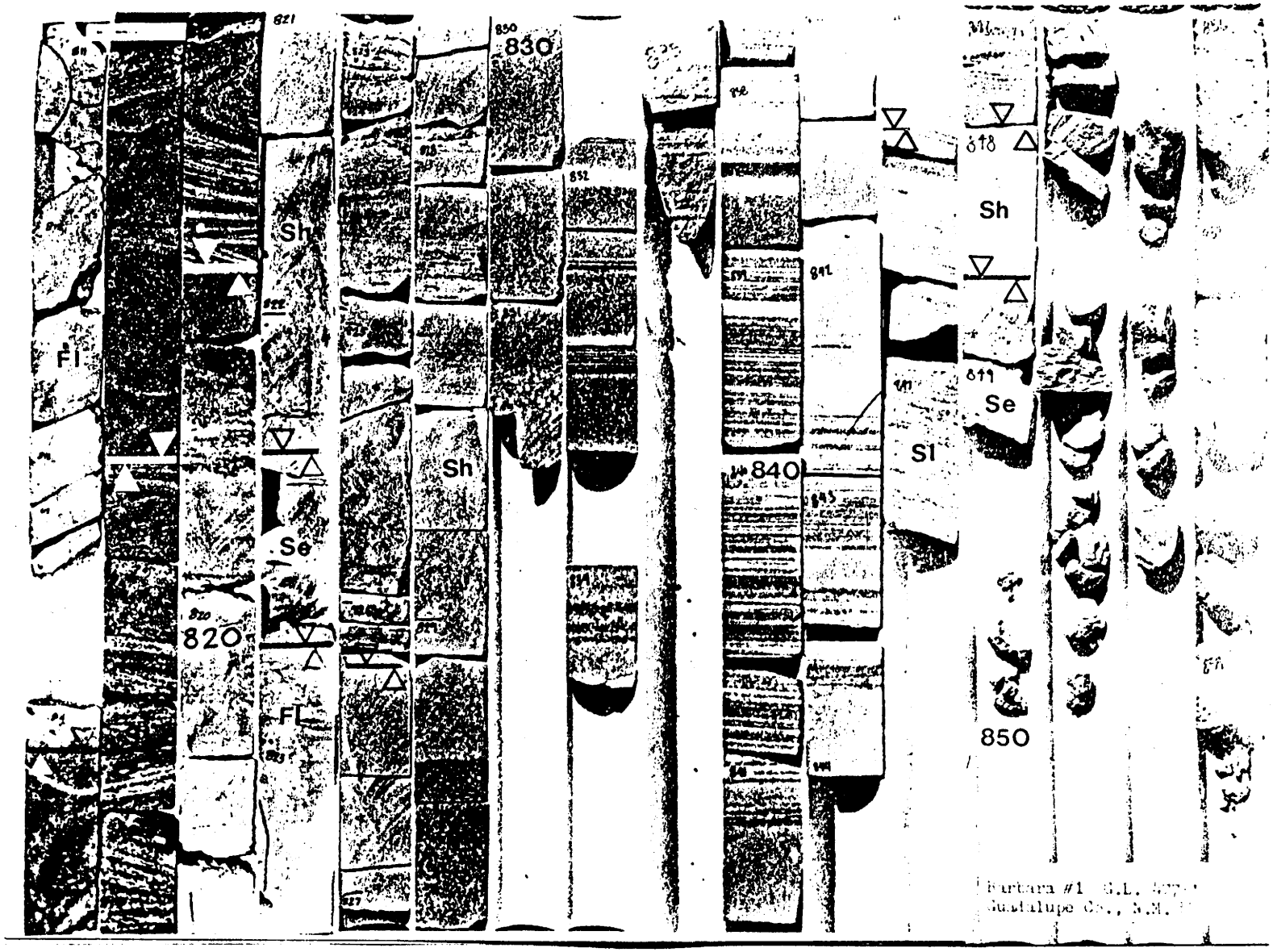

Fig. 5c: Core photographs and lithofacies: P.L.E.I. Barbara No. 1

N.M.I.M.I.
LIBRARY

Table 1: Petrography of the upper Santa Rosa Sandstone

(Miller, 1966)		(Broadhead, 1983)		THIS STUDY		(CORE LABS, 1983)	
Quartz (well-rounded, abraded)	50-70%	silt - very coarse sand size predominantly monocrystalline	40-70%	Anhedral - subhedral .05 - .2 mm diameter some with inclusions straight extinction	50-90%	predominantly monocrystalline straight extinction	82%
Composite (undulose extinction)	10%						
Milky (vacuoles)	5%						
Colorless (plutonic with rutile)	85%						
Orthoclase	10%	total feldspars range from 0 - 10% (little alteration)	trace		trace	Feldspars: Albite twinned and untwinned	4-6%
Colorless (fresh)	50%						
Bubbly alteration	50%						
Microcline	2%		trace		trace		
Plagioclase (sericitized)	1%		trace	sericitized	1-3%	sericitization noted	
Chert (well rounded and elongate)	5-25%						
Micas (Muscovite, biotite, chlorite)	1%			as deformed flakes	0-5%		
Rock fragments (metaquartzites, mineral aggregates with schistose or slaty structure)	10%	predominantly altered volcanics granite, and microcrystalline limestone.	10%	micrite, siltstone	0-9%		
Magnetite-ilmenite (occurs in the red, hematite-stained sands but does not occur in the grey beds because of diagenetic dissolution.)	2%	hematite, pyrite	trace	pyrite cubes in silty intervals	0-2%	framboidal pyrite	
Leucoxene, Zircon, Tourmaline, garnet, rutile (See Sidwell, 1945, p. 50-54.)	trace					garnet, zircon, sillimanite, tourmaline	
Sparry calcite cement		ranges from 0 - 40%	20%	fine internal structure	10-20%	dolomite cement	trace
Quartz overgrowths		common - not abraded		common		common	
Clays		ranges from 0 - 50%		authigenic kaolinite	5%		
Porosity (maximum)		ranges from 15 - 36%	10%	visible in thin section 5-10% 80% is effective porosity		approximately	10%

(23b)

N.M.I.M.T.
LIBRARY

during burial. (Sediments of Jurassic and Cretaceous age buried the upper Santa Rosa Sandstone to approximately 4000 feet before uplift and erosion exhumed the reservoir sand to its present position at 350 to 800 feet below the surface.) Core photos of the Barbara No. 1 well from 777 ft. to 779 ft (Fig. 5b) show cemented laminations which indicate that some cementation had already taken place before migration of the oil.

Since migration of the oil predated the major episode of cementation which in turn predates significant burial, a major migration of oil probably took place sometime in late Triassic or Jurassic time. This would mean that the oil has been exposed to degradation and loss of volatiles in a near-surface environment twice: once when it migrated into the reservoir sands before they were deeply buried and recently when the reservoir sands have been uplifted. The low oil gravity caused by biodegradation of the oil (as determined by geochemical studies (Budding, 1979)) also supports this conclusion. Vermicular books of authigenic kaolinite seen in scanning electron photomicrographs of the reservoir sand are the result of an early period of flushing with low pH waters. Their preservation in oil-filled zones suggests that the oil has played a role in preventing illitization (Chepilov, 1959). Cubic, framboidal, and disseminated authigenic pyrite (FeS_2) is found in interbedded grey siltstones and mudstones. Sulfur for the formation of this pyrite comes from the bacterial reduction of dissolved sulfate and the decomposition of organic sulfur compounds (Berner, 1970).

Slumping due to the dissolution of underlying beds of gypsum suggests that they are a major source of dissolved sulfates. The sulfate is reduced to form H_2S by anaerobic bacteria and this disassociates in water to yield sulfur. The sulfur ions combined with dissolved iron from detrital iron-bearing minerals such as magnetite and biotite to form pyrite. Plant remains found in the formation serve as a source of nutrients for the bacteria. Berner (1970) has shown that the amount of pyrite formed is usually a linear function of the amount of organic carbon available. The amount of total organic carbon present also indirectly controls the color of shales. Potter et al. (1980) demonstrated that the degree of oxidation of shale is affected by the amount of organic carbon it contains. The degree of oxidation determines the Fe3+/Fe2+ ratio which directly affects the color of the shale (Tomlinson, 1916). A shale with a high ratio is red and one with a low ratio is grey-green. The red and grey-green shales present in the Newkirk cores represent a partially complete diagenetic oxidation cycle. No attempt was made to correlate the red shale as it appeared to be almost random in occurrence.

Source Rocks and Oil Migration

The geochemical studies of oil from the Santa Rosa tar sands by Budding (1979) and the work of others provide data from which a model of constraining factors governing oil genesis and migration can be built. An underlying assumption is the oil at Santa Rosa was derived from the same formation or formations as that at Newkirk. This assumption is based on the heavy, black, low

API gravity nature of the oil, the fact that it is trapped in the same formation, and saturation patterns are the same as seen in outcrops and wells. Sample logs from wells between the two areas commonly show traces of asphaltic oil in the Santa Rosa sandstone which supports a similar origin for oil in the two areas.

Geochemistry of the Santa Rosa Oils

Budding (1979) found the oil at Santa Rosa had a napthene content of approximately 98%. Bacterial action typically removes normal paraffins thus enriching the relative proportion of other components such as the napthene fraction. N-alkanes were present in a bimodal distribution with maxima near C17-18 and C25-26 suggesting a mixed marine and terrestrial origin similar to that found in Green River oil shales. The pristane-to-phytane ratio ranges -from 0.52 to 0.67 suggesting a reducing environment at the time the organic material, which was the source of the oil, was deposited. Oxidizing conditions were prevalent during deposition of the Santa Rosa sandstone and would not have been favorable for preservation of organic matter. Stable carbon isotope data from the Santa Rosa oils yield values (delta C13 = -28.5 to -28.3) similar to isotope data from Permian and Pennsylvanian oils of the Permian Basin. Biodegradation typically has little effect on stable isotope data. The carbon preference index (CPI) was measured and ranged from 0.94 to 1.19 and suggests a low amount of terrestrial organic matter in the original material from which the oil was derived.

N.M.I.M.T. LIBRARY

Maturity of Potential Source Rocks

Vitrinite reflectance of a sample from Pennsylvanian rocks in the Trans Pecos Latigo Ranch Block D, No. 1 well in section 26 of Township 10 North, Range 23 East (16 miles southwest of Newkirk field) taken at a depth of 6050 feet showed a reflectance value (Ro) of 0.85% (Geochem Laboratories, 1983). Organic rich sediments which yield Ro values in this range typically yield mature oil or immature heavy oil (Geochem Laboratories, 1983) and are classed as moderately mature to mature. This value also correlated positively with thermal alteration values (TAI) from kerogen in the same interval (Geochem Laboratories, 1983).

A gradient of vitrinite reflectance values is shown in Fig. 6. It was constructed assuming that the Ro of 0.85% was the result of thermal gradients existing at the time of maximum burial of the earliest Mississippian or Pennsylvanian sediments. The region of peak oil generation indicates the times at which sediments of different formations became hot enough to generate oil. This figure supports generation from Pennsylvanian or Mississippian source rocks and shows that rocks of the Permian San Andres Formation, which is a major producing formation in the Permian Basin, were probably not buried deep enough near Newkirk to become thermally mature. Indeed, only the lowest Pennsylvanian and Mississippian rocks were within the oil generation region before the estimated time of migration and this lends further support to their being the source of the oil. Geochemical data was not available for the San Andres Formation.

Geochemistry of Source Rocks

Total organic carbon in shales below 2000' depth (Abo, Sangre de Cristo, Granite Wash, and Pennsylvanian formations) averaged 0.08% total organic carbon (TOC) with the exception of one shale zone between 7056 and 7258 feet which had a high of 0.84% TOC. These poor percentages (1-2% is regarded to be good and more than 4% is excellent (Geochem Labororatories, 1983)) are probably related to the generally oxidizing environments in which most of these sediments were deposited and which prevented the preservation of large amounts of organic matter.

Migration Paths

The low amounts of organic carbon in potential source rocks raises the question of how sufficient oil was generated under poor conditions to form the large oil accumulations of Santa Rosa (57-90 million bbls.) and Newkirk (30- 60 million bbls.). In a statistical survey of several hundred fields, Sluijk and Nederlof (1984) found effective drainage areas were concentrated between 10 and 5000 square kilometers (3.9-1928) square miles), net source rock thicknesses generally lay between 5 and 100 meters (16 to 328 feet), vertical migration distances were concentrated between 100 and 5000 meters (328 and 16395 feet) and lateral migration distances were typically between 5 and 50 kilometers (3 - 31 miles). A longer lateral migration distance over a wide area of source shales could collect greater amounts of petroleum. The conditions for long lateral migration pathways are regional dips

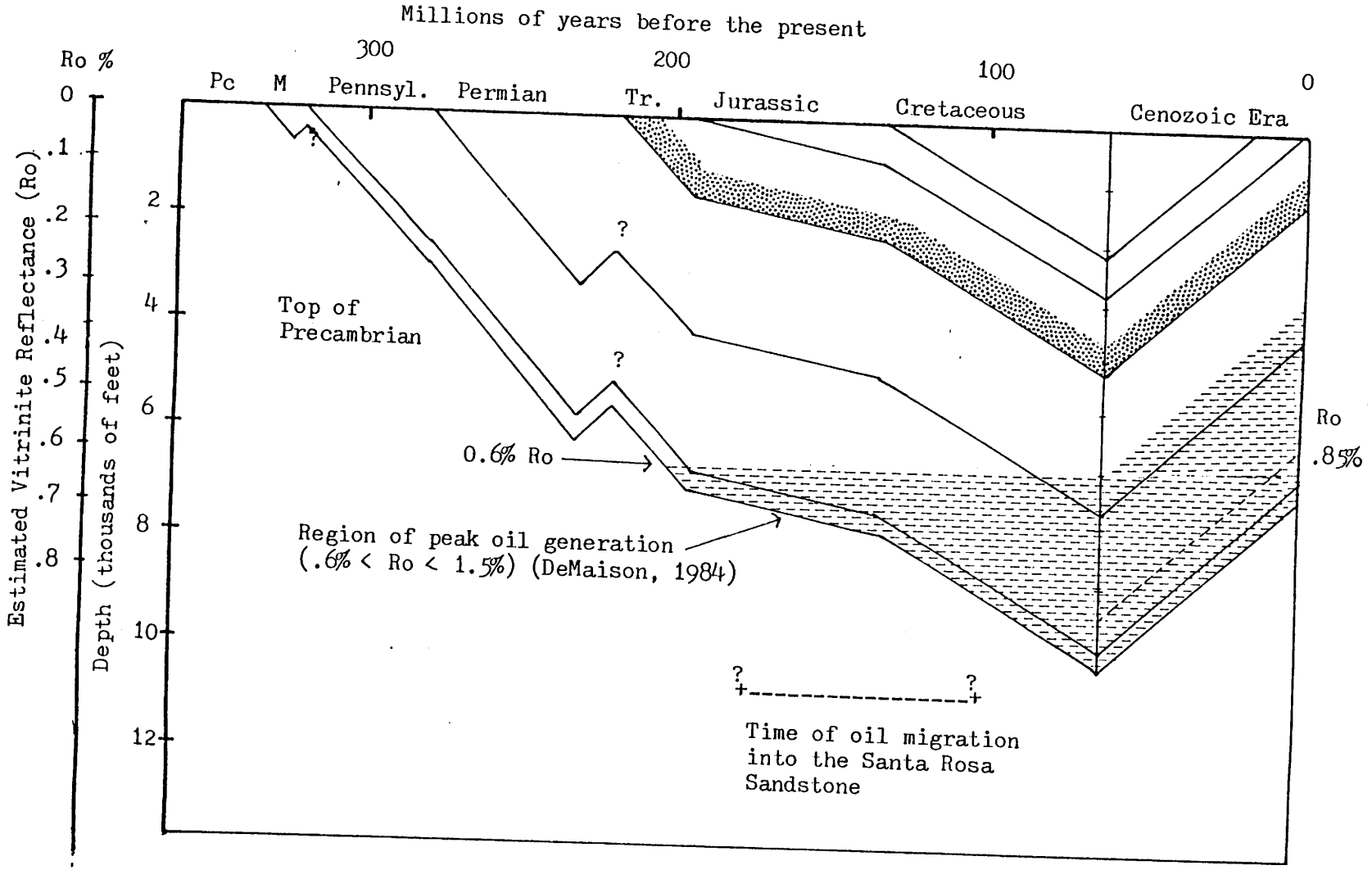

Fig. 6: Newkirk Area Subsidence History

N.M.I.M.T.
LIBRARY

of porous rocks effectively sealed against vertical migration which channel the oil toward the trap. In the Newkirk and Santa Rosa areas, fracturing caused by salt solution and collapse have affected overlying shales and some fractures show evidence of oil migration through them. Cementation of the Santa Rosa and other sands and their generally fine-grained nature tend to limit their oil conducting capacity. Formations in the area are interrupted by local slumps and structural features which might either form traps, outlets, or blockages to long range oil migration. Shows of predominantly dead oil in Bernal, Yeso, Abo, and Pennsylvanian sediments were common in the Trans Pecos Latigo Ranch Block D, No. 1 well. Pyrolysis analysis of cuttings from the Yeso Formation in that well indicated the oil shows were migrated hydrocarbons and were probably not formed in place. This suggests that vertical migration is the predominant migration direction in the area. Shows become more common in the Pennsylvanian and several wells produce gas and condensate from formations of this age in eastern Guadalupe and western Quay counties.

Migration Timing

The onset of petroleum generation may have been closely followed by migration before the oil became mature. It is probable that immature heavy oil migrated into the trap and was later subject to biodegradation which further reduced its API gravity. The observation that oil saturation is sensitive to slight changes in grain size in the reservoir also suggests the oil was too viscous to migrate into the finer-grained areas of

LIBRARY

the trap. Sample logs of the Latigo Ranch Block D, No. 1 well indicate numerous shows of dead oil over an interval of several thousand feet in Permian sands, shales, and anhydrites where water washing and biodegradation is less active than at shallower depths also supports migration of a low API gravity oil. The oil would have migrated through these sediments in fractures.

Trapping Mechanism

Newkirk Field has some aspects in common with other major oil deposits. Solution of underlying evaporites occurs beneath the Athabasca tar sands of Canada, above the Yates Field in West Texas, and in the Ochoan salts along a north-south producing trend in the Permian Basin. Roberts (1978) related these similarities to a fundamental change in direction of water movement in the subsurface from lateral to vertical which causes separation of organic components from water in traps. The mechanism for separation involves a combination of temperature drop, pressure drop, and salinity increase (due to deeper, more saline waters moving closer to the surface).

Roberts (1978) also asserts that good traps are commonly related to local weaknesses in one or more of the otherwise competent, covering strata such as shales. The reservoir sand and shale covering act as a selective membrane. The Newkirk reservoir sand allowed inward oil migration as long as the bouyant head of oil was sufficient to push the oil into the pores. Cartmill (1976) estimated that a fine-grained sandstone would require a bouyant head of 10 ft. of heavy oil to allow migration. A medium

LIBRARY

coarse sandstone would require only about 1 ft. of oil. Hubbert (1953) estimated that a shale would require a displacement pressure of 40 atmospheres (588 psi) to permit passage of petroleum versus only 0.1 amospheres (1.47 psi) for a sandstone. Since the reservoir sand is generally more than 10 feet thick, sufficient head exists to cause oil to push through the reservoir and to be conducted vertically through fractures in the Chinle shale and into the Cuervo sands. Muskat (1949) estimated that a single 0.001 inch wide fracture overlying a 500 ft. oil column could drain 150 million barrels of oil from a reservoir in 1000 years. Although the oil column at Newkirk is only on the order of tens of feet, this suggests that significant amounts of oil have escaped from the trap in the past through vertical fractures. Migration of slugs of oil in a separate phase also explains the anomalous character of the oil- water contact. Some structurally high sands contain no oil. These sands are finer than average and the bouyant head of oil was not sufficient to force the oil throught the narrow pore throats. Lower portions of the reservoir show gilsonite and oil in fractures. Oil migrated through these sands and left behind the heaviest, least mobile constituents. This portion of the sand shows little cementation indicating that calcite cementation may be related to changes in pressure and temperature conditions in the upper part of the reservoir rather than an overall change in water chemistry.

LIBRARY

CHAPTER THREE

Cross Sections

East - west cross section A-A' (Plates 2,3, and 4 in pocket) consists of three sheets and is sub-perpendicular to the southeast regional paleoflow direction. The westernmost sheet (Plate 2) shows a flat lying sand which splits and thins to the west. Several of the wells on this sheet had oil shows within 100 feet of the surface in the Cuervo sandstone. A continuous layer of mudstone between these near-surface sands and the main reservoir sands has not formed a complete seal to the reservoir and has allowed oil to migrate into the Cuervo.

The middle sheet (Plate 3) shows the upper and lower Santa Rosa sandstones slumping into a karst sinkhole. The upper sand was not deposited continuously across this area. The area may have contained topographic highs in the form of low hills of eroding lacustrine mudstones at the time of deposition. The braided streams depositing the sands would have been confined to valleys up to several miles wide flanking this low hill or other topographic highs of moderate relief (see the block diagrams in Fig. 7). The interruption in deposition of the Santa Rosa may have provided a weak point at which slumping began. Some of the Cuervo sands (unshaded) may be seen dipping into the sink area which has a total relief of approximately 120 feet over a distance of 1500 feet at the west edge. Aerial photographs show

LIBRARY

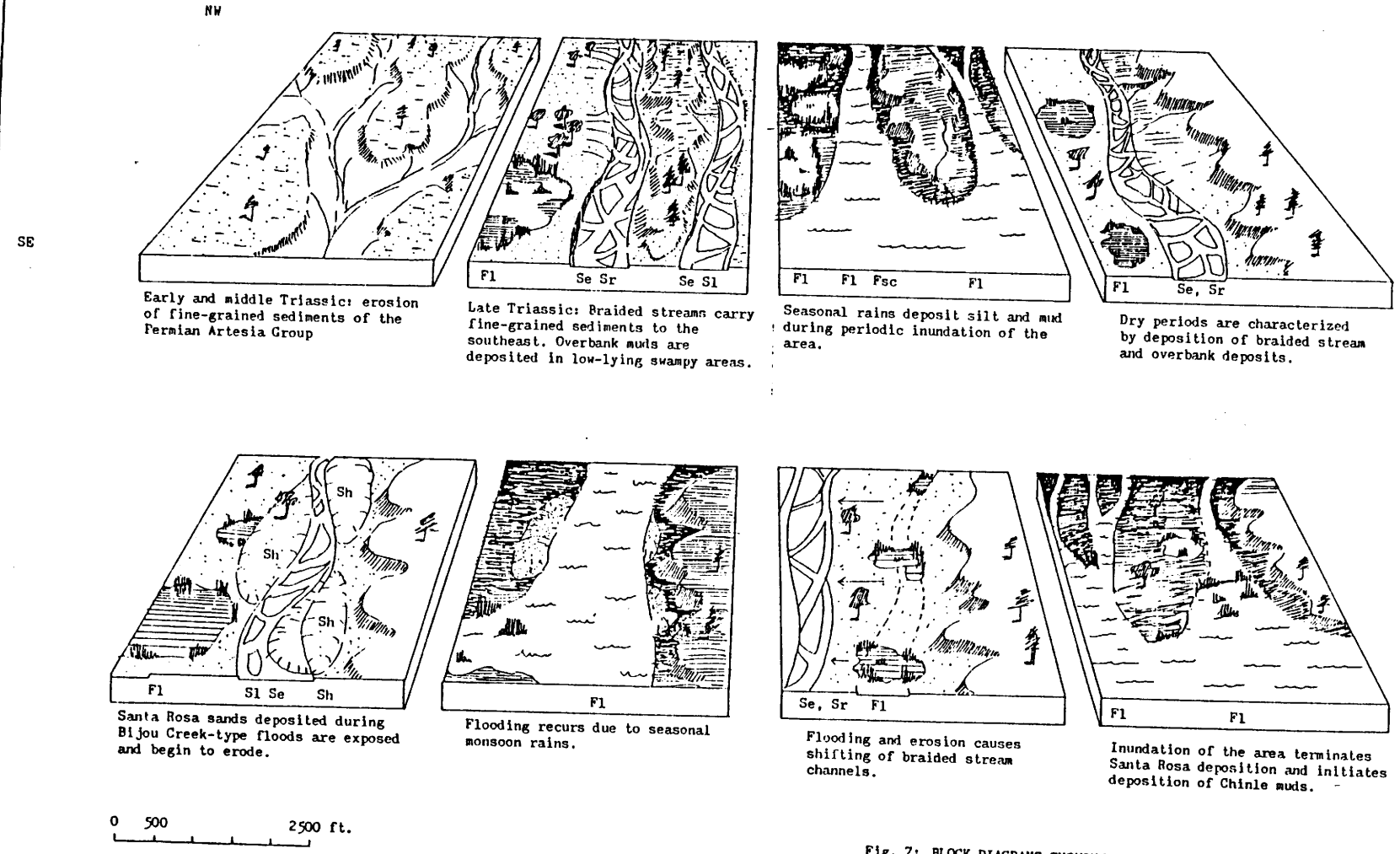

Early and middle Triassic: erosion of fine-grained sediments of the Permian Artesia Group

Late Triassic: Braided streams carry fine-grained sediments to the southeast. Overbank muds are deposited in low-lying swampy areas.

Seasonal rains deposit silt and mud during periodic inundation of the area.

Dry periods are characterized by deposition of braided stream and overbank deposits.

Santa Rosa sands deposited during Bijou Creek-type floods are exposed and begin to erode.

Flooding recurs due to seasonal monsoon rains.

Flooding and erosion causes shifting of braided stream channels.

Inundation of the area terminates Santa Rosa deposition and initiates deposition of Chinle muds.

Fig. 7: BLOCK DIAGRAMS SHOWING DEPOSITIONAL ENVIRONMENTS OF THE SANTA ROSA SANDSTONE IN THE NEWKIRK AREA

LIBRARY

that the sink may have influenced the course of north-flowing streams in section 14 of Township 11 North, Range 26 East. Sands of the Cuervo (unshaded) may be seen slumping into the sink in cross-section AA-2 indicating that slumping took place after deposition of the Cuervo.

The eastern sheet of the cross section (Plate 4) shows the discontinuous nature of the upper sand and undulatory nature of its structure. These undulations may be related to karst slumping on a smaller scale than that shown in the middle sheet or they may be tectonically formed. Oil saturation is not continuous throughout the wells in the section, indicating changes in sand permeability and porosity. The lower sand has abundant oil shows and oil-filled fractures but did not trap significant amounts of oil. Fractures in the intervening mudstone and absence of the mudstone because of erosion could have provided conduits for migration of the oil into the upper sands. If fractures were a factor they would be more numerous around the perimeters of sinkholes, at the crest of the anticline, and along flexures at its flanks. The west-side steamflood pilot has exhibited better performance than its easterly counterpart. Siphoning-off of the steam by fractures in the more karst-affected east side could have prevented it from heating the sand effectively.

Fence Diagrams

Fence diagrams of the steamflood pilot wells are shown in Plates 9 and 10 (in pocket). The sands are very continuous over the scale of the pilot operation. The uppermost sand, however,

LIBRARY

grades laterally into shale in some wells. Perforations are shown. Steam flow should occur in the most continuous intervals. The easternmost north-south cross section DD' (Plate 7 in pocket) shows an anticline. This cross section crosses section AA-3 about 200 east of the Jeannie No. 3 well. The Jeannie No. 5 well was used in order to include lithologic information from cores on the cross sections. The relationship and correlation of these two wells is shown in detail on the fence diagram of the east pilot (Plate 9 in pocket). These wells are close to each other and there is little variation in the sands between them. Fault gouge was noted in cores in the Beryl No. 1 and possibly in the Daisy No. 1. This may have been related to minor faulting caused by flexing of the sand as it draped over the underlying Precambrian horst or faulting associated with the sinking of the Santa Rosa into sinkholes. No direct evidence of a large offset fault along the flanks of the structure was seen in cross sections or on the surface. The core from the Barbara No. 2 well showed oil in fractures at the 892 ft. depth. The oil can be seen diffusing into the surrounding uncemented sandstone. At the 902 ft. depth oil is trapped in laminations which may have been surrounded by cemented sandstone at one time but which are now surrounded by porous uncemented medium grained sandstone.

North-south cross section CC' (Plate 6 in pocket) shows the reservoir sands dip to the north. Opposing dip to the south like that shown in cross section DD' is absent . A discrepancy exists where the gamma ray log of the State No. 4 well shows sand but

LIBRARY

the sample log shows shale in the upper sand. Oil is absent, probably because pore throats were too narrow to permit oil migration into the pore space. Note that the sand in this well is structurally higher than the oil saturated sand of the State No. 11 and would normally be expected to contain oil.

North-south cross section BB' (Plate 5 in pocket) shows dip of the reservoir sand similar to that in CC'. However, the upper sand pinches out to the north instead of to the south as in CC'. The core at 416 ft. depth in the O'Connell No. 1 shows that oil migrated into laminations before the major phase of calcite cementation began. These laminations were truncated by an erosional scour surface during deposition. An interesting comparison can be made of the character of the oil saturation in this sketch to sketches on cross section DD'.

Structure and Isopach Maps

A structure contour map of the top of the upper sand is shown in Fig. 8 . This map shows structural closure of several hundred feet. An inward curving of the contour lines in section 14 is the result of slumping of the sand into a sinkhole. The structure contours are continued across areas where no sand was deposited in order to show the structure clearly.

Two isopach maps were prepared. Fig. 9 shows the thickness of the upper Santa Rosa sand (including shale stringers). A comparison with Fig. 8 shows that initiation of slumping may have begun in the area where the sandstone is absent and failure was more likely to occur. Fig. 10 shows the thickness of a

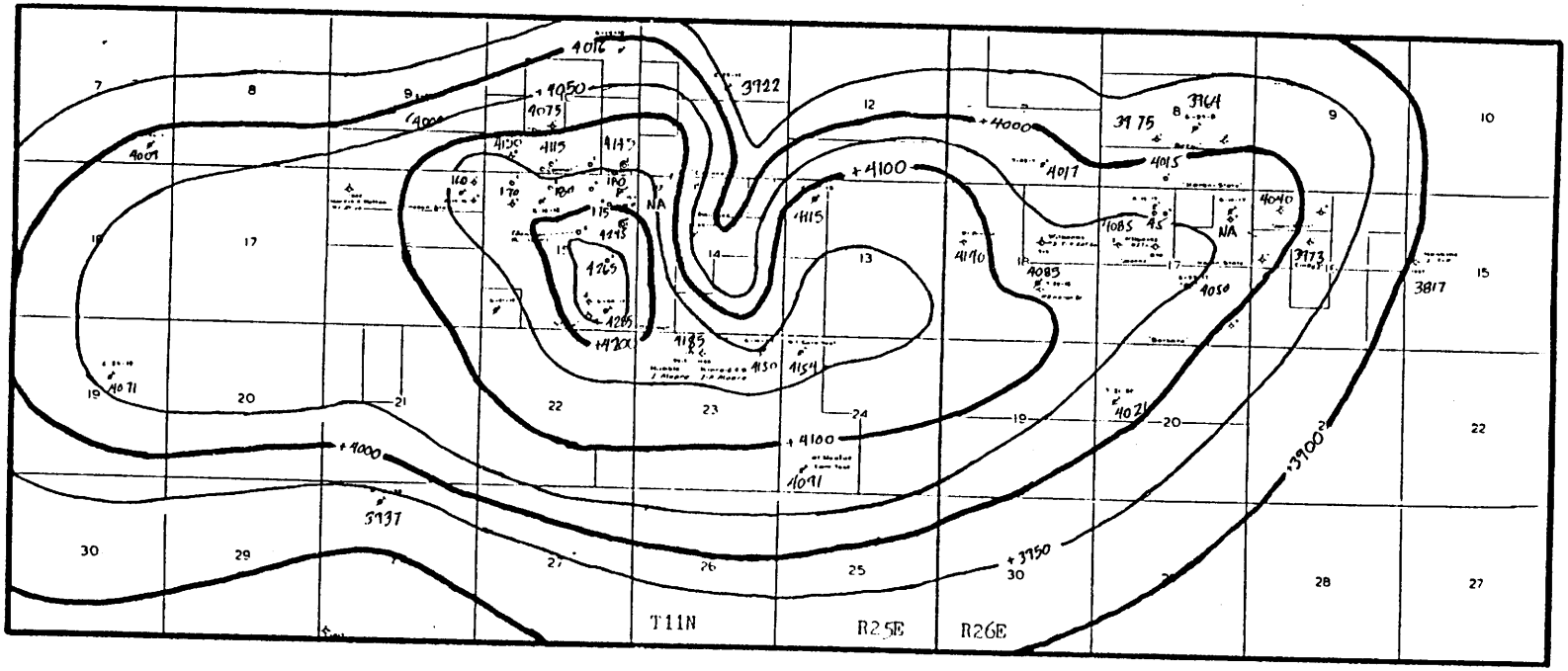

Fig. 8: Structure contour map on top of the upper Santa Rosa Sandstone
Contour interval: 50 ft.

LIBRARY

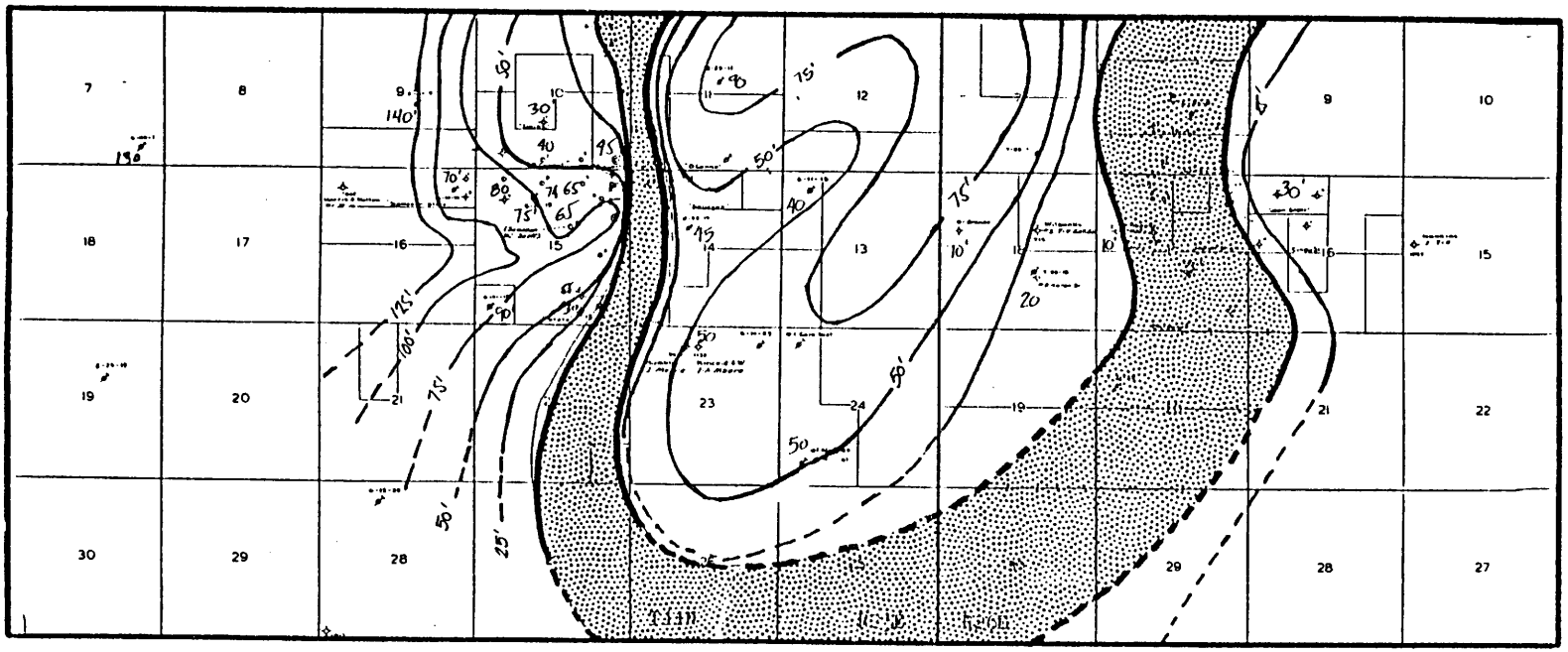

Fig. 9: Isopach map of the upper stringer of the upper Santa Rosa Sandstone
Contour interval: 25 ft. Shaded where zero thickness

LIBRARY

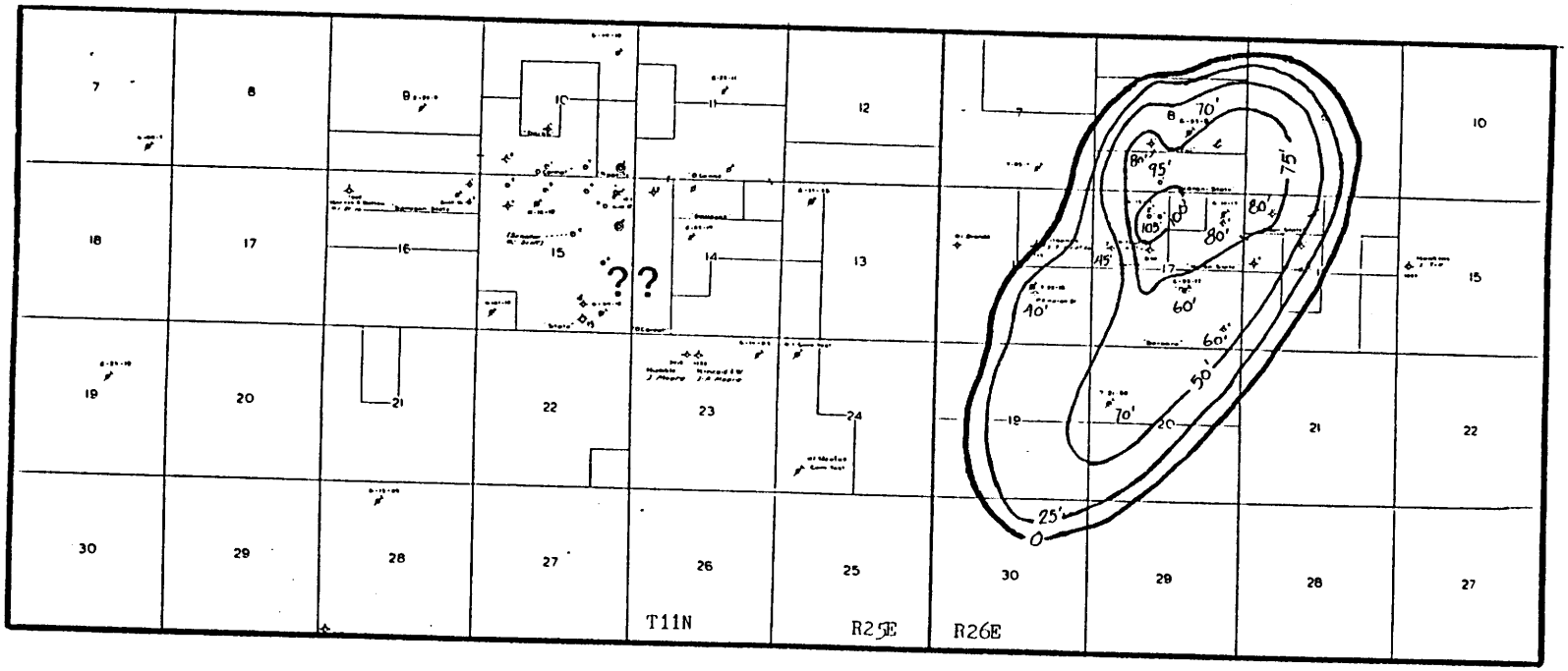

Fig. 10: Isopach map of the lower stringer (?) of the upper Santa Rosa Sandstone
Contour interval: 25 ft.

(140)

LIBRARY
SOCORRO N.M.

lower stringer (?) of the upper sand. It is very difficult to determine how much of the thick sequences present in cross section DD' should be assigned to each of these two stringers. The lower stringer (?) may actually be the middle Santa Rosa Sandstone mentioned by McDowell (1972) but petrographic studies to determine this were not made. Based on stratigraphic positions in the Jeannie No. 3 (Plate 4) and Jeannie No. 5 (Plate 7) wells, it was decided that the full sand thickness should be assigned to the lower stringer. Its isopach map shows that a thick area of the lower stringer underlies an area of zero thickness of the upper stringer. This may be the result of a paleo high caused by the resistant character of the lower stringer discouraging deposition of the upper stringer at this location. Alternatively, the full thickness of sand should not have all been assigned to the lower stringer. Note that the trend of these areas of zero sand thickness seen in Fig. 9 trend south or south-southwest in an area where the regional paleocurrent directions are southeast.

LIBRARY

CHAPTER FOUR

Depositional Environment

The Dockum Group of eastern New Mexico (of which the Santa Rosa Sandstone is a part) was deposited in a continental basin (McGowen et al., 1983). A large lake with fluctuating shorelines was centered on the Texas - New Mexico border during the Triassic period Braided and meandering streams flowed into this lake (Fig. 11). High and low stands of the lake created cyclic fluvial, deltaic, and lacustrine deposits.

The source area for the Santa Rosa in the study area includes the Sierra Grande arch and Pedernal uplift. These uplifts were partially covered by Pennsylvanian and Permian sediments at the time of Triassic deposition (Kottlowski and Stewart, 1970).

Lupe (1977) concluded that the Santa Rosa Sandstone in the vicinity of Santa Rosa was deposited as a complex of braided streams, floodplains, and lakes. Paleocurrent directions were generally east and south (McGowen et al., 1979). These directions are supported by paleocurrent measurements taken on the Cuervo (Fig. 12 - a,b,c), the upper Santa Rosa Sandstone (Fig. 12-d), and east and southeast trending sandstone bodies separated by muddy areas noted by Broadhead (1984). The muddy areas were deposited in interfluvial and lacustrine environments (Broadhead, 1984). The lower sandstone has a sheetlike morphology and was

LIBRARY

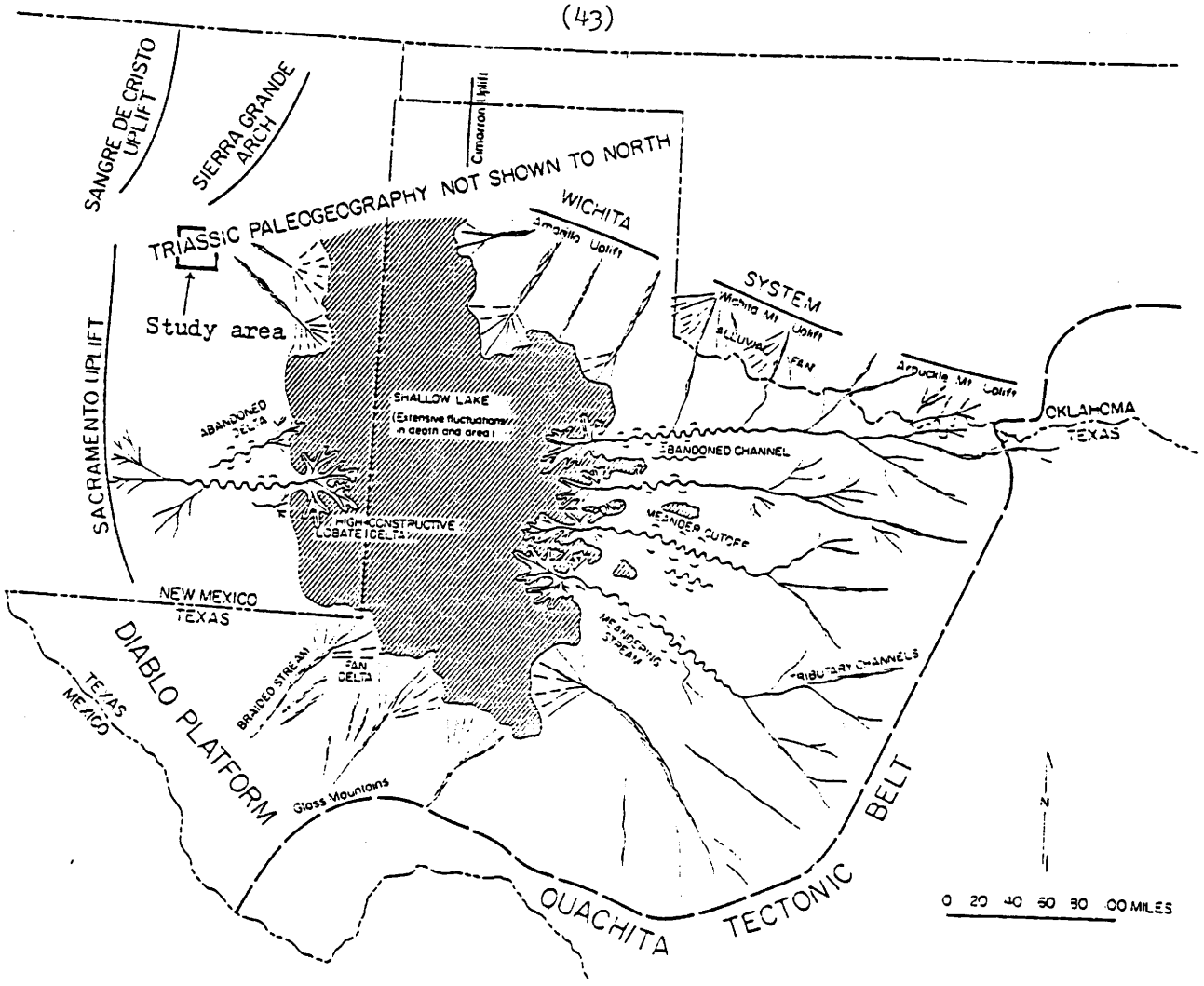

Fig. 11: Triassic Paleogeography
(McGowen et al., 1979)

☐ Approximate location of the Newkirk Field

LIBRARY SOCORRO, N.M.

probably deposited by braided streams flowing over an alluvial plain (Broadhead, 1984). The middle mudstone unit of the Santa Rosa Sandstone may have been deposited by a lacustrine transgression by the Dockum lake and contains widespread lacustrine muds and local deltaic and lacustrine sands (Broadhead, 1984 and McGowen et al., 1979).

The upper sandstone unit is interpreted as a fan-delta deposit by McGowen et al. (1979, pp. 8-9) that prograded southeast over the lacustrine deposits of the middle mudstone unit. Both upward-fining and upward coarsening sequences are present in cores and logs in the field. Broadhead (1984) reports the upper unit was probably deposited as an alluvial sheet sand dominated by braided streams.

McGowen et al. (1979, p. 9) described the upper sandstone unit at one locality as being composed of 20 feet of basal ripple drifted, horizontal and broadly undulatory laminated very fine-grained to fine-grained sandstone and 10 feet of superposed trough-filling cross-stratified, fine-to medium-grained sandstone. The upper unit is overlain by red, brown, and gray lacustrine mudstones of the Chinle Formation. The Cuervo sandstones were deposited by braided streams (Broadhead, 1984) flowing southeast as shown by paleocurrent measurements on ripple marks (Fig. 12b) and other data.

Core Descriptions

Cores from the upper Santa Rosa Sandstone in the Newkirk Field formed the primary data for this study. The cores were

LIBRARY

(a)

Cuervo Sandstone: on low dome-shaped outcrop 1 mile southwest of west pilot

n = 39

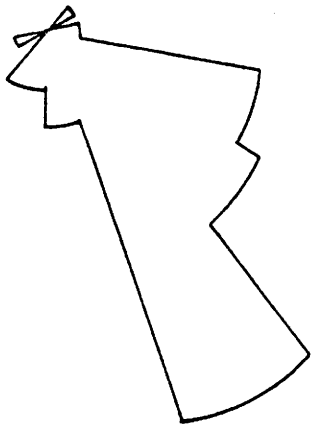

(b)

Upper Santa Rosa Sandstone: near Santa Rosa Lake dam

n = 19

Scale

n = 18

(c)

Cuervo Sandstone: top of mesa 3 miles west of wes pilot

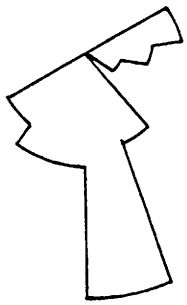

n = 32

(d)

Cuervo Sandstone: 1 mile southwest of east pilot

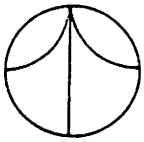

Fig. 12:
Paleocurrent Rose Diagrams
(from asymmetrical ripple marks)

LIBRARY

described using a grain-size comparator, dilute HCL for identification of calcite cement, and a hand lens. Details of the lithology, cement, sedimentary structure, fractures, plant fragments, pyrite, and oil saturation were logged on a scale of 5 inches = 100 ft. to facilitate correlation with geophysical logs of the same scale. Sketches were made where this scale did not allow sufficient room to show important features. The cores were not azimuth oriented, which would have contributed important paleocurrent information from cross bedding directions. Each core consisted of 3 foot segments commonly broken into shorter segments of a few inches to two feet. Recovery was excellent in the sandstone intervals and good to poor in the mudstone intervals.

The cores show two dominant lithologies. One is a very fine to fine-grained brown sandstone with planar laminations and medium scale cross laminations. The second is grey mudstone and siltstone which is interlaminated with the sandstone. It varies from being finely laminated to structureless This facies was examined in thin section and with X-Ray diffraction methods. It is composed of smectite and illite with varying amounts of angular silt-size quartz. In some cores the mudstone is colored red due to the presence of iron oxides. The clay composition is the same in both cases. The two dominant lithologies contain sedimentary structures which repeated in the section and suggested cycles of deposition. The data collected are shown on the cross sections (Plates 2 - 8, in pocket) in order to

LIBRARY

facilitate an understanding of the interrelationship of lithologies and stratigraphy.

The cyclic nature of the cores suggested that they could be related to Miall's classification of fluvial lithofacies on the basis of grain size and sedimentary structures. Examples of the lithofacies is shown in the core photos (Fig. 5) of the Barbara No. 1 from 709 ft. to 860 ft.. The approximate contacts between lithofacies is shown by a bar with pointers on both sides. Darker areas in the cores are the result of various amounts of oil saturation. The original color of the lithologies pictured varies between light brown and light grey. Some sections of the cores did not fit the criteria of Miall exactly and these sections were fit into an existing lithofacies. A common example was the existence of gravel-sized material. Instead of being at the base of a scour, it occasionally appeared near the top of what otherwise might be lithofacies Se. In addition, lithofacies Gm and Se both can have gravel-size material and sometimes were difficult to distinguish. The following is a description of the lithofacies:

CODE: Gm Lithofacies: Gravel, structureless to crudely bedded

SEDIMENTARY STRUCTURES: horizontal bedding, imbrication

INTERPRETATION: longitudinal bars, lag and sieve deposits

LIBRARY SOCORRO, N.M.

CODE: Sr Lithofacies: sand, very fine to coarse

SEDIMENTARY STRUCTURES: ripple marks of all types.

INTERPRETATION: (lower flow regime).

These sequences were represented in the cores by wavy laminated fine and very fine-grained sandstones and siltstones.

CODE: Sh LITHOFACIES: sand, very fine to coarse

SEDIMENTARY STRUCTURES: Horizontal lamination, parting or streaming lineation.

INTERPRETATION: upper flow regime deposits.

Many of the cores contain internally structureless fine grained sandstone ranging from a few feet to a few tens of feet thick which is assigned to this lithofacies. This is based upon the possibility that it contains stratification which is too faint to detect by the naked eye and upon a process of elimination. This lithofacies may have sharp or gradational upper and lower contacts with grey siltstones.

CODE: Se LITHOFACIES: sand: erosional scours with clasts

SEDIMENTARY STRUCTURES: Crude crossbedding

INTERPRETATION: Scour fills

Some sandstone sequences contained clasts of mudstone near the base. These clasts were generally a few millimeters to a few centimeters in size, subrounded to rounded, and grey in color.

LIBRARY

Very elongate angular fragments, which probably represent mudcracked mud, occur.

CODE: S1 LITHOFACIES: fine sand

SEDIMENTARY STRUCTURES: low angle (<10 degree) crossbeds

INTERPRETATION: scour fills, crevasse splays

CODE: F1 LITHOFACIES: sand, silt, mud

SEDIMENTARY STRUCTURES: fine lamination, very small ripples

INTERPRETATION: overbank or waning flood deposits

This was a very common lithofacies, present in every core to some extent. The laminations may be straight or wavy. Abundant plant fragments and pyrite usually occur in this facies.

CODE: Fsc LITHOFACIES: silt, mud

SEDIMENTARY STRUCTURES: laminated to structureless

INTERPRETATION: backswamp deposits

Some grey siltstone sequences were structureless and crumbly and contained plant fragments and abundant pyrite.

CODE: Fm LITHOFACIES: mud, silt

SEDIMENTARY STRUCTURES: structureless, dessication cracks

INTERPRETATION: overbank or drape deposits

External molds of invertebrate fossils were found in both the mudstone and sandstone facies. These molds, however, were rare and not well preserved.

According to Miall (1982) , a systematic study of fluvial deposits requires at least three main steps: First, the major and minor lithofacies components should be identified. Secondly, these should be grouped into associations and internal relationships of the lithofacies should be determined. Thirdly, the geometry and orientation of the depositional units should be studied. The results from these studies can then be related to a series of facies models.

The strongly cyclical nature of fluvial systems means they tend to generate distinctive vertical profiles. The facies cycles as seen in vertical sections such as cores can be classified as either autocyclic or allocyclic. Autocyclic processes are those which occur as an integral part of the depositional environment, such as lateral meander migration or seasonal floods (Miall, 1981). Allocyclic processes are those external to the system, such as tectonic events or climatic changes (Miall, 1982). Overprinting of allocyclic processes (essentially random from the standpoint of the fluvial system) over autocyclic processes (essentially deterministic) is common and leads to complex sequences.

Library

Markov Analysis

In order to extract the fluvially determined cycle from the vertical profile, Miall (1982) recommends the use of Markov chain analysis. A Markov process is one "in which the probability of the process being in a given state at a particular time may be deduced from knowledge of the immediately preceding state" (Harbaugh and Bonham-Carter, 1970, p. 98). The particular Markov method used here is the "single-dependency, embedded chain" method (Krumbein and Dacey, 1969) which corresponds to "method 1" of Miall (1973) in which the thickness of individual beds is not taken into consideration.

The initial data for the Markov calculation is shown in Fig. 13a. This table shows the number of transitions in all the cores from the lithology listed along the left hand side to the lithology at the top. Fig. 13b shows the probabilities of the different combinations of lithologies arising, given a starting lithology at the left. It was calculating by dividing each cell by the total for its row. Fig. 14a, the difference matrix, was calculated in two steps. First an independent trials probability matrix (not shown) was constructed using data from Fig. 13a. The row total for each cell was subtracted from the total number of transitions (107) and the result divided into the column total for that cell. This procedure corresponds to equation 1 of Miall (1973). Finally, each cell of the independent trials matrix was subtracted from the corresponding cell in Fig. 13b. Positive numbers are underlined in the difference matrix to emphasize

transitions which occurred with greater than random frequencies. Fig. 14b, the Chi - Square Table, shows the Chi - Square calculations after the method of Till (1974, p. 75). Each cell is calculated by the following formula:

$$T * \ln(P/S)$$

where: T = transitions for that cell in Fig. 13a.
P = probability of transition from Fig. 13b.
S = probability column sum from Fig. 13b.

The cells are then summed and doubled to arrive at the Chi - Square value and compared with values in Chi - Square tables. The degrees of freedom are calculated by the following formula:

$$(\text{number of rows in matrix} - 1)^2 - (\text{number of rows})$$

For the Newkirk cores we arrive at a Chi - Square value of 110 for a matrix with 41 degrees of freedom. This is well in excess of the 57 needed to prove that there is a less than a 5% chance the observed transitions are solely random. This means there is a 95% probability that the observed transitions are autocyclic.

The Solvex cores had a Chi - Square value of 172 (Figs. 15-16), also indicating a very high probability that the observed transitions are autocyclic rather than random. This shows that

there is a high degree of autocorrelation within the observed interval created by clyclical pattern of depositional energy levels. The most probable cause of these patterns is an annual monsoonal or rainy season followed by a dry period. A difference matrix diagram of the upper Santa Rosa Sandstone is shown in Fig. 17. This diagram shows the important non-random transitions. Fig. 18 shows the number of transitions between lithofacies and indicates which transitions are the most common.

LIBRARY

Fig. 13a markl.mp
Markov Analysis: (after Miall and Gibling, 1978)
Newkirk Cores

Lithofacies (after Miall, 1978a)

	Gm	Sr	Sh	Sl	Se	Fl	Fsc	Fm	Total
Gm (long. bars, lag, sieve)	0	0	0	0	0	1	0	0	1
Sr (ripples (LFR)	0	0	1	0	0	4	0	0	5
Sh (planar bed: LFR & UFR)	1	2	0	2	4	17	1	0	27
Sl (scour fill, splays)	0	2	0	0	1	11	0	0	14
Se (scour fills)	0	0	7	1	0	6	1	0	15
Fl (overbank deposits)	0	0	18	8	9	0	3	0	38
Fsc (backswamp deposits)	0	1	1	2	1	0	0	0	5
Fm (overbank & drape)	0	0	0	0	0	2	0	0	2
	1	5	27	13	15	41	5	0	107

Fig. 13b:

Probability matrix	Gm	Sr	Sh	Sl	Se	Fl	Fsc	Fm	Total
Gm (long. bars, lag, sieve)	0%	0%	0%	0%	0%	100%	0%	0%	100%
Sr (ripples (LFR)	0%	0%	20%	0%	0%	80%	0%	0%	100%
Sh (planar bed: LFR & UFR)	4%	7%	0%	7%	15%	63%	4%	0%	100%
Sl (scour fill, splays)	0%	14%	0%	0%	7%	79%	0%	0%	100%
Se (scour fills)	0%	0%	47%	7%	0%	40%	7%	0%	100%
Fl (overbank deposits)	0%	0%	47%	21%	24%	0%	8%	0%	100%
Fsc (backswamp deposits)	0%	20%	20%	40%	20%	0%	0%	0%	100%
Fm (overbank & drape)	0%	0%	0%	0%	0%	100%	0%	0%	100%
Totals:	1%	5%	25%	12%	14%	38%	5%	0%	107

LIBRARY
SOCORRO, N.M.

Fig. 14a
Newkirk Field Cores
Difference Matrix

	Gm	Sr	Sh	Sl	Se	Fl	Fsc	Fm	Totals:
Gm (long. bars, lag, sieve)	-1%	-5%	-25%	-12%	-14%	61%	-5%	0%	-1%
Sr (ripples (LFR)	-1%	-5%	-6%	-13%	-15%	40%	-5%	0%	-5%
Sh (planar bed: LFR & UFR)	2%	1%	-34%	-9%	-4%	12%	-3%	0%	-34%
Sl (scour fill, splays)	-1%	9%	-29%	-14%	-9%	34%	-5%	0%	-15%
Se (scour fills)	-1%	-5%	17%	-7%	-16%	-5%	1%	0%	-16%
Fl (overbank deposits)	-1%	-7%	8%	2%	2%	-59%	1%	0%	-55%
Fsc (backswamp deposits)	-1%	15%	-6%	27%	5%	-40%	-5%	0%	-5%
Fm (overbank & drape)	-1%	-5%	-26%	-12%	-14%	61%	-5%	0%	-2%
Totals:	-5%	-2%	-101%	-38%	-65%	104%	-25%	0%	-133%

Fig. 14b Chi - Square Test
Newkirk Field Cores
X - Square Calculation

	Gm	Sr	Sh	Sl	Se	Fl	Fsc	Fm	Totals:
Gm (long. bars, lag, sieve)	0	0	0	0	0	1	0	0	0.9592568
Sr (ripples (LFR)	0	0	-0	0	0	3	0	0	2.7120069
Sh (planar bed: LFR & UFR)	1	1	0	-1	0	8	-0	0	9.7400378
Sl (scour fill, splays)	0	2	0	0	-1	8	0	0	9.4597247
Se (scour fills)	0	0	4	-1	0	0	0	0	4.3169296
Fl (overbank deposits)	0	0	11	4	5	0	2	0	22.02688
Fsc (backswamp deposits)	0	1	-0	2	0	0	0	0	3.9600253
Fm (overbank & drape)	0	0	0	0	0	2	0	0	1.9185135
Totals:	1.376992	4.610317	15.175068	5.1912652	4.62176	22.421826	1.6961459	0	55.093374

Total X Square Value: 110.18675
for 41 degrees of freedom

Fig. 15a: mark2.mp
Markov Analysis: (after Miall and Gibling, 1978)
Solvex Cores

Lithofacies (after Miall, 1978a)

	Gm	Sr	Sh	Sl	Se	Fl	Fsc	Fm	Total
Gm (long. bars, lag, sieve)	0	0	6	1	0	0	3	0	10
Sr (ripples (LFR)	0	0	0	0	0	0	0	0	0
Sh (planar bed: LFR & UFR)	1	0	0	21	0	1	19	0	42
Sl (scour fill, splays)	0	0	17	0	0	0	6	0	23
Se (scour fills)	0	0	0	0	0	0	0	0	0
Fl (overbank deposits)	0	0	1	0	0	0	0	0	1
Fsc (backswamp deposits)	9	0	20	2	0	0	0	0	31
Fm (overbank & drape)	0	8	19	0	0	2	0	0	29
	10	8	63	24	0	3	28	0	136

Fig. 15b:
Probability matrix

	Gm	Sr	Sh	Sl	Se	Fl	Fsc	Fm	Total
Gm (long. bars, lag, sieve)	0%	0%	60%	10%	0%	0%	30%	0%	100%
Sr (ripples (LFR)	0%	0%	0%	0%	0%	0%	0%	0%	0%
Sh (planar bed: LFR & UFR)	2%	0%	0%	50%	0%	2%	45%	0%	100%
Sl (scour fill, splays)	0%	0%	74%	0%	0%	0%	26%	0%	100%
Se (scour fills)	0%	0%	0%	0%	0%	0%	0%	0%	0%
Fl (overbank deposits)	0%	0%	100%	0%	0%	0%	0%	0%	100%
Fsc (backswamp deposits)	29%	0%	65%	6%	0%	0%	0%	0%	100%
Fm (overbank & drape)	0%	28%	66%	0%	0%	7%	0%	0%	100%
Totals:	7%	6%	46%	18%	0%	2%	21%	0%	100%

Fig. 16a:
Solvex Cores
Difference Matrix

	Gm	Sr	Sh	Sl	Se	Fl	Fsc	Fm	Totals:
Gm (long. bars, lag, sieve)	-8%	-6%	10%	-9%	0%	-2%	8%	0%	-8%
Sr (ripples (LFR)	-7%	-6%	-46%	-18%	0%	-2%	-21%	0%	-100%
Sh (planar bed: LFR & UFR)	-8%	-9%	-67%	24%	0%	-1%	15%	0%	-45%
Sl (scour fill, splays)	-9%	-7%	18%	-21%	0%	-3%	1%	0%	-20%
Se (scour fills)	-7%	-6%	-46%	-18%	0%	-2%	-21%	0%	-100%
Fl (overbank deposits)	-7%	-6%	53%	-18%	0%	-2%	-21%	0%	-1%
Fsc (backswamp deposits)	20%	-8%	5%	-16%	0%	-3%	-27%	0%	-30%
Fm (overbank & drape)	-9%	20%	7%	-22%	0%	4%	-26%	0%	-27%
Totals:	-37%	-27%	-67%	-98%	0%	-11%	-90%	0%	-330%

Fig. 16b:

Solvex Cores
X - Square Calculation

	Gm	Sr	Sh	Sl	Se	Fl	Fsc	Fm	Totals:
Gm (long. bars, lag, sieve)	0	0	2	-1	0	0	1	0	2.1136159
Sr (ripples (LFR)	0	0	0	0	0	0	0	0	0
Sh (planar bed: LFR & UFR)	-1	0	0	22	0	0	15	0	35.77648
Sl (scour fill, splays)	0	0	8	0	0	0	1	0	9.3633617
Se (scour fills)	0	0	0	0	0	0	0	0	0
Fl (overbank deposits)	0	0	1	0	0	0	0	0	0.7695202
Fsc (backswamp deposits)	12	0	7	-2	0	0	0	0	16.972591
Fm (overbank & drape)	0	12	7	0	0	2	0	0	21.229263
Totals:	11.232165	12.362872	23.476663	19.290069	0	2.3561609	17.506901	0	86.224832

Total X Square Value: 172.44966
for 41 degrees of freedom

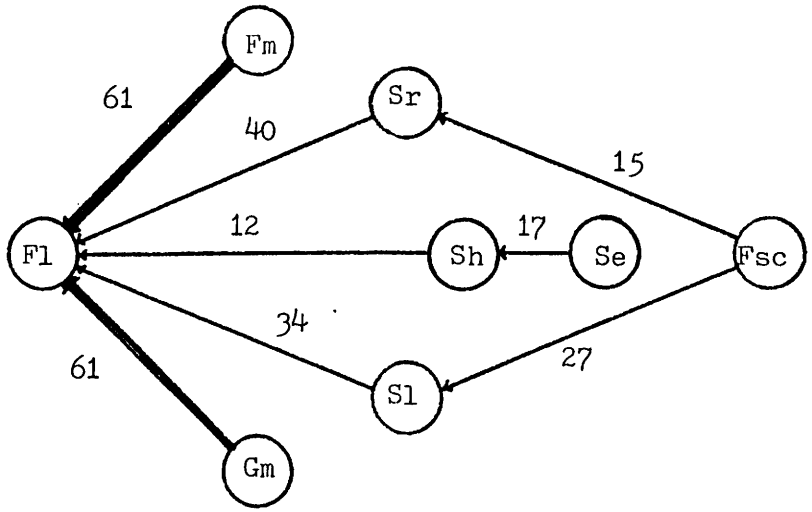

Newkirk Field: Upper Santa Rosa Sandstone

Difference Matrix Diagram

(Numbers are percentages greater than 10% from Fig. 14a.)

Fig. 17

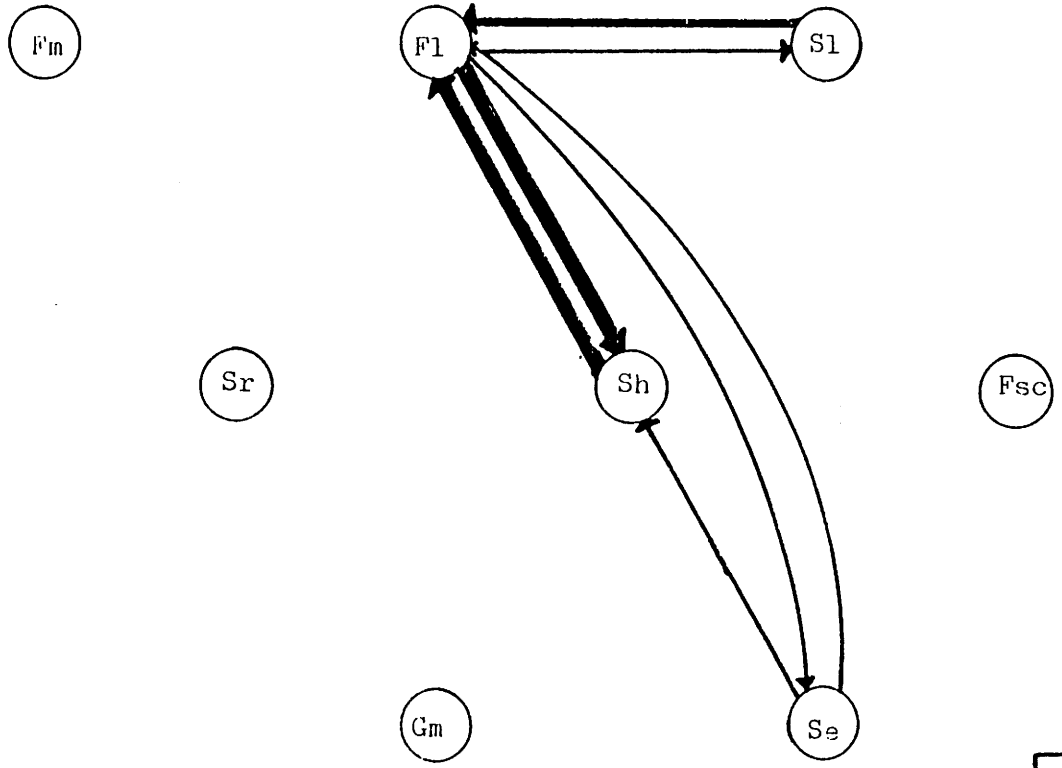

15 - 20

10 - 15

5 - 10

0 - 5 (not shown)

Number of transitions (n=107)

Newkirk Field: Upper Santa Rosa Sandstone

Strength Diagram

(Transitions from Fig. 13a)

Fig. 18

CHAPTER FIVE

Comparisons with Modern Environments

Miall lists six principal lithofacies assemblage models for low sinuosity, multiple channel rivers. The model which most closely fits the observed facies patterns of the Santa Rosa Sandstone is the Bijou Creek type with major facies Sh (lower and upper flow regime) and Sl (fine sand with low angle crossbeds representative of scour fills.) The environmental setting for the Bijou Creek type is ephemeral or perennial rivers subject to flash floods (Miall, 1981).

Bijou Creek, Colorado

The Bijou Creek type is named for Bijou Creek, Colorado (McKee et al., 1967) which drains an area of 1444 square miles underlain by the Pierre Shale, Fox Hills Sandstone, and Laramie Formation of the Late Cretaceous series. These formations consist of shales, sandy shales, sandstones, and lignitic coal beds with little coarse material. Annual precipitation ranges widely about an average of 13 inches per year. McKee et al. (1967) studied the deposition of sand during flood and found that it consisted of 90% horizontal strata with minor amounts of tabular planar crossbedding at the outer edges of the flood sheets. Local climbing ripple laminae and convolute bedding formed during waning stages of the flood and are characteristic of relatively sheltered areas away from the path of the main flood. Erosional

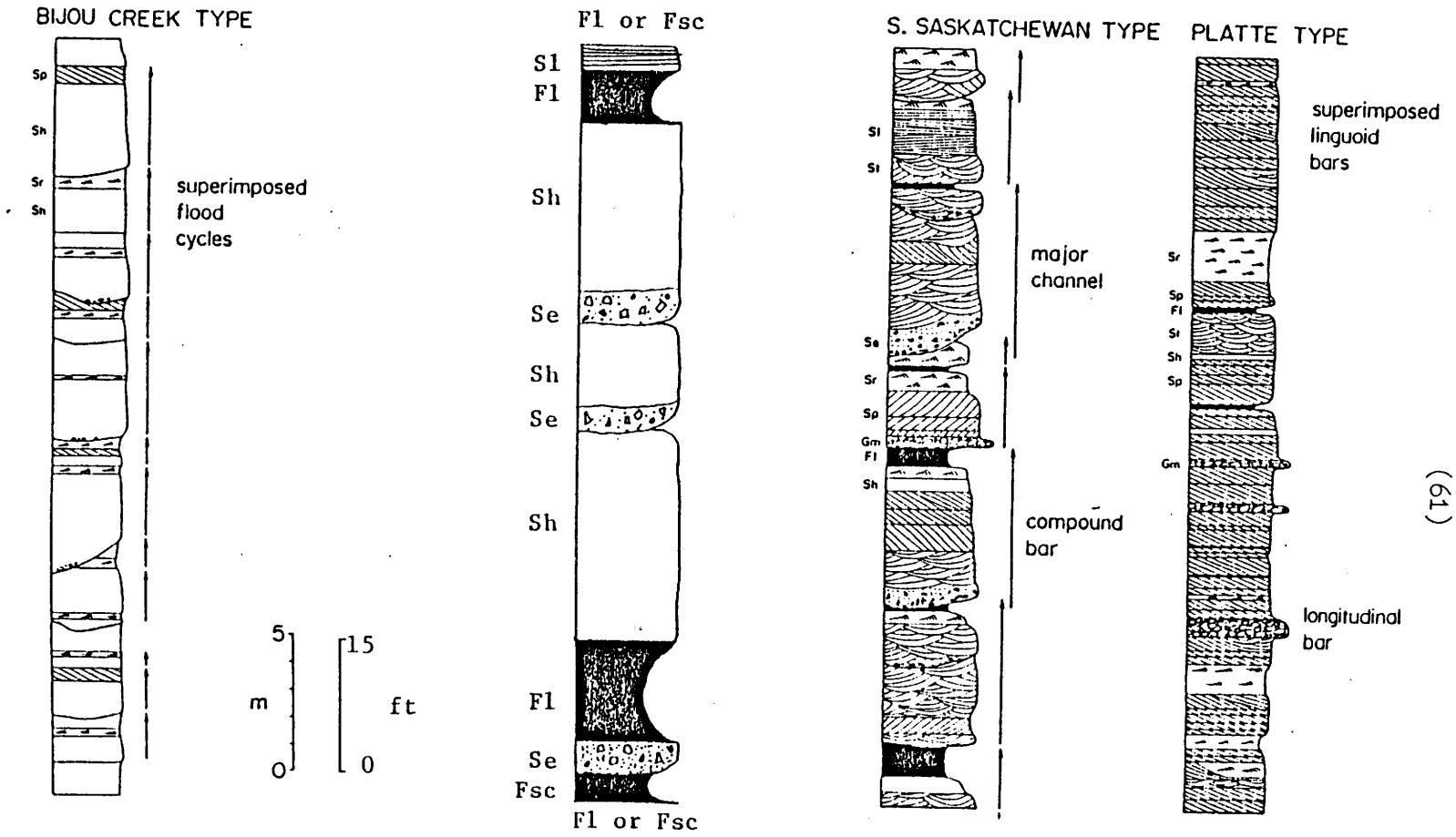

Newkirk Field, N.M.

Fig. 19: Generalized vertical profiles compared (Miall, 1978 and this paper)

surfaces and soft sediment deformation structures were rare. A comparison of typical vertical sequences in the Newkirk cores with that of the Bijou Creek and other types is shown in Fig. 19. The flood occurred in two stages and the waning phases at the end of each stage are characterized by climbing ripple laminae. Convolute laminae were developed during late flood stages during lower flow regime conditions and represent a time when the sediment was in a quicksand-like state.

The flood sheets were deposited 0.25 to 0.5 mile beyond the banks on each side of the stream and averaged two to three feet thick with a maximum of 12 feet. The dominant lithology consists of moderately well-sorted, medium-grained sand with minor amounts of fine and coarse-grained material. The flood moved large concrete slabs proving that the source area exerted control over the grain size. The mean velocity computed on the basis of a total cross-sectional area of 28,380 square feet for the channel and overbank flow was 16.4 feet per second (11.2 miles per hour). In the main channel it was computed to be 21.83 feet per second (14.9 m.p.h.). Both calculations were made using a measured peak discharge of 466,000 cubic feet per second. This volume of water was the result of rainfall rates of up to 12 inches in several hours along the upper reaches of the creek and approximately equals the amount of rain which normally falls in one year in the area. The width of the Bijou Creek channel and flood plain during years of average flow is about .25 to .75 miles and is confined by easily eroded alluvial deposits which

filled a wide valley 5 to 10 miles wide during the Pleistocene Epcoh. Loess and sand dunes are present in the area above the level of present flood plains. Cottonwood trees grow on the flood plains. The flood waters spread sand across the flood plain in a downstream direction by jumping out of the banks of the sinuous channel rather than laterally spilling over them. (See Fig. 20). The preflood surface of the flood plain was a maximum of 10 feet above the present level of the streambed. On this surface the flood deposited a sheet of sand about 800 feet wide and 1500 to 2000 feet long. Near the cutbank along the channel the flood sand ranged from 20 to 30 inches thick; a maximum thickness of 40 inches was observed about 300 feet north of the channel edge. Debris on trees suggests the flood waters reached a depth of 9 feet above the flood plain and approximately 19 feet above the stream bottom. Froude numbers for channel flow and overbank flow are 0.88 and 0.97 respectively and represent subcritical tranquil flow ($Fr < 1$).

As shown in Fig. 20, West Bijou Creek had a sinuosity of 1.33 on a scale of 1.0 for straight streams to 2.0 for highly tortuous streams (Schumm, 1963). The meander wavelength (or distance from one point of inflection to the next) was 2100 feet. The meander amplitude was 1500 feet and the channel width to depth ratio (F) varies between 1.2 and 6.6 at different locations. The average channel gradient of Bijou Creek over its 80 mile course is approximately 25 feet per mile. There may have been local changes in gradient in the study area which

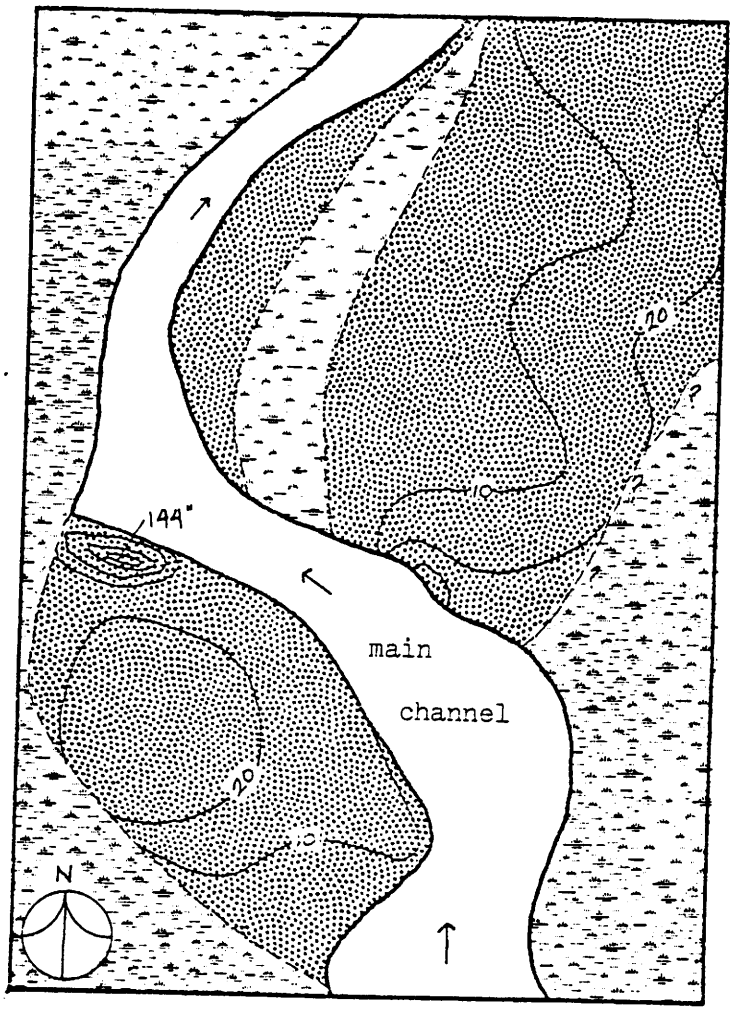

Fig. 20: West Bijou Creek, Colorado

Shaded areas are flood deposits
Contour interval - 10 inches
(modified from McKee et al, 1967)

contributed to the flooding. Channel morphology in ephemeral streams is more closely related to annual flooding events than average annual discharge.

The Santa Rosa Sandstone in the study area consists of fine and medium-grained sandstones with planar horizontal bedding and interlaminated siltstone. Convolute bedding is present. The morphology of the upper Santa Rosa is sheet-like, as well. The total thickness of the Santa Rosa is much thicker than at Bijou Creek because it is made up of intervals typically 1 to 6 feet thick separated by siltstone intervals approximately one half to 2 feet thick. This comparison suggests the upper Santa Rosa Sandstone may be a composite of sheet flood deposits separated by overbank deposits deposited during periods of normal stream flow.

Lake Eyre, Australia

The sand-bed ephemeral streams of the western Lake Eyre basin of Australia (Williams, 1971) also afford examples with striking similarity to the study area. The inland drainage over deeply weathered Mesozoic sediments and mudstones into a large fluctuating interior lake is similar to the drainage of Triassic streams in the Santa Rosa area into a shallow lake straddling the Texas - New Mexico border. Streams in both areas rise in Precambrian crystalline rocks one hundred to two hundred miles from the lake. The climate in the Lake Eyre basin is generally arid but may be subject to winter monsoonal rains of approximately 5 to 14 inches (120 - 350 mm) in one month causing stream flooding. The climate of the Triassic in the study area of

this report was warm and humid with arid cycles and wide seasonal variations possibly caused by monsoonal rains (McGowen et al., 1979) In a study covering 250,000 square kilometers Williams (1971) found that the most common bed forms preserved in channels were large-scale ripples with local longitudinal, transverse, small-scale ripples, and lingoid bars. Minor bed forms were upper flow regime plane beds and flute marks. Lower flow regime prevailed in the area. The streams drain crystalline Precambrian rocks near their headwaters and then traverse wide expanses of deeply weathered Mesozoic sandstones and mudstones. Lithofacies Sp, Sr, Fl, and Fm may be produced in waning flood stages, generating thin fining upward cycles. A thickness of sediment in excess of 1.5 meters (4.5 feet) may be deposited in a single flood. Lithofacies Se represents erosional surfaces with clasts. Sl represents low angle cross beds and dessication features may be present. All of these lithofacies are common in the cores.

A comparison between vertical sequences typical of the Bijou Creek, Lake Eyre, and Newkirk areas is presented in Fig. 21. The Newkirk cores show an oscillation between laminated sandstone and mudstone and another oscillation between these sediments and structureless sandstones. The greater abundance of finer material at Newkirk than at Bijou Creek may be a reflection of study methods. At Bijou Creek, the depth of investigation was only a few feet. At Newkirk, the interval investigated ranged from 50 to 150 feet. Also, the Newkirk Field cores represent ancient facies which may have undergone any number of cycles of erosion and

deposition as compared to the recent environments studied at Bijou Creek and Lake Eyre. Indeed, the Bijou Creek environment may not survive erosion, thus disappearing from the geologic record entirely.

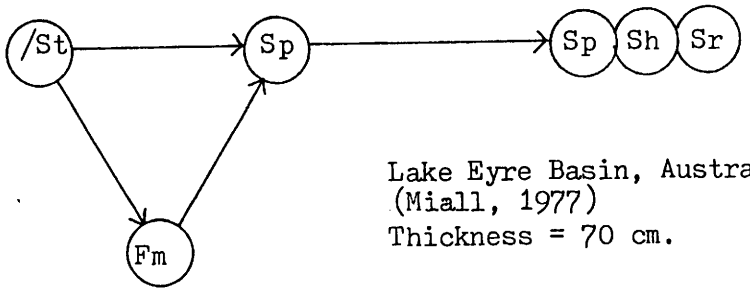

Lake Eyre Basin, Australia
(Miall, 1977)
Thickness = 70 cm.

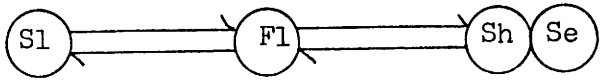

Newkirk Field Cores (Santa Rosa Ss.)

Thickness = 100 cm. - 500 cm.

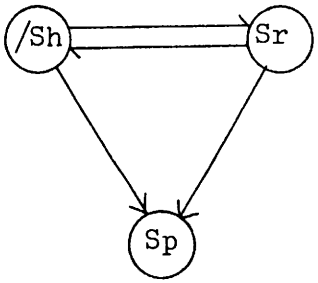

Bijou Creek, Colorado
(Miall, 1977)
Thickness = 15 - 140 cm.

Fig. 21 : Vertical Sequences

/ = major scour surface

→ = upward bed transition

Thickness given is for a typical sequence.

CHAPTER SIX

Paleoclimatology

Paleomagnetic studies show the study area moving from a few degrees south of the equator during the Upper Permian Epoch to approximately 10 degrees north of the equator during the Upper Triassic Epoch (Robinson, 1973). An arid climate during the Permian created thick sequences of evaporites in the Delaware Basin of west Texas (Miller, 1966). The climate then became more humid as suggested by the greater degree of alteration of feldspars in the Triassic Santa Rosa Sandstone (Miller, 1966 and Adams, 1929). Green (1954) suggested the climate alternated between humid and semi-arid. Dubiel (1984), in work on the Triassic Chinle Formation in southeastern Arizona, found lungfish burrows and seed ferns buried by rapid sedimentation in anastomosing stream sediments indicate a monsoonal-type climate with alternating wet and dry seasons. Diastems in Gilbert deltas there were caused by fluctuating lake levels. In the Santa Rosa Formation of Quay County, New Mexico Berkstresser and Mourant (1966) found beds of low-grade coal about 3 inches thick interbedded with beds of black clay containing clam shells. Rainfall was sufficient to maintain swampy areas and associated plant growth which formed these coals. Alternating wet and dry seasons would also provide the variable discharge generally associated with braided streams (Smith, 1970). Climatic studies

using hypothetical models show the study area would lie in an area characterized by seasonal rainfall and subhumid to semiarid conditions, depending on the elevation of the landmass (Robinson, 1973).

Geomorphology

Regional studies indicate that relief on the top of Permian sediments influenced deposition of Triassic sediments. The top of the Artesia Group was partly planed off in response to the reactivation of the Sierra Grande and Pedernal uplifts after deposition of the Permian San Andres Formation and before the onset of Dockum sedimentation (Broadhead, 1984).

The Lower Santa Rosa Sandstone was deposited over the surface of the Artesia Group in two stages. The first stage occurred as alluvial fans or fan deltas (McGowen et al., 1979) spread over the red, fine-grained sandstones and mudstones of the Artesia Group. These were followed by coarse-grained sands of a meandering alluvial system (McGowen et al., 1979) flowing generally southeast. An increase in the level of the Dockum lake centered on the Texas- New Mexico border or local lakes deposited the middle mudstone unit which formed the base upon which the upper Santa Rosa Sandstone was deposited.

The coincidence of thick-sandstone trends with underlying thin areas in the Artesia Group may be evidence of deposition of fluvial Dockum sandstones in broad valleys eroded into the Artesia Group (Broadhead, 1984). A sandstone isolith map of both upper and lower sandstone units shows east and southeast trending sandstone

bodies separated by parallel-trending muddy areas (Broadhead, 1984) which may be the result of valleys formed parallel to the paleoflow direction. Relief of these valleys was probably low because they were cut into easily eroded mudstones and fine-grained sandstones. The features discussed here were derived from studies of the lower sandstone but could apply to the upper sandstone unit as well because it was deposited by streams with the same paleoflow direction over lacustrine mudstones and sandstones of similar composition and properties.

Ablock diagram of this model is shown in Fig. 7. The proposed existence of valleys cut into mudstones implies that some of the mudstone laterally equivalent to the upper sandstone may pre-date the sandstone. Abrupt lateral facies changes are also implied and are observed as shown on Plate 3 between the State No. 11 well and the O'Connell No. 3 well. Lateral facies changes would be expected to be more abrupt perpendicular to paleoflow or from southwest to northeast in this case.

Sands undergo erosion after floods and parts of the upper cycle such as clays and silts deposited by the waning stage of the flood, are lost. The next flood will deposit sands directly on top of this erosional surface resulting in very thick sands after several cycles. Because the intervening erosional cycle is difficult to characterize, the number of flood cycles responsible for a given thickness of sand may only be estimated. Best preservation of sequences would occur in the middle of channels and topographically low areas such as abandoned channels. Miall

(1978) shows flood cycles of sand approximately 3 to 15 feet thick separated by 1 to 3 foot intervals of mud for this type of stream. Williams (1971) noted that the most common bed forms in the Lake Eyre drainage basins were large-scale catenary transverse ripples, transverse and linguoid channel bars, sinuous and lunate small-scale ripples, and lower flow regime plane beds in decreasing order of abundance. The general distribution and degree of dip of cross stratification in the Bijou Creek flood-deposits agrees with those seen in cores of the Newkirk Field. Most strata were horizontal or sub-horizontal with a few dips as high as 25 degrees. Dips greater than this such as the 75 degree dip in the Beryl No.1 or 30 degrees in the Barbara No. 2 probably result from structural or soft sediment deformations.

Miall (1981) notes that the dominant bar in sandy braided rivers is the simple foreset bar with internal planar cross-bedding, a height of 1 to 3 feet, and a length of several hundred meters. Other names for this type of bar are linguoid, transverse, lobate, and chute bars. These mesoform bars form in response to individual dynamic events such as seasonal floods. They may coalesce over a period of years to form macroform compound bars with complex internal structures composed of several types of complex cross-bedding and internal erosional surfaces. The planar crossbedding seen in cores of the Barbara No. 1 well (Fig. 5b) at 785 ft. was probably part of a foreset bar. Longitudinal facies within the braided stream channels should be influenced by the tendency of fine-grained sediments in braided stream channels

to form transverse bars as opposed to longitudinal bars for coarser sediments (Smith, 1970). This results in an increase in the ratio of planar cross-stratification to horizontal stratification when transverse bars are present. Visher (1965) suggests that fluvial sequences may be subdivided into four lithologic units. The lowest basal unit contains poorly sorted coarse clastic detritus transported by traction along the channel bottom, which occasionally occurs in the cores. The zone is occasionally found in the cores. An example is the Joan No. 1 well at 850 feet. The second zone which may be tens of feet thick, is composed of well-sorted festoon or planar cross-bedded sands associated with migrating dunes and sand waves with up to 20 feet of relief. Planar cross-bedded sands may also be associated with transverse bars as discussed above and can be seen in the Jeannie No. 3 at approximately 775 feet below the surface.

Overlying this is horizontally bedded fine sand and silt of Visher's third unit. This zone may range from a few inches to tens of feet thick and may be a product of upper flow regime as it exhibits no ripples or cross-bedding and can be seen in the Joan No. 1 well at 810 ft. to 820 ft. below the surface and in core photos of the Barbara No. 1 from 730 ft. to 738 ft. (Fig. 5a).

The topmost ripple cross-laminated zone is composed of very fine sands, silts, and clays and reaches a maximum development of only a few feet. The sediments are generally deposited outside the fluvial channel except during falling flood stages. This zone

may be seen in the Roberts No. 1 well between 470 ft. and 485 ft. and in the Barbara No. 1 from 742 ft. to 745 ft.. The Roberts No. 1 well appears to be near the bank of the fluvial channel of the upper sand because of its lack of sand.

CONCLUSION

The vertical lithofacies sequences observed in cores of the upper Santa Rosa Sandstone in the Newkirk field indicate that it was deposited in a braided stream environment subject to seasonal flooding similar to the conditions which prevail today at Bijou Creek, Colorado. Oil migrated into permeable laminae of the sandstone before calcite cementation became widespread. Burial of the sequence occurred after calcite had filled the pore space, preventing significant compaction. Fracturing occurred in several different episodes due to compaction, structural movement, and slumping.

Implications for Petroleum Exploration

A viable exploration strategy in the Newkirk area would take the following issues into consideration:

Oil or gas? If oil is sought, where is the gravity of the oil likely to be high enough for it to be produced by conventional methods? This question requires knowledge of geothermal gradients, source material, and maturity. Traps in Pennsylvanian rocks might yield producible oil whereas shallower formations may yield heavy oils similar to that at Newkirk. Locating areas where sediments have been buried to sufficient depths for thermal maturation to occur is very important. A basin study should attempt to locate sediments deposited in environments conducive to the production and preservation of large amounts of organic matter. Geochemical studies of the North

Sea, Syrte Basin (North Africa), and Gippsland Basin (Southeast Australia) (DeMaison, 1984) show that the largest fields consistently occur where organic-rich sediments have been buried to optimum depths for oil generation.

Type of trap? Whether the anticline at Newkirk is due to tectonic movement of the Precambrian horst or due to dissolution of Permian evaporites or both would have major implications for prospective traps above the Permian. Stratigraphic traps formed by pinchouts and unconfomities are other possible exploration targets. If heavy oil is predicted, permeabilities need to be high enough to permit production by conventional means.

Diagenesis? The Glorieta sandstone is medium-grained but appears to be well cemented and no shows were reported in it in the Trans-Pecos Latigo Ranch Unit 1, Well A (S2 T9N R23E) that had shows in shales, sands, and evaporites nearby. This implies that some prospective reservoir rocks may be cemented and form poor reservoirs.

Timing of trap formation and oil migration? Oil migrated into Newkirk field in several episodes which probably began in Jurassic time. Migration pathways through underlying shales were probably fractures which formed by tectonic movement or compaction of sediments. Calcite cementation which began shortly before oil migrated into the trap reduced the porosity slightly in some parts of the sandstone. Oil has leaked from the trap into the Cuervo sandstone (Plate 2, State No. 3 and State No. 5) indicating that fracturing of the intervening mudstones is

allowing oil to escape from the trap. Source rocks for the oil lie directly beneath the field and may be in either Permian or Pennsylvanian formations. This model implies that traps formed after the Jurassic or early Cretaceous may not contain oil or will contain oil which has spilled from earlier traps. Alternately, oil may have been generated during the Cenozoic. Further checking of this model and construction of a similar one for future exploration targets should be done.

Suggestions for Future Work

The depositional environment of the Santa Rosa Sandstone should be further studied by examining cores from the M.A.J.A. Mining Company cores stored with the New Mexico Bureau of Mines Several thousand feet of small diameter cores were taken from the Santa Rosa tar sands deposit in the Santa Rosa Sandstone and could be studied by the methods of Miall (1982) used in this paper. These cores were looked at briefly in preparation of this study and appeared to be composed of the same lithofacies present at the Newkirk field.

Geochemical studies of the oil from Newkirk should be compared with that of the Santa Rosa tar sands. Comparison with geochemical studies of source rocks is needed to establish the origin of the oil. Further geochemical studies of cores from the region are needed to pinpoint potential source rocks and maturity gradients. Reconstruction of depositional environments of potential source beds might yield areas where source rocks are most likely to be organic rich.

Petrographic and dating work should be done on the intrusions at Newkirk and at Santa Rosa. Comparison between the two and basalt flows in the region would yield interesting clues to the tectonic movements in the area.

REFERENCES CITED

Adams, J.E., 1929, Triassic of west Texas: American Association of Petroleum Geologists, Bulletin, v. 13, p. 1045-1055.

Beerbower, J.R., 1978, Cyclothems and cyclic depositional mechanisms in alluvial plain sedimentation: In D.F. Merriam, ed., Cyclic Sedimentation, Geol. Surv. Kansas Bull. 169, p. 31-42.

Berkstresser, C.F., Jr. and Mourant, W.A., 1966, Groundwater resources and geology of Quay County, New Mexico: New Mexico Bur. Mines and Min. Res. Groundwater Report 9, 115 p.

Berner, R.A., 1970, Sedimentary pyrite formation: American Journal of Science, v. 268, p. 1-23.

Broadhead, R.F., 1984, Subsurface petroleum geology of Santa Rosa Sandstone (Triassic), northeast New Mexico: New Mexico Bureau of Mines and Mineral Resources, Circular 193, 23 pp.

Budding, A.J., 1979, Geology and oil characteristics of the Santa Rosa tar sands, Guadalupe County, New Mexico: New Mexico Energy Research and Development Program, Report EMD 78-3316, 19 pp.

Cambell, C.V., 1976, Reservoir geometry of a fluvial sheet sandstone: American Association of Petroleum Geologists, Bulletin, v. 50, no. 7., pp. 1009 - 1020.

Camp, W.H., 1956, Forests of the past and present. In: A world geography of forest resources, edited by Haden-Guest and others, pp. 13-47. Am. Geog. Soc., Spec. Pub. 33, Ronald Press, N.Y.

Cartmill, J.C., 1976, Obscure nature of petroleum migration and entrapment: American Association of Petroleum Geologists, Bulletin, v. 60, p. 1520-1530.

Chepilov, K.R., Ermolova, E.P. and Orlova, N.A., 1959, Epigenetic minerals as indicators of time arrival of petroleum into commercial sand reservoirs. Dokl. Akad. Nauk S.S.S.R. v. 125, p. 1097-1099.

Colbert, E.H. and Gregory, J.T., 1957, Correlation of continental Triassic sediments by vertebrate fossils: Geological Society America, Bulletin, v. 68, pp. 1456-1467.

Core Labs, 1980, Screening tests for thermal oil recovery: Core Labs, Inc., confidential report to Public Lands Exploration, Inc., August 12, 1980.

Darton, N.H., 1921, Geologic structure of parts of New Mexico: U.S. Geol. Survey Bull. 725-E, p. 173-276.

Davis, J.C. and Cocke, J.M., 1972, Interpretation of complex lithologic associations by substitutability analysis: in Cubitt, J.M. and Henley, S., Statistical Analysis in Geology:,1978, Dowden, Hutchinson, & Ross, Inc., Pa., pp. 262-287.

DeMaison, G., 1984, The generative basin concept: In DeMaison, G. and Murris, R.J. eds, Petroleum geochemistry and basin evaluation: American Association of Petroleum Geologists, Memoir 35, pp. 1-14.

Downey, Marlan W., 1984, Evaluating seals for hydrocarbon accumulations: American Association of Petroleum Geologists, Bulletin, v. 68, no. 11, pp. 1752-1763.

Dubiel, R.F., 1984, Evidence for wet paleoenvironments, Upper Triassic Chinle Formtation, Utah: talk given at 37th annual meeting of Rocky Mtn. Section, G.S.A.

Flugel, E., 1982, Microfacies analysis of limestones: Springer-Verlag, New York, p. 42-46.

Folk, R.L., 1961, Petrology of sedimentary rocks: Univ. Texas, Hemphills, Austin, 184 p.

Foster, R.W., Frentress, R.M., and Riese, W.C., 1972, Subsurface geology of east-central New Mexico: New Mexico Geological Society, Special Publication 4, 22 pp.

Geochemical Laboratories, 1983, Geochemical service report on the Trans Pecos Latigo Ranch Block D No. 1 Well: Report to Kriti Exploration Inc., Houston, Texas, 56 p..

Gorman, J.M. and Robeck, R.C., 1946, Geology and asphalt deposits of north-central Guadalupe county, New Mexico: United States Geological Survey, Oil and Gas Investigations Preliminary Map PM 44.

Granata, F.E., 1982, Regional sedimentation of the Late Triassic Dockum Group, West Texas and eastern New Mexico: Unpub. M.S. thesis, Ausin, Univ. Texas, 198 p..

Green, F.E., 1954, The Triassic deposits of northwestern Texas: Unpub. PH.D. dissert., Texas Tech. Coll., Lubbock, 196 pp.

Gustavson, T.C., Finley, R.J. and McGillis, K.A., 1980, Regional dissolution of Permian salt in the Anadarko, Dalhart, and Palo Duro basins of the Texas Panhandle: Bur. of Econ. Geol. of Univ. of Texas Report of Investigations No. 106, 40 pp.

Hahn, A., 1971, Types of magnetic anomalies measured on land and general aspects of their geologic meaning, International Association of Geomagnetism and Aeronomy Bulletin, v. 28, p. 134-143.

Harbaugh, J. and Bonham-Carter, G., 1970, Computer simulation in Geology, Wiley, N.Y., 575 p.

Hubbert, M.K., 1953, Entrapment of petroleum under hydrodynamic conditions: American Association of Petroleum Geologists, Bulletin, v. 37, pp. 1954-2026.

Kelley, V.C., 1972, Triassic rocks of the Santa Rosa Country: New Mexico Geological Society, 23rd Field Conference, Guidebook, pp. .

Keplinger and Associates, 1980, An appraisal of estimated heavy oil recovery via steamflood from the Newkirk East and Newkirk West prospects, Guadalupe County, New Mexico: unpublished report to Public Lands Exploration Company.

Kluth, C.F. and Coney, P.J., 1981, Plate tectonics of the ancestral Rocky Mountains: Geology, v. 9, p. 10-15.

Kottlowski F.E. and Stewart, W.J., 1970, The Wolfcampian Joyita uplift in central New Mexico: New Mexico Bureau of Mines and Mineral Resources, Memoir 23, pt. I, pp. 1-31.

Krumbein, W.C. and Dacey, M.F., 1969, Markov chains and embedded Markov chains in geology: Jour. Internat. Assoc. for Mathematical Geology, v. 1, p. 79-96.

Lazurus, J., Martin, K.W., Culver, C.N., 1983, Geology, hydrology, and ore reserves on a portion of the Solv-Ex corporation tar sand lease near Santa Rosa, New Mexico: Volume I Geology and Hydrology: Unpublished report.

Lee, W.T. 1923, Erosion by solution and fill: U.S. Geological Survey, Bulletin 760-C, p. 107-121.

Lemley, K.R., 1984, Analysis and paleoenvironmental interpretation of the Abo Formation, Abo Canyon area, Valencia, Torrance, and Socorro counties, New Mexico: unpublished Masters thesis, New Mexico Institute of Mining and Technology, 91 pp.

Lupe, R., 1977, Depositional history of the Triassic Santa Rosa Sandstone, Santa Rosa, New Mexico: Geological Society of America, South-Central Section, 11th Annual Meeting, March 17-18, 1977, El Paso, Texas, p. 61.

Martin, David F., 1983, Steamflood pilot in the O'Connell Ranch Field: New Mexico Energy Research and Development Institute, Report NMERDI 2-69-3302, 70 pp.

McDowell, T.E., 1972, Geology of Los Esteros dam site: New Mexico Geological Society, 23rd Field Conference, Guidebook, pp. 178-183.

McGowen, J.H., Granata, G.E., and Seni, S.J., 1979, Depositonal framework of the lower Dockum Group (Triassic), Texas Panhandle: Texas Bur. Econ. Geol., Rept. Inv. 97, 60 pp.

McKee, E.D., Crosby, E.J., and Berryhill, H.L., 1967, Flood deposits, Bijou Creek, Colorado: J. Sed. Petrol., v. 37, p. 829-851.

McKee, E.D., and Weir, G.W., 1953, Terminology for stratification and cross-stratification in sedimentary rocks: Geol. Soc. of America Bull., v. 64, pp. 381-390.

Miall, A.D., 1973, Markov chain analysis applied to an ancient alluvial plain succession, Sedimentology, v. 20, p. 347-364.

_____, 1977, A review of the braided river depositional environment: Earth Science Reviews, v. 13, p. 1-62.

_____, 1978, Lithofacies types and vertical profile models in braided rivers: a summary; in A.D. Miall, ed., Fluvial Sedimentology, Canadian Society of Petroleum Geologists, Memoir 5, p. 597-604.

_____, 1982, Analysis of Fluvial Depositional Systems, American Association of Petroleum Geologists, Education Course Note Series #20, 76 p.

Miller, D.N., 1966, Petrology of Pierce Canyon redbeds, Delaware Basin, Texas and New Mexico: American Association of Petroleum Geologists, Bulletin Bull., v. 50, No. 2, pp. 283-307.

Morgan, A.M., 1941, Solution phenomena in New Mexico: in Symposium on relations of geology to the groundwater problems of the Southwest: American Geophysical Union Transactions, 23rd. annual meeting, pt. I, p. 27-35.

Muskat, M., 1949, Physical principles of oil production: New York, McGraw-Hill Book Co., section 6.3, p. 241-250.

Potter, P.E., Maynard, J.B., and Pryor, W.A., 1980, Sedimentology of shale, Springer-Verlag, New York, p. 55-56.

Roberts, W.H. 1978, Design and function of oil and gas traps. In: Problems of Petroleum Migration, edited by Roberts, W.H. and Cordell, R.J., American Association of Petroleum Geologists, Studies in Geology No. 10., pp. 217-240.

Roberts, J.L., 1970, The intrusion of magma into brittle rocks: in Newall, G. and Rast, N. eds., Mechanism of igneous intrusion, Gallery Press London, p. 327-328.

Robinson, P.L., 1973, Palaeoclimatology and continental drift. In: Implications of Continental drift to the earth sciences, edited by Tarling, D.H. and Runcorn, S.K., Academic Press, London., pp. 451-485.

Schumm, S.A., 1963, Sinuosity of alluvial rivers on the Great Plains: Geological Association of America, Bulletin, v. 74, pp. 1089-1100.

Scott, G., 1979, Newkirk Area heavy oil prospects: report to investors, 26 pp.

Sidwell, R., 1945, Triassic sediments in west Texas and eastern New Mexico: J. Sed. Pet., v. 15, no. 2, pp. 50-54

Sluijk, D. and Nederlof, M.H., 1984, Worldwide geological experience as a systematic basis for prospect appraisal: In DeMaison, G. and Murris, R.J. eds, Petroleum geochemistry and basin evaluation: American Association of Petroleum Geologists, Memoir 35, pp. 15-26.

Smith, N.D., 1970, The braided stream depositional environment: comparison of the Platte River with some Silurian clastic rocks, north-central Appalachians: G.S.A. Bull., v. 81, p. 2993-3014.

Stearns, D.W., 1972, Structural interpretation of fractures associated with the Bonita Fault: New Mexico Geological Society, 23rd Field Conference, Guidebook, pp. 161-64.

Till, R., 1974, Statistical methods for the earth scientist: John Wiley and Sons, New York, pp. 121 - 122.

Tomlinson, C.W., 1916, The origin of red beds: American Journal of Science, v. 24, p. 153-179.

Visher, G.S., 1965, Use of vertical profile in environmental reconstruction: American Association of Petroleum Geologists, Bulletin, v. 49, No. 1, pp. 41-61.

_____, 1969, Grain size distributions and depositional processes: J. Sed. Petr., v. 39, no. 3, p. 1074-1106.

Wash, R., 1982, Low Gravity, high viscosity oil is target of New Mexico's first pilot: Drill Bit, March, pp. 97-99.

Welte, D.H., 1965, Relation between petroleum and source rock: American Association of Petroleum Geologists, Bulletin, v. 49, no. 12, pp.

Williams, G.E., 1971, Flood deposits of the sand-bed ephemeral streams of central Australia: Sedimentology, v. 17, p. 1-40.

Williams, P. F. and Rust, B.R., 1969, The sedimentology of a braided river: J. Sed. Petr., v. 39, no. 2, p. 649-679.

Wolski, J. and Kozushko, P., 1983, General evaluation of the oil sands deposit south of Los Esteros Lake, Santa Rosa, New Mexico: Solv-Ex Corporation unpublished report.

Wright, M.D., 1959, The formation of cross-bedding by a meandering or braided stream: J. Sed. Pet., v. 29, pp. 610-615

APPENDIX A

PERMEABILITY MEASUREMENTS

PROCEDURE:

Cores were obtained from wells in the Newkirk field.

Water permeability was tested by placing a non-extracted core in a Hassler holder, and pressurizing it to an overburden pressure of 550 psi (37.4 atm.) with nitrogen. The holder was placed in a hot water bath and water formulated to match that of the injection water was pumped through it. Acknowledgements and thanks for help in performing these tests go to Joe Triana, Doug Wilson, and Zeke Sherman of the Petroleum Research and Recovery Center.

RESULTS:

TABLE 2

TEMPERATURE Centigrade	VOLUME ml.	TIME sec.	PRESSURE atmos.	VISCOSITY cp.	PERMEABILITY millidarcies
Core: Jeannie No. 3, 737 FT. Fine grained quartz arenite impregnated with oil. (Length=6.055 cm., d=2.533 cm.)					
25	2.3	300	2.42	.8937	3.4
25	2.3	300	2.42	.8937	3.4
58	3.3	300	1.84	.4832	3.5
58	3.7	300	1.84	.4832	3.9
66	7.3	600	1.90	.4293	3.3
69	3.6	300	1.9	.4117	3.12
25	3.5	300	2.79	.8937	4.5
Core: State #9, 469 FT. Medium grained quartz arenite with a show of oil. (Length=6.467 cm., d=2.533 cm.)					
25	12.0	30	0.68	.8937	675.0

Formula for calculating permeability to water:

$$k \text{ (darcies)} = \frac{[\text{Vol/Time}] * [\text{viscosity}] * [\text{length}]}{[\text{area}]\,[\text{pressure}]}$$

AIR PERMEABILITY:

Air permeabilties were measured by placing the extracted core in the Hassler holder under overburden pressure as before. Nitrogen pressure was measured with a mercury manometer and volume displaced was measured with a soap bubble tube.

PRESSURE (mm of mercury) LEFT	RIGHT	Time (sec.)	VOLUME (ml.)
Core: Jeannie No. 3, 737 ft. (extracted)			
40	60	18.9	20
37	57	20.13	20
50	70	15.42	20
50	70	15.05	20
50	70	15.9	20
50	70	15.27	20
Mean dP cm = 11.233		16.778	20

The formula used to calculate air permeability was:

$$k\ (\text{darcies}) = \frac{[\text{length}]\ [4.446*10^{6}]}{[\text{time}]\ [\text{pressleft} + \text{pressright}]\ [\text{area}]\ [130+P]}$$

k (md) = 200.67 md

JOINTING

The orientation of joints seen on the surface of the Cuervo Sandstone is shown below. Joints in the subsurface would impart a preferential direction to flow of fluids because of greater permeability along them. The following readings were taken at widely spaced locations in the field area:

Joint	Direction		
1	N45W	3	N50W
2	N50W	4	N50W

APPENDIX B

The following lists show information about wells drilled in the area by PLEI and Rio Petro. The first shows the following:

CODE: a code assigned to each well as follows:

BA	BARBARA	JE	Jeannie
BE	Beryl	JO	Joan
BR	Brenda	KA	Karen
CI	Cindy	OC	O'Connell
DA	Daisy	RO	Roberts
ST	State	SA	Samedan State
SX	State water well		

SEC: Section TWP: Township RANG: Range LOCATION: survey

GROU LEVL: ground level

TD: Total depth (ft.) TD ABS: Total depth in feet above sea level

TOP CORE: Depth to top of core (ft.) TC ABS: Top of core above sea level

BOT CORE: Depth to bottom of core BC ABS: (above sea level)

CORE: S = stored in Socorro, NM. M = stored in Midland, Tx.

SAMP: S = drilling samples available

TYPE LOGS AVAL: types of logs available:

SL = Sample log
PP = Porosity & Permeability from Core Labs
CNL = Compensated Neutron log
KPHI = Permeability and porosity in detail from Core Labs

Table 4 shows wells drilled in the area by Humble (Exxon) and other companies. Most of these wells were drilled in the 1960's. Abbreviations are the same as above.

HU = Humble core test

TABLE 3: List of P.L.E.I. and Rio Petro wells

CODE	SEC	TWP	RANG	LOCATION	GL RE OV UL	TD	TD ABS	TC COPRE	TC ABS	BC COTRE	BC ABS	COREE	SAMP	TLYOPGES	AVAL	
BA1	17	11N	26E	2030 SL 2030 EL	4775	937	3838	739	4036	859	3916	S	S	SL		CNL
BA2	17	11N	26E	660 SL 660 EL	4768	993	3775	680	4095	912	3863	S	S	SL	PP	
BE1	8	11N	26E	1650 SL 1980 WL	4762	1050	2813	762	4000	934	3828	M	S	SL	PP	
BE2	8	11N	26E	1650 SL 990 EL	4759	975	2853	815	3944	921	3838	M	-	SL	PP	
BE3												-	-			
BE4												M	-			
BR1	18	11N	26E	660 NL 1980 WL	4785	815	3023	650	4135	720	4065	M	S	SL	PP	CNL
CI1	16	11N	26E	1650 NL 980 WL				751		824		M	S			
DA1	10	11N	25E	1650 SL 2310 WL				338		456		S	-		PP	
JE1	17	11N	26E	800 NL 1980 WL	4746	840	3906	694	4091	753	4032	M	S	SL	PP	CNL
JE2	17	11N	26E	1980 NL 660 WL	4771	899	3872	708	4063	796	3975	S	-	SL	PP	
JE3	17	11N	26E	800 NL 2310 WL	4771	836	3935	701	4070	825	3946	M	-		PP	CNL
JE4	17	11N	26E	635 NL 2145 WL	4763	764	3182					-	-			CNL
JE5	17	11N	26E	800 NL 2145 WL	4759	829	3930					-	-			CNL
JE6	17	11N	26E	965 NL 2145 WL	4753	758	3995					-	-			
JO1	16	11N	26E	660 NL 990 WL	4758	900	3858	751	4007	855	3903	M	-	SL	PP	
JO2	16	11N	26E	660 NL 2310 WL	4738	925	3813	781	3957	847	3891	M	S	SL	PP	
KA1	8	11N	26E	330 SL 2310 WL	4770	866	3025	762	4008	863	3907	M	S	SL	PP	CNL
KA2	17	11N	26E	990 NL 660 EL	4802	943	3859	803	3999	887	3915	S	-	SL	PP	
KA3	18	11N	26E	1800 SL 1980 EL	4825	900	3925	730	4095	812	4013	M	S	SL	PP	
KA4	16	11N	26E	2310 NL 330 WL	4766	900	3866	750	4016	850	3916	M	S	SL		CNL
KW1												-	-			
OC1	10	11N	25E	330 SL 2310 WL	4518	443	4075	93	4425	430	4088	S	-	SL		
OC2												-	-			
OC3	14	11N	25E	500 NL 660 WL	4755	813	3942					-	-	SL		
OC4								319		439		-	-		PP	
OC5	10	11N	25E	330 SL 1650 EL				371		461		-	S		PP	
OC6	10	11N	25E	500 SL 990 WL	4480	500	3980					-	S	SL		
OC7	10	11N	25E	330 SL 1650 EL	4555	550	4005					-	-	SL		
RO1	10	11N	25E	330 SL 500 EL	4592	695	3897	457	4135	530	4062	S	-	SL		CNL
SA1	16	11N	25E	330 NL 330 EL	4484	500	3984	378	4106	387	4097	S	-	SL		CNL
SA2	16	11N	25E	990 NL 330 EL	4488	440	4048	267	4221	316	4172	-	-	SL		
ST1	15	11N	25E	540 NL 560 EL								-	-			
ST2	15	11N	25E	500 NL 1650 EL	4551	456	4095	375	4176	456	4095	M	-	SL		CNL
ST3	15	11N	25E	500 NL 2310 WL	4516	429	4087	335	4181	413	4103	M	-	SL		CNL
ST4	15	11N	25E	1650 NL 500 EL	4581	600	3981	408	4173	433	4148	-	-	SL		CNL
ST5	15	11N	25E	330 NL 990 WL	4495	454	4041	56	4439	454	4207	S	-	SL		CNL
ST6												-	-			
ST7	15	11N	25E	990 NL 990 WL	4515	445	4070	88	4427	394	4121	S	-	SL		
ST8	15	11N	25E	990 NL 990 EL	4559	500	4059	321	4238	432	4127	S	-	SL	PP	
ST9	15	11N	25E	2310 SL 990 EL				351		481		S	-		PP	
ST10	15	11N	25E	352 NL 665 EL	4579	515	4064	416		476		M	S	SL	PP	CNL KPHI
ST11	15	11N	25E	353 NL 672 EL		510		406		475		M	S	SL	PP	CNL KPHI
ST12	15	11N	25E	519 NL 832 EL	4572	510	4062	398		469		M	S	SL	PP	CNL KPHI
ST13	10	11N	25E	519 NL 506 EL	4582	492	4090					-	-			CNL
ST14	10	11N	25E	35 NL 672 EL	4578	478	4100					-	-			CNL
ST15	15	11N	25E	330 SL 1650 EL	4574	415	4159	305	4269	416	4158	M	-	SL	PP	
SX3	15	11N	25E	480 NL 2310 WL	4516	122	4394	87	4429	122	4394	-	-	SL		
SX7	15	11N	25E	20 FT FROM S3	4515	66	4449					S	-	SL		
ST16	15	11N	25E	810SL 1650EL	4585	1186						S		SL		CNL

TABLE 4

Humble & other wells

CODE	SEC	TWP	RANG	LOCATION	GL	TD	TYPE LOGS
HU225	5	6N	25E	1980 FNL 1980 FWL	4542	1018	GR
HU413	3	10N	22E	660 FSL 660 FWL	4882	740	SP Res
HUMONS1	1	11N	25E	1980 FNL 1980 FEL	4610	910	GR-Acoustic
HU447	7	11N	25E	660 FSL 660 FEL	4775	1305	" "
HU339	9	11N	25E	1910 FEL 2210 FSL	4482	848	" "
HU1410	10	11N	25E	990 FNL 660 FEL	4556	680	" "
HU2311	11	11N	25E	2210 FNL 2210 FEL	4684	848	SP - Induc
HU1113	13	11N	25E		4830	1160	" "
HU214	14	11N	25E	1980 FNL & FWL	4855	870	" "
HU1215	15	11N	25E	990 FNL 1980 FWL	4513	380	Sonic - GR
HU1415	15	11N	25E	660 FNL 660 FEL	4564	482	GR - CNL
HU4115	15	11N	25E	500 FSL 500 FWL	4509	820	GR
HU1416	16	11N	25E	730 FNL & FEL	4492	550	SP - Ind
HU4415	15	11N	25E	660 FSL & 980 FEL	4576	458	" "
HU1423	23	11N	25E		4942	1155	GR
HU1228	28	11N	25E	660 FNL 1980 FWL	4562	1095	SP - Ind
HU437	7	11N	26E	660 FSL 1980 FEL	4703	806	GR - Sonic
HU3317	17	11N	26E	1980 FSL 1980 FEL	4772	880	SP - Ind
HU3318	18	11N	26E	1980 FSL & FEL	4119	870	GR - Sonic
HU2120	20	11N	26E	1980 FNL 660 FWL	4801	870	" "
HU3413	13	14N	22E	1980 FSL 660 FEL	5172	920	GR - Sonic
HU1435	35	15N	22E	506 FNL 506 FEL	4820	484	" "
HUNEAFUS	24	11N	25E				
HW1	4	11N	25E			1235	GR
1HIGGINS	28	11N	25E				
HANKINS	15	11N	25E				

APPENDIX C

Genesis of Clays and their Effect on Steamflood Performance in the Santa Rosa Formation Guadalupe County, NM

by

Curtis McKallip Jr.

December 1983

ABSTRACT

The O'Connell Ranch steamflood project in the Triassic Santa Rosa Formation of Eastern New Mexico injects steam into a heavy oil sandstone reservoir.

Samples taken from oil well cores were examined using X-Ray diffraction and Scanning Electron Microscope techniques.

The adjacent siltstones and shales contain kaolinite, illite, and smectites or mixed layer clays. These clays exist as an overlapping, interleaved mass of flakes as identified by SEM study in contrast to the highly ordered crystalline kaolinite in the sandstone.

Previous studies indicate that kaolinite containing sandstones are sensitive to hot water, brine, and NaOH solutions. The injection of steam may interact with kaolinite and illite in the formation to reduce permeability by dispersal of clays.

INTRODUCTION

The Triassic Santa Rosa Formation in Guadalupe County, New Mexico, consists of the Upper Sand, Middle Shale, and Lower Sand members. The Upper Sand is separated from the Lower sand by a bed of grey to red siltstone (Fig. 1; Fig. 2).

Several deposits of heavy oil occur in the Upper Sand. The deposit at Santa Rosa is estimated to contain approximately 90 million barrels of oil (Budding, 1979) and the one at Newkirk, which is currently being steamflooded, 33 million barrels (Martin, 1983). The Petroleum Research and Recovery Center at Socorro, New Mexico is currently consulting on the engineering of the project. The steamflood has produced less than 100 barrels of oil since its inception two years ago. The limited success of the project can be related to several factors. The pay sand (40 ft.) thickness is insufficient to prevent heat loss, porosity (20%) and steam permeability (<60 millidarcies) restrict the flow of heavy oil (17 degrees API), and mechanical difficulties have led to a loss of consistent heat input. Low injection pressures must be maintained in order to avoid fracturing the formation (Keplinger, 1980). None of the problems of the steamflood are directly attributable to the clays in the formation. However, they are a primary factor in reducing the permeability of the reservoir and this inhibits steamflood performance.

COMPOSITE STRATIGRAPHIC SECTION

GUADALUPE CTY., NM.

FIG. 1

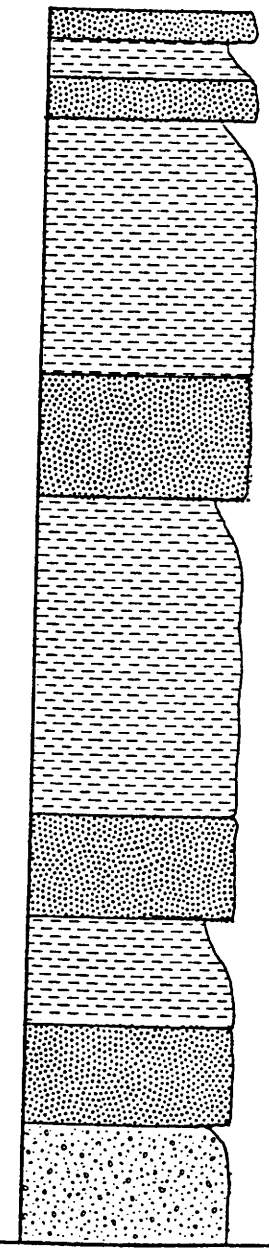

		FEET	LITHOLOGY	ENVIRONMENT (Lupe, 1977)
Triassic	Cuervo Ss.	20	MED GRAINED SS.	
		30	RED-BROWN MUDSTONE	
		30	MED-FINE SS.	
	Lower Chinle	200	RED-BROWN FINE SS.	
		100	MED-FINE Grained Ss. w/ Grey Shale	
		250	Red-Brown MUDSTONE AND Grey Shale	
Perm.	Artesia Santa Rosa Lower Shale Upper	80	Brn-Grey v. fine-fine Ss.	Fan delta
		80	Red-Grey mudstone	Prodelta Lacustrine
		80-160	Brn-Grey fine Ss.	Coarse grained meanderbelt ALLUVIAL FAN
			Red-orange Ss.	

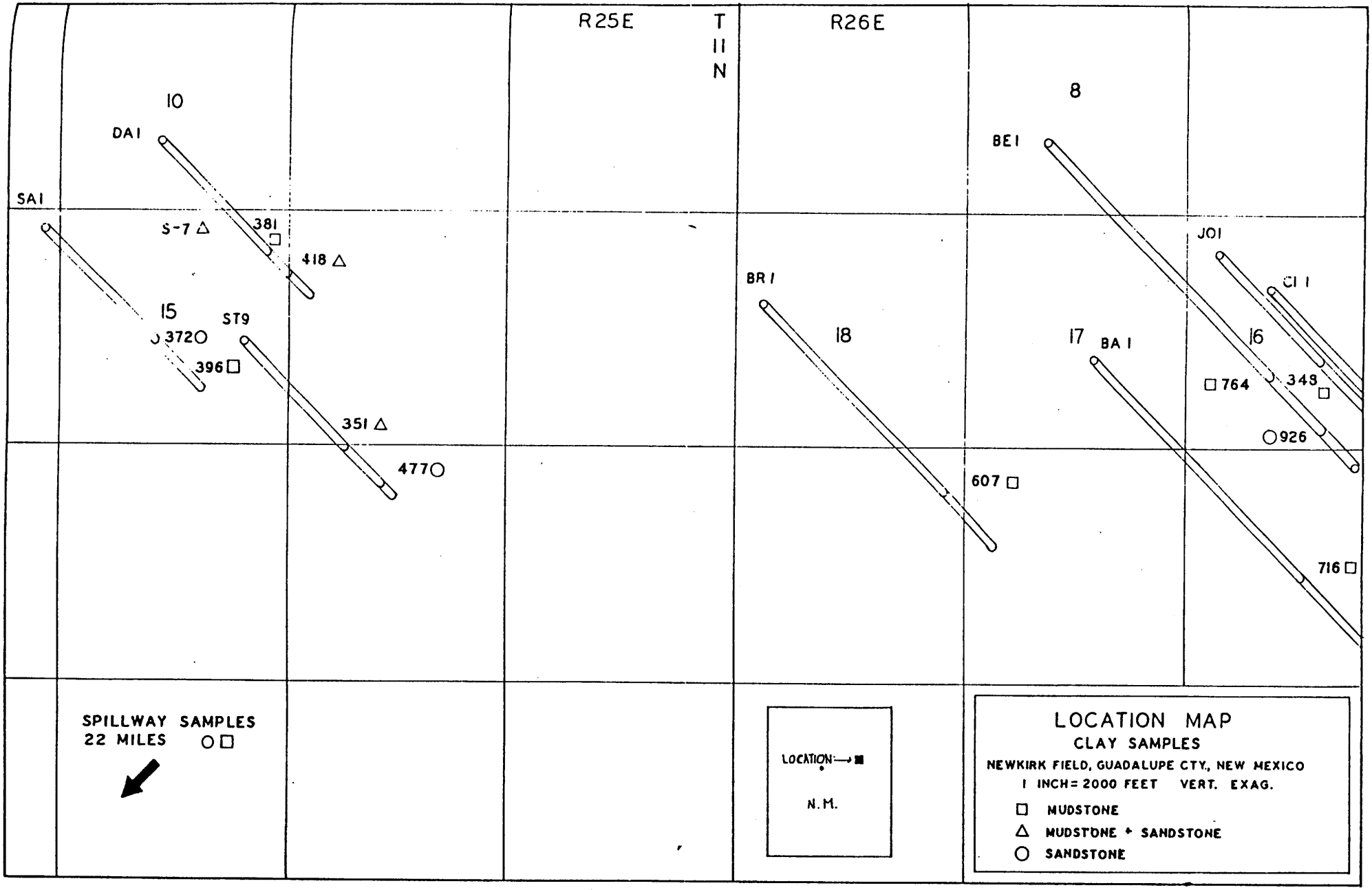
R25E
T
11
N
R26E
10
DA1
SA1
S-7 △
381 □
418 △
15
ST9
3720
396 □
351 △
4770
8
BE1
JO1
CI 1
BR 1
18
17
BA 1
16
□ 764
348 □
926
607 □
716 □
SPILLWAY SAMPLES
22 MILES ○ □
LOCATION
N.M.
LOCATION MAP
CLAY SAMPLES
NEWKIRK FIELD, GUADALUPE CTY., NEW MEXICO
1 INCH = 2000 FEET VERT. EXAG.
□ MUDSTONE
△ MUDSTONE + SANDSTONE
○ SANDSTONE

FIG. 2

PURPOSE

The purpose of this study is to determine the clay minerals present and how they are related to the pore space. Are they lining pore throats? Are they intergranular? Are expandable clays present? How are the clays affected by the heat of the steam (155° C at 250 psi)? Would there be porosity and permeability trends that could be predicted by a model of the depostional environment (Wilson, 1982)? As part of the answer to this question, the possible origins of the clays will be examined.

PROCEDURE

SAMPLE PREPARATION:

Sampling was planned to encompass the Santa Rosa Formation laterally across the steamflood project area and vertically within the area. Several samples from an exposure of the Santa Rosa at the Santa Rosa Dam Spillway 22 miles to the southwest were also run as well as one sample from the overlying Cuervo Sandstone at the steamflood site. One of the samples from the Santa Rosa spillway was highly oil impregnated.

A description of the samples is given below in Table 1. The descriptions were made using Folk's 1966 classification system. For the purposes of this experiment, the samples were divided into three dominant lithologies which reflect different energy

levels in the depositional environment. The squares (□) represent low energy mudstones and siltstones. The circles (○) represent higher-energy generally well sorted, calcite cemented, fine to medium grained sandstones. The triangles (△) represent a transistion between the first two. These rocks are grey siltstones with laminations of brown fine grained sandstone.

The numbers beside the samples from the Newkirk Field designate depths in feet below the surface. The variance in surface elevation of the wells was less than 50 feet so these depths are roughly correlatable. These samples were taken from cores which had been removed from the ground for approximately one year and stored. Formation water and volatiles had evaporated from the core soon after removal from the ground.

Three samples were taken from cuttings and their parent lithology was estimated by comparison with intact core. The other samples were taken from surface exposures and had been subject to long term weathering. However, results showed that exposure had not changed the clays under study significantly.

Table 1: Samples Analyzed

Sample #	Symbol	Description of Rock (Location)
BA1-716		Grey calclitharenite (Newkirk Fld.)
BE1-764		Grey pyritic siltstone (Newkirk Fld.)
BE1-926		Grey gilsonitic quartz arenite (Newkirk Fld.)
BR1-607		Mudstone (well cuttings) (Newkirk Fld.)
CI1-480		Mudstone (well cuttings) (Newkirk Fld.)
DA1-381		Grey micaceous siltstone (Newkirk Fld.)
DA1-418		Finely laminated sandstone and siltstone (NKF)
FS 2-7		Red hematitic sublitharenite (Cuervo Ss.)
JO1-348		Mudstone (well cuttings) (Newkirk Fld.)
SA1-394		Grey calclitharenite (Newkirk Fld.)
SA1-396		Red calcareous mudstone (Newkirk Fld.)
SA1-372		Gilsonite-bearing sublitharenite (Newkirk Fld.)
SRS-1		Red and Grey micaceous mudstone (S.R. dam)
SRS-oil		Fine grained sublitharenite (S.R. dam)
ST9-351		Micaceous fine laminated grey brown siltstone and sandstone (Newkirk Field)
ST9-459		Grey fine-medium grained sublitharenite (NKF)

Samples were disaggregated and crushed with a mortar and pestle for about 5 minutes. They were then placed in 250 ml beakers filled with deionized water and allowed to settle for approximately 15-20 minutes. If flocculation occurred and there was insufficient clay in suspension to sediment a slide, the sample was washed again. If the second treatment failed to produce the desired suspension, the sample was treated with 6 drops of "Calgon". This universally produced the suspension desired. The oil in some of the samples did not appear to inhibit suspension of the clays - possibly because it had dried out for over a year.

Samples from the upper 1 cm of solution were dropped onto glass slides and allowed to dry for 24 hours.

EXAMINATION:

Diffractograms of the slides were made with Ni filtered, Cu radiation (wavelength = 1.542 angstroms). The 2 theta values were converted to angstroms for clay identification (Figs. 3-6). Two theta values are shown in parentheses in this paper.

Several slides were treated with ethylene glycol for 24 hours and two porcelain plates were made and heated to 325 degrees Centigrade for 1 hour and then rerun.

Samples of freshly broken rock were sputter coated with gold for 3 minutes at a pressure of 50 microns in preparation for use with the scanning electron microscope. The samples were then examined and photographed at magnifications ranging from 400 to 2500 times. Higher magnifications were tried but generally had poor resolution.

Many of the samples contained heavy oil. These samples were tested under a vacuum to determine the release of volatiles which might be potentially harmful to the Scanning Electron Microscope (SEM). However, the samples had been exposed to the atmosphere long enough for volatiles to have been driven off. To check the effects of cleaning the samples on the clays, a sample of sandstone which had been Soxlet extracted using toluene for approximately 10 hours was examined by SEM. Almost all the clay had been washed from the sample (as determined by comparison with an identical, non-extracted sample) with the exception of a few scattered

kaolinite plates. A call to CORE LABS indicated that they use a solution of 90% methylene chloride and 10% methanol for extraction (Scott, 1983). Due to the highly dangerous nature of methylene chloride and the ability to use oil impregnated samples in this particular case, this method was not tried.

RESULTS OF X-RAY DIFFRACTION STUDY

KAOLINITE

The most obvious peaks on the diffractograms of all three lithologies belonged to kaolinite. No attempt was made to differentiate kaolinite from dickite which has been noted in sedimentary rocks (Hemingway, and Brindley, 1948). However, the appearance of the kaolinite differed from the dickite pictured in SEM photos (Keller, 1976) although this,too, is not diagnostic.

Kaolinite appeared as two peaks: 7.15 A (12.4 2θ), and 3.58 A (24.9 2θ). The abundance and degree of crystallinity of kaolinite both affect the height of the peaks.

A comprehensive quantitative analysis was not undertaken. Instead, a semi-quantitative method of comparison was used. Peak heights were normalized to an X-Ray count scale of 2000. Therefore a peak from a run done on a scale of 1000 was considered to be twice as high as it would have been if it had been run on a scale of 2000 and a peak from a run done on a scale of 4000 was considered to be half as high as it should have been.

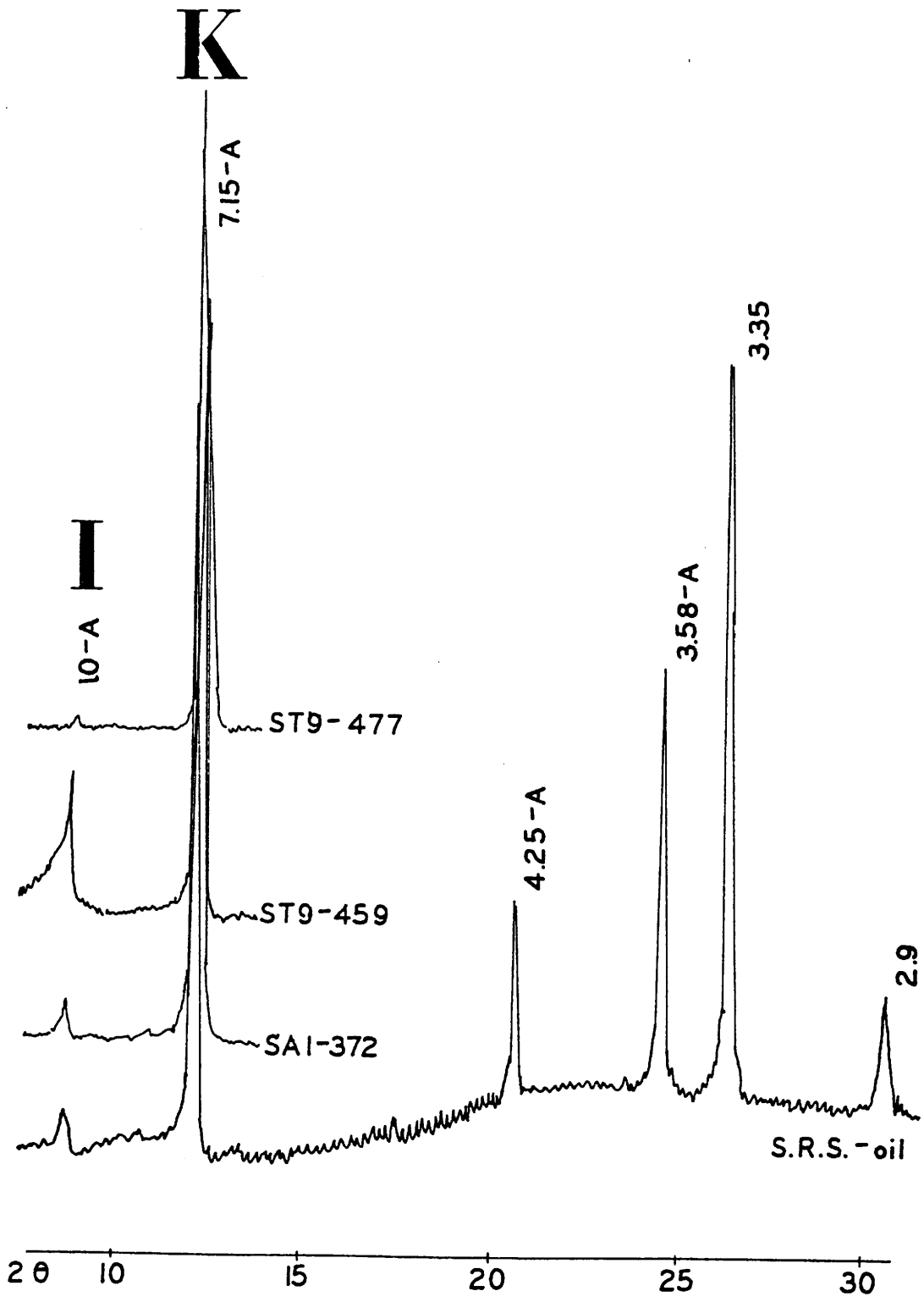

SANDSTONES ◯

FIG. 3

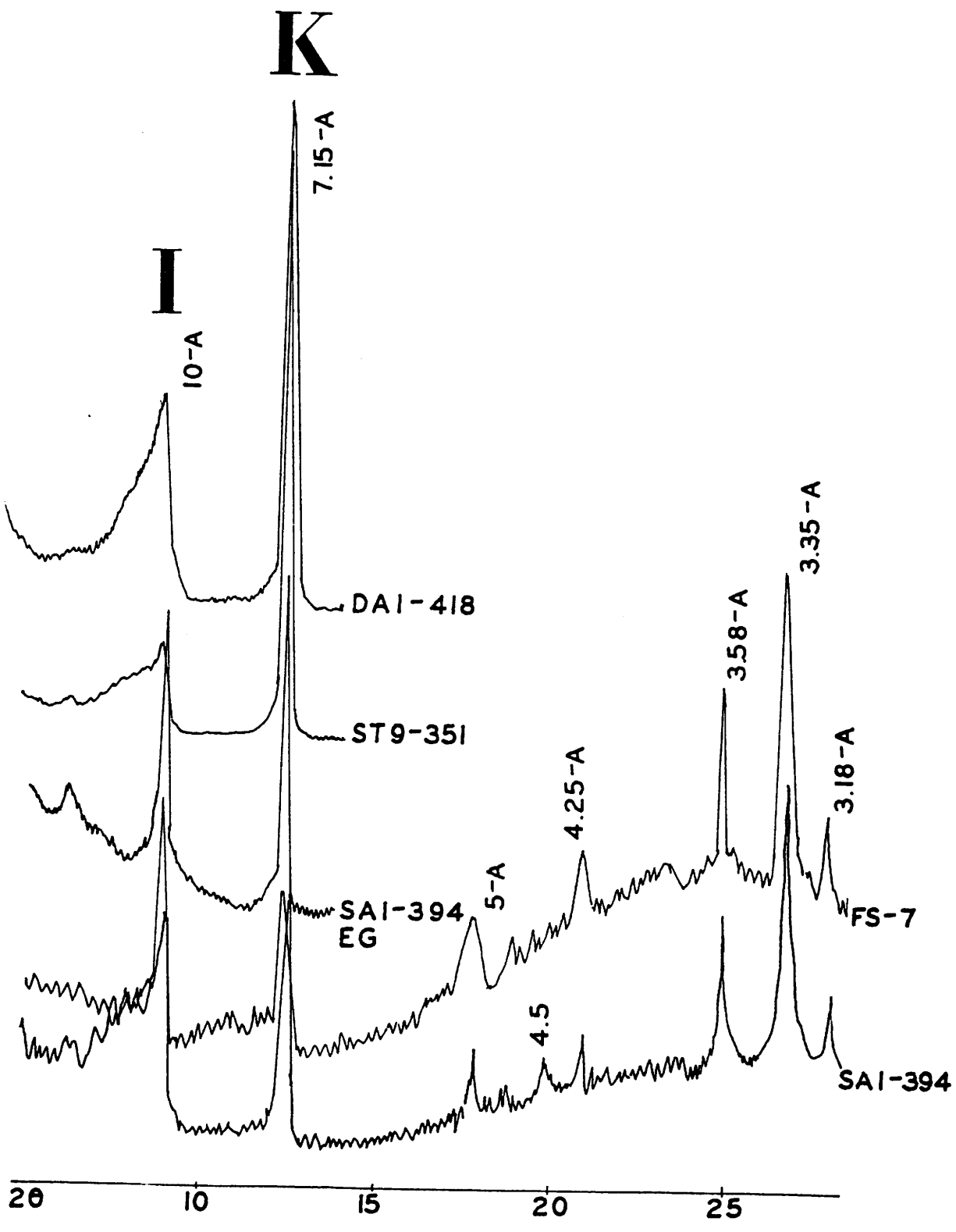

MUDSTONE AND SANDSTONE △

FIG. 4

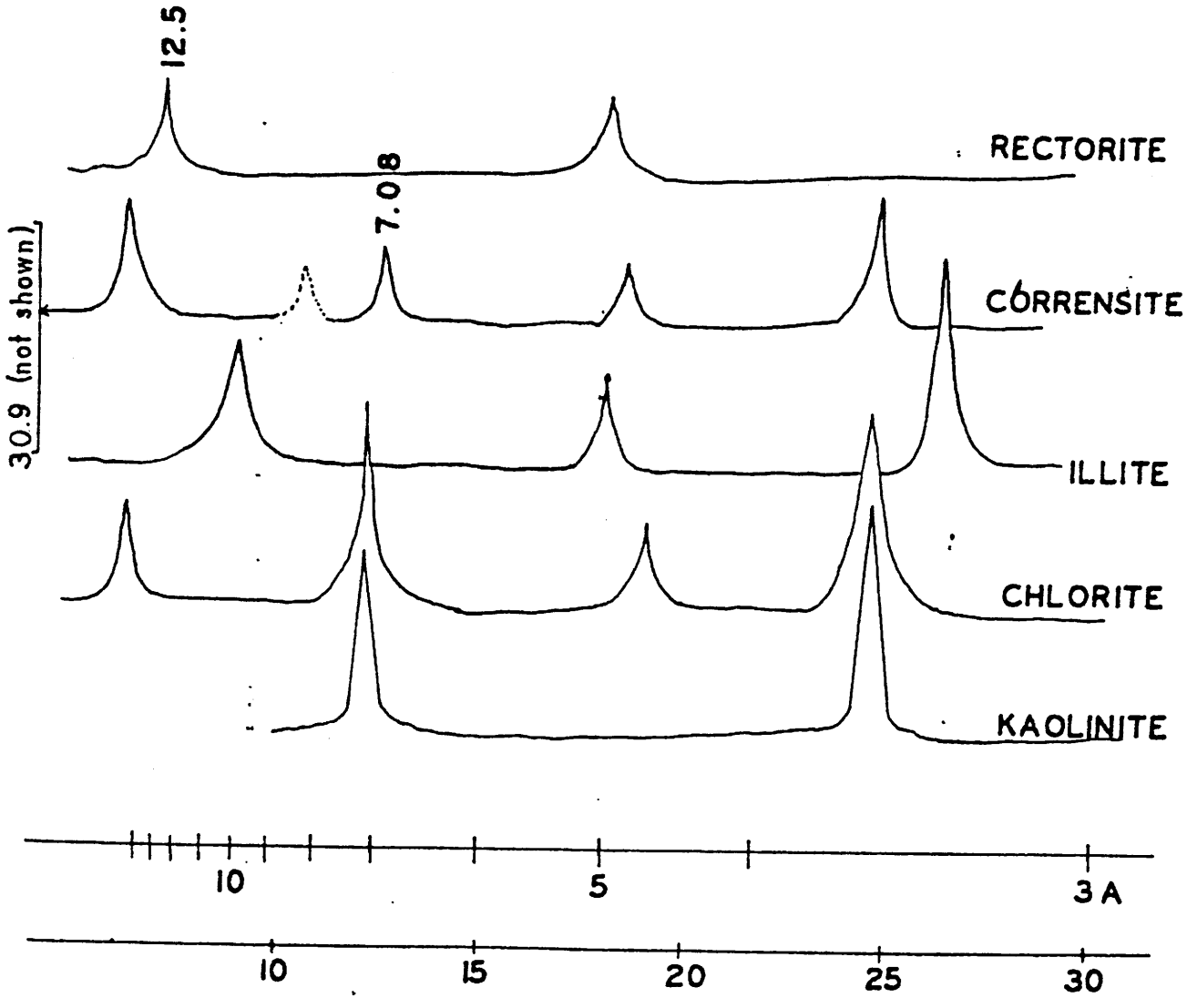

CHARACTERISTIC CURVES

FIG. 5

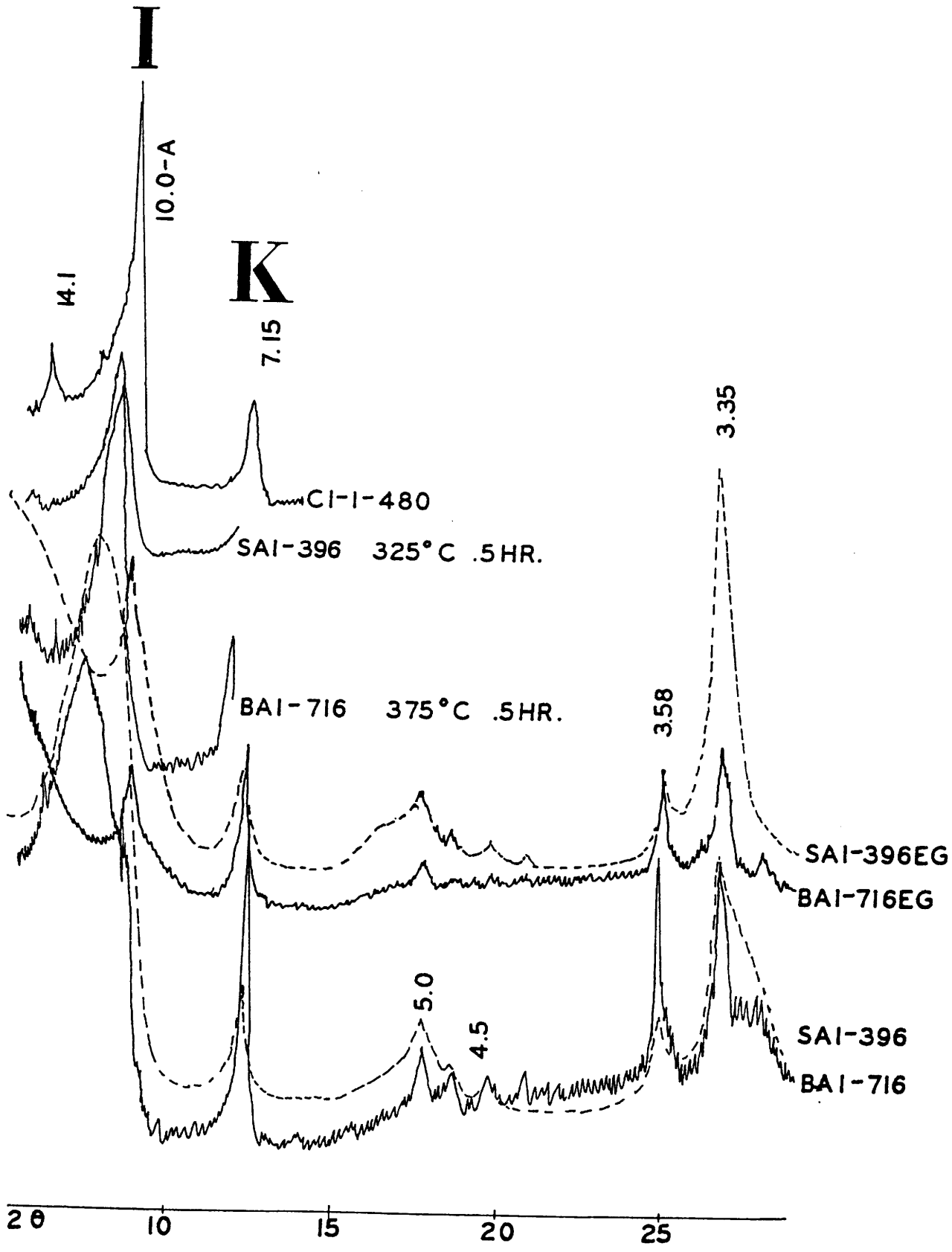

MUDSTONES ☐

FIG. 6

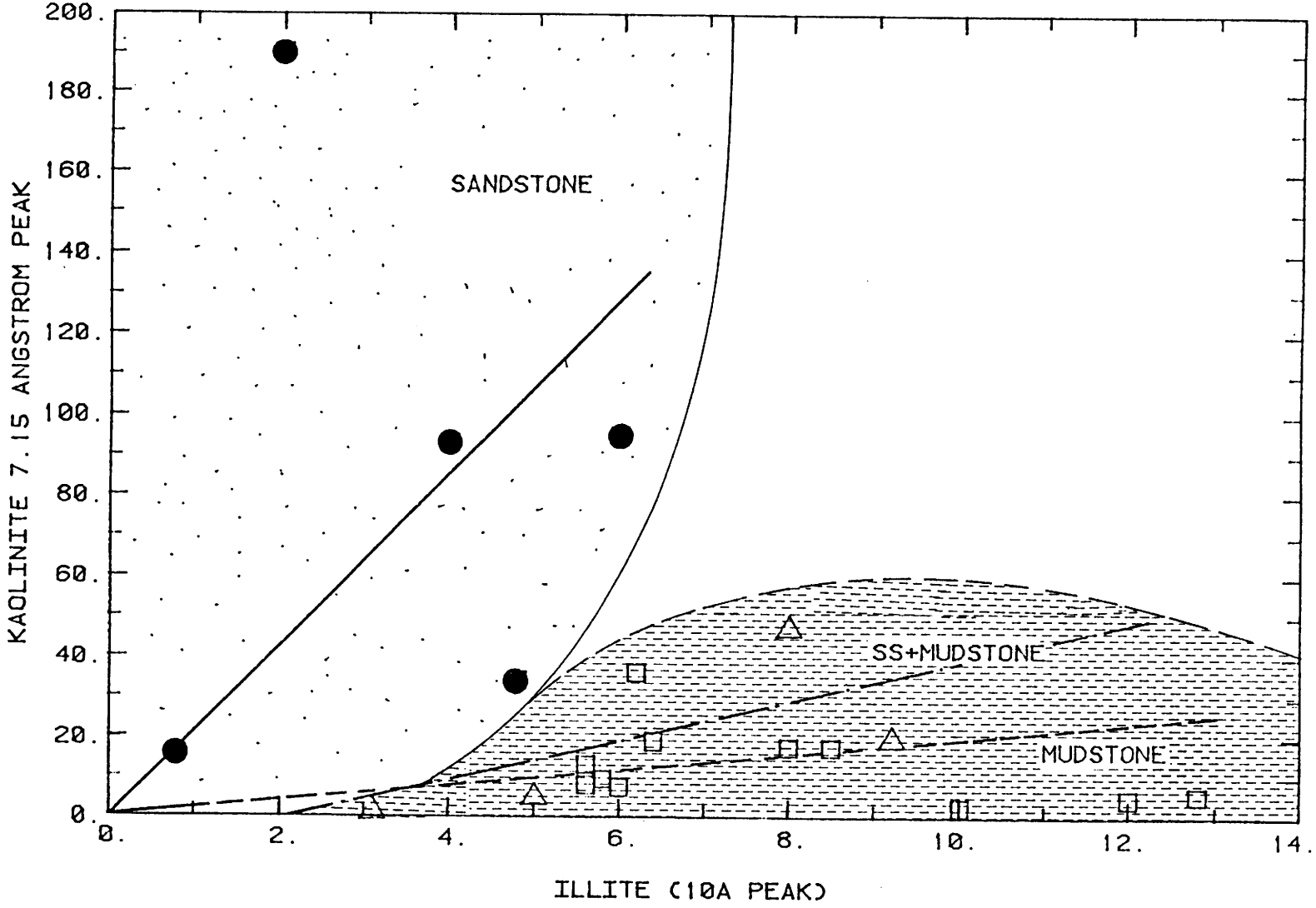

KAOLINITE V. ILLITE

FIG. 7

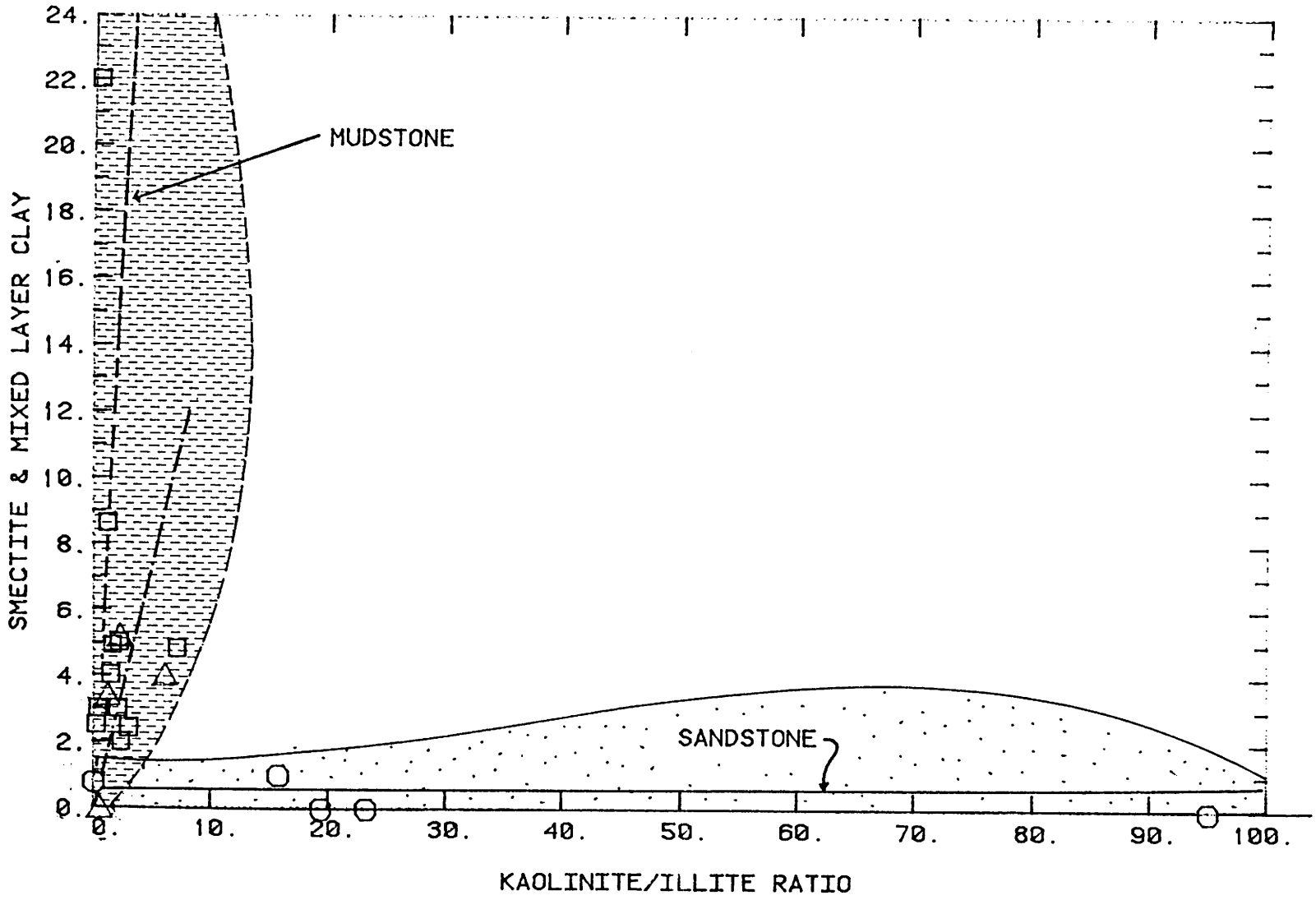

KAOLINITE/ILLITE RATIO V. SMECTITE & ML CLAYS

FIG. 8

Some of the sandstones had to be run on a scale of 20,000 due to the highly crystallized nature of the kaolin.

This method is similar to that used by Esquevin (1969) to analyze the crystallinity of illite. By measuring the intensity of the 5 A and 10 A peaks (I(002)/I(001)) he showed that a contour of the ratio of peak heights was related to specific episodes of diagenetic evolution.

The peaks in Figs. 3-6 are a mixture of scales and represent a sample of the original data of this project.

Percentage compositions were not calculated because the peak heights were so greatly affected by crystallinity and would distort calculated compositions. The area under the curve method would give more representative compositions.

The marked contrast between the kaolinite peaks in the sandstones (very sharp) and mudstones (diffuse) is a caused by their higher crystallinity and greater percentage abundance (very little illite) in the sandstones.

Kaolinite may be detrital, but is generally the result of erosion of weathering profiles in leached acidic environments in hot and humid climates. Basic K-rich interstitial solutions can cause illitization of kaolinite during diagenesis (Chepilov, 1959).

ILLITES

The illite peaks at 10 A (8.8 2θ) and 5 A (17.8 2θ) showed in various intensities on all of the diffractograms. Some of the illite peak intensity may be due to illites in mixed layer clays as will be discussed later.

Fig. 7 shows the normalized peak heights of illite (10 A) plotted against kaolinite (7.15 A). These peaks were chosen as representative of the amount of and crystallinity of these particular clays. Lines were drawn for the three lithologies which seem to best fit the data. An attempt was made to formally regress the data but the results seemed relatively less meaningful than an educated guess at best fit. Also, the degree of precision of the data did not warrant formal mathematical treatment. Contours were drawn to represent the field of variation of each lithology after the method of Esquivin (1969).

This plot suggests that kaolinite and illite may have existed together as a detrital mixture in the mudstones. Later solutions transported kaolinite from these mudstones or another source into the sandstones.

Illites exist as three common polymorphs. The 1Md form develops during weathering and transport. A 1M illite is formed under varying conditions. A 2M illite is found in micas of the metamorphic zones or in detrital illites from continents where the cold and dry climate was not favourable to hydrolysis.

No attempt to determine the polymorphic type was made as it is difficult in the presence of other minerals. The above indicates it should be 1Md.

SMECTITES

The presence of smectites on the diffractograms is indicated by peaks at 12.0 A (7) and 4.5 A (19.8). The 12.0 A peak expands on glycolation to approximately 17.8 A (5.2) in a very similar manner to an example of a random mixed layer 14 A montmorillonite - illite investigated by Thorez (1975). Heating to 375 C. for 30 minutes collapses the peak back to close to 10 A.

Figure 8 shows that smectite is associated with illite (low kaolinite/illite ratio) in the mudstones and is absent in the sandstones.

Dunoyer de Segonzac (1970) gives the following table describing the evolution of smectite into illite during burial diagenesis in Logbaba boreholes:

Table 4:Smectite-->Mixed layers-->Illite

Depth (m)	Type	d(001) no tr.	d(001) E.G.	d(001) Heated
915	M	14	17	10
1350	I-M	11.5	17	10
1497	I-M	12	14	10
2041	I-M	11	12.5	10
3423	I-M	10.5	12	10
3586	I-M	10.5	12 broad	10
4019	I	10	10	10

There is a similarity in the behavior of the test run at 1350 meters (4050 feet) and the behavior of the smectites from the mudstones at Santa Rosa.

The environmental significance of I-M mixed layer clays lies in the fact that they represent the fixation of K+ by smectites in a potassium-rich environment of early diagenesis.

The work of several authors indicates that the zone of stability of mixed layers to be between 80-200 degrees C.

CHLORITE

The presence of small peaks at 14.1 A (6.2) and 4.7 A (18.7) indicate that chlorite may be present in small quantities. Chlorite is difficult to distinguish in the presence of kaolinite because its very strong 7 A peak is obscured by that of kaolinite (001).

The chlorite may be detrital or it may be a result of diagenetic aggradation and reordering of illites. Chlorites are unstable in highly leached environments.

CORRENSITE

The presence of corrensite in a sandstone from the Santa Rosa was reported by Glass et al (1973). The corrensite of Lippman (1954) has peaks at 14.2-A, (VS) 10-A (M), 7.08 (W), 4.72 (M), and 3.34-A (VS). These peaks coincide well with the peaks observed on an untreated diffractogram of the mudstone. However, the diagnostic 30.8-A (2.9) peak is missing.

Corrensite represents an intermediate step in the evolution of illites towards chlorite by fixation of magnesium (Dunoyer de Segonzac, 1970). It is generally associated with evaporites in Permian and Triassic rocks of Europe.

ANALYSIS BY SEM

Scanning electron microscope photographs indicate well crystallized books of kaolinite in the sandstones and a layering of illite-montmorillonite flakes in the mudstones. Kaolinite may exist as a poorly crystallized variety which may be hidden by the "leaves" of illite and mixed layer clays.

Figure 9 shows quartz qrains in the sandstone which was sawed. The water associated with sawing may have washed out the kaolinite. Visible is a 100 micron (.1 mm) wide muscovite flake.

Figure 10 shows quartz grains surrounded by stacks of kaolinite flakes 6-10 microns in diameter and 10-20 microns long.

Figure 11 of mudstone shows mixed layer illite-smectite flakes 2-15 microns in size. Ordered kaolinite is conspicuously absent.

Figure 12 shows a closer view of I-M mixed layer clay.

SEM study (Kotelnikov (1965) suggests that detrital illite may occur as isometric flakes and diagenetic illite may appear as elongated flakes in the form of slabs. Based on this, the illite in the mudstone as shown in SEM micrographs is detrital.

Considerable microporosity exists between the kaolinite books in the sandstone. The kaolinite in general shows the structure described by Keller (1976). Loose packing of the stacks of plates differentiates this kaolinite from one produced in a hydrothermal environment which would have a tighter packing.

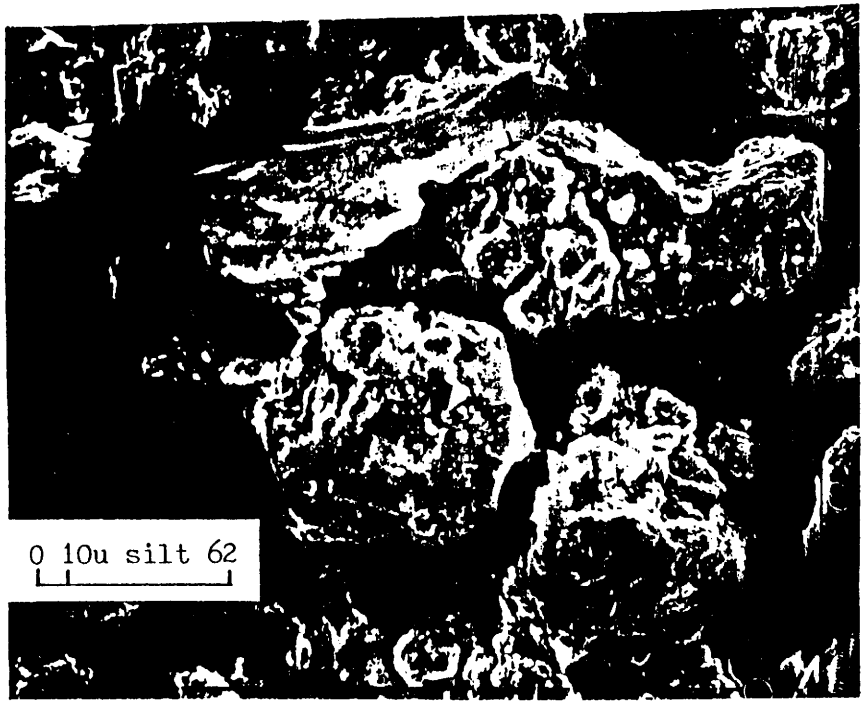

ST8-396
X410

FIG. 9

ST8-396
X2000

FIG. 10

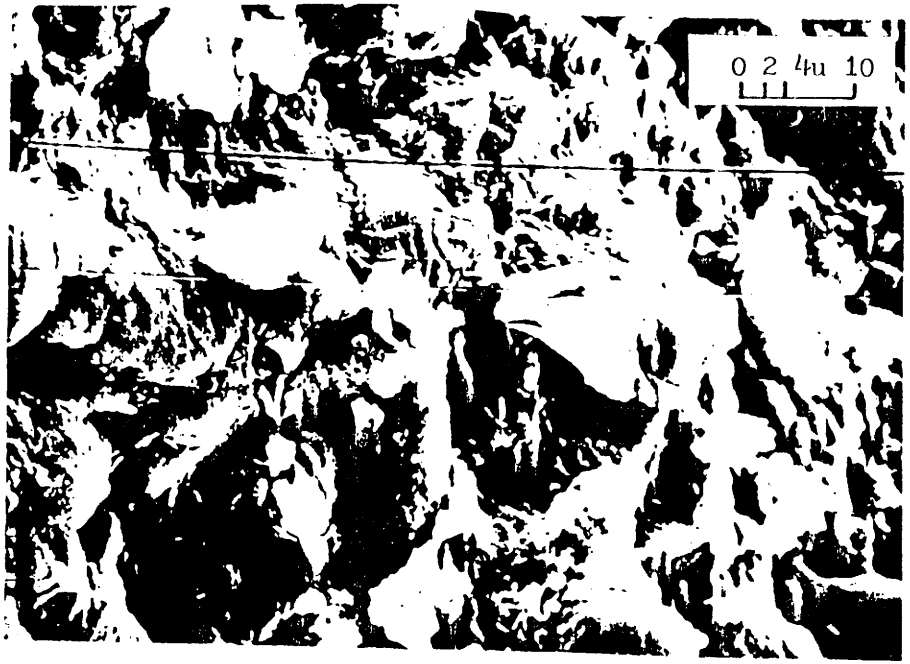

SAI-396
X1500

FIG. 11

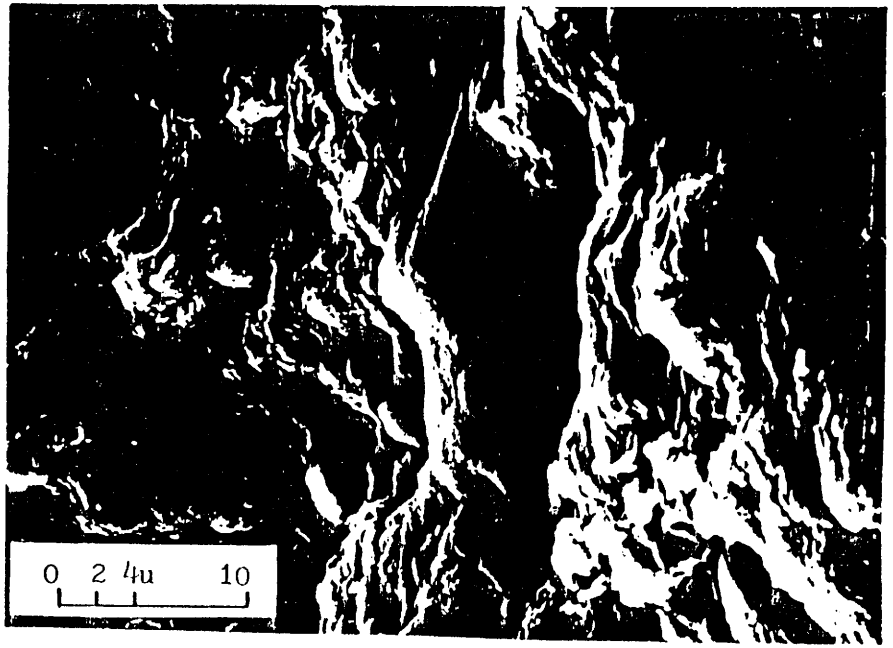

SAI-396
X 2500

FIG. 12

CORE LABS also made and analyzed SEM micrographs of the cores. Their analysis was similar to the above. They noted abraded kaolinite (possibly detrital?) in the sandstone and a clay coating on some of the grains of undetermined composition.

In general, kaolinites are easy to identify by SEM because of their platelet morphology. Illites and smectites exhibit a soggy cornflake-like morphology but their diffentiation and percentage determination is very difficult.

ANALYSIS BY THIN SECTION

The sandstones were composed of well-sorted silt size (.05 mm) - med. sand size (.3 mm) quartz (80%), feldspar (5%), chert (5%), with traces of dolomite, muscovite, hematite, and clays. Grain contacts are tangential and concavo-convex. Cement occurs in the form of quartz overgrowths and dolomite.

The clays were difficult to identify in thin section. Identification was made even more difficult be the presence of oil which masks the true features of the clays. Since prior identification was made by X-Ray this was not a cause for concern.

The clays exist as intergranular matrix. Little primary (except for the previously described microporosity) porosity is evident. Secondary porosity seems absent as well. Visual estimates of the blue epoxy impregnated slides gave an effective porosity of 10-12%.

Several photographs of Triassic sandstone thin sections are used as examples in AAPG Memoir 22:A Color Guide to Sandstone Petrology (1979) and show visible kaolinite stacks. Other clays are described as well.

GENESIS OF THE CLAYS

The Santa Rosa sandstone was deposited in a humid to semi-humid climate by a terrestrial fluvial system which flowed over Permian carbonates, shales, and evaporites (McGowen, 1983). Flow was to the southeast towards a lake basin at the Texas border. Deposited with the sandstone were numerous plant fragments which were later coalified. Their presence along with pyrite indicates an acidic reducing environment similar to that of coal swamps The area was later subjected to sufficient chemical and physical diagenesis to produce coalification. A rough estimate of maximum burial based on personal observation of the remnant mesas capped by rocks as young as the Cretaceous age would be 3000-5000 feet. These depths are sufficient to produce a temperature of 150 degrees farenheit.

The almost complete absence of feldspars in the rock indicate either their absence in the source rocks or their complete alteration. The few grains which were found were altered so as to be almost unrecognizable.

The probable sequence of genesis probably included these steps:

1. Overbank muds of mixed kaolinite, smectite, and illite from the Permian formations were deposited by the river system.

2. The system was later covered by sediments. Ion concentration in the pore water began to increase as temperature increased solubilities. Conversion of smectites to illites began after the model of Hower et al (1976).

3. The area began to be eroded and water began to circulate through the formation. Kaolinite was precipitated in the pore space of the sandstone.

STEAMFLOOD PERFORMANCE

Water temperature, ion content of the water, and type of clay are major factors affecting steamflood performance.

The approximate composition of the injection water currently used at the site is shown below in Table 3:

Table 3: Water Analyses (Martin, 1983)

	Injected Steam Water	
pH	8.6	
Alkalinity as HCO3	524	mg/liter
Chlorides as Cl	57	mg/liter
Sulfates as SO4	510	mg/liter
Hardness as CaCO3	0	
Calcium as Ca	0	
Magnesium as Mg	0	

Steam is being injected at the rate of 60 barrels of water/day at a temperature of 310 degrees F. (333°C) and under a pressure of 250 psi (Martin, 1983). Average porosity of the formation is 20% and average air permeability is 200 md.

To demonstrate the sensitivity of clays to different solutions Mungan (1963) tested cores of St. Peter sandstone consisting of very pure silica sand and 0.4% kaolinite with a 30,000 ppm NaCl solution and a 0.5 N NaOH solution. The brine reduced permeability by about a third while the NaOH solution reduced it by half (Fig. 13).

Mungan (1963) also investigated the effects of flooding with a 30,000 ppm NaCl solution followed by distilled water on a core of Berea sandstone containing illite, chlorite, kaolinite, and interlayered illite. The permeability dropped from 190 md to 0.9 md. almost immediately upon introduction of distilled water to the core. Clays were also produced in the effluent indicating dispersal of grains was occurring (Fig. 14).

These effects can be alleviated by eliminating the 'shock' effect of fresh water and reducing the salinity very gradually as was shown in another experiment.

Experiments with NaOH solutions at 180 degrees F. produced a permeability reduction from 240 md. to 180 md. in an oil-wet core. Following the caustic flood with distilled water at 180 deg. F. produced a further reduction of permeability to 55 md. (Mungan, 1963) Fig. 14.

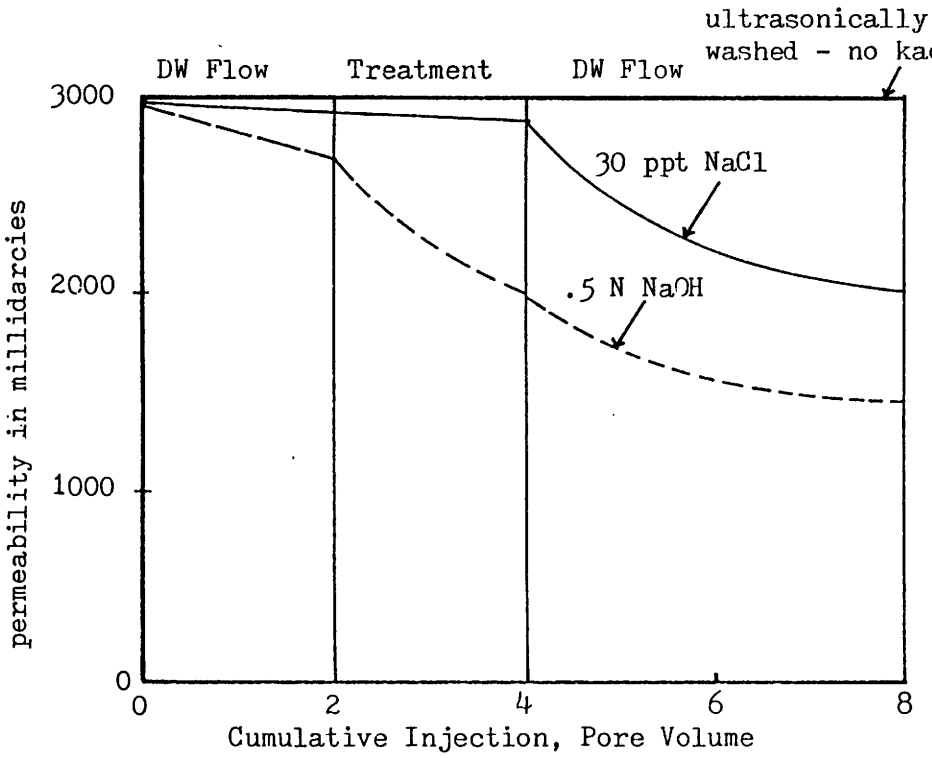

The Effect of Small Quantity of Indigenous Kaolinite on the Permeability of Unconsolidated St. Peter Sand Cores (approx. 0.4% kaolinite)

FIG. 13

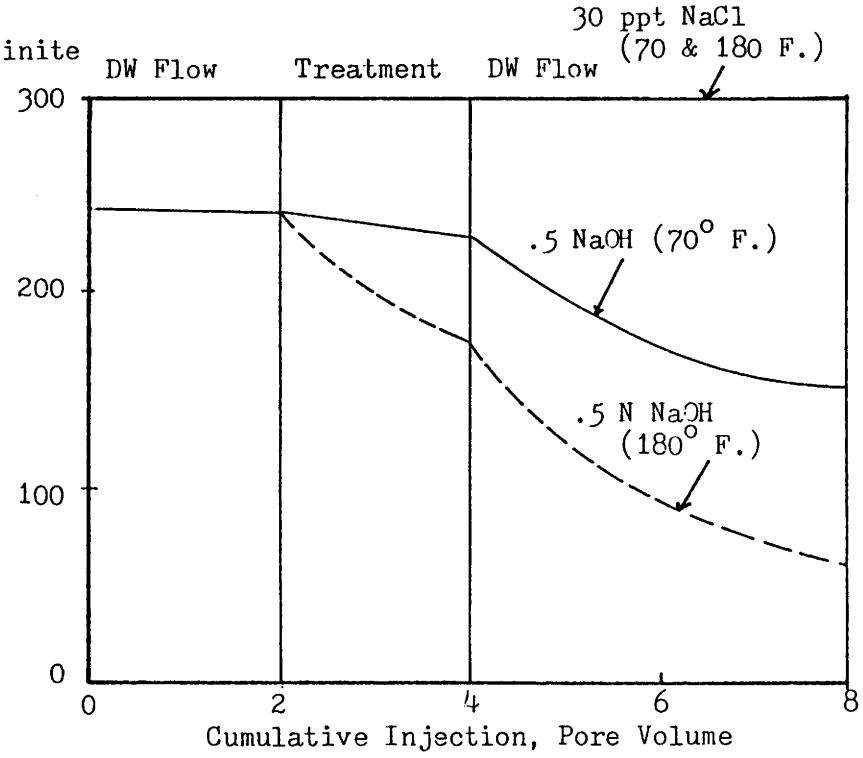

The Effect of Temperature on Sensitivity of Nonextracted Cores from Formation A. (approx. 1% kaolinite)

FIG. 14

(after Mungan, 1963)

NEWKIRK FIELD CORES

FIG. 15

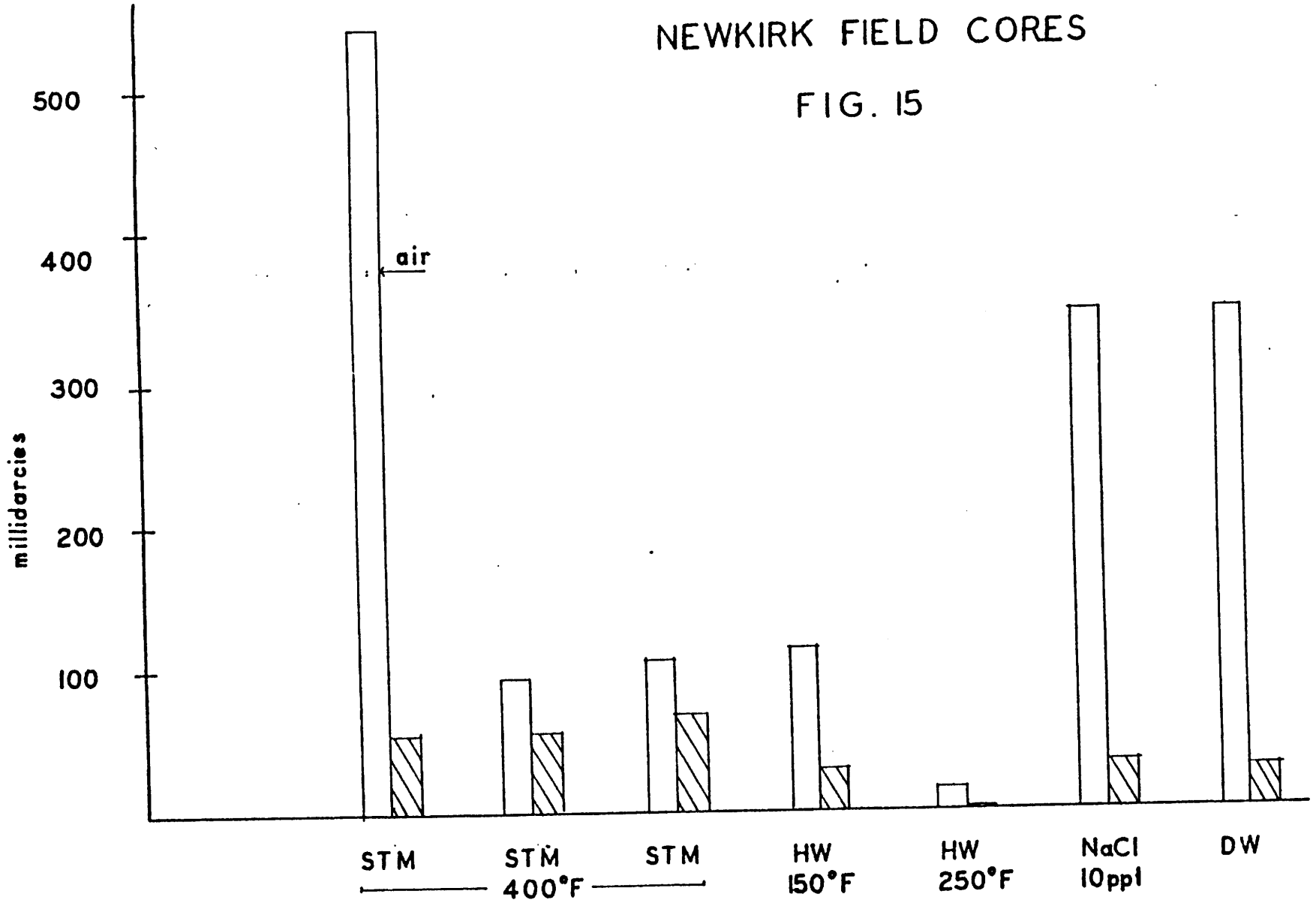

AIR PERMEABILITY V. WATER PERMEABILITY (after CORE LABS)

The conclusions of these experiments are:

1. The primary cause of permeability reduction is blocking of the pore passages by dispersed particles.

2. Permeability reduction due to salinity changes occurs regardless of the type of clay.

3. NaOH generally caused more damage than brine solutions because it dissolves matrix material, disperses clays, and dislodges fine material which then block pore throats.

Little work has been done on the long term (1-15 years) effects of steamflooding on clays. The similarity to hydrothermal systems is evident with the main difference being the vast difference in time. Potential exists for illitization of kaolins and destruction of permeability, in effect, creating a shale where a sandstone once was. Theoretically, this condition would show as a pressure buildup in injection pressure. This has not been the case at the steamflood project.

CORE LABS ran several tests on oil saturated cores from the Newkirk Field to determine steamflood viability. The tests included steamflood (400 degrees F.) sensitivity, Hot water (150 & 250 degrees F.), and water sensitivity for 10,000 ppm NaCl and distilled water. The results are summarized in Fig. 15.

The tests indicated that steam was effective at removing most of the oil while hot water was not.

According to these tests, permeability to steam was actually twice that of distilled water. Permeability was not affected by 150 degree F. hot water or a brine solution. Only the 250 degree F. hot water reduced permeability significantly (to < 2 md.). Also, air permeabilites were a poor guide to fluid permeabilities due in part to the clays in the pores.

CONCLUSION

Kaolinites, illites, and mixed layer clays in the fluvial fine grained Santa Rosa sandstone constitute the major impediment to fluid flow in the formation. Steamflooding in progress may be further aggravating the situation by:

1. Increasing the temperature
2. Introducing water of lower ion content which disperses the clays.
3. Introducing water of higher OH- content which also aids dispersal of the clays.
4. Potentially creating illites from kaolinites which have a greater potential for blocking pores.

The state of current work is insufficient to construct models which might predict trends of reduced kaolinite and greater permeability.

More study on the long term effects of steam would be helpful in determining effects on clays and potential permeability reduction.

BIBLIOGRAPHY

Budding, A.J., (1979) Geology and oil characteristics of the Santa Rosa tar sands, Guadalupe County, N.M.. Prepared under grant number 78-3316, N.M. Energy Institute at NMIMT, Socorro, N.M.

Chepilov, K.R., Ermolova, E.P. and Orlova, N.A. (1959) Epigenetic minerals as indicators of time arrival of petroleum into commercial sand reservoirs. Dokl. Akad. Nauk S.S.S.R. 125:1097-1099.

CORE LABS (1980) Screening tests for thermal oil recovery for Public Lands Exploration, INC., report to George Scott, consulting geologist, Roswell, N.M..

Donoyer de Segonzac, G. (1970) Clay-minerals diagenesis and low grade metamorphism. Sedimentology, V. 15, p. 281-346.

Esquivan, J., (1969) Influence de la composition chimique des illites sur leur cristallinite. Bull. Centre Rech. Pau-SNPA, 3:147-632.

Hemingway, J.E. and Brindley, G.W. (1948) The occurrence of dickite in some sedimentary rocks. Intern. Geol. Congr., 18th, London, 1948, Rept.,13:308.

Hower, J., Eslinger, E., Hower, C., Perry, H. (1976) Mechanism of burial metamorphism of argillaceous sediment: 1. Mineralogical and chemical evidence. GSA Bull. v. 87, p. 725-737.

Keller, W.D., (1976) Scan electron micrographs of kaolins collected from diverse environments of origin (parts I and II). Clays and Clay Min., Vol 24.

Keplinger and associates, Inc. (1980) An appraisal of estimated heavy oil recovery via steamflood from the Newkirk East and Newkirk West Prospects, Guadalupe County, NM, submitted to Public Lands Exploration Co., Dallas, Tx.

Kelley, Vincent C. (1972) Triassic Rocks of the Santa Rosa Country. N.M.Geol. Soc. Guidebook, 23 Fld. conf., E-Central NM.

Kotelnikov, D.D. (1965) Sur les caracteres morphologiques des illites dans les roches sedimentaires. Mineral. Sb., 19:26-35.

Lippman, Friedrich (1954) Uber einen Keuperton von Zaisersweiher bei Maulbronn. Heidelberg Geitr. Min., v. 4, p. 130-134.

Lindquist, Sandra J. (1983) Nugget Formation Reservoir Characteristics Affecting Production in the Overthrust Belt of Southwestern Wyoming., J. Pet. Tech., July, 1983.

Martin, Dave (1983) Steamflood pilot in the O'Connell Ranch Field. PRRC Report 83-9, Socorro, NM.

Mcgowen, J.H., Granata, G.E., Seni, S.J.. (1983) Depositional Setting of the Triassic Dockum Group, Texas Panhandle and Eastern New Mexico. Mesozoic Paleogeography of west-central U.S. (Reynolds, M.W. and Dolly, E.D. eds.), Denver, Colorado.

Mungan, Necmettin (1963) Permeability Reduction through changes in pH and Salinity. J. Pet. Tech., Dec. 1963.

Scott, Andy (1983) personal communication (CORE LABS).

Thorez, J. (1975) Phyllosilicates and clay minerals. Editions G. Lelotte, Dison, Belgium.

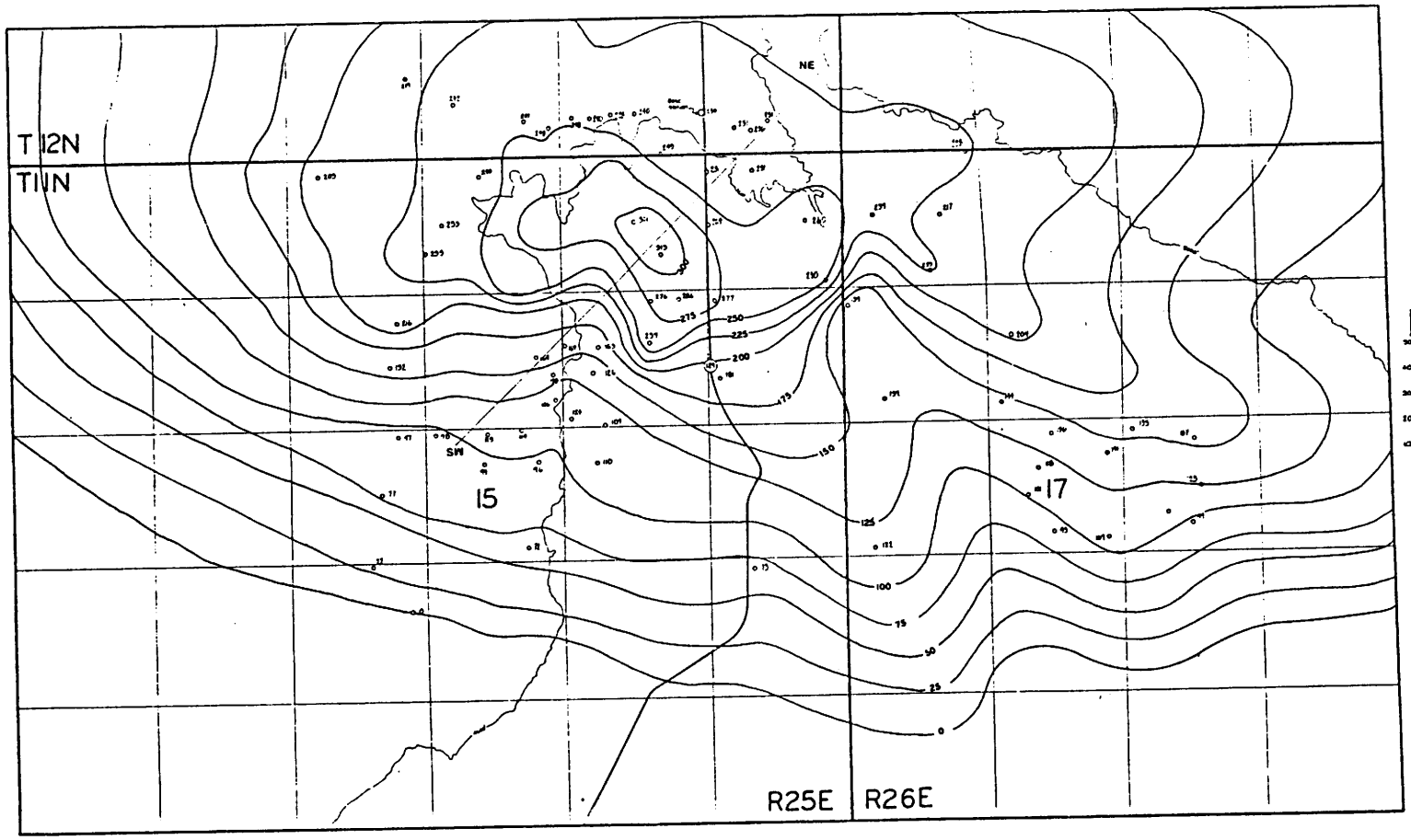

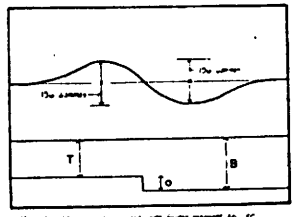

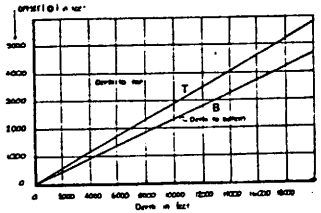

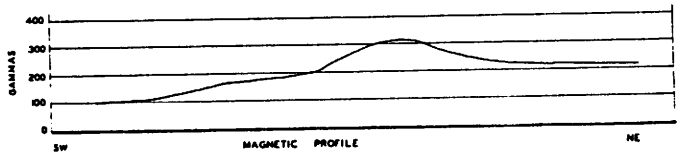

MAGNETIC ANOMALIES MAP

CONTOUR INTERVAL: 25 GAMMAS

COUNTY: GUADALUPE
STATE: NEW MEXICO
BY: J. Curtis McKallip Jr.

0 1 mi

PLATE 1

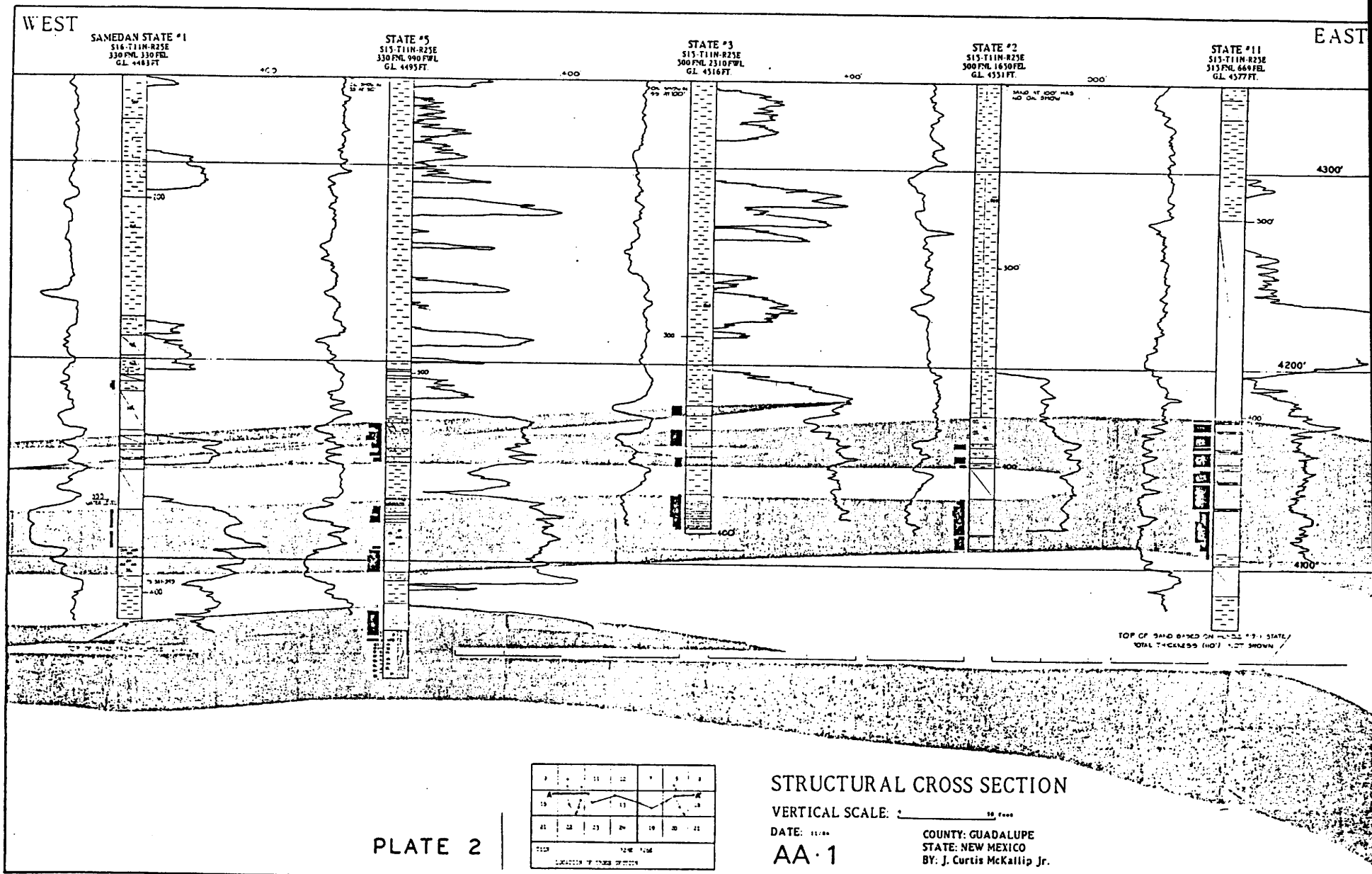

PLATE 2

STRUCTURAL CROSS SECTION

VERTICAL SCALE:

DATE:

AA·1

COUNTY: GUADALUPE
STATE: NEW MEXICO
BY: J. Curtis McKallip Jr.

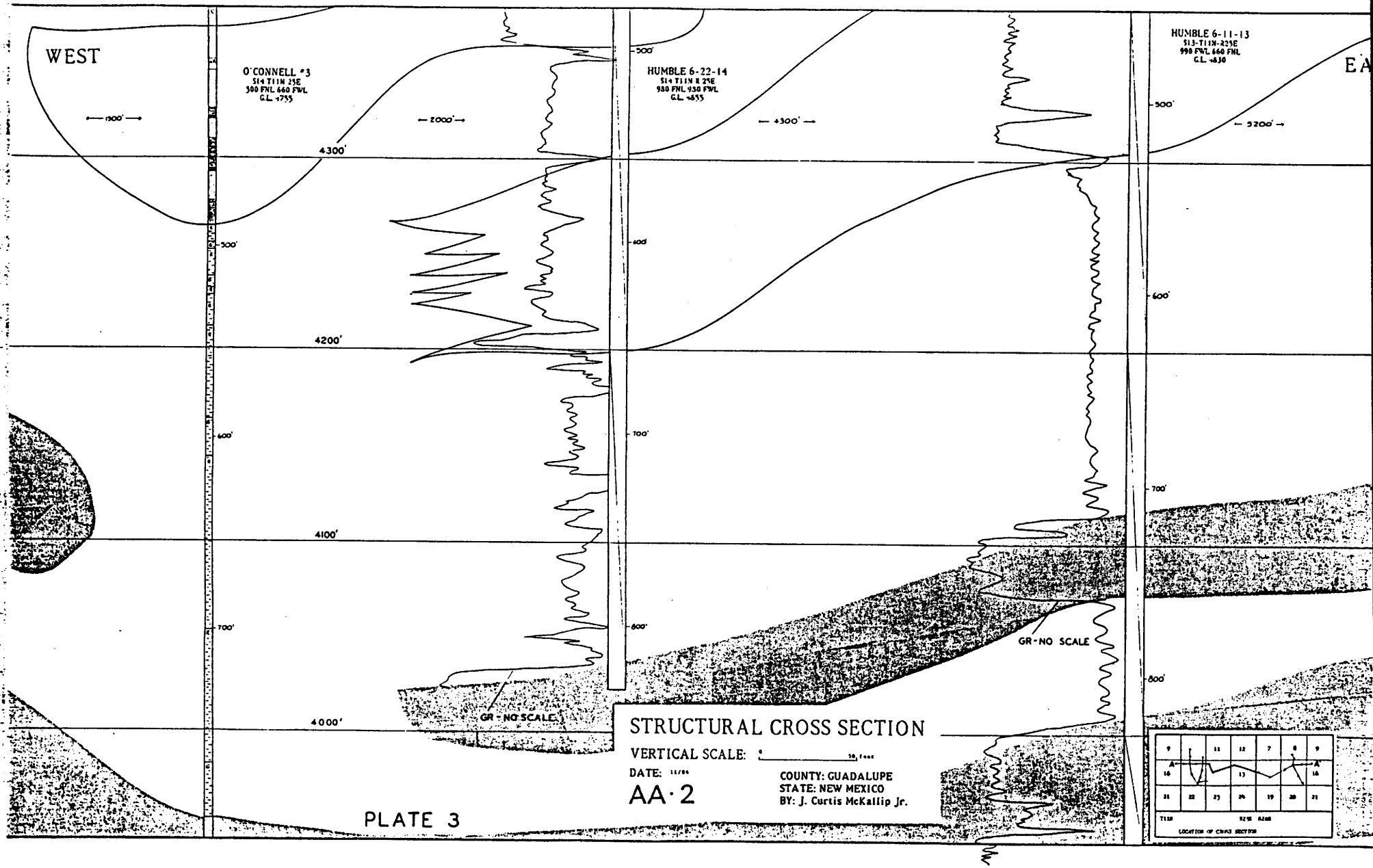
WEST
O'CONNELL #3
S14 T11N 25E
500 FNL 660 FWL
G.L. 4755
HUMBLE 6-22-14
S14 T11N R 25E
980 FNL 950 FWL
G.L. 4835
HUMBLE 6-11-13
S13-T11N-R25E
990 FWL 660 FNL
G.L. 4830
EA
1500'
2000'
4300'
3200'
4300'
4200'
4100'
4000'
500'
600'
700'
800'
GR - NO SCALE
GR-NO SCALE
STRUCTURAL CROSS SECTION
VERTICAL SCALE:
DATE:
AA·2
COUNTY: GUADALUPE
STATE: NEW MEXICO
BY: J. Curtis McKallip Jr.
PLATE 3

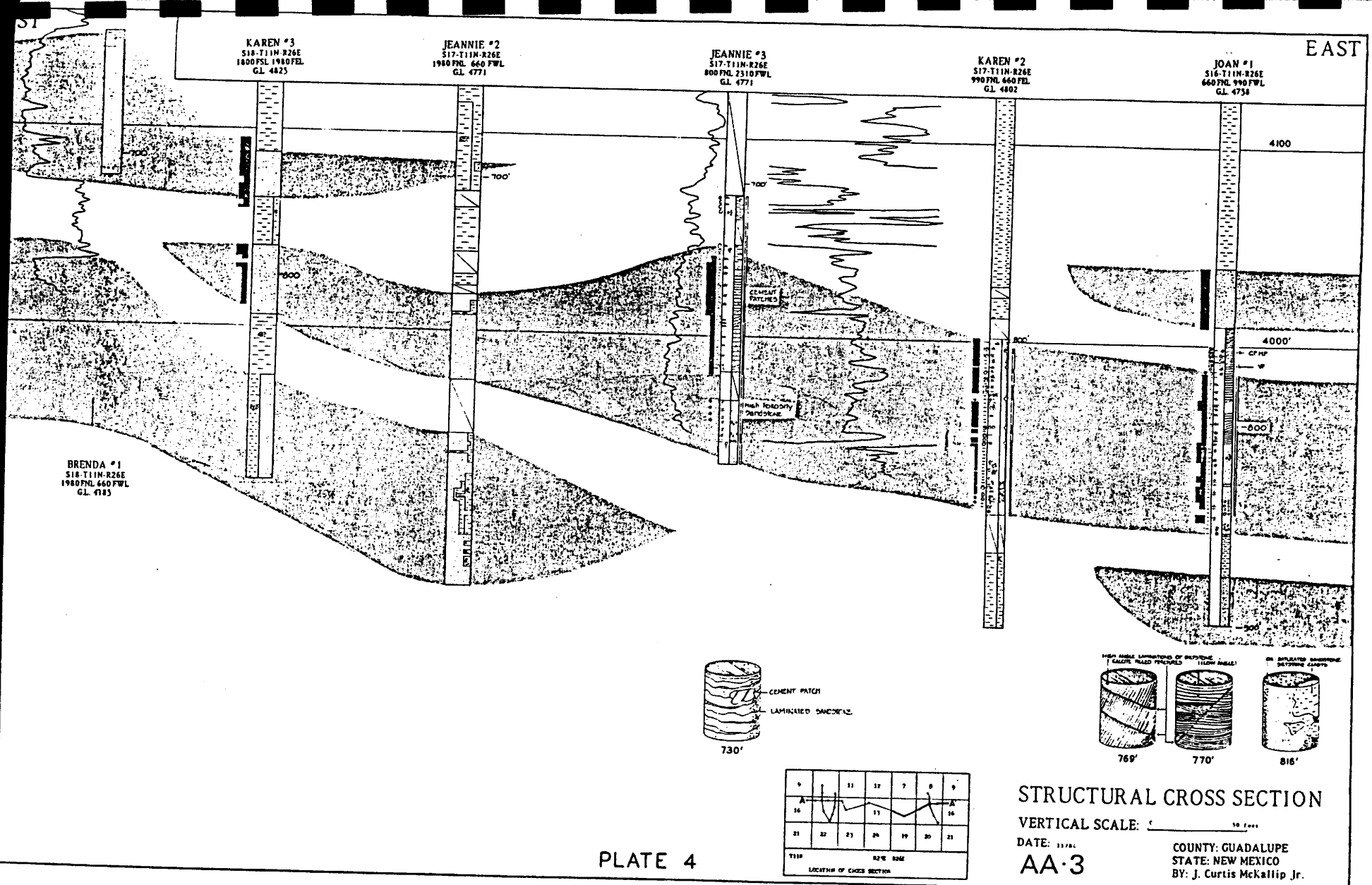

PLATE 4

STRUCTURAL CROSS SECTION

VERTICAL SCALE: 1" = 50 Feet

DATE: 11/84

AA·3

COUNTY: GUADALUPE
STATE: NEW MEXICO
BY: J. Curtis McKallip Jr.

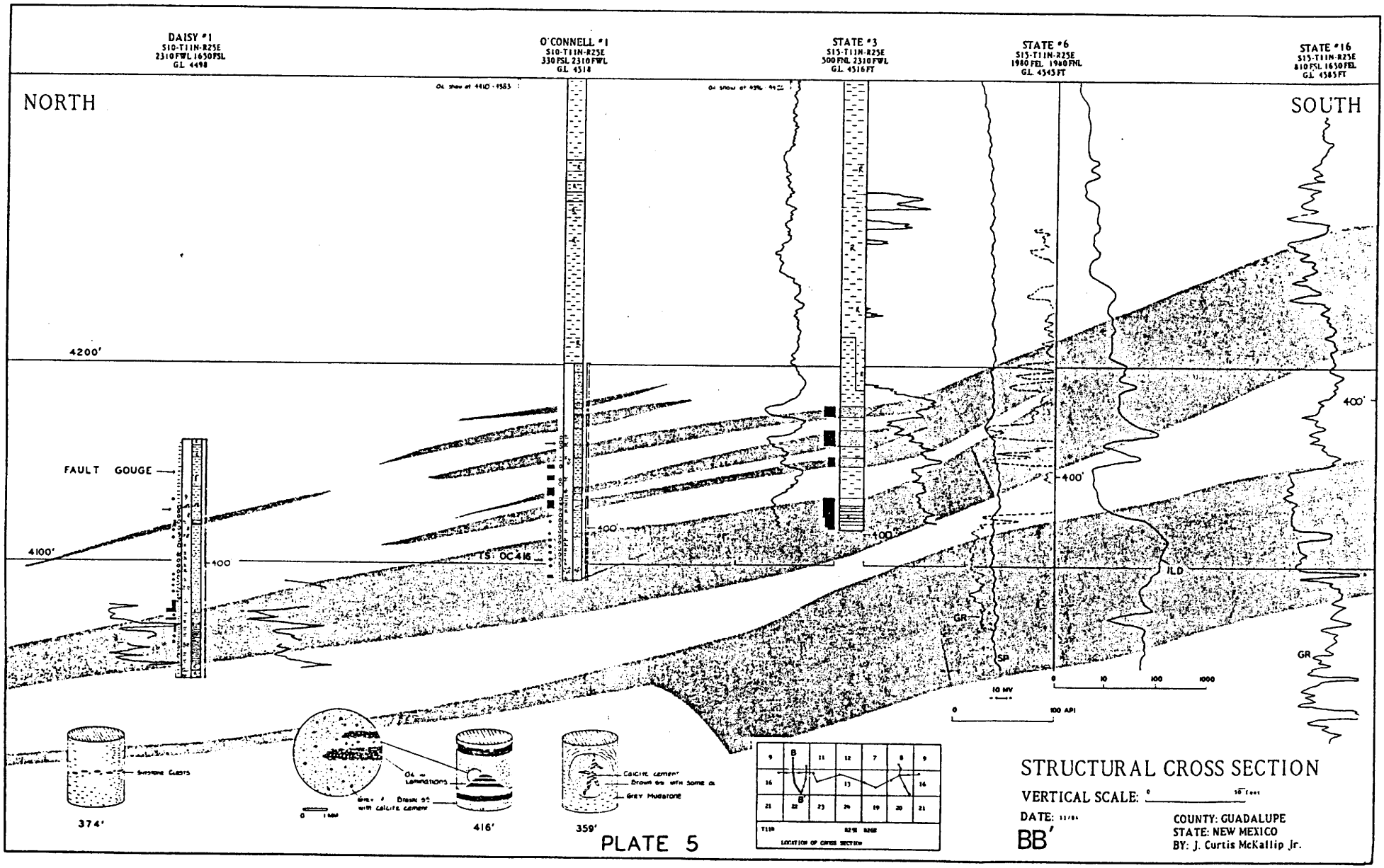
DAISY #1
S10-T11N-R25E
2310FWL 1650FSL
GL 4498
O'CONNELL #1
S10-T11N-R25E
330FSL 2310FWL
GL 4518
STATE #3
S15-T11N-R25E
500FNL 2310FWL
GL 4516FT
STATE #6
S15-T11N-R25E
1980 FEL 1980 FNL
GL 4545FT
STATE #16
S15-T11N-R25E
810FSL 1650FEL
GL 4585FT
NORTH
SOUTH
4200'
4100'
400'
FAULT GOUGE
TS OC416
GR
SP
ILD
10 MV
100 API
Siltstone Clasts
Oil in Laminations
Grey & Brown ss with calcite cement
Calcite cement
Brown ss with some oil
Grey Mudstone
374'
416'
359'
PLATE 5
STRUCTURAL CROSS SECTION
VERTICAL SCALE:
DATE:
BB'
COUNTY: GUADALUPE
STATE: NEW MEXICO
BY: J. Curtis McKallip Jr.

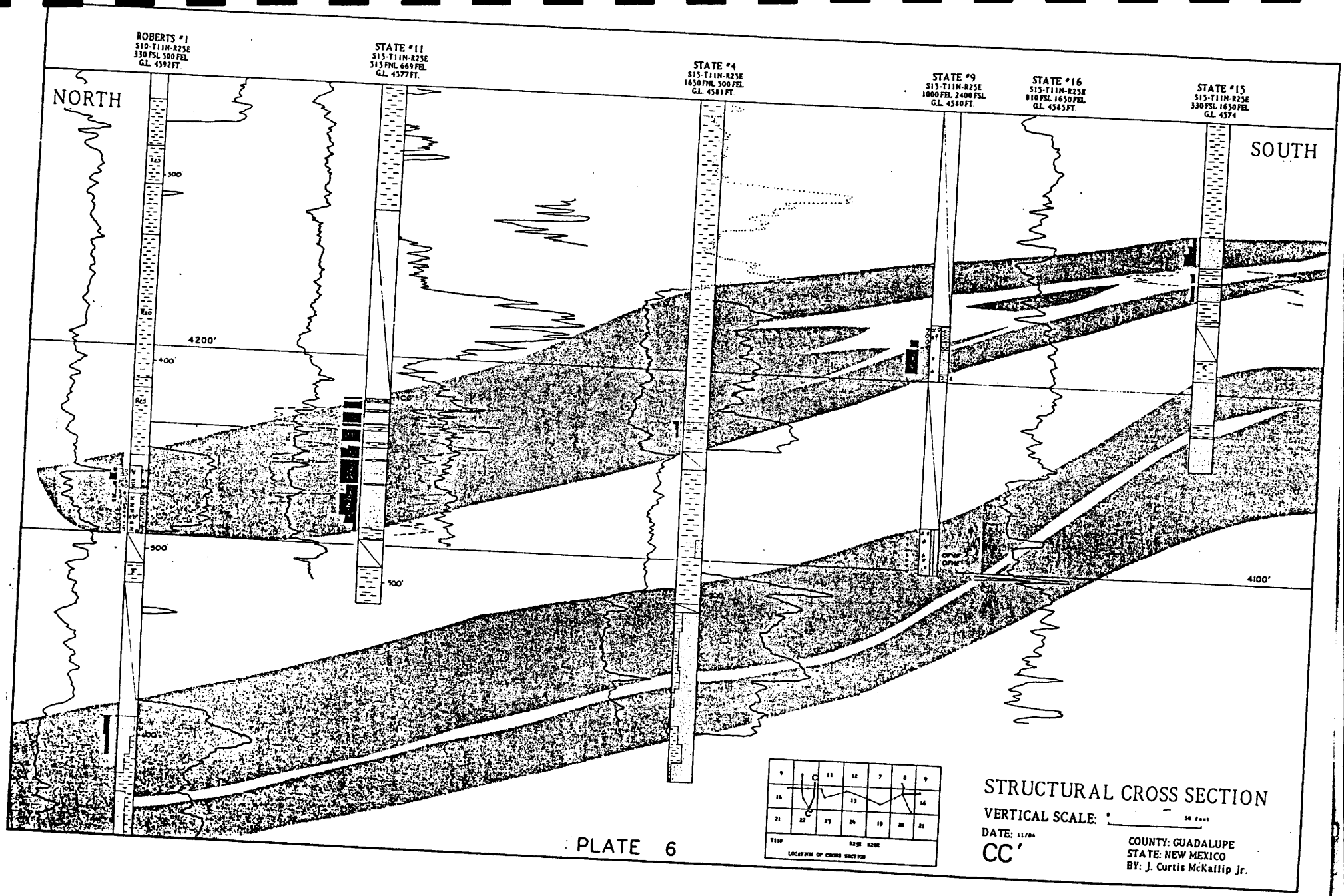

PLATE 6

STRUCTURAL CROSS SECTION

VERTICAL SCALE: 1" = 50 Feet

DATE: 11/84

CC'

COUNTY: GUADALUPE
STATE: NEW MEXICO
BY: J. Curtis McKallip Jr.

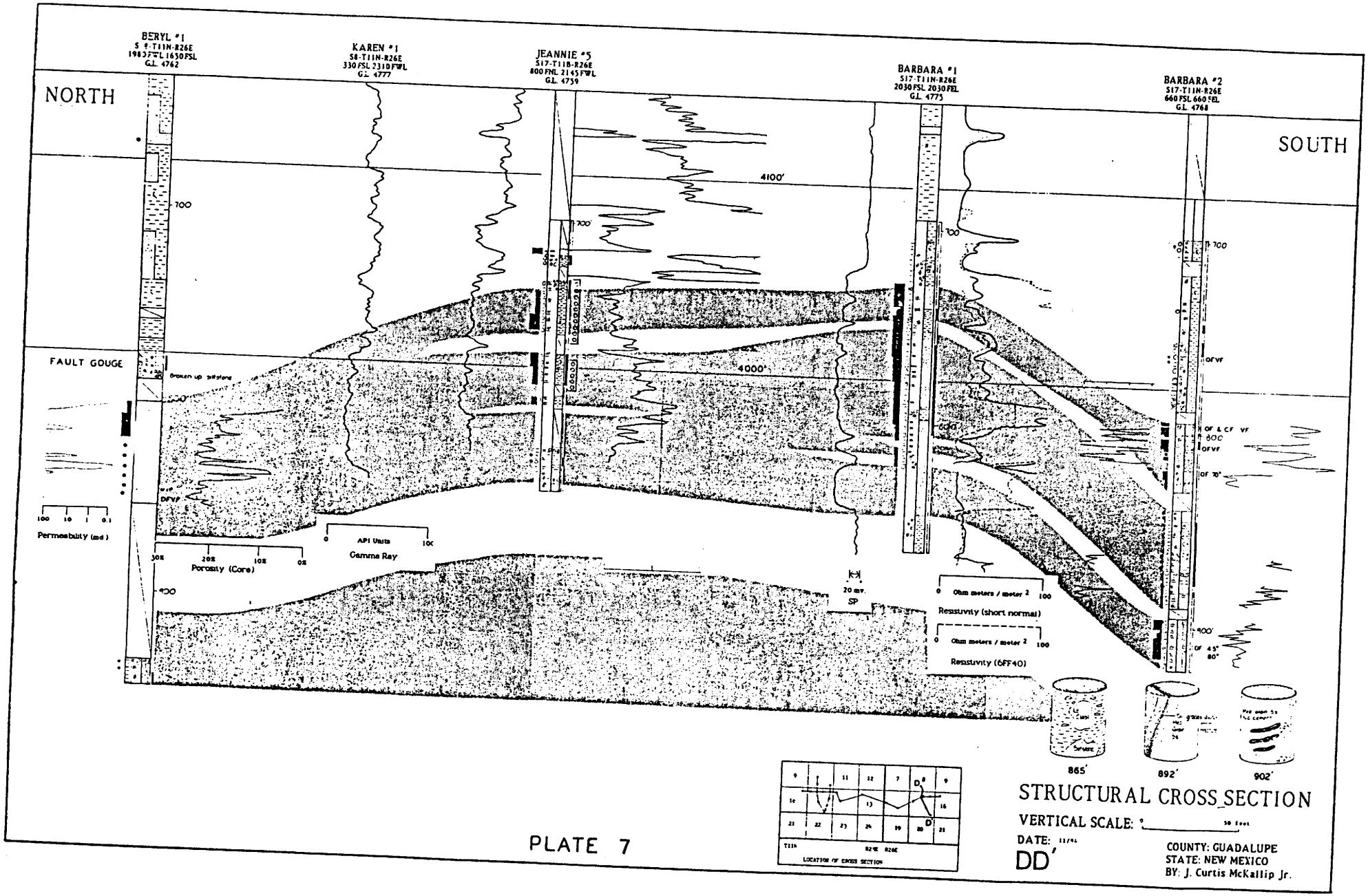
BERYL #1
S 8-T11N-R26E
1983 FEL 1650 FSL
G.L. 4762
KAREN #1
S8-T11N-R26E
330 FSL 2310 FWL
G.L. 4777
JEANNIE #5
S17-T11S-R26E
800 FNL 2145 FWL
G.L. 4759
BARBARA #1
S17-T11N-R26E
2030 FSL 2030 FEL
G.L. 4775
BARBARA #2
S17-T11N-R26E
660 FSL 660 FEL
G.L. 4768
NORTH
SOUTH
FAULT GOUGE
4100'
4000'
700
800
900
Permeability (md)
Porosity (Core)
Gamma Ray
API Units
SP
20 mv.
Resistivity (short normal)
Resistivity (6FF40)
Ohm meters / meter 2
865'
892'
902'
STRUCTURAL CROSS SECTION
VERTICAL SCALE:
DATE:
DD'
COUNTY: GUADALUPE
STATE: NEW MEXICO
BY: J. Curtis McKallip Jr.
LOCATION OF CROSS SECTION

PLATE 7

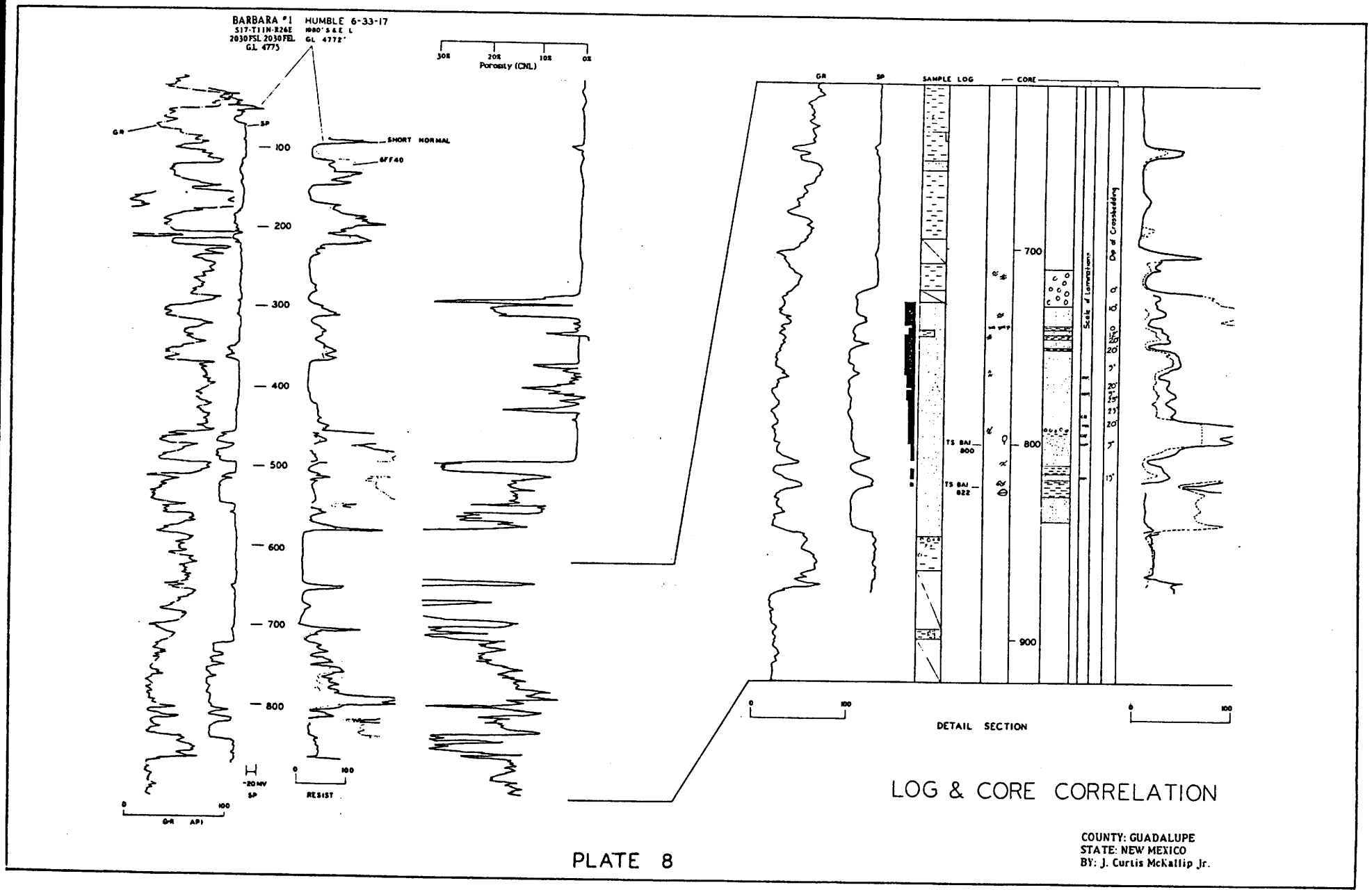
BARBARA #1
S17-T11N-R26E
2030FSL 2030FEL
GL 4775
HUMBLE 6-33-17
1980' S & E L
GL 4772'
30% 20% 10% 0%
Porosity (CNL)
GR
SP
SHORT NORMAL
6FF40
100
200
300
400
500
600
700
800
-20 MV
SP
0
100
RESIST
0
100
GR API
GR
SP
SAMPLE LOG
CORE
700
800
900
TS BAI 800
TS BAI 822
Scale of Lamination
Dip of Crossbedding
0
100
0
100
DETAIL SECTION
LOG & CORE CORRELATION
COUNTY: GUADALUPE
STATE: NEW MEXICO
BY: J. Curtis McKallip Jr.

PLATE 8

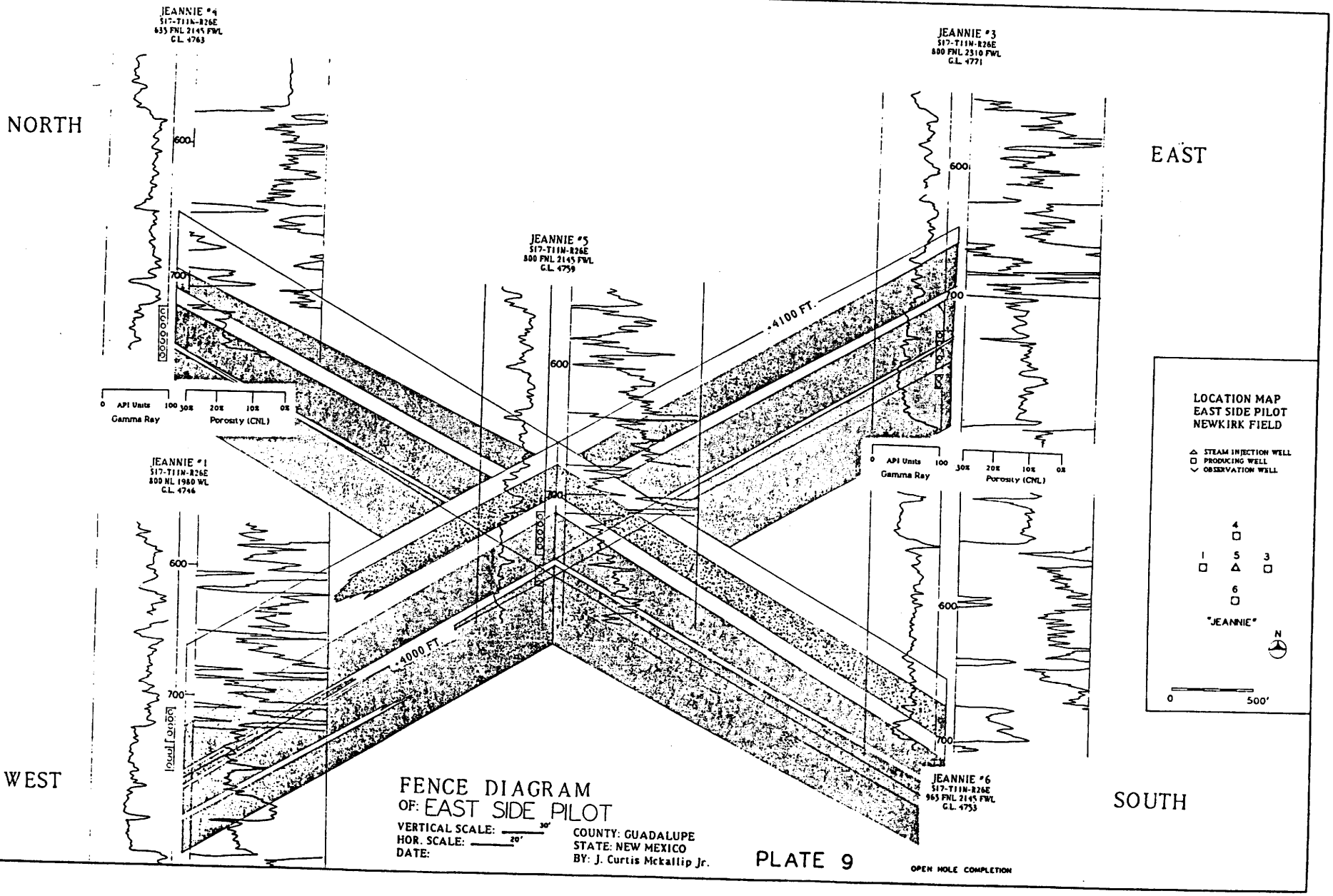
NORTH
EAST
WEST
SOUTH
JEANNIE #4
S17-T11N-R26E
635 FNL 2145 FWL
G.L. 4763
JEANNIE #3
S17-T11N-R26E
800 FNL 2510 FWL
G.L. 4771
JEANNIE #5
S17-T11N-R26E
800 FNL 2145 FWL
G.L. 4759
JEANNIE #1
S17-T11N-R26E
800 NL 1980 WL
G.L. 4746
JEANNIE #6
S17-T11N-R26E
965 FNL 2145 FWL
G.L. 4753
4100 FT.
4000 FT.
600
700
API Units
Gamma Ray
Porosity (CNL)
LOCATION MAP
EAST SIDE PILOT
NEWKIRK FIELD
STEAM INJECTION WELL
PRODUCING WELL
OBSERVATION WELL
"JEANNIE"
0
500'
FENCE DIAGRAM
OF: EAST SIDE PILOT
VERTICAL SCALE: 30'
HOR. SCALE: 20'
DATE:
COUNTY: GUADALUPE
STATE: NEW MEXICO
BY: J. Curtis Mckallip Jr.
PLATE 9
OPEN HOLE COMPLETION

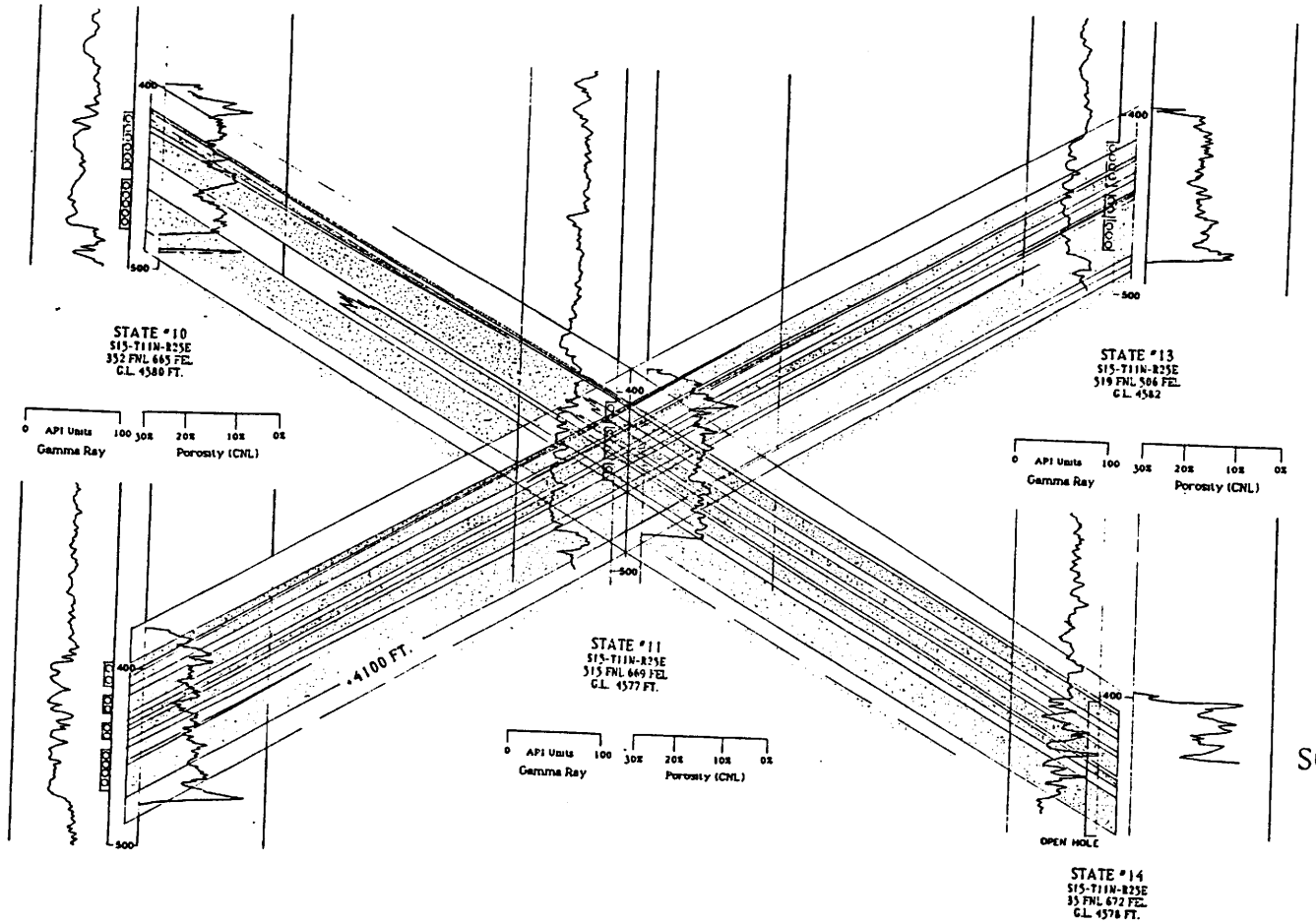

FENCE DIAGRAM
OF: WEST PILOT

VERTICAL SCALE: 30'
HOR. SCALE: 20'
DATE: 7-84

COUNTY: GUADALUPE
STATE: NEW MEXICO
BY: J. Curtis Mckallip Jr.

LEGEND:
- SANDSTONE
- MUDSTONE
- PERFORATIONS

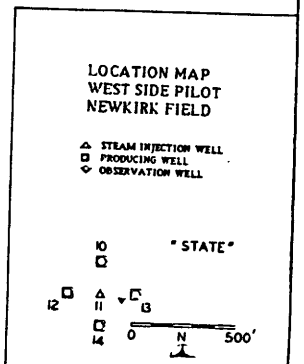

PLATE 10

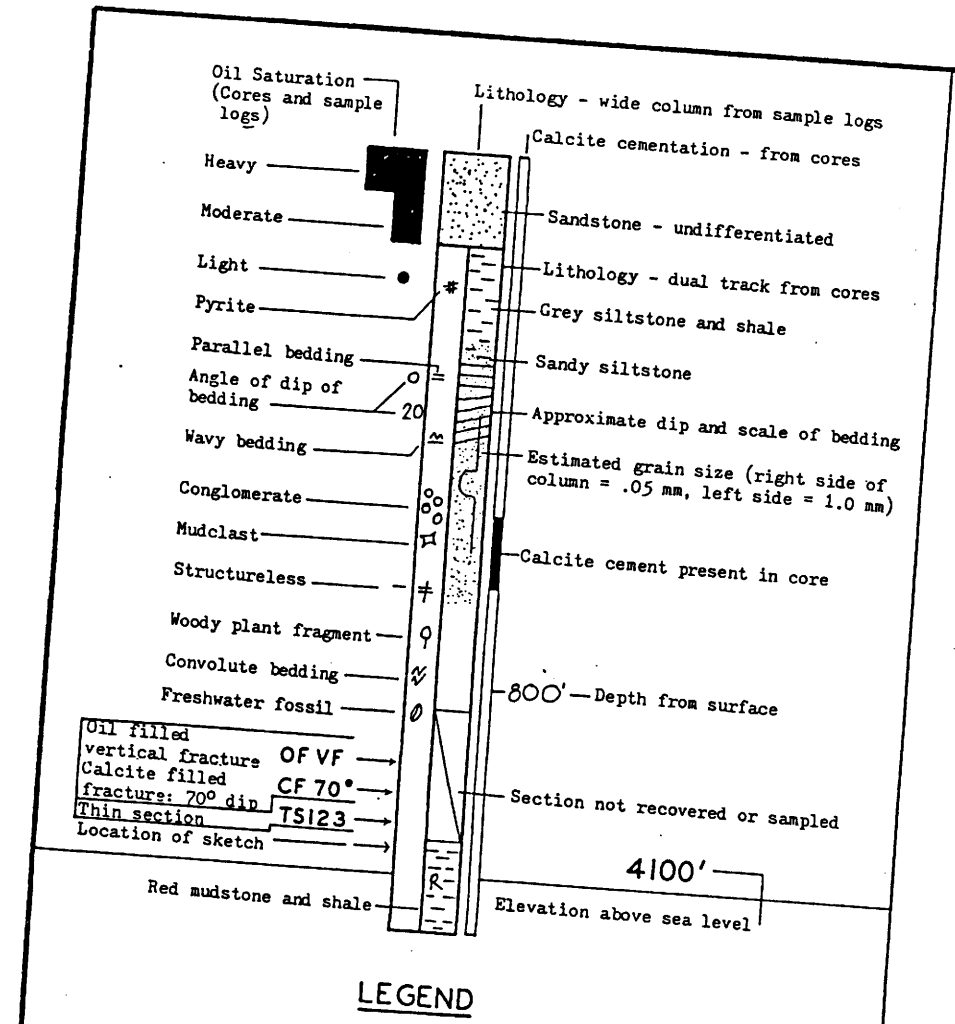

LEGEND

PLATE II

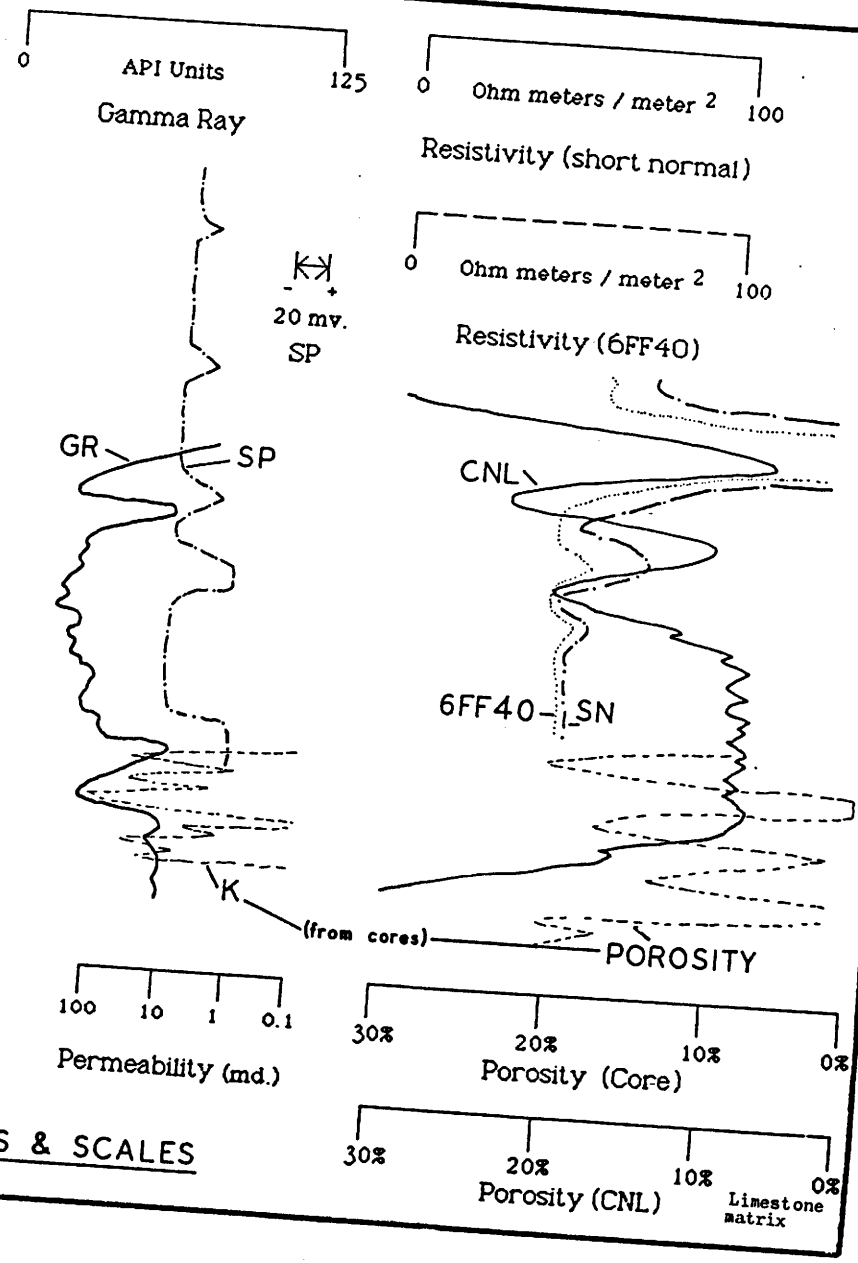

LOGS & SCALES

T 12N

T 11N

R25E

R26E

NE

SW

15

17

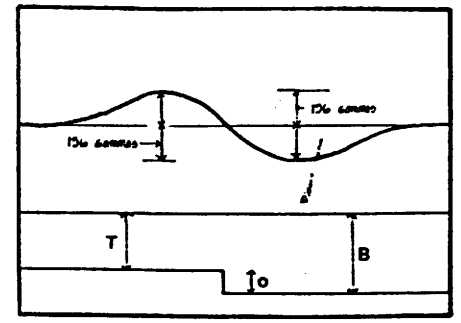

Magnetic anomaly associated with faulted basement key to relationships shown below

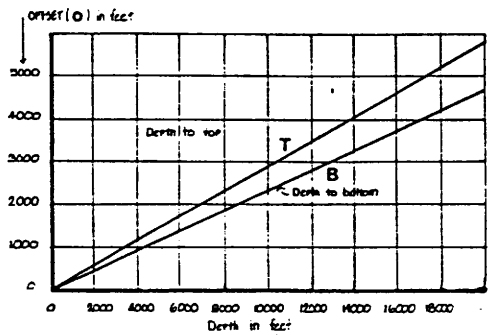

Possible combinations of effect and depths for an anomaly of 150 gammas

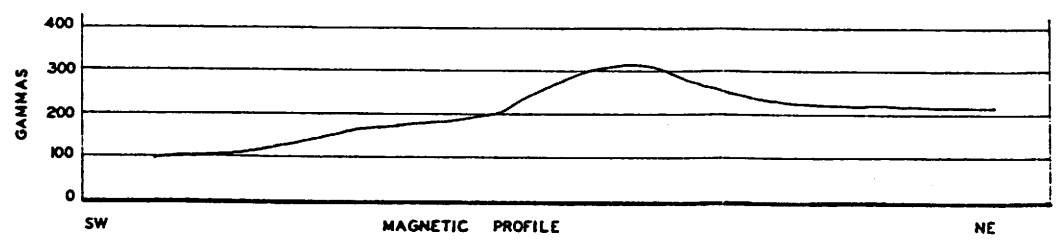

MAGNETIC ANOMALIES MAP

CONTOUR INTERVAL: 25 GAMMAS

0 1 mi

COUNTY: GUADALUPE
STATE: NEW MEXICO
BY: J. Curtis McKallip Jr.

PLATE 1

WEST

SAMEDAN STATE #1
S16-T11N-R25E
330 FNL 330 FEL
G.L. 4483 FT.

STATE #5
S15-T11N-R25E
330 FNL 990 FWL
G.L. 4495 FT.

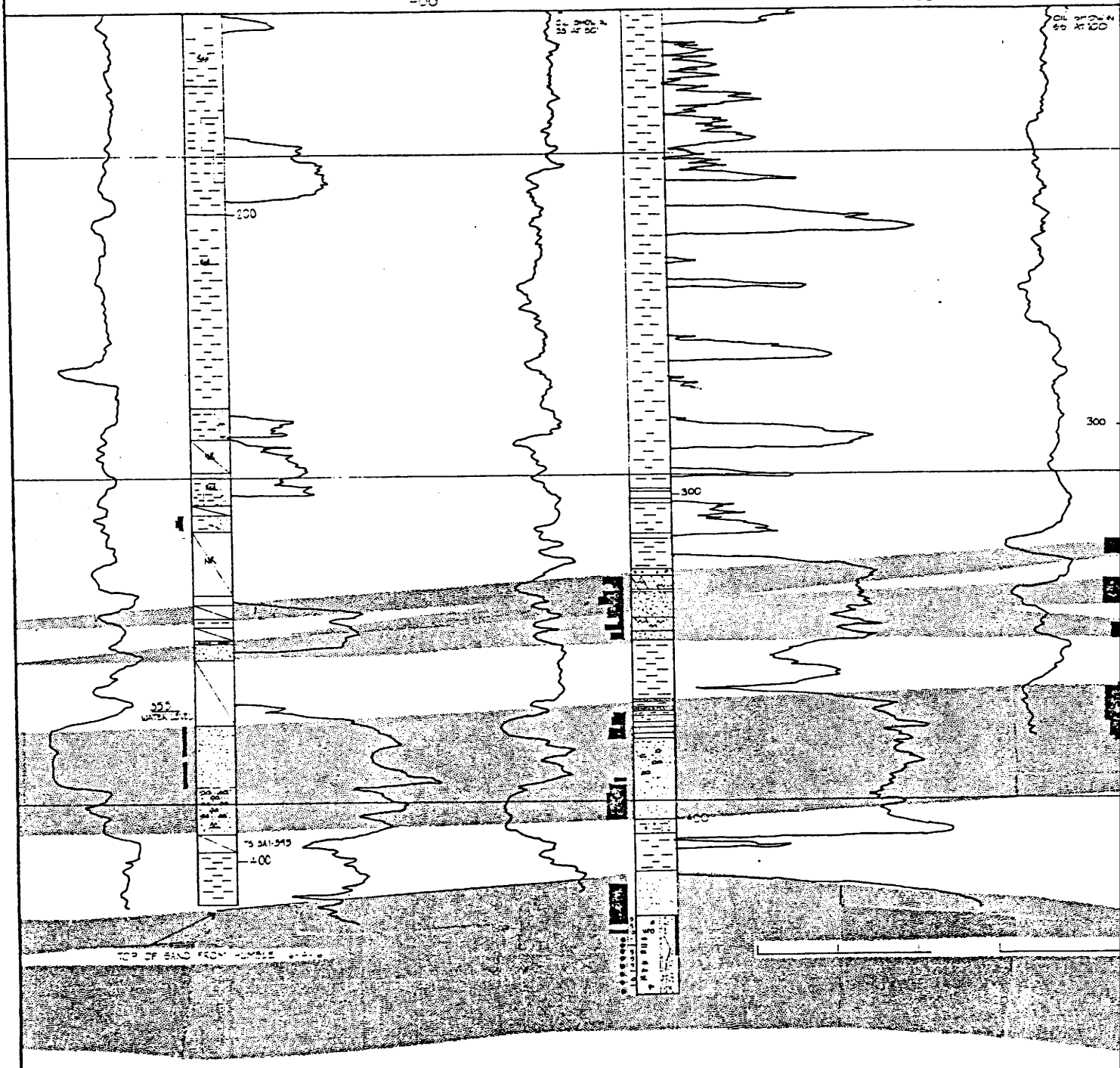

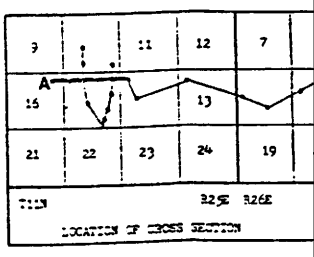

PLATE 2

WEST

O'CONNELL #3
S14 T11N 25E
500 FNL 660 FWL
G.L. 4755

HUMBLE 6-22-14
S14 T11N R 25E
980 FNL 980 FWL
G.L. 4855

HUMBLE 6-11-13
S13-T11N-R25E
990 FWL 660 FNL
G.L. 4830

EAST

1500'

2000'

4300'

500'

4300'

500'

600'

4200'

600'

700'

4100'

700'

800'

700'

800'

4000'

GR-NO SCALE

GR-NO SCALE

STRUCTURAL CROSS SECTION

VERTICAL SCALE: 1" = 50 feet

DATE: 11/84

AA·2

COUNTY: GUADALUPE
STATE: NEW MEXICO
BY: J. Curtis McKallip Jr.

PLATE 3

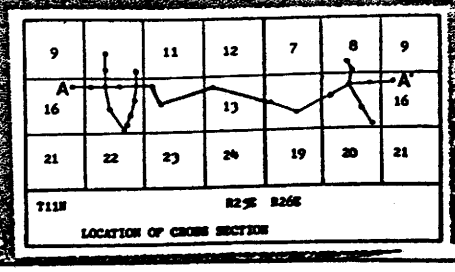

WEST

EAST

KAREN #3
S18-T11N-R26E
1800FSL 1980FEL
G.L. 4825

JEANNIE #2
S17-T11N-R26E
1980FNL 660FWL
G.L. 4771

JEANNIE #3
S17-T11N-R26E
800FNL 2310FWL
G.L. 4771

KAREN #2
S17-T11N-R26E
990FNL 660FEL
G.L. 4802

JOAN #1
S16-T11N-R26E
660FNL 990FWL
G.L. 4758

BRENDA #1
S18-T11N-R26E
1980FNL 660FWL
G.L. 4785

700'

600

700'

700'

CEMENT PATCHES

High Porosity Sandstone

800'

4'100

4000'

GR

VF

600'

500'

CEMENT PATCH

LAMINATED SANDSTONE

730'

HIGH ANGLE LAMINATIONS OF SILTSTONE
CALCITE FILLED FRACTURES

(LOW ANGLE)

OIL-SATURATED SANDSTONE
SILTSTONE CLASTS

769'

770'

816'

9		11	12	7	8	9
A 16			13			A' 16
21	22	23	24	19	20	21

T11N R25E R26E

LOCATION OF CROSS SECTION

STRUCTURAL CROSS SECTION

VERTICAL SCALE: 0 50 feet

DATE: 11/84

AA·3

COUNTY: GUADALUPE
STATE: NEW MEXICO
BY: J. Curtis McKallip Jr.

PLATE 4

DAISY #1
S10-T11N-R25E
2310FWL 1650FSL
G.L. 4498

O'CONNELL #1
S10-T11N-R25E
330FSL 2310FWL
G.L. 4518

STATE #3
S15-T11N-R25E
500FNL 2310FWL
G.L. 4516FT.

STATE #6
S15-T11N-R25E
1980FEL 1980FNL
G.L. 4545FT.

STATE #16
S15-T11N-R25E
810FSL 1650FEL
G.L. 4585FT.

NORTH

SOUTH

Oil show at 4410'-4555'

Oil show at 4516'-4625'

4200'

4100'

400'

FAULT GOUGE

TS OC416

ILD

GR

SP

10 MV

0 100 API

0 10 100 1000

Siltstone Clasts

374'

Oil in Laminations

Grey & Brown SS with calcite cement

0 1MM

416'

Calcite cement

Brown SS with some oil

Grey Mudstone

359'

9	B	11	12	7	8	9
16			13			16
21	22	B' 23	24	19	20	21

T11N R25E R26E

LOCATION OF CROSS SECTION

STRUCTURAL CROSS SECTION

VERTICAL SCALE: 0 50 feet

DATE: 11/84

BB'

COUNTY: GUADALUPE
STATE: NEW MEXICO
BY: J. Curtis McKallip Jr.

PLATE 5

ROBERTS #1
S10-T11N-R25E
330 FSL 500 FEL
G.L. 4592 FT.

STATE #11
S15-T11N-R25E
515 FNL 669 FEL
G.L. 4577 FT.

STATE #4
S15-T11N-R25E
1650 FNL 500 FEL
G.L. 4581 FT.

STATE #9
S15-T11N-R25E
1000 FEL 2400 FSL
G.L. 4580 FT.

STATE #16
S15-T11N-R25E
810 FSL 1650 FEL
G.L. 4585 FT.

STATE #15
S15-T11N-R25E
330 FSL 1650 FEL
G.L. 4574

NORTH

SOUTH

300'

4200'

400'

500'

500'

300'

4100'

600'

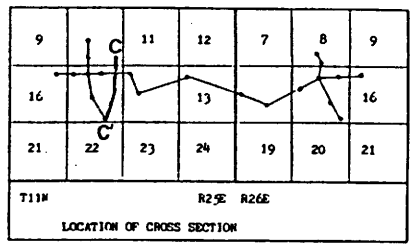

STRUCTURAL CROSS SECTION

VERTICAL SCALE: 0 50 feet

DATE: 11/84

CC'

COUNTY: GUADALUPE
STATE: NEW MEXICO
BY: J. Curtis McKallip Jr.

PLATE 6

BERYL #1
S 2-T11N-R26E
1980 FWL 1650 FSL
G.L. 4762

KAREN #1
S8-T11N-R26E
330 FSL 2310 FWL
G.L. 4777

JEANNIE #5
S17-T11B-R26E
800 FNL 2145 FWL
G.L. 4759

BARBARA #1
S17-T11N-R26E
2030 FSL 2030 FEL
G.L. 4775

BARBARA #2
S17-T11N-R26E
660 FSL 660 FEL
G.L. 4768

NORTH

SOUTH

4100'

4000'

700'

800'

900'

FAULT GOUGE

Broken up siltstone

OF VF

OF & CF VF

OF 70°

OF 45°
80°

100 10 1 0.1
Permeability (md.)

0 API Units 100
Gamma Ray

30% 20% 10% 0%
Porosity (Core)

20 mv.
SP

0 Ohm meters / meter² 100
Resistivity (short normal)

0 Ohm meters / meter² 100
Resistivity (6FF40)

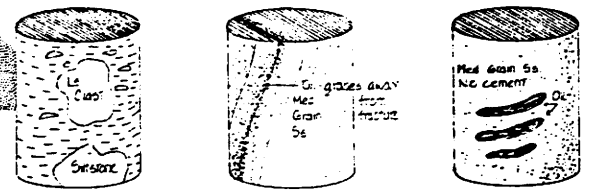

865' 892' 902'

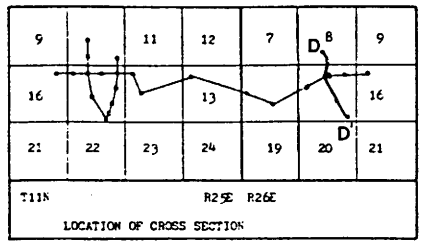

STRUCTURAL CROSS SECTION

VERTICAL SCALE: 0 50 feet

DATE: 11/84

DD'

COUNTY: GUADALUPE
STATE: NEW MEXICO
BY: J. Curtis McKallip Jr.

PLATE 7

BARBARA #1
S17-T11N-R26E
2030 FSL 2030 FEL
G.L. 4775

HUMBLE 6-33-17
1980' S & E L
GL 4772'

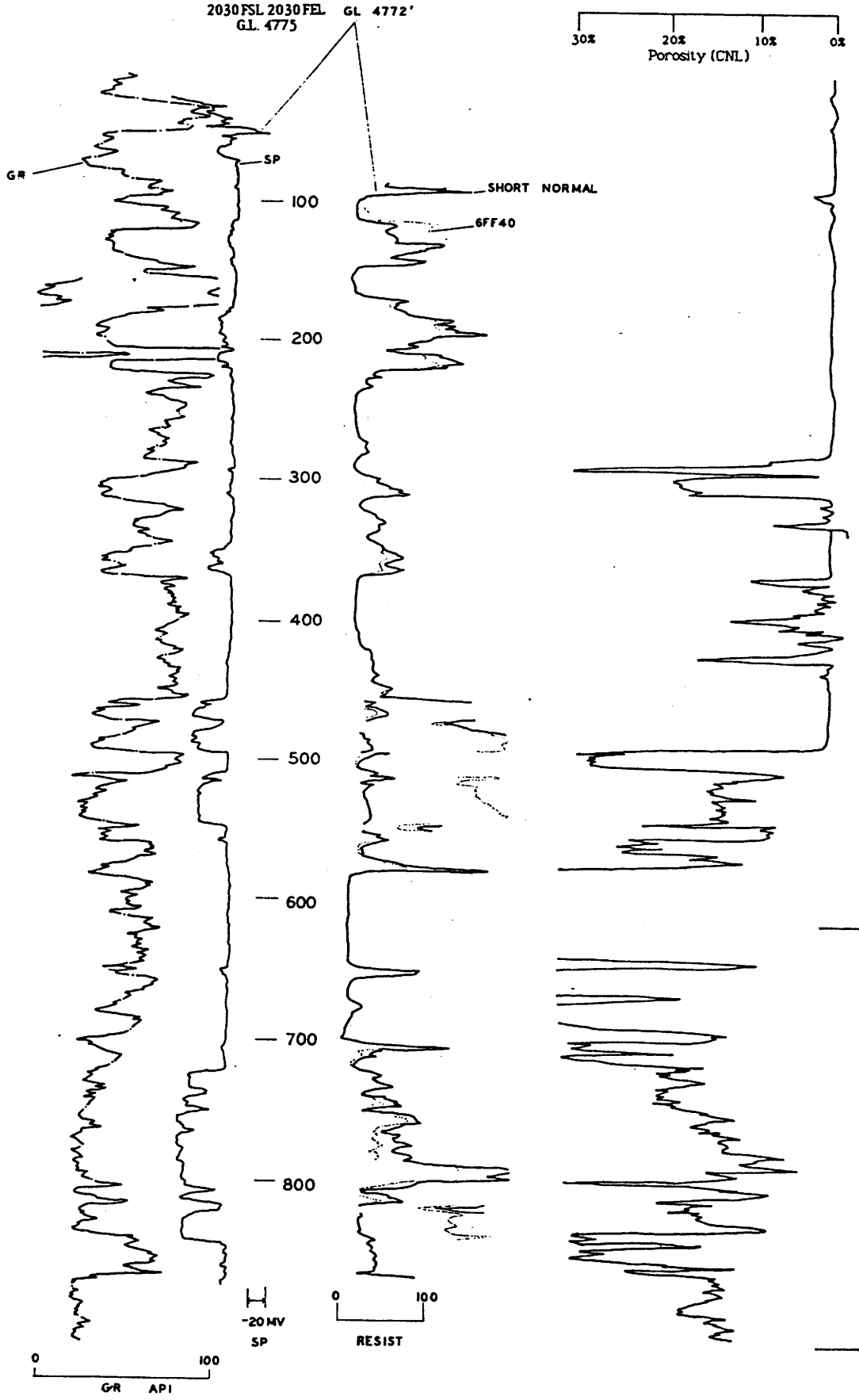

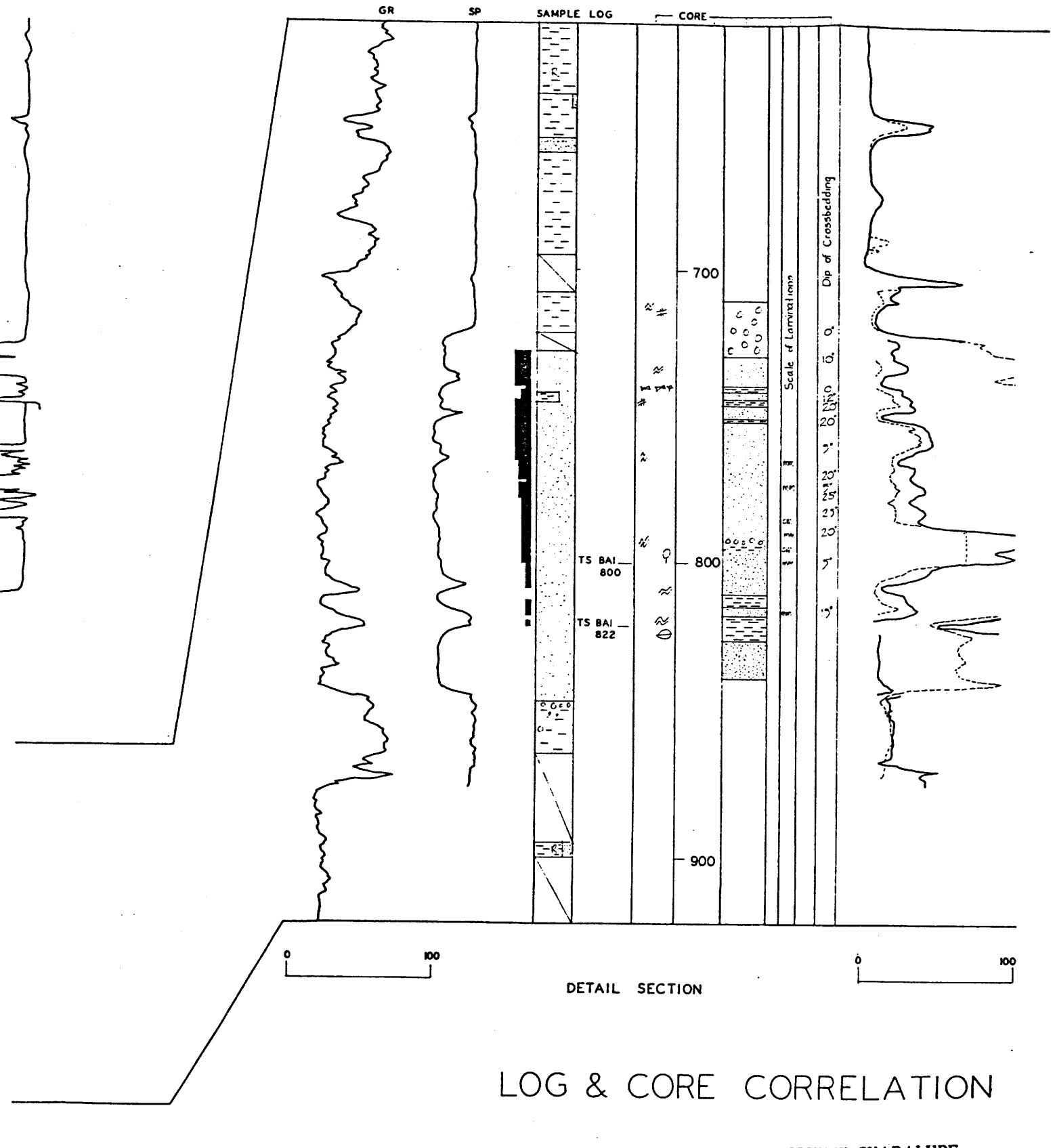

LOG & CORE CORRELATION

COUNTY: GUADALUPE
STATE: NEW MEXICO
BY: J. Curtis McKallip Jr.

PLATE 8

NORTH

EAST

WEST

SOUTH

JEANNIE #4
S17-T11N-R26E
635 FNL 2145 FWL
G.L. 4763

JEANNIE #3
S17-T11N-R26E
800 FNL 2310 FWL
G.L. 4771

JEANNIE #5
S17-T11N-R26E
800 FNL 2145 FWL
G.L. 4759

JEANNIE #1
S17-T11N-R26E
800 NL 1980 WL
G.L. 4746

JEANNIE #6
S17-T11N-R26E
965 FNL 2145 FWL
G.L. 4753

600

700

0 API Units 100
Gamma Ray

30% 20% 10% 0%
Porosity (CNL)

+4100 FT.

+4000 FT.

LOCATION MAP
EAST SIDE PILOT
NEWKIRK FIELD

△ STEAM INJECTION WELL
□ PRODUCING WELL
◇ OBSERVATION WELL

4 □
1 □ 5 △ 3 □
6 □

"JEANNIE"

N

0 500'

FENCE DIAGRAM
OF: EAST SIDE PILOT

VERTICAL SCALE: 30'
HOR. SCALE: 20'
DATE:

COUNTY: GUADALUPE
STATE: NEW MEXICO
BY: J. Curtis Mckallip Jr.

PLATE 9

OPEN HOLE COMPLETION

NORTH

EAST

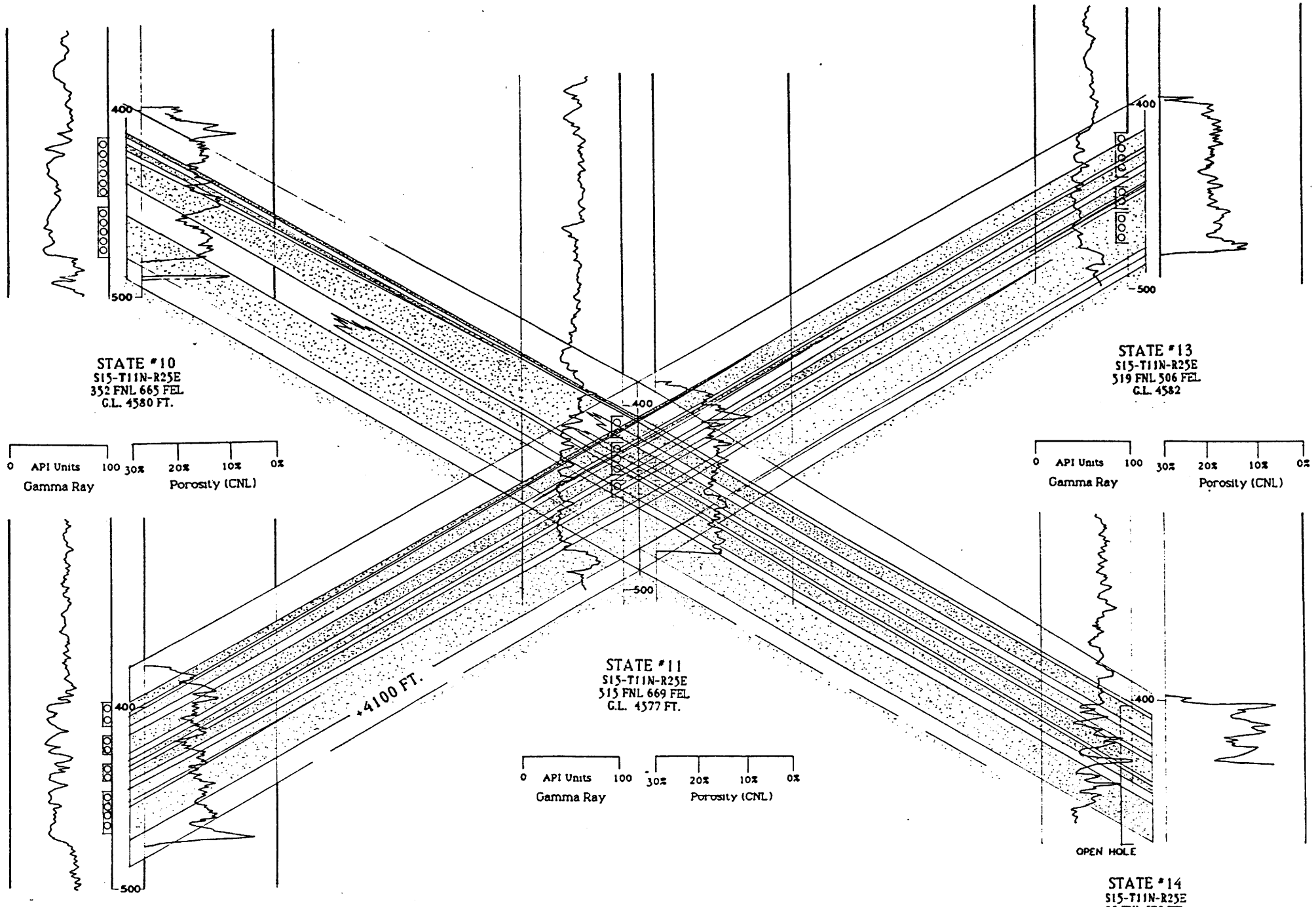

SOUTH

WEST

FENCE DIAGRAM
OF: WEST PILOT

VERTICAL SCALE: 30'
HOR. SCALE: 20'
DATE: 7-84

COUNTY: GUADALUPE
STATE: NEW MEXICO
BY: J. Curtis Mckallip Jr.

LEGEND:
- SANDSTONE
- MUDSTONE
- PERFORATIONS

LOCATION MAP
WEST SIDE PILOT
NEWKIRK FIELD

- STEAM INJECTION WELL
- PRODUCING WELL
- OBSERVATION WELL

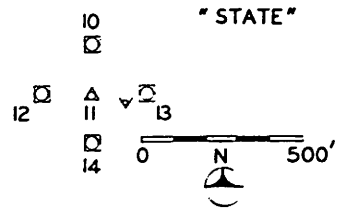

PLATE 10

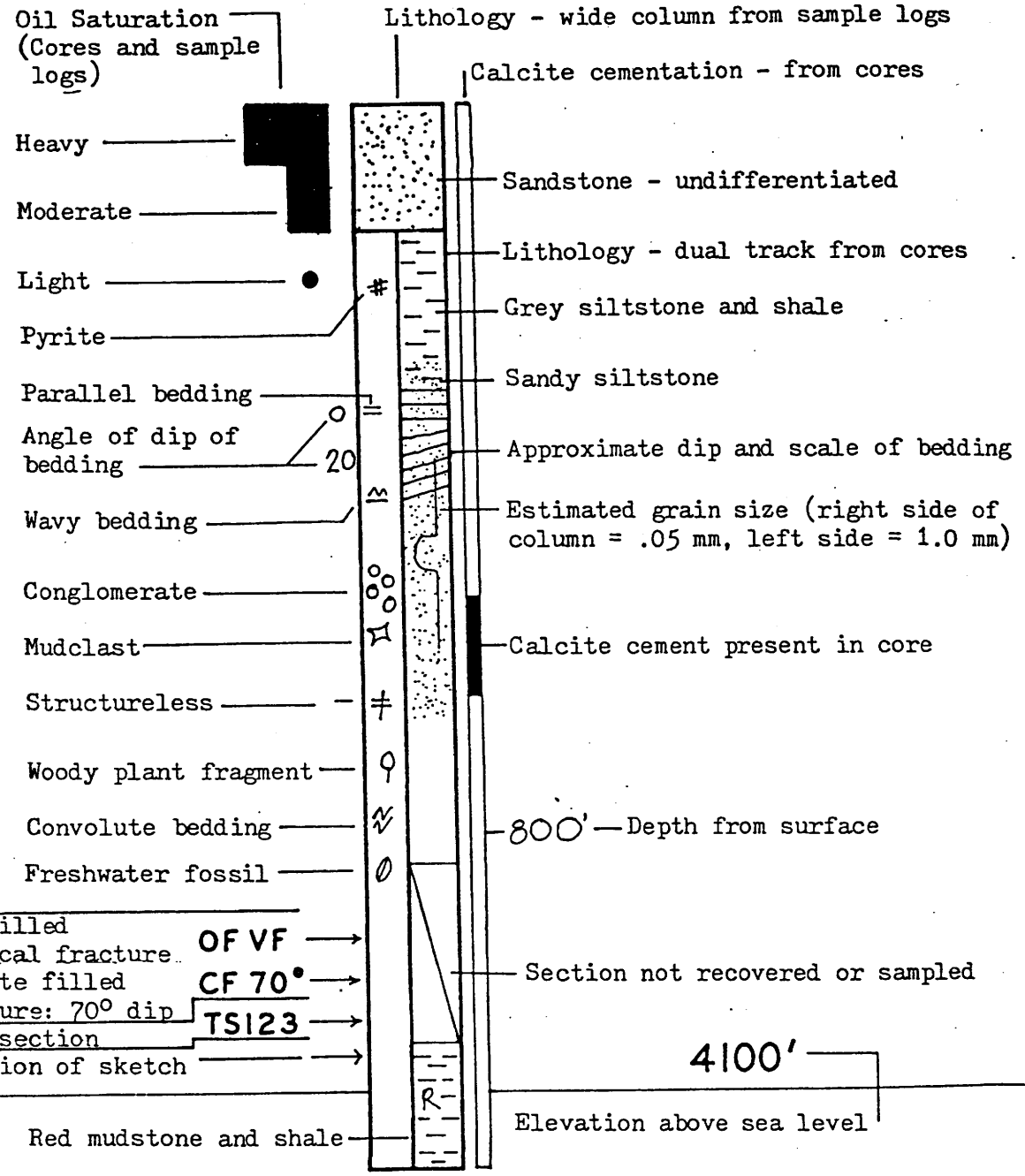

LEGEND

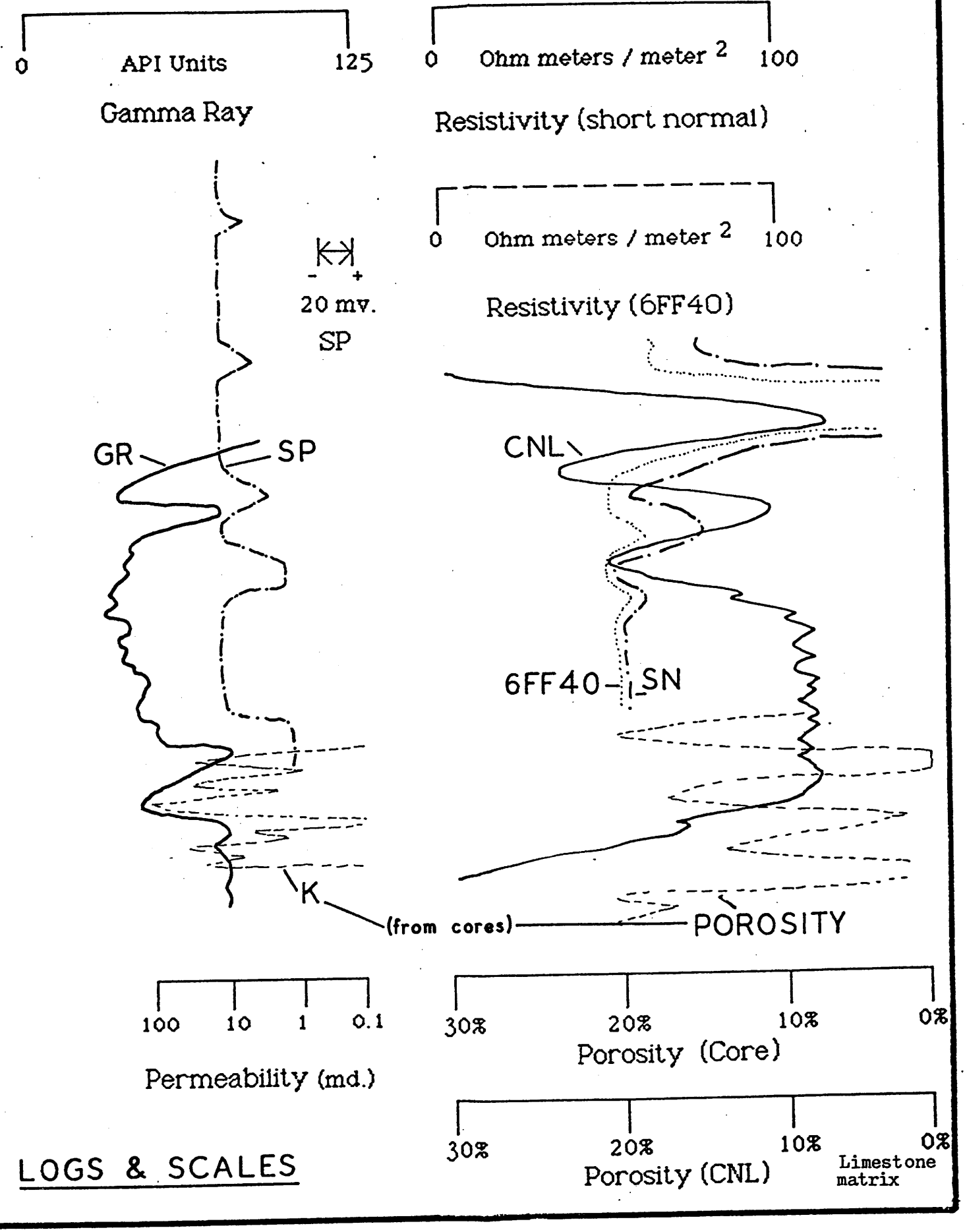

LOGS & SCALES

PLATE II

Fig. 13a markl.mp
Markov Analysis: (after Miall and Gibling, 1978)
Newkirk Cores

Lithofacies (after Miall, 1978a)

	Gm	Sr	Sh	Sl	Se	Fl	Fsc	Fm	Total
Gm (long. bars, lag, sieve)	0	0	0	0	0	1	0	0	1
Sr (ripples (LFR)	0	0	1	0	0	4	0	0	5
Sh (planar bed: LFR & UFR)	1	2	0	2	4	17	1	0	27
Sl (scour fill, splays)	0	2	0	0	1	11	0	0	14
Se (scour fills)	0	0	7	1	0	6	1	0	15
Fl (overbank deposits)	0	0	18	8	9	0	3	0	38
Fsc (backswamp deposits)	0	1	1	2	1	0	0	0	5
Fm (overbank & drape)	0	0	0	0	0	2	0	0	2
	1	5	27	13	15	41	5	0	107

Fig. 13b:

Probability matrix	Gm	Sr	Sh	Sl	Se	Fl	Fsc	Fm	Total
Gm (long. bars, lag, sieve)	0%	0%	0%	0%	0%	100%	0%	0%	100%
Sr (ripples (LFR)	0%	0%	20%	0%	0%	80%	0%	0%	100%
Sh (planar bed: LFR & UFR)	4%	7%	0%	7%	15%	63%	4%	0%	100%
Sl (scour fill, splays)	0%	14%	0%	0%	7%	79%	0%	0%	100%
Se (scour fills)	0%	0%	47%	7%	0%	40%	7%	0%	100%
Fl (overbank deposits)	0%	0%	47%	21%	24%	0%	8%	0%	100%
Fsc (backswamp deposits)	0%	20%	20%	40%	20%	0%	0%	0%	100%
Fm (overbank & drape)	0%	0%	0%	0%	0%	100%	0%	0%	100%
Totals:	1%	5%	25%	12%	14%	38%	5%	0%	107

LIBRARY
SOCORRO, N.M.

Fig. 14a
Newkirk Field Cores
Difference Matrix

	Gm	Sr	Sh	Sl	Se	Fl	Fsc	Fm	Totals:
Gm (long. bars, lag, sieve)	-1%	-5%	-25%	-12%	-14%	61%	-5%	0%	-1%
Sr (ripples (LFR)	-1%	-5%	-6%	-13%	-15%	40%	-5%	0%	-5%
Sh (planar bed: LFR & UFR)	2%	1%	-34%	-9%	-4%	12%	-3%	0%	-34%
Sl (scour fill, splays)	-1%	9%	-29%	-14%	-9%	34%	-5%	0%	-15%
Se (scour fills)	-1%	-5%	17%	-7%	-16%	-5%	1%	0%	-16%
Fl (overbank deposits)	-1%	-7%	8%	2%	2%	-59%	1%	0%	-55%
Fsc (backswamp deposits)	-1%	15%	-6%	27%	5%	-40%	-5%	0%	-5%
Fm (overbank & drape)	-1%	-5%	-26%	-12%	-14%	61%	-5%	0%	-2%
Totals:	-5%	-2%	-101%	-38%	-65%	104%	-25%	0%	-133%

Fig. 14b Chi - Square Test
Newkirk Field Cores
X - Square Calculation

	Gm	Sr	Sh	Sl	Se	Fl	Fsc	Fm	Totals:
Gm (long. bars, lag, sieve)	0	0	0	0	0	1	0	0	0.9592568
Sr (ripples (LFR)	0	0	-0	0	0	3	0	0	2.7120069
Sh (planar bed: LFR & UFR)	1	1	0	-1	0	8	-0	0	9.7400378
Sl (scour fill, splays)	0	2	0	0	-1	8	0	0	9.4597247
Se (scour fills)	0	0	4	-1	0	0	0	0	4.3169296
Fl (overbank deposits)	0	0	11	4	5	0	2	0	22.02688
Fsc (backswamp deposits)	0	1	-0	2	0	0	0	0	3.9600253
Fm (overbank & drape)	0	0	0	0	0	2	0	0	1.9185135
Totals:	1.376992	4.610317	15.175068	5.1912652	4.62176	22.421826	1.6961459	0	55.093374

Total X Square Value: 110.18675
for 41 degrees of freedom

Fig. 15a: mark2.mp
Markov Analysis: (after Miall and Gibling, 1978)
Solvex Cores

Lithofacies (after Miall, 1978a)

	Gm	Sr	Sh	Sl	Se	Fl	Fsc	Fm	Total
Gm (long. bars, lag, sieve)	0	0	6	1	0	0	3	0	10
Sr (ripples (LFR)	0	0	0	0	0	0	0	0	0
Sh (planar bed: LFR & UFR)	1	0	0	21	0	1	19	0	42
Sl (scour fill, splays)	0	0	17	0	0	0	6	0	23
Se (scour fills)	0	0	0	0	0	0	0	0	0
Fl (overbank deposits)	0	0	1	0	0	0	0	0	1
Fsc (backswamp deposits)	9	0	20	2	0	0	0	0	31
Fm (overbank & drape)	0	8	19	0	0	2	0	0	29
	10	8	63	24	0	3	28	0	136

Fig. 15b:
Probability matrix

	Gm	Sr	Sh	Sl	Se	Fl	Fsc	Fm	Total
Gm (long. bars, lag, sieve)	0%	0%	60%	10%	0%	0%	30%	0%	100%
Sr (ripples (LFR)	0%	0%	0%	0%	0%	0%	0%	0%	0%
Sh (planar bed: LFR & UFR)	2%	0%	0%	50%	0%	2%	45%	0%	100%
Sl (scour fill, splays)	0%	0%	74%	0%	0%	0%	26%	0%	100%
Se (scour fills)	0%	0%	0%	0%	0%	0%	0%	0%	0%
Fl (overbank deposits)	0%	0%	100%	0%	0%	0%	0%	0%	100%
Fsc (backswamp deposits)	29%	0%	65%	6%	0%	0%	0%	0%	100%
Fm (overbank & drape)	0%	28%	66%	0%	0%	7%	0%	0%	100%
Totals:	7%	6%	46%	18%	0%	2%	21%	0%	100%

Fig. 16a:
Solvex Cores
Difference Matrix

	Gm	Sr	Sh	Sl	Se	Fl	Fsc	Fm	Totals:
Gm (long. bars, lag, sieve)	-8%	-6%	10%	-9%	0%	-2%	8%	0%	-8%
Sr (ripples (LFR)	-7%	-6%	-46%	-18%	0%	-2%	-21%	0%	-100%
Sh (planar bed: LFR & UFR)	-8%	-9%	-67%	24%	0%	-1%	15%	0%	-45%
Sl (scour fill, splays)	-9%	-7%	18%	-21%	0%	-3%	1%	0%	-20%
Se (scour fills)	-7%	-6%	-46%	-18%	0%	-2%	-21%	0%	-100%
Fl (overbank deposits)	-7%	-6%	53%	-18%	0%	-2%	-21%	0%	-1%
Fsc (backswamp deposits)	20%	-8%	5%	-16%	0%	-3%	-27%	0%	-30%
Fm (overbank & drape)	-9%	20%	7%	-22%	0%	4%	-26%	0%	-27%
Totals:	-37%	-27%	-67%	-98%	0%	-11%	-90%	0%	-330%

Fig. 16b:

Solvex Cores
X - Square Calculation

	Gm	Sr	Sh	Sl	Se	Fl	Fsc	Fm	Totals:
Gm (long. bars, lag, sieve)	0	0	2	-1	0	0	1	0	2.1136159
Sr (ripples (LFR)	0	0	0	0	0	0	0	0	0
Sh (planar bed: LFR & UFR)	-1	0	0	22	0	0	15	0	35.77648
Sl (scour fill, splays)	0	0	8	0	0	0	1	0	9.3633617
Se (scour fills)	0	0	0	0	0	0	0	0	0
Fl (overbank deposits)	0	0	1	0	0	0	0	0	0.7695202
Fsc (backswamp deposits)	12	0	7	-2	0	0	0	0	16.972591
Fm (overbank & drape)	0	12	7	0	0	2	0	0	21.229263
Totals:	11.232165	12.362872	23.476663	19.290069	0	2.3561609	17.506901	0	86.224832

Total X Square Value: 172.44966
for 41 degrees of freedom

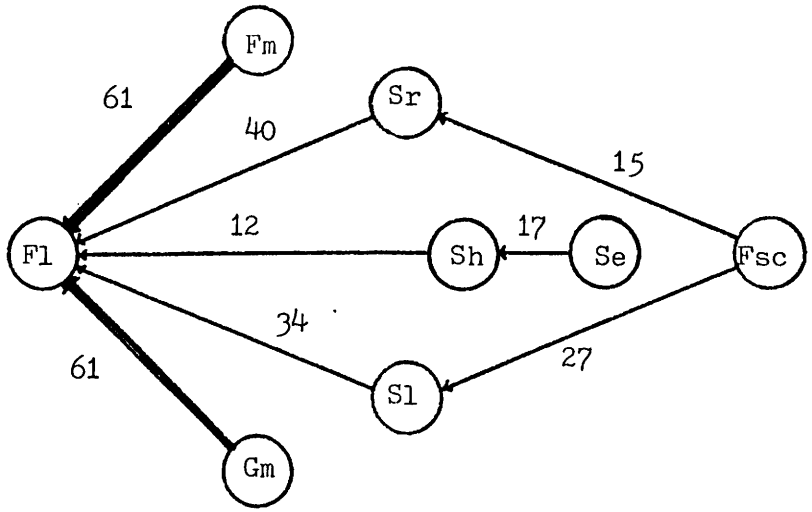

Newkirk Field: Upper Santa Rosa Sandstone

Difference Matrix Diagram

(Numbers are percentages greater than 10% from Fig. 14a.)

Fig. 17

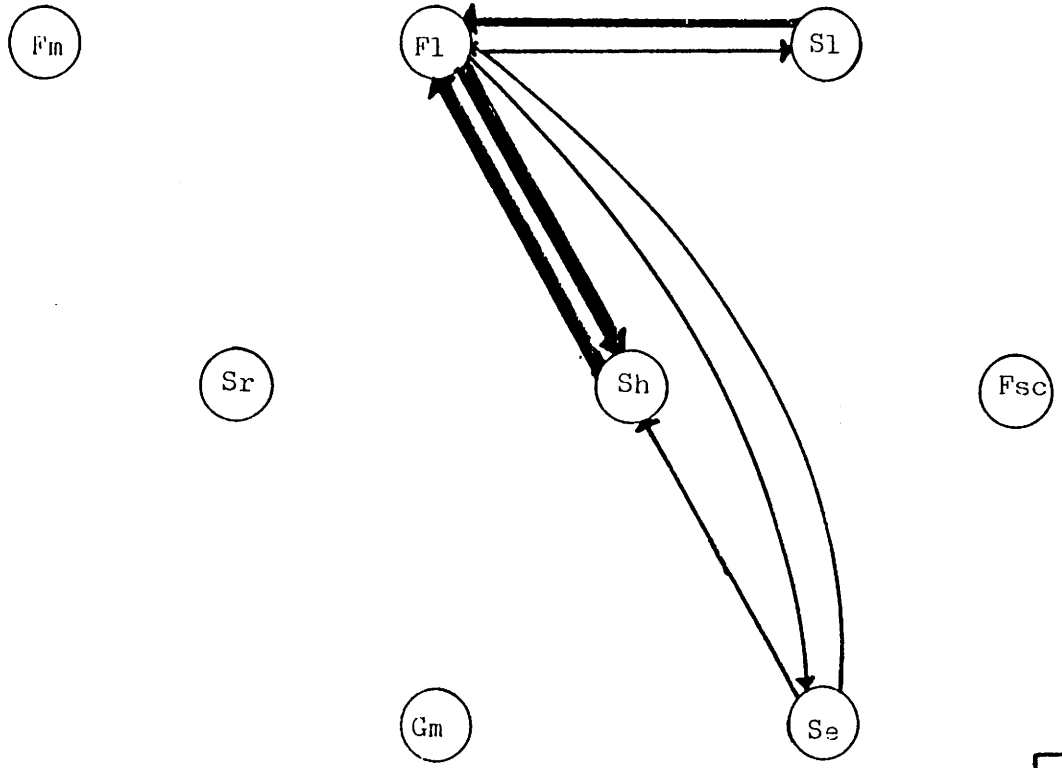

15 - 20

10 - 15

5 - 10

0 - 5 (not shown)

Number of transitions (n=107)

Newkirk Field: Upper Santa Rosa Sandstone

Strength Diagram

(Transitions from Fig. 13a)

Fig. 18

CHAPTER FIVE

Comparisons with Modern Environments

Miall lists six principal lithofacies assemblage models for low sinuosity, multiple channel rivers. The model which most closely fits the observed facies patterns of the Santa Rosa Sandstone is the Bijou Creek type with major facies Sh (lower and upper flow regime) and Sl (fine sand with low angle crossbeds representative of scour fills.) The environmental setting for the Bijou Creek type is ephemeral or perennial rivers subject to flash floods (Miall, 1981).

Bijou Creek, Colorado

The Bijou Creek type is named for Bijou Creek, Colorado (McKee et al., 1967) which drains an area of 1444 square miles underlain by the Pierre Shale, Fox Hills Sandstone, and Laramie Formation of the Late Cretaceous series. These formations consist of shales, sandy shales, sandstones, and lignitic coal beds with little coarse material. Annual precipitation ranges widely about an average of 13 inches per year. McKee et al. (1967) studied the deposition of sand during flood and found that it consisted of 90% horizontal strata with minor amounts of tabular planar crossbedding at the outer edges of the flood sheets. Local climbing ripple laminae and convolute bedding formed during waning stages of the flood and are characteristic of relatively sheltered areas away from the path of the main flood. Erosional

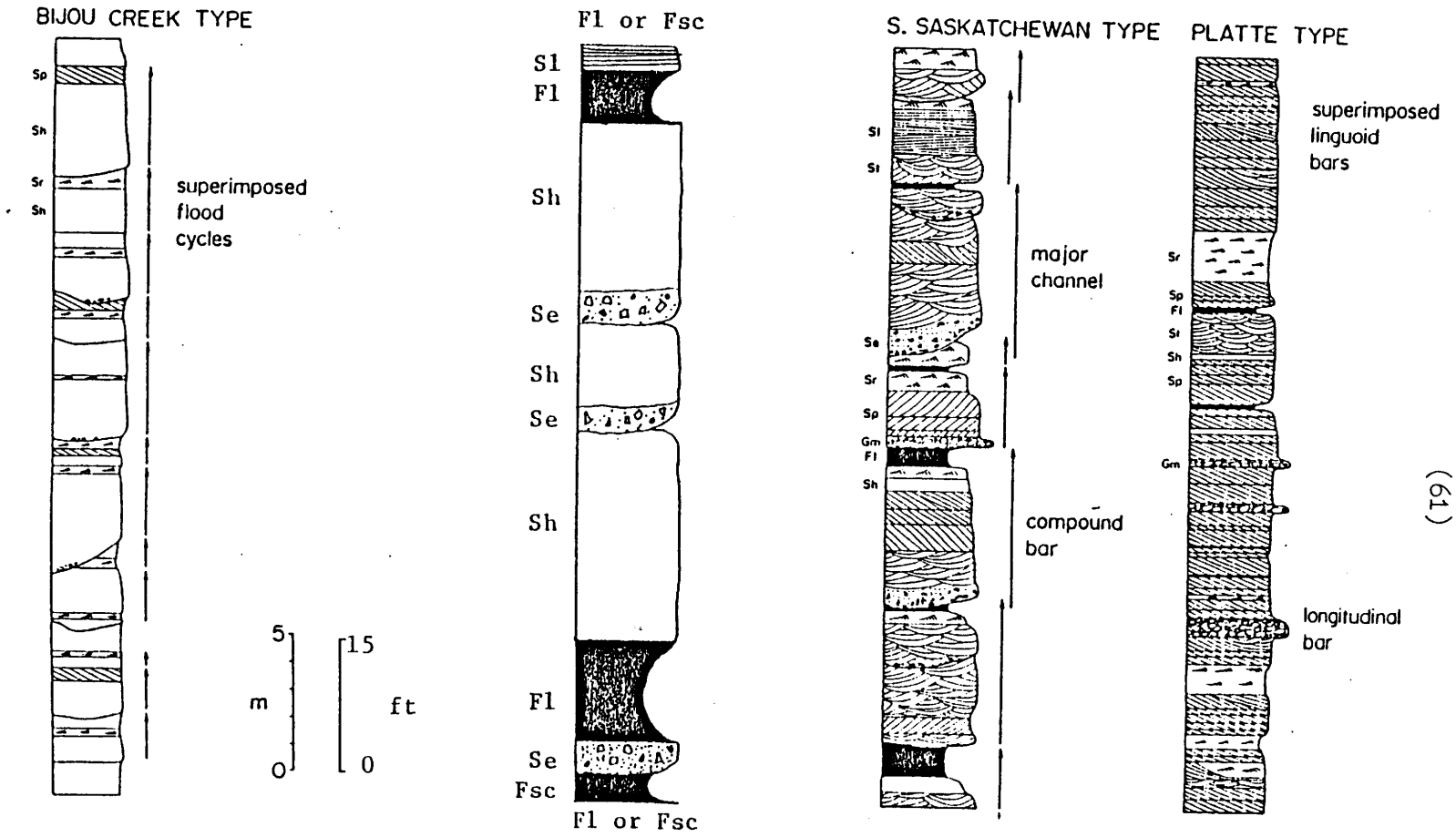

Newkirk Field, N.M.

Fig. 19: Generalized vertical profiles compared (Miall, 1978 and this paper)

surfaces and soft sediment deformation structures were rare. A comparison of typical vertical sequences in the Newkirk cores with that of the Bijou Creek and other types is shown in Fig. 19. The flood occurred in two stages and the waning phases at the end of each stage are characterized by climbing ripple laminae. Convolute laminae were developed during late flood stages during lower flow regime conditions and represent a time when the sediment was in a quicksand-like state.

The flood sheets were deposited 0.25 to 0.5 mile beyond the banks on each side of the stream and averaged two to three feet thick with a maximum of 12 feet. The dominant lithology consists of moderately well-sorted, medium-grained sand with minor amounts of fine and coarse-grained material. The flood moved large concrete slabs proving that the source area exerted control over the grain size. The mean velocity computed on the basis of a total cross-sectional area of 28,380 square feet for the channel and overbank flow was 16.4 feet per second (11.2 miles per hour). In the main channel it was computed to be 21.83 feet per second (14.9 m.p.h.). Both calculations were made using a measured peak discharge of 466,000 cubic feet per second. This volume of water was the result of rainfall rates of up to 12 inches in several hours along the upper reaches of the creek and approximately equals the amount of rain which normally falls in one year in the area. The width of the Bijou Creek channel and flood plain during years of average flow is about .25 to .75 miles and is confined by easily eroded alluvial deposits which

filled a wide valley 5 to 10 miles wide during the Pleistocene Epcoh. Loess and sand dunes are present in the area above the level of present flood plains. Cottonwood trees grow on the flood plains. The flood waters spread sand across the flood plain in a downstream direction by jumping out of the banks of the sinuous channel rather than laterally spilling over them. (See Fig. 20). The preflood surface of the flood plain was a maximum of 10 feet above the present level of the streambed. On this surface the flood deposited a sheet of sand about 800 feet wide and 1500 to 2000 feet long. Near the cutbank along the channel the flood sand ranged from 20 to 30 inches thick; a maximum thickness of 40 inches was observed about 300 feet north of the channel edge. Debris on trees suggests the flood waters reached a depth of 9 feet above the flood plain and approximately 19 feet above the stream bottom. Froude numbers for channel flow and overbank flow are 0.88 and 0.97 respectively and represent subcritical tranquil flow ($Fr < 1$).

As shown in Fig. 20, West Bijou Creek had a sinuosity of 1.33 on a scale of 1.0 for straight streams to 2.0 for highly tortuous streams (Schumm, 1963). The meander wavelength (or distance from one point of inflection to the next) was 2100 feet. The meander amplitude was 1500 feet and the channel width to depth ratio (F) varies between 1.2 and 6.6 at different locations. The average channel gradient of Bijou Creek over its 80 mile course is approximately 25 feet per mile. There may have been local changes in gradient in the study area which

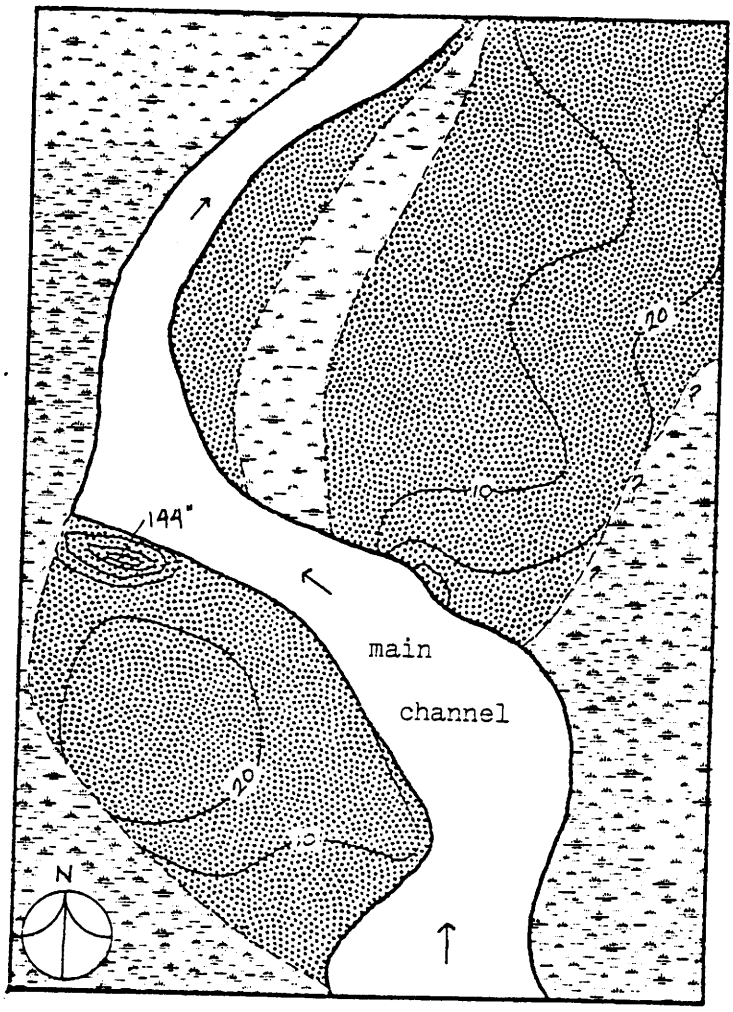

Fig. 20: West Bijou Creek, Colorado

Shaded areas are flood deposits
Contour interval - 10 inches
(modified from McKee et al, 1967)

contributed to the flooding. Channel morphology in ephemeral streams is more closely related to annual flooding events than average annual discharge.

The Santa Rosa Sandstone in the study area consists of fine and medium-grained sandstones with planar horizontal bedding and interlaminated siltstone. Convolute bedding is present. The morphology of the upper Santa Rosa is sheet-like, as well. The total thickness of the Santa Rosa is much thicker than at Bijou Creek because it is made up of intervals typically 1 to 6 feet thick separated by siltstone intervals approximately one half to 2 feet thick. This comparison suggests the upper Santa Rosa Sandstone may be a composite of sheet flood deposits separated by overbank deposits deposited during periods of normal stream flow.

Lake Eyre, Australia

The sand-bed ephemeral streams of the western Lake Eyre basin of Australia (Williams, 1971) also afford examples with striking similarity to the study area. The inland drainage over deeply weathered Mesozoic sediments and mudstones into a large fluctuating interior lake is similar to the drainage of Triassic streams in the Santa Rosa area into a shallow lake straddling the Texas - New Mexico border. Streams in both areas rise in Precambrian crystalline rocks one hundred to two hundred miles from the lake. The climate in the Lake Eyre basin is generally arid but may be subject to winter monsoonal rains of approximately 5 to 14 inches (120 - 350 mm) in one month causing stream flooding. The climate of the Triassic in the study area of

this report was warm and humid with arid cycles and wide seasonal variations possibly caused by monsoonal rains (McGowen et al., 1979) In a study covering 250,000 square kilometers Williams (1971) found that the most common bed forms preserved in channels were large-scale ripples with local longitudinal, transverse, small-scale ripples, and lingoid bars. Minor bed forms were upper flow regime plane beds and flute marks. Lower flow regime prevailed in the area. The streams drain crystalline Precambrian rocks near their headwaters and then traverse wide expanses of deeply weathered Mesozoic sandstones and mudstones. Lithofacies Sp, Sr, Fl, and Fm may be produced in waning flood stages, generating thin fining upward cycles. A thickness of sediment in excess of 1.5 meters (4.5 feet) may be deposited in a single flood. Lithofacies Se represents erosional surfaces with clasts. Sl represents low angle cross beds and dessication features may be present. All of these lithofacies are common in the cores.

A comparison between vertical sequences typical of the Bijou Creek, Lake Eyre, and Newkirk areas is presented in Fig. 21. The Newkirk cores show an oscillation between laminated sandstone and mudstone and another oscillation between these sediments and structureless sandstones. The greater abundance of finer material at Newkirk than at Bijou Creek may be a reflection of study methods. At Bijou Creek, the depth of investigation was only a few feet. At Newkirk, the interval investigated ranged from 50 to 150 feet. Also, the Newkirk Field cores represent ancient facies which may have undergone any number of cycles of erosion and

deposition as compared to the recent environments studied at Bijou Creek and Lake Eyre. Indeed, the Bijou Creek environment may not survive erosion, thus disappearing from the geologic record entirely.

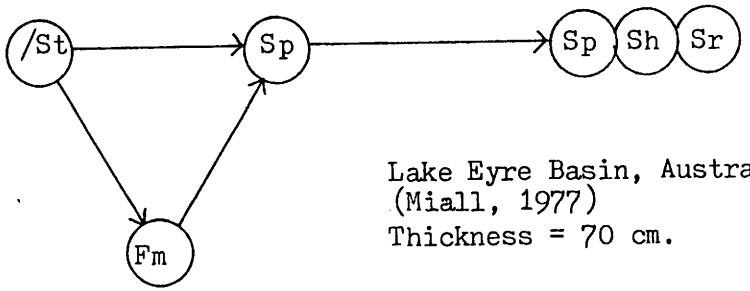

Lake Eyre Basin, Australia
(Miall, 1977)
Thickness = 70 cm.

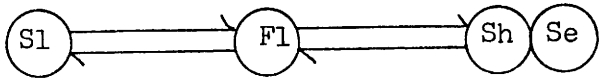

Newkirk Field Cores (Santa Rosa Ss.)

Thickness = 100 cm. - 500 cm.

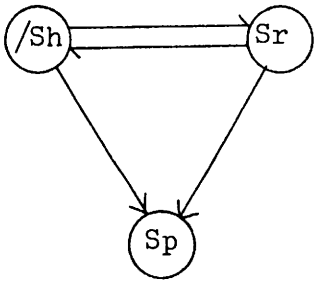

Bijou Creek, Colorado
(Miall, 1977)
Thickness = 15 - 140 cm.

Fig. 21 : Vertical Sequences

/ = major scour surface

→ = upward bed transition

Thickness given is for a typical sequence.

CHAPTER SIX

Paleoclimatology

Paleomagnetic studies show the study area moving from a few degrees south of the equator during the Upper Permian Epoch to approximately 10 degrees north of the equator during the Upper Triassic Epoch (Robinson, 1973). An arid climate during the Permian created thick sequences of evaporites in the Delaware Basin of west Texas (Miller, 1966). The climate then became more humid as suggested by the greater degree of alteration of feldspars in the Triassic Santa Rosa Sandstone (Miller, 1966 and Adams, 1929). Green (1954) suggested the climate alternated between humid and semi-arid. Dubiel (1984), in work on the Triassic Chinle Formation in southeastern Arizona, found lungfish burrows and seed ferns buried by rapid sedimentation in anastomosing stream sediments indicate a monsoonal-type climate with alternating wet and dry seasons. Diastems in Gilbert deltas there were caused by fluctuating lake levels. In the Santa Rosa Formation of Quay County, New Mexico Berkstresser and Mourant (1966) found beds of low-grade coal about 3 inches thick interbedded with beds of black clay containing clam shells. Rainfall was sufficient to maintain swampy areas and associated plant growth which formed these coals. Alternating wet and dry seasons would also provide the variable discharge generally associated with braided streams (Smith, 1970). Climatic studies

using hypothetical models show the study area would lie in an area characterized by seasonal rainfall and subhumid to semiarid conditions, depending on the elevation of the landmass (Robinson, 1973).

Geomorphology

Regional studies indicate that relief on the top of Permian sediments influenced deposition of Triassic sediments. The top of the Artesia Group was partly planed off in response to the reactivation of the Sierra Grande and Pedernal uplifts after deposition of the Permian San Andres Formation and before the onset of Dockum sedimentation (Broadhead, 1984).

The Lower Santa Rosa Sandstone was deposited over the surface of the Artesia Group in two stages. The first stage occurred as alluvial fans or fan deltas (McGowen et al., 1979) spread over the red, fine-grained sandstones and mudstones of the Artesia Group. These were followed by coarse-grained sands of a meandering alluvial system (McGowen et al., 1979) flowing generally southeast. An increase in the level of the Dockum lake centered on the Texas- New Mexico border or local lakes deposited the middle mudstone unit which formed the base upon which the upper Santa Rosa Sandstone was deposited.

The coincidence of thick-sandstone trends with underlying thin areas in the Artesia Group may be evidence of deposition of fluvial Dockum sandstones in broad valleys eroded into the Artesia Group (Broadhead, 1984). A sandstone isolith map of both upper and lower sandstone units shows east and southeast trending sandstone

bodies separated by parallel-trending muddy areas (Broadhead, 1984) which may be the result of valleys formed parallel to the paleoflow direction. Relief of these valleys was probably low because they were cut into easily eroded mudstones and fine-grained sandstones. The features discussed here were derived from studies of the lower sandstone but could apply to the upper sandstone unit as well because it was deposited by streams with the same paleoflow direction over lacustrine mudstones and sandstones of similar composition and properties.

Ablock diagram of this model is shown in Fig. 7. The proposed existence of valleys cut into mudstones implies that some of the mudstone laterally equivalent to the upper sandstone may pre-date the sandstone. Abrupt lateral facies changes are also implied and are observed as shown on Plate 3 between the State No. 11 well and the O'Connell No. 3 well. Lateral facies changes would be expected to be more abrupt perpendicular to paleoflow or from southwest to northeast in this case.

Sands undergo erosion after floods and parts of the upper cycle such as clays and silts deposited by the waning stage of the flood, are lost. The next flood will deposit sands directly on top of this erosional surface resulting in very thick sands after several cycles. Because the intervening erosional cycle is difficult to characterize, the number of flood cycles responsible for a given thickness of sand may only be estimated. Best preservation of sequences would occur in the middle of channels and topographically low areas such as abandoned channels. Miall

(1978) shows flood cycles of sand approximately 3 to 15 feet thick separated by 1 to 3 foot intervals of mud for this type of stream. Williams (1971) noted that the most common bed forms in the Lake Eyre drainage basins were large-scale catenary transverse ripples, transverse and linguoid channel bars, sinuous and lunate small-scale ripples, and lower flow regime plane beds in decreasing order of abundance. The general distribution and degree of dip of cross stratification in the Bijou Creek flood-deposits agrees with those seen in cores of the Newkirk Field. Most strata were horizontal or sub-horizontal with a few dips as high as 25 degrees. Dips greater than this such as the 75 degree dip in the Beryl No.1 or 30 degrees in the Barbara No. 2 probably result from structural or soft sediment deformations.

Miall (1981) notes that the dominant bar in sandy braided rivers is the simple foreset bar with internal planar cross-bedding, a height of 1 to 3 feet, and a length of several hundred meters. Other names for this type of bar are linguoid, transverse, lobate, and chute bars. These mesoform bars form in response to individual dynamic events such as seasonal floods. They may coalesce over a period of years to form macroform compound bars with complex internal structures composed of several types of complex cross-bedding and internal erosional surfaces. The planar crossbedding seen in cores of the Barbara No. 1 well (Fig. 5b) at 785 ft. was probably part of a foreset bar. Longitudinal facies within the braided stream channels should be influenced by the tendency of fine-grained sediments in braided stream channels

to form transverse bars as opposed to longitudinal bars for coarser sediments (Smith, 1970). This results in an increase in the ratio of planar cross-stratification to horizontal stratification when transverse bars are present. Visher (1965) suggests that fluvial sequences may be subdivided into four lithologic units. The lowest basal unit contains poorly sorted coarse clastic detritus transported by traction along the channel bottom, which occasionally occurs in the cores. The zone is occasionally found in the cores. An example is the Joan No. 1 well at 850 feet. The second zone which may be tens of feet thick, is composed of well-sorted festoon or planar cross-bedded sands associated with migrating dunes and sand waves with up to 20 feet of relief. Planar cross-bedded sands may also be associated with transverse bars as discussed above and can be seen in the Jeannie No. 3 at approximately 775 feet below the surface.

Overlying this is horizontally bedded fine sand and silt of Visher's third unit. This zone may range from a few inches to tens of feet thick and may be a product of upper flow regime as it exhibits no ripples or cross-bedding and can be seen in the Joan No. 1 well at 810 ft. to 820 ft. below the surface and in core photos of the Barbara No. 1 from 730 ft. to 738 ft. (Fig. 5a).

The topmost ripple cross-laminated zone is composed of very fine sands, silts, and clays and reaches a maximum development of only a few feet. The sediments are generally deposited outside the fluvial channel except during falling flood stages. This zone

may be seen in the Roberts No. 1 well between 470 ft. and 485 ft. and in the Barbara No. 1 from 742 ft. to 745 ft.. The Roberts No. 1 well appears to be near the bank of the fluvial channel of the upper sand because of its lack of sand.

CONCLUSION

The vertical lithofacies sequences observed in cores of the upper Santa Rosa Sandstone in the Newkirk field indicate that it was deposited in a braided stream environment subject to seasonal flooding similar to the conditions which prevail today at Bijou Creek, Colorado. Oil migrated into permeable laminae of the sandstone before calcite cementation became widespread. Burial of the sequence occurred after calcite had filled the pore space, preventing significant compaction. Fracturing occurred in several different episodes due to compaction, structural movement, and slumping.

Implications for Petroleum Exploration

A viable exploration strategy in the Newkirk area would take the following issues into consideration:

Oil or gas? If oil is sought, where is the gravity of the oil likely to be high enough for it to be produced by conventional methods? This question requires knowledge of geothermal gradients, source material, and maturity. Traps in Pennsylvanian rocks might yield producible oil whereas shallower formations may yield heavy oils similar to that at Newkirk. Locating areas where sediments have been buried to sufficient depths for thermal maturation to occur is very important. A basin study should attempt to locate sediments deposited in environments conducive to the production and preservation of large amounts of organic matter. Geochemical studies of the North

Sea, Syrte Basin (North Africa), and Gippsland Basin (Southeast Australia) (DeMaison, 1984) show that the largest fields consistently occur where organic-rich sediments have been buried to optimum depths for oil generation.

Type of trap? Whether the anticline at Newkirk is due to tectonic movement of the Precambrian horst or due to dissolution of Permian evaporites or both would have major implications for prospective traps above the Permian. Stratigraphic traps formed by pinchouts and unconfomities are other possible exploration targets. If heavy oil is predicted, permeabilities need to be high enough to permit production by conventional means.

Diagenesis? The Glorieta sandstone is medium-grained but appears to be well cemented and no shows were reported in it in the Trans-Pecos Latigo Ranch Unit 1, Well A (S2 T9N R23E) that had shows in shales, sands, and evaporites nearby. This implies that some prospective reservoir rocks may be cemented and form poor reservoirs.

Timing of trap formation and oil migration? Oil migrated into Newkirk field in several episodes which probably began in Jurassic time. Migration pathways through underlying shales were probably fractures which formed by tectonic movement or compaction of sediments. Calcite cementation which began shortly before oil migrated into the trap reduced the porosity slightly in some parts of the sandstone. Oil has leaked from the trap into the Cuervo sandstone (Plate 2, State No. 3 and State No. 5) indicating that fracturing of the intervening mudstones is

allowing oil to escape from the trap. Source rocks for the oil lie directly beneath the field and may be in either Permian or Pennsylvanian formations. This model implies that traps formed after the Jurassic or early Cretaceous may not contain oil or will contain oil which has spilled from earlier traps. Alternately, oil may have been generated during the Cenozoic. Further checking of this model and construction of a similar one for future exploration targets should be done.

Suggestions for Future Work

The depositional environment of the Santa Rosa Sandstone should be further studied by examining cores from the M.A.J.A. Mining Company cores stored with the New Mexico Bureau of Mines Several thousand feet of small diameter cores were taken from the Santa Rosa tar sands deposit in the Santa Rosa Sandstone and could be studied by the methods of Miall (1982) used in this paper. These cores were looked at briefly in preparation of this study and appeared to be composed of the same lithofacies present at the Newkirk field.

Geochemical studies of the oil from Newkirk should be compared with that of the Santa Rosa tar sands. Comparison with geochemical studies of source rocks is needed to establish the origin of the oil. Further geochemical studies of cores from the region are needed to pinpoint potential source rocks and maturity gradients. Reconstruction of depositional environments of potential source beds might yield areas where source rocks are most likely to be organic rich.

Petrographic and dating work should be done on the intrusions at Newkirk and at Santa Rosa. Comparison between the two and basalt flows in the region would yield interesting clues to the tectonic movements in the area.

REFERENCES CITED

Adams, J.E., 1929, Triassic of west Texas: American Association of Petroleum Geologists, Bulletin, v. 13, p. 1045-1055.

Beerbower, J.R., 1978, Cyclothems and cyclic depositional mechanisms in alluvial plain sedimentation: In D.F. Merriam, ed., Cyclic Sedimentation, Geol. Surv. Kansas Bull. 169, p. 31-42.

Berkstresser, C.F., Jr. and Mourant, W.A., 1966, Groundwater resources and geology of Quay County, New Mexico: New Mexico Bur. Mines and Min. Res. Groundwater Report 9, 115 p.

Berner, R.A., 1970, Sedimentary pyrite formation: American Journal of Science, v. 268, p. 1-23.

Broadhead, R.F., 1984, Subsurface petroleum geology of Santa Rosa Sandstone (Triassic), northeast New Mexico: New Mexico Bureau of Mines and Mineral Resources, Circular 193, 23 pp.

Budding, A.J., 1979, Geology and oil characteristics of the Santa Rosa tar sands, Guadalupe County, New Mexico: New Mexico Energy Research and Development Program, Report EMD 78-3316, 19 pp.

Cambell, C.V., 1976, Reservoir geometry of a fluvial sheet sandstone: American Association of Petroleum Geologists, Bulletin, v. 50, no. 7., pp. 1009 - 1020.

Camp, W.H., 1956, Forests of the past and present. In: A world geography of forest resources, edited by Haden-Guest and others, pp. 13-47. Am. Geog. Soc., Spec. Pub. 33, Ronald Press, N.Y.

Cartmill, J.C., 1976, Obscure nature of petroleum migration and entrapment: American Association of Petroleum Geologists, Bulletin, v. 60, p. 1520-1530.

Chepilov, K.R., Ermolova, E.P. and Orlova, N.A., 1959, Epigenetic minerals as indicators of time arrival of petroleum into commercial sand reservoirs. Dokl. Akad. Nauk S.S.S.R. v. 125, p. 1097-1099.

Colbert, E.H. and Gregory, J.T., 1957, Correlation of continental Triassic sediments by vertebrate fossils: Geological Society America, Bulletin, v. 68, pp. 1456-1467.

Core Labs, 1980, Screening tests for thermal oil recovery: Core Labs, Inc., confidential report to Public Lands Exploration, Inc., August 12, 1980.

Darton, N.H., 1921, Geologic structure of parts of New Mexico: U.S. Geol. Survey Bull. 725-E, p. 173-276.

Davis, J.C. and Cocke, J.M., 1972, Interpretation of complex lithologic associations by substitutability analysis: in Cubitt, J.M. and Henley, S., Statistical Analysis in Geology:,1978, Dowden, Hutchinson, & Ross, Inc., Pa., pp. 262-287.

DeMaison, G., 1984, The generative basin concept: In DeMaison, G. and Murris, R.J. eds, Petroleum geochemistry and basin evaluation: American Association of Petroleum Geologists, Memoir 35, pp. 1-14.

Downey, Marlan W., 1984, Evaluating seals for hydrocarbon accumulations: American Association of Petroleum Geologists, Bulletin, v. 68, no. 11, pp. 1752-1763.

Dubiel, R.F., 1984, Evidence for wet paleoenvironments, Upper Triassic Chinle Formtation, Utah: talk given at 37th annual meeting of Rocky Mtn. Section, G.S.A.

Flugel, E., 1982, Microfacies analysis of limestones: Springer-Verlag, New York, p. 42-46.

Folk, R.L., 1961, Petrology of sedimentary rocks: Univ. Texas, Hemphills, Austin, 184 p.

Foster, R.W., Frentress, R.M., and Riese, W.C., 1972, Subsurface geology of east-central New Mexico: New Mexico Geological Society, Special Publication 4, 22 pp.

Geochemical Laboratories, 1983, Geochemical service report on the Trans Pecos Latigo Ranch Block D No. 1 Well: Report to Kriti Exploration Inc., Houston, Texas, 56 p..

Gorman, J.M. and Robeck, R.C., 1946, Geology and asphalt deposits of north-central Guadalupe county, New Mexico: United States Geological Survey, Oil and Gas Investigations Preliminary Map PM 44.

Granata, F.E., 1982, Regional sedimentation of the Late Triassic Dockum Group, West Texas and eastern New Mexico: Unpub. M.S. thesis, Ausin, Univ. Texas, 198 p..

Green, F.E., 1954, The Triassic deposits of northwestern Texas: Unpub. PH.D. dissert., Texas Tech. Coll., Lubbock, 196 pp.

Gustavson, T.C., Finley, R.J. and McGillis, K.A., 1980, Regional dissolution of Permian salt in the Anadarko, Dalhart, and Palo Duro basins of the Texas Panhandle: Bur. of Econ. Geol. of Univ. of Texas Report of Investigations No. 106, 40 pp.

Hahn, A., 1971, Types of magnetic anomalies measured on land and general aspects of their geologic meaning, International Association of Geomagnetism and Aeronomy Bulletin, v. 28, p. 134-143.

Harbaugh, J. and Bonham-Carter, G., 1970, Computer simulation in Geology, Wiley, N.Y., 575 p.

Hubbert, M.K., 1953, Entrapment of petroleum under hydrodynamic conditions: American Association of Petroleum Geologists, Bulletin, v. 37, pp. 1954-2026.

Kelley, V.C., 1972, Triassic rocks of the Santa Rosa Country: New Mexico Geological Society, 23rd Field Conference, Guidebook, pp. .

Keplinger and Associates, 1980, An appraisal of estimated heavy oil recovery via steamflood from the Newkirk East and Newkirk West prospects, Guadalupe County, New Mexico: unpublished report to Public Lands Exploration Company.

Kluth, C.F. and Coney, P.J., 1981, Plate tectonics of the ancestral Rocky Mountains: Geology, v. 9, p. 10-15.

Kottlowski F.E. and Stewart, W.J., 1970, The Wolfcampian Joyita uplift in central New Mexico: New Mexico Bureau of Mines and Mineral Resources, Memoir 23, pt. I, pp. 1-31.

Krumbein, W.C. and Dacey, M.F., 1969, Markov chains and embedded Markov chains in geology: Jour. Internat. Assoc. for Mathematical Geology, v. 1, p. 79-96.

Lazurus, J., Martin, K.W., Culver, C.N., 1983, Geology, hydrology, and ore reserves on a portion of the Solv-Ex corporation tar sand lease near Santa Rosa, New Mexico: Volume I Geology and Hydrology: Unpublished report.

Lee, W.T. 1923, Erosion by solution and fill: U.S. Geological Survey, Bulletin 760-C, p. 107-121.

Lemley, K.R., 1984, Analysis and paleoenvironmental interpretation of the Abo Formation, Abo Canyon area, Valencia, Torrance, and Socorro counties, New Mexico: unpublished Masters thesis, New Mexico Institute of Mining and Technology, 91 pp.

Lupe, R., 1977, Depositional history of the Triassic Santa Rosa Sandstone, Santa Rosa, New Mexico: Geological Society of America, South-Central Section, 11th Annual Meeting, March 17-18, 1977, El Paso, Texas, p. 61.

Martin, David F., 1983, Steamflood pilot in the O'Connell Ranch Field: New Mexico Energy Research and Development Institute, Report NMERDI 2-69-3302, 70 pp.

McDowell, T.E., 1972, Geology of Los Esteros dam site: New Mexico Geological Society, 23rd Field Conference, Guidebook, pp. 178-183.

McGowen, J.H., Granata, G.E., and Seni, S.J., 1979, Depositonal framework of the lower Dockum Group (Triassic), Texas Panhandle: Texas Bur. Econ. Geol., Rept. Inv. 97, 60 pp.

McKee, E.D., Crosby, E.J., and Berryhill, H.L., 1967, Flood deposits, Bijou Creek, Colorado: J. Sed. Petrol., v. 37, p. 829-851.

McKee, E.D., and Weir, G.W., 1953, Terminology for stratification and cross-stratification in sedimentary rocks: Geol. Soc. of America Bull., v. 64, pp. 381-390.

Miall, A.D., 1973, Markov chain analysis applied to an ancient alluvial plain succession, Sedimentology, v. 20, p. 347-364.

_____, 1977, A review of the braided river depositional environment: Earth Science Reviews, v. 13, p. 1-62.

_____, 1978, Lithofacies types and vertical profile models in braided rivers: a summary; in A.D. Miall, ed., Fluvial Sedimentology, Canadian Society of Petroleum Geologists, Memoir 5, p. 597-604.

_____, 1982, Analysis of Fluvial Depositional Systems, American Association of Petroleum Geologists, Education Course Note Series #20, 76 p.

Miller, D.N., 1966, Petrology of Pierce Canyon redbeds, Delaware Basin, Texas and New Mexico: American Association of Petroleum Geologists, Bulletin Bull., v. 50, No. 2, pp. 283-307.

Morgan, A.M., 1941, Solution phenomena in New Mexico: in Symposium on relations of geology to the groundwater problems of the Southwest: American Geophysical Union Transactions, 23rd. annual meeting, pt. I, p. 27-35.

Muskat, M., 1949, Physical principles of oil production: New York, McGraw-Hill Book Co., section 6.3, p. 241-250.

Potter, P.E., Maynard, J.B., and Pryor, W.A., 1980, Sedimentology of shale, Springer-Verlag, New York, p. 55-56.

Roberts, W.H. 1978, Design and function of oil and gas traps. In: Problems of Petroleum Migration, edited by Roberts, W.H. and Cordell, R.J., American Association of Petroleum Geologists, Studies in Geology No. 10., pp. 217-240.

Roberts, J.L., 1970, The intrusion of magma into brittle rocks: in Newall, G. and Rast, N. eds., Mechanism of igneous intrusion, Gallery Press London, p. 327-328.

Robinson, P.L., 1973, Palaeoclimatology and continental drift. In: Implications of Continental drift to the earth sciences, edited by Tarling, D.H. and Runcorn, S.K., Academic Press, London., pp. 451-485.

Schumm, S.A., 1963, Sinuosity of alluvial rivers on the Great Plains: Geological Association of America, Bulletin, v. 74, pp. 1089-1100.

Scott, G., 1979, Newkirk Area heavy oil prospects: report to investors, 26 pp.

Sidwell, R., 1945, Triassic sediments in west Texas and eastern New Mexico: J. Sed. Pet., v. 15, no. 2, pp. 50-54

Sluijk, D. and Nederlof, M.H., 1984, Worldwide geological experience as a systematic basis for prospect appraisal: In DeMaison, G. and Murris, R.J. eds, Petroleum geochemistry and basin evaluation: American Association of Petroleum Geologists, Memoir 35, pp. 15-26.

Smith, N.D., 1970, The braided stream depositional environment: comparison of the Platte River with some Silurian clastic rocks, north-central Appalachians: G.S.A. Bull., v. 81, p. 2993-3014.

Stearns, D.W., 1972, Structural interpretation of fractures associated with the Bonita Fault: New Mexico Geological Society, 23rd Field Conference, Guidebook, pp. 161-64.

Till, R., 1974, Statistical methods for the earth scientist: John Wiley and Sons, New York, pp. 121 - 122.

Tomlinson, C.W., 1916, The origin of red beds: American Journal of Science, v. 24, p. 153-179.

Visher, G.S., 1965, Use of vertical profile in environmental reconstruction: American Association of Petroleum Geologists, Bulletin, v. 49, No. 1, pp. 41-61.

_____, 1969, Grain size distributions and depositional processes: J. Sed. Petr., v. 39, no. 3, p. 1074-1106.

Wash, R., 1982, Low Gravity, high viscosity oil is target of New Mexico's first pilot: Drill Bit, March, pp. 97-99.

Welte, D.H., 1965, Relation between petroleum and source rock: American Association of Petroleum Geologists, Bulletin, v. 49, no. 12, pp.

Williams, G.E., 1971, Flood deposits of the sand-bed ephemeral streams of central Australia: Sedimentology, v. 17, p. 1-40.

Williams, P. F. and Rust, B.R., 1969, The sedimentology of a braided river: J. Sed. Petr., v. 39, no. 2, p. 649-679.

Wolski, J. and Kozushko, P., 1983, General evaluation of the oil sands deposit south of Los Esteros Lake, Santa Rosa, New Mexico: Solv-Ex Corporation unpublished report.

Wright, M.D., 1959, The formation of cross-bedding by a meandering or braided stream: J. Sed. Pet., v. 29, pp. 610-615

APPENDIX A

PERMEABILITY MEASUREMENTS

PROCEDURE:

Cores were obtained from wells in the Newkirk field.

Water permeability was tested by placing a non-extracted core in a Hassler holder, and pressurizing it to an overburden pressure of 550 psi (37.4 atm.) with nitrogen. The holder was placed in a hot water bath and water formulated to match that of the injection water was pumped through it. Acknowledgements and thanks for help in performing these tests go to Joe Triana, Doug Wilson, and Zeke Sherman of the Petroleum Research and Recovery Center.

RESULTS:

TABLE 2

TEMPERATURE Centigrade	VOLUME ml.	TIME sec.	PRESSURE atmos.	VISCOSITY cp.	PERMEABILITY millidarcies
Core: Jeannie No. 3, 737 FT. Fine grained quartz arenite impregnated with oil. (Length=6.055 cm., d=2.533 cm.)					
25	2.3	300	2.42	.8937	3.4
25	2.3	300	2.42	.8937	3.4
58	3.3	300	1.84	.4832	3.5
58	3.7	300	1.84	.4832	3.9
66	7.3	600	1.90	.4293	3.3
69	3.6	300	1.9	.4117	3.12
25	3.5	300	2.79	.8937	4.5
Core: State #9, 469 FT. Medium grained quartz arenite with a show of oil. (Length=6.467 cm., d=2.533 cm.)					
25	12.0	30	0.68	.8937	675.0

Formula for calculating permeability to water:

$$k \text{ (darcies)} = \frac{[\text{Vol/Time}] * [\text{viscosity}] * [\text{length}]}{[\text{area}]\,[\text{pressure}]}$$

AIR PERMEABILITY:

Air permeabilties were measured by placing the extracted core in the Hassler holder under overburden pressure as before. Nitrogen pressure was measured with a mercury manometer and volume displaced was measured with a soap bubble tube.

PRESSURE (mm of mercury) LEFT	RIGHT	Time (sec.)	VOLUME (ml.)
Core: Jeannie No. 3, 737 ft. (extracted)			
40	60	18.9	20
37	57	20.13	20
50	70	15.42	20
50	70	15.05	20
50	70	15.9	20
50	70	15.27	20
Mean dP cm = 11.233		16.778	20

The formula used to calculate air permeability was:

$$k\ (\text{darcies}) = \frac{[\text{length}]\ [4.446*10^{6}]}{[\text{time}]\ [\text{pressleft} + \text{pressright}]\ [\text{area}]\ [130+P]}$$

k (md) = 200.67 md

JOINTING

The orientation of joints seen on the surface of the Cuervo Sandstone is shown below. Joints in the subsurface would impart a preferential direction to flow of fluids because of greater permeability along them. The following readings were taken at widely spaced locations in the field area:

Joint	Direction		
1	N45W	3	N50W
2	N50W	4	N50W

APPENDIX B

The following lists show information about wells drilled in the area by PLEI and Rio Petro. The first shows the following:

CODE: a code assigned to each well as follows:

BA	BARBARA	JE	Jeannie
BE	Beryl	JO	Joan
BR	Brenda	KA	Karen
CI	Cindy	OC	O'Connell
DA	Daisy	RO	Roberts
ST	State	SA	Samedan State
SX	State water well		

SEC: Section TWP: Township RANG: Range LOCATION: survey

GROU LEVL: ground level

TD: Total depth (ft.) TD ABS: Total depth in feet above sea level

TOP CORE: Depth to top of core (ft.) TC ABS: Top of core above sea level

BOT CORE: Depth to bottom of core BC ABS: (above sea level)

CORE: S = stored in Socorro, NM. M = stored in Midland, Tx.

SAMP: S = drilling samples available

TYPE LOGS AVAL: types of logs available:

SL = Sample log
PP = Porosity & Permeability from Core Labs
CNL = Compensated Neutron log
KPHI = Permeability and porosity in detail from Core Labs

Table 4 shows wells drilled in the area by Humble (Exxon) and other companies. Most of these wells were drilled in the 1960's. Abbreviations are the same as above.

HU = Humble core test

TABLE 3: List of P.L.E.I. and Rio Petro wells

CODE	SEC	TWP	RANG	LOCATION	GL RE OV UL	TD	TD ABS	TC COPRE	TC ABS	BC COTRE	BC ABS	COREE	SAMP	TLYOPGES	AVAL	
BA1	17	11N	26E	2030 SL 2030 EL	4775	937	3838	739	4036	859	3916	S	S	SL		CNL
BA2	17	11N	26E	660 SL 660 EL	4768	993	3775	680	4095	912	3863	S	S	SL	PP	
BE1	8	11N	26E	1650 SL 1980 WL	4762	1050	2813	762	4000	934	3828	M	S	SL	PP	
BE2	8	11N	26E	1650 SL 990 EL	4759	975	2853	815	3944	921	3838	M	-	SL	PP	
BE3												-	-			
BE4												M	-			
BR1	18	11N	26E	660 NL 1980 WL	4785	815	3023	650	4135	720	4065	M	S	SL	PP	CNL
CI1	16	11N	26E	1650 NL 980 WL				751		824		M	S			
DA1	10	11N	25E	1650 SL 2310 WL				338		456		S	-		PP	
JE1	17	11N	26E	800 NL 1980 WL	4746	840	3906	694	4091	753	4032	M	S	SL	PP	CNL
JE2	17	11N	26E	1980 NL 660 WL	4771	899	3872	708	4063	796	3975	S	-	SL	PP	
JE3	17	11N	26E	800 NL 2310 WL	4771	836	3935	701	4070	825	3946	M	-		PP	CNL
JE4	17	11N	26E	635 NL 2145 WL	4763	764	3182					-	-			CNL
JE5	17	11N	26E	800 NL 2145 WL	4759	829	3930					-	-			CNL
JE6	17	11N	26E	965 NL 2145 WL	4753	758	3995					-	-			
JO1	16	11N	26E	660 NL 990 WL	4758	900	3858	751	4007	855	3903	M	-	SL	PP	
JO2	16	11N	26E	660 NL 2310 WL	4738	925	3813	781	3957	847	3891	M	S	SL	PP	
KA1	8	11N	26E	330 SL 2310 WL	4770	866	3025	762	4008	863	3907	M	S	SL	PP	CNL
KA2	17	11N	26E	990 NL 660 EL	4802	943	3859	803	3999	887	3915	S	-	SL	PP	
KA3	18	11N	26E	1800 SL 1980 EL	4825	900	3925	730	4095	812	4013	M	S	SL	PP	
KA4	16	11N	26E	2310 NL 330 WL	4766	900	3866	750	4016	850	3916	M	S	SL		CNL
KW1												-	-			
OC1	10	11N	25E	330 SL 2310 WL	4518	443	4075	93	4425	430	4088	S	-	SL		
OC2												-	-			
OC3	14	11N	25E	500 NL 660 WL	4755	813	3942					-	-	SL		
OC4								319		439		-	-		PP	
OC5	10	11N	25E	330 SL 1650 EL				371		461		-	S		PP	
OC6	10	11N	25E	500 SL 990 WL	4480	500	3980					-	S	SL		
OC7	10	11N	25E	330 SL 1650 EL	4555	550	4005					-	-	SL		
RO1	10	11N	25E	330 SL 500 EL	4592	695	3897	457	4135	530	4062	S	-	SL		CNL
SA1	16	11N	25E	330 NL 330 EL	4484	500	3984	378	4106	387	4097	S	-	SL		CNL
SA2	16	11N	25E	990 NL 330 EL	4488	440	4048	267	4221	316	4172	-	-	SL		
ST1	15	11N	25E	540 NL 560 EL								-	-			
ST2	15	11N	25E	500 NL 1650 EL	4551	456	4095	375	4176	456	4095	M	-	SL		CNL
ST3	15	11N	25E	500 NL 2310 WL	4516	429	4087	335	4181	413	4103	M	-	SL		CNL
ST4	15	11N	25E	1650 NL 500 EL	4581	600	3981	408	4173	433	4148	-	-	SL		CNL
ST5	15	11N	25E	330 NL 990 WL	4495	454	4041	56	4439	454	4207	S	-	SL		CNL
ST6												-	-			
ST7	15	11N	25E	990 NL 990 WL	4515	445	4070	88	4427	394	4121	S	-	SL		
ST8	15	11N	25E	990 NL 990 EL	4559	500	4059	321	4238	432	4127	S	-	SL	PP	
ST9	15	11N	25E	2310 SL 990 EL				351		481		S	-		PP	
ST10	15	11N	25E	352 NL 665 EL	4579	515	4064	416		476		M	S	SL	PP	CNL KPHI
ST11	15	11N	25E	353 NL 672 EL		510		406		475		M	S	SL	PP	CNL KPHI
ST12	15	11N	25E	519 NL 832 EL	4572	510	4062	398		469		M	S	SL	PP	CNL KPHI
ST13	10	11N	25E	519 NL 506 EL	4582	492	4090					-	-			CNL
ST14	10	11N	25E	35 NL 672 EL	4578	478	4100					-	-			CNL
ST15	15	11N	25E	330 SL 1650 EL	4574	415	4159	305	4269	416	4158	M	-	SL	PP	
SX3	15	11N	25E	480 NL 2310 WL	4516	122	4394	87	4429	122	4394	-	-	SL		
SX7	15	11N	25E	20 FT FROM S3	4515	66	4449					S	-	SL		
ST16	15	11N	25E	810SL 1650EL	4585	1186						S		SL		CNL

TABLE 4

Humble & other wells

CODE	SEC	TWP	RANG	LOCATION	GL	TD	TYPE LOGS
HU225	5	6N	25E	1980 FNL 1980 FWL	4542	1018	GR
HU413	3	10N	22E	660 FSL 660 FWL	4882	740	SP Res
HUMONS1	1	11N	25E	1980 FNL 1980 FEL	4610	910	GR-Acoustic
HU447	7	11N	25E	660 FSL 660 FEL	4775	1305	" "
HU339	9	11N	25E	1910 FEL 2210 FSL	4482	848	" "
HU1410	10	11N	25E	990 FNL 660 FEL	4556	680	" "
HU2311	11	11N	25E	2210 FNL 2210 FEL	4684	848	SP - Induc
HU1113	13	11N	25E		4830	1160	" "
HU214	14	11N	25E	1980 FNL & FWL	4855	870	" "
HU1215	15	11N	25E	990 FNL 1980 FWL	4513	380	Sonic - GR
HU1415	15	11N	25E	660 FNL 660 FEL	4564	482	GR - CNL
HU4115	15	11N	25E	500 FSL 500 FWL	4509	820	GR
HU1416	16	11N	25E	730 FNL & FEL	4492	550	SP - Ind
HU4415	15	11N	25E	660 FSL & 980 FEL	4576	458	" "
HU1423	23	11N	25E		4942	1155	GR
HU1228	28	11N	25E	660 FNL 1980 FWL	4562	1095	SP - Ind
HU437	7	11N	26E	660 FSL 1980 FEL	4703	806	GR - Sonic
HU3317	17	11N	26E	1980 FSL 1980 FEL	4772	880	SP - Ind
HU3318	18	11N	26E	1980 FSL & FEL	4119	870	GR - Sonic
HU2120	20	11N	26E	1980 FNL 660 FWL	4801	870	" "
HU3413	13	14N	22E	1980 FSL 660 FEL	5172	920	GR - Sonic
HU1435	35	15N	22E	506 FNL 506 FEL	4820	484	" "
HUNEAFUS	24	11N	25E				
HW1	4	11N	25E			1235	GR
1HIGGINS	28	11N	25E				
HANKINS	15	11N	25E				

APPENDIX C

Genesis of Clays and their Effect on Steamflood Performance in the Santa Rosa Formation Guadalupe County, NM

by

Curtis McKallip Jr.

December 1983

ABSTRACT

The O'Connell Ranch steamflood project in the Triassic Santa Rosa Formation of Eastern New Mexico injects steam into a heavy oil sandstone reservoir.

Samples taken from oil well cores were examined using X-Ray diffraction and Scanning Electron Microscope techniques.

The adjacent siltstones and shales contain kaolinite, illite, and smectites or mixed layer clays. These clays exist as an overlapping, interleaved mass of flakes as identified by SEM study in contrast to the highly ordered crystalline kaolinite in the sandstone.

Previous studies indicate that kaolinite containing sandstones are sensitive to hot water, brine, and NaOH solutions. The injection of steam may interact with kaolinite and illite in the formation to reduce permeability by dispersal of clays.

INTRODUCTION

The Triassic Santa Rosa Formation in Guadalupe County, New Mexico, consists of the Upper Sand, Middle Shale, and Lower Sand members. The Upper Sand is separated from the Lower sand by a bed of grey to red siltstone (Fig. 1; Fig. 2).

Several deposits of heavy oil occur in the Upper Sand. The deposit at Santa Rosa is estimated to contain approximately 90 million barrels of oil (Budding, 1979) and the one at Newkirk, which is currently being steamflooded, 33 million barrels (Martin, 1983). The Petroleum Research and Recovery Center at Socorro, New Mexico is currently consulting on the engineering of the project. The steamflood has produced less than 100 barrels of oil since its inception two years ago. The limited success of the project can be related to several factors. The pay sand (40 ft.) thickness is insufficient to prevent heat loss, porosity (20%) and steam permeability (<60 millidarcies) restrict the flow of heavy oil (17 degrees API), and mechanical difficulties have led to a loss of consistent heat input. Low injection pressures must be maintained in order to avoid fracturing the formation (Keplinger, 1980). None of the problems of the steamflood are directly attributable to the clays in the formation. However, they are a primary factor in reducing the permeability of the reservoir and this inhibits steamflood performance.

COMPOSITE STRATIGRAPHIC SECTION

GUADALUPE CTY., NM.

FIG. 1

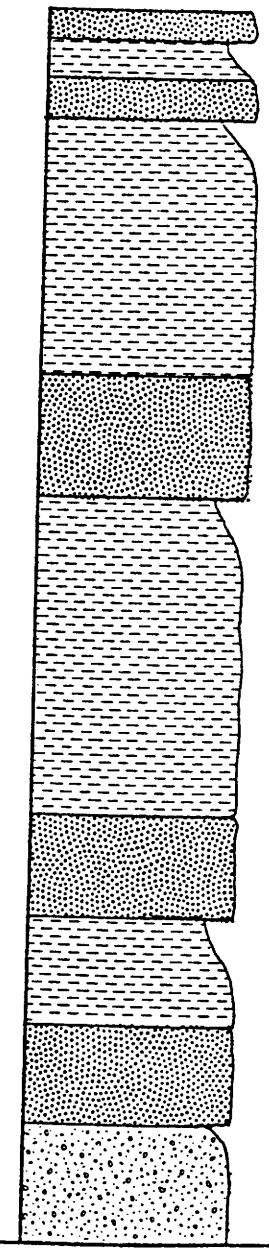

		FEET	LITHOLOGY	ENVIRONMENT (Lupe, 1977)
Triassic	Cuervo Ss.	20	MED GRAINED SS.	
		30	RED-BROWN MUDSTONE	
		30	MED-FINE SS.	
	Lower Chinle	200	RED-BROWN FINE SS.	
		100	MED-FINE Grained Ss. w/ Grey Shale	
		250	Red-Brown MUDSTONE AND Grey Shale	
Perm.	Artesia Santa Rosa Lower Shale Upper	80	Brn-Grey v. fine-fine Ss.	Fan delta
		80	Red-Grey mudstone	Prodelta Lacustrine
		80-160	Brn-Grey fine Ss.	Coarse grained meanderbelt ALLUVIAL FAN
			Red-orange Ss.	

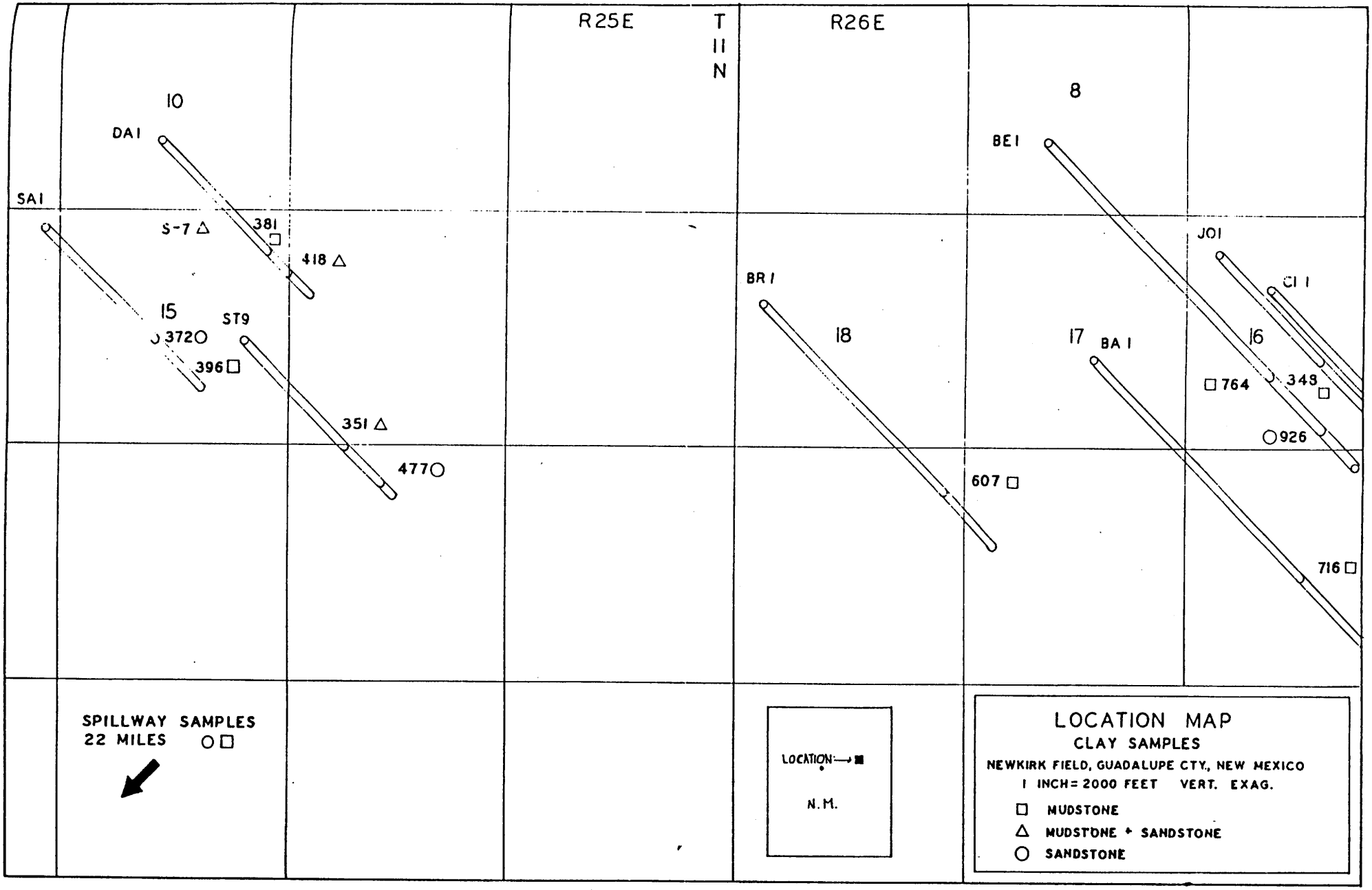
R25E
T
11
N
R26E
10
DA1
SA1
S-7 △
381 □
418 △
15
ST9
3720
396 □
351 △
4770
8
BE1
JO1
CI 1
BR 1
18
17
BA 1
16
□ 764
348 □
926
607 □
716 □
SPILLWAY SAMPLES
22 MILES ○ □
LOCATION
N.M.
LOCATION MAP
CLAY SAMPLES
NEWKIRK FIELD, GUADALUPE CTY., NEW MEXICO
1 INCH = 2000 FEET VERT. EXAG.
□ MUDSTONE
△ MUDSTONE + SANDSTONE
○ SANDSTONE

FIG. 2

PURPOSE

The purpose of this study is to determine the clay minerals present and how they are related to the pore space. Are they lining pore throats? Are they intergranular? Are expandable clays present? How are the clays affected by the heat of the steam (155° C at 250 psi)? Would there be porosity and permeability trends that could be predicted by a model of the depostional environment (Wilson, 1982)? As part of the answer to this question, the possible origins of the clays will be examined.

PROCEDURE

SAMPLE PREPARATION:

Sampling was planned to encompass the Santa Rosa Formation laterally across the steamflood project area and vertically within the area. Several samples from an exposure of the Santa Rosa at the Santa Rosa Dam Spillway 22 miles to the southwest were also run as well as one sample from the overlying Cuervo Sandstone at the steamflood site. One of the samples from the Santa Rosa spillway was highly oil impregnated.

A description of the samples is given below in Table 1. The descriptions were made using Folk's 1966 classification system. For the purposes of this experiment, the samples were divided into three dominant lithologies which reflect different energy

levels in the depositional environment. The squares (□) represent low energy mudstones and siltstones. The circles (○) represent higher-energy generally well sorted, calcite cemented, fine to medium grained sandstones. The triangles (△) represent a transistion between the first two. These rocks are grey siltstones with laminations of brown fine grained sandstone.

The numbers beside the samples from the Newkirk Field designate depths in feet below the surface. The variance in surface elevation of the wells was less than 50 feet so these depths are roughly correlatable. These samples were taken from cores which had been removed from the ground for approximately one year and stored. Formation water and volatiles had evaporated from the core soon after removal from the ground.

Three samples were taken from cuttings and their parent lithology was estimated by comparison with intact core. The other samples were taken from surface exposures and had been subject to long term weathering. However, results showed that exposure had not changed the clays under study significantly.

Table 1: Samples Analyzed

Sample #	Symbol	Description of Rock (Location)
BA1-716		Grey calclitharenite (Newkirk Fld.)
BE1-764		Grey pyritic siltstone (Newkirk Fld.)
BE1-926		Grey gilsonitic quartz arenite (Newkirk Fld.)
BR1-607		Mudstone (well cuttings) (Newkirk Fld.)
CI1-480		Mudstone (well cuttings) (Newkirk Fld.)
DA1-381		Grey micaceous siltstone (Newkirk Fld.)
DA1-418		Finely laminated sandstone and siltstone (NKF)
FS 2-7		Red hematitic sublitharenite (Cuervo Ss.)
JO1-348		Mudstone (well cuttings) (Newkirk Fld.)
SA1-394		Grey calclitharenite (Newkirk Fld.)
SA1-396		Red calcareous mudstone (Newkirk Fld.)
SA1-372		Gilsonite-bearing sublitharenite (Newkirk Fld.)
SRS-1		Red and Grey micaceous mudstone (S.R. dam)
SRS-oil		Fine grained sublitharenite (S.R. dam)
ST9-351		Micaceous fine laminated grey brown siltstone and sandstone (Newkirk Field)
ST9-459		Grey fine-medium grained sublitharenite (NKF)

Samples were disaggregated and crushed with a mortar and pestle for about 5 minutes. They were then placed in 250 ml beakers filled with deionized water and allowed to settle for approximately 15-20 minutes. If flocculation occurred and there was insufficient clay in suspension to sediment a slide, the sample was washed again. If the second treatment failed to produce the desired suspension, the sample was treated with 6 drops of "Calgon". This universally produced the suspension desired. The oil in some of the samples did not appear to inhibit suspension of the clays - possibly because it had dried out for over a year.

Samples from the upper 1 cm of solution were dropped onto glass slides and allowed to dry for 24 hours.

EXAMINATION:

Diffractograms of the slides were made with Ni filtered, Cu radiation (wavelength = 1.542 angstroms). The 2 theta values were converted to angstroms for clay identification (Figs. 3-6). Two theta values are shown in parentheses in this paper.

Several slides were treated with ethylene glycol for 24 hours and two porcelain plates were made and heated to 325 degrees Centigrade for 1 hour and then rerun.

Samples of freshly broken rock were sputter coated with gold for 3 minutes at a pressure of 50 microns in preparation for use with the scanning electron microscope. The samples were then examined and photographed at magnifications ranging from 400 to 2500 times. Higher magnifications were tried but generally had poor resolution.

Many of the samples contained heavy oil. These samples were tested under a vacuum to determine the release of volatiles which might be potentially harmful to the Scanning Electron Microscope (SEM). However, the samples had been exposed to the atmosphere long enough for volatiles to have been driven off. To check the effects of cleaning the samples on the clays, a sample of sandstone which had been Soxlet extracted using toluene for approximately 10 hours was examined by SEM. Almost all the clay had been washed from the sample (as determined by comparison with an identical, non-extracted sample) with the exception of a few scattered

kaolinite plates. A call to CORE LABS indicated that they use a solution of 90% methylene chloride and 10% methanol for extraction (Scott, 1983). Due to the highly dangerous nature of methylene chloride and the ability to use oil impregnated samples in this particular case, this method was not tried.

RESULTS OF X-RAY DIFFRACTION STUDY

KAOLINITE

The most obvious peaks on the diffractograms of all three lithologies belonged to kaolinite. No attempt was made to differentiate kaolinite from dickite which has been noted in sedimentary rocks (Hemingway, and Brindley, 1948). However, the appearance of the kaolinite differed from the dickite pictured in SEM photos (Keller, 1976) although this,too, is not diagnostic.

Kaolinite appeared as two peaks: 7.15 A (12.4 2θ), and 3.58 A (24.9 2θ). The abundance and degree of crystallinity of kaolinite both affect the height of the peaks.

A comprehensive quantitative analysis was not undertaken. Instead, a semi-quantitative method of comparison was used. Peak heights were normalized to an X-Ray count scale of 2000. Therefore a peak from a run done on a scale of 1000 was considered to be twice as high as it would have been if it had been run on a scale of 2000 and a peak from a run done on a scale of 4000 was considered to be half as high as it should have been.

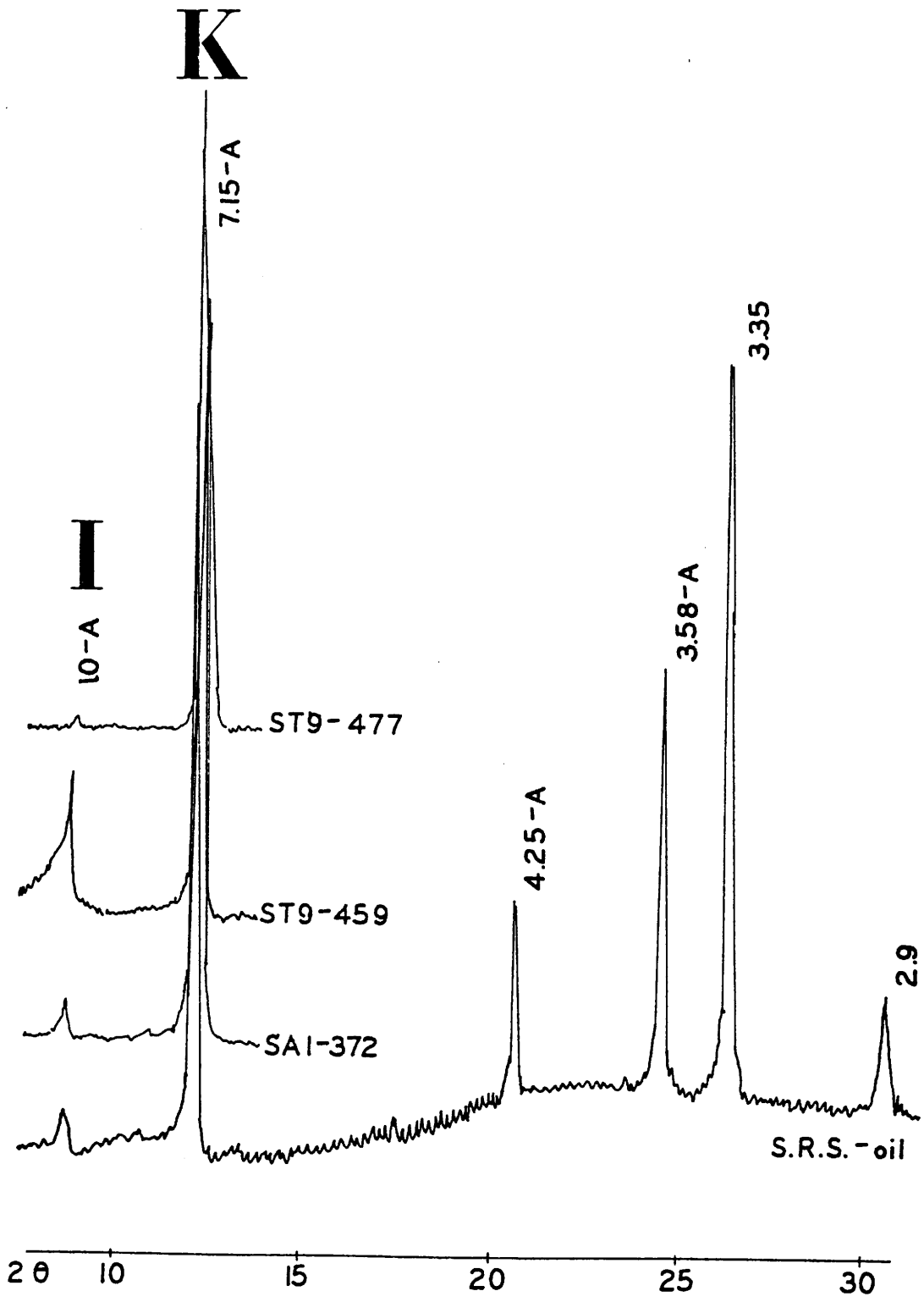

SANDSTONES ◯

FIG. 3

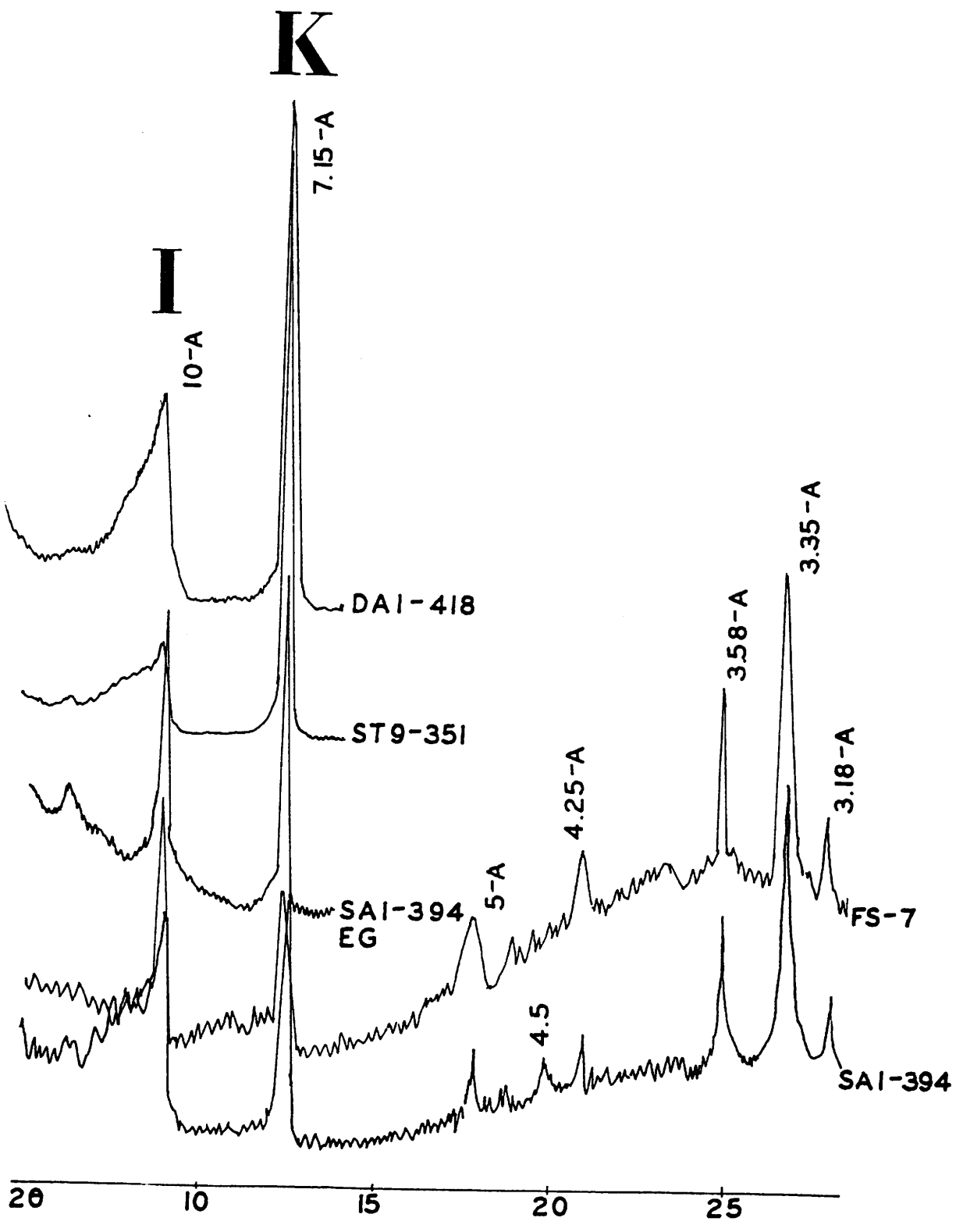

MUDSTONE AND SANDSTONE △

FIG. 4

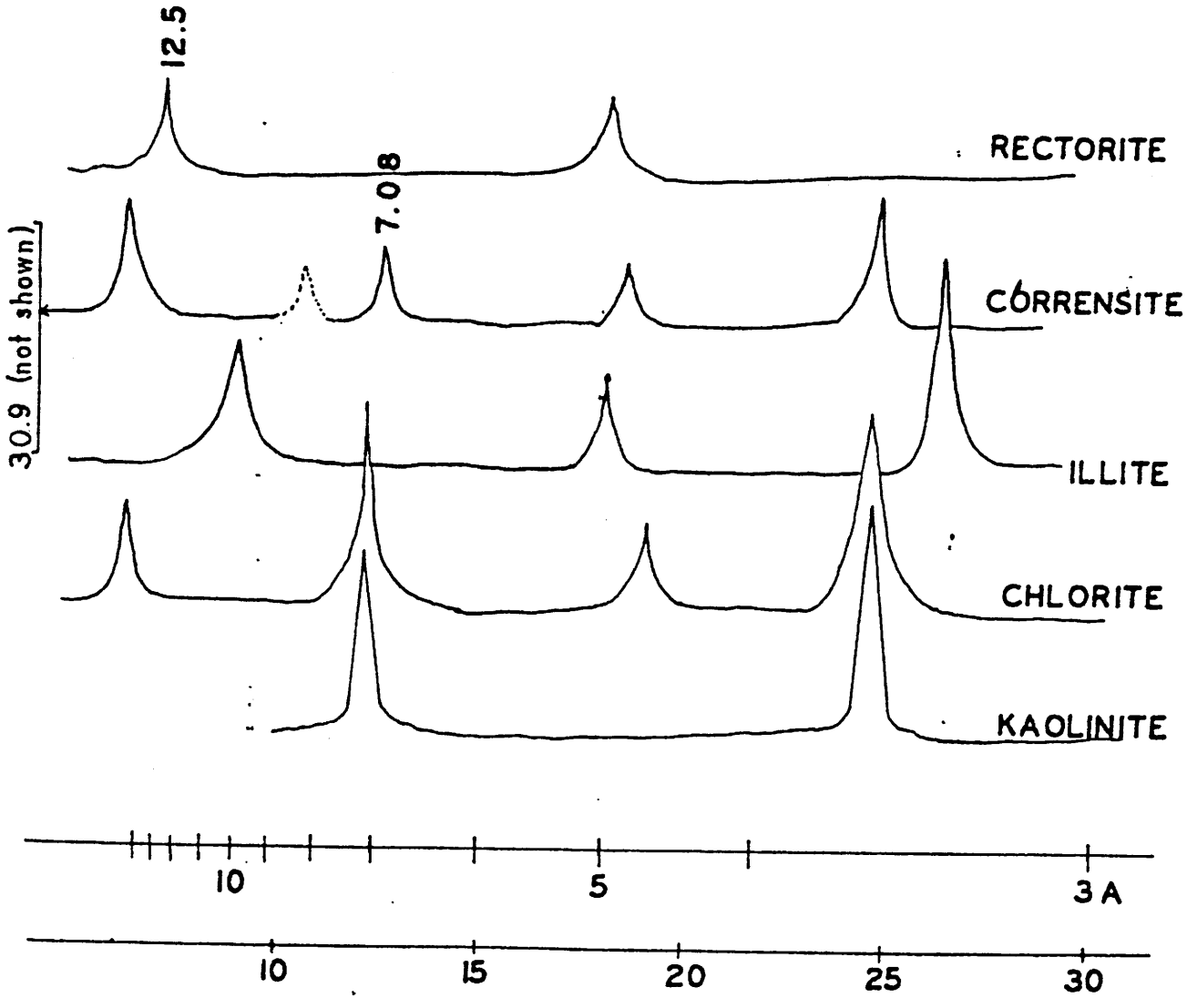

CHARACTERISTIC CURVES

FIG. 5

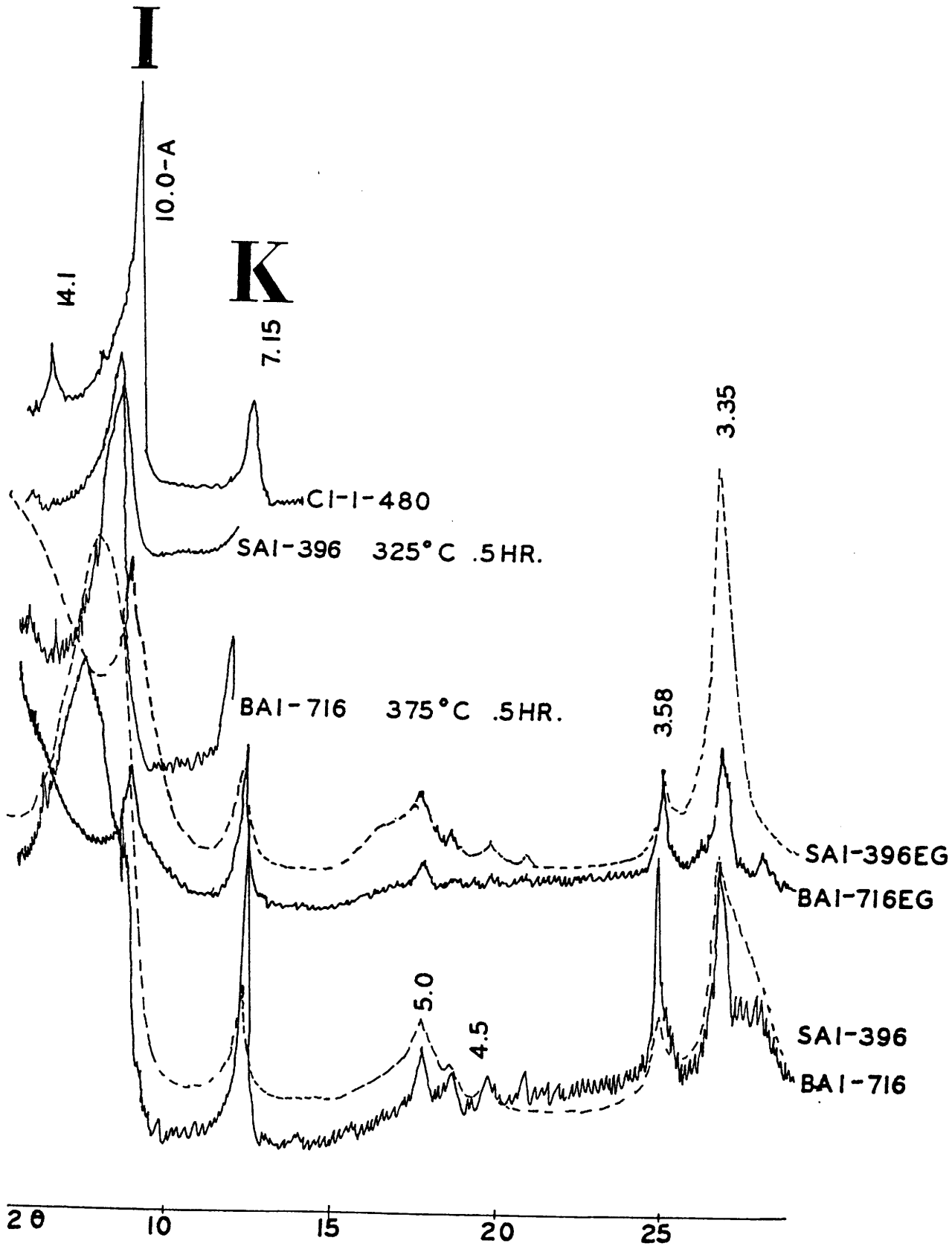

MUDSTONES ☐

FIG. 6

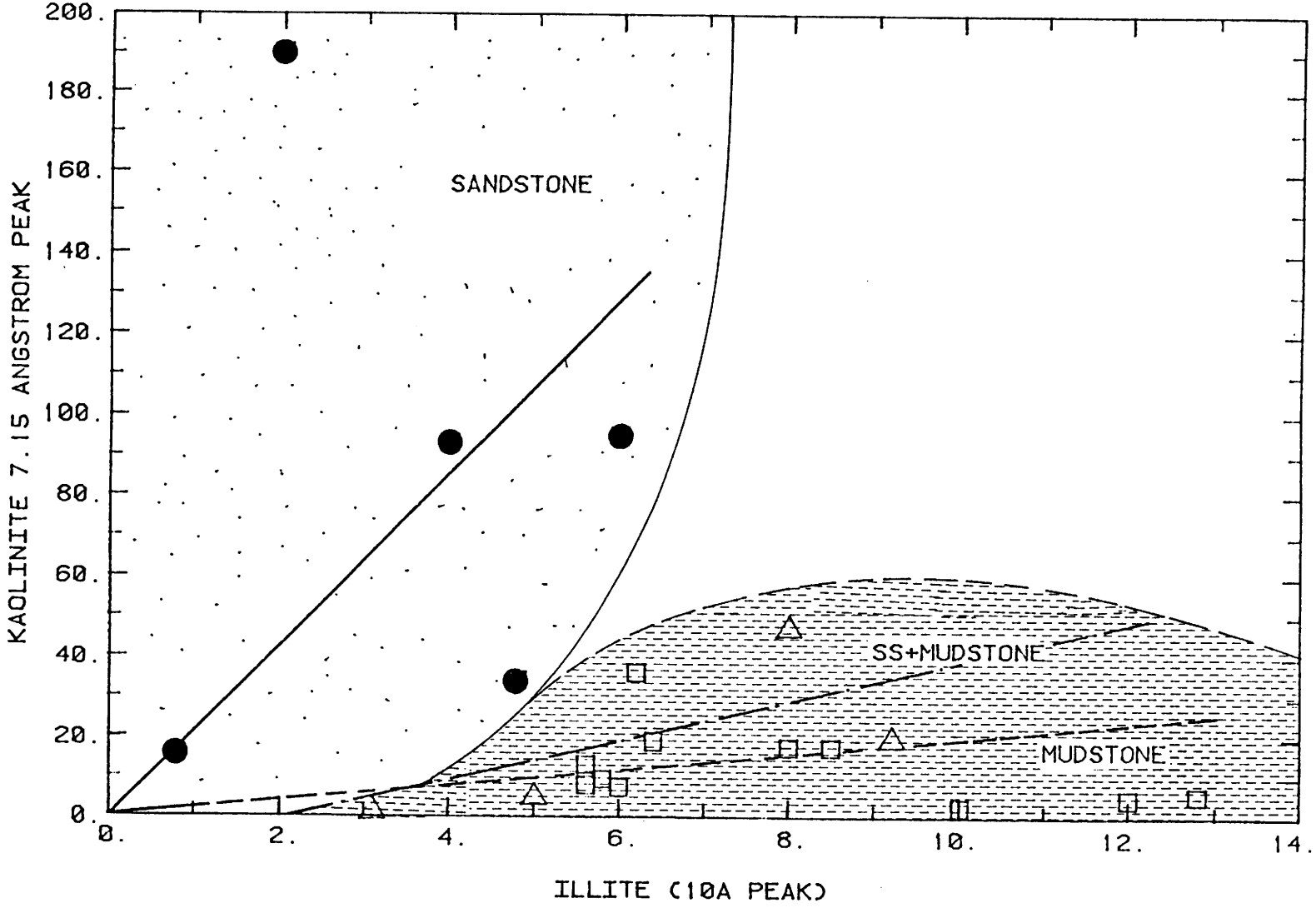

KAOLINITE V. ILLITE

FIG. 7

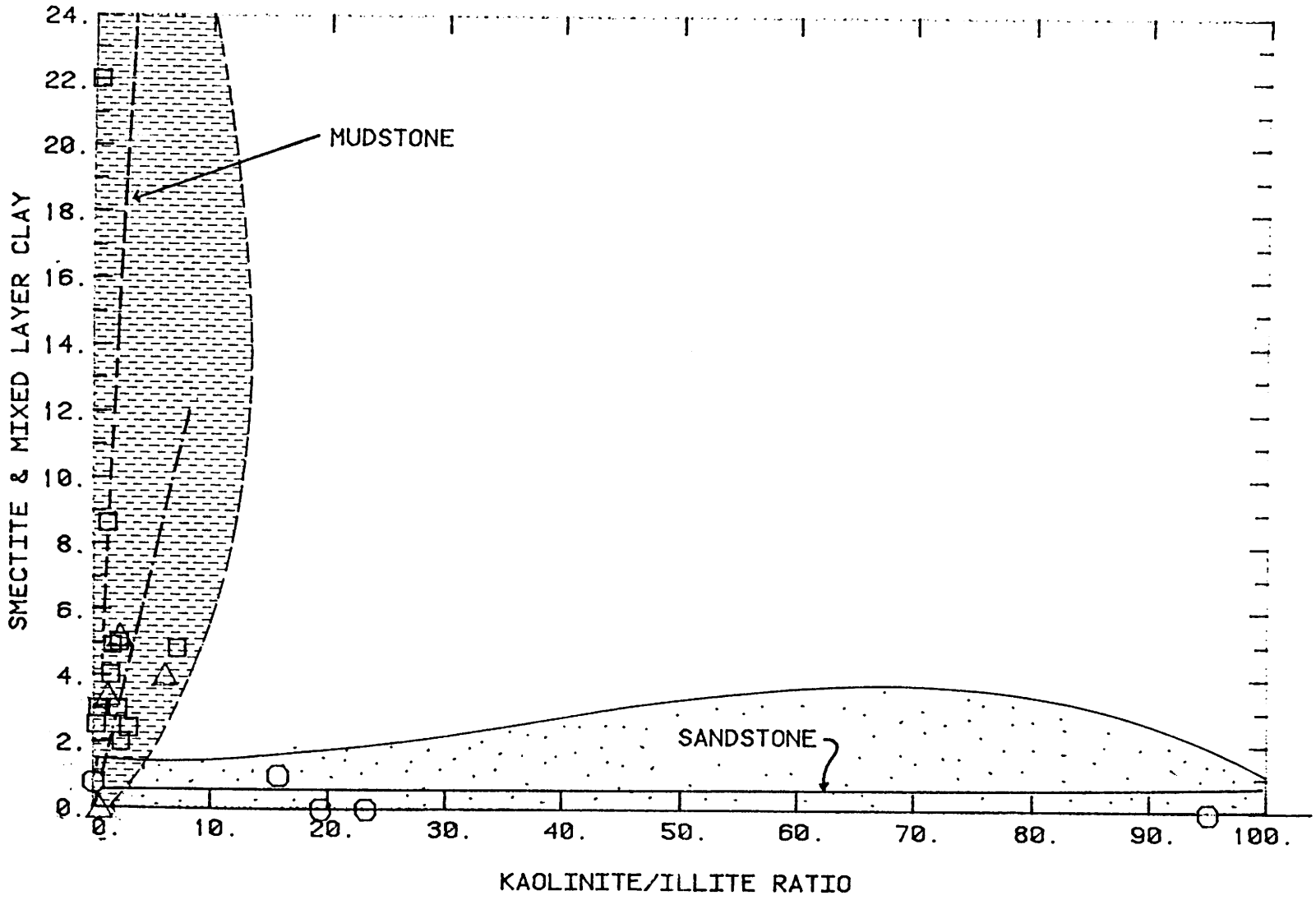

KAOLINITE/ILLITE RATIO V. SMECTITE & ML CLAYS

FIG. 8

Some of the sandstones had to be run on a scale of 20,000 due to the highly crystallized nature of the kaolin.

This method is similar to that used by Esquevin (1969) to analyze the crystallinity of illite. By measuring the intensity of the 5 A and 10 A peaks (I(002)/I(001)) he showed that a contour of the ratio of peak heights was related to specific episodes of diagenetic evolution.

The peaks in Figs. 3-6 are a mixture of scales and represent a sample of the original data of this project.

Percentage compositions were not calculated because the peak heights were so greatly affected by crystallinity and would distort calculated compositions. The area under the curve method would give more representative compositions.

The marked contrast between the kaolinite peaks in the sandstones (very sharp) and mudstones (diffuse) is a caused by their higher crystallinity and greater percentage abundance (very little illite) in the sandstones.

Kaolinite may be detrital, but is generally the result of erosion of weathering profiles in leached acidic environments in hot and humid climates. Basic K-rich interstitial solutions can cause illitization of kaolinite during diagenesis (Chepilov, 1959).

ILLITES

The illite peaks at 10 A (8.8 2θ) and 5 A (17.8 2θ) showed in various intensities on all of the diffractograms. Some of the illite peak intensity may be due to illites in mixed layer clays as will be discussed later.

Fig. 7 shows the normalized peak heights of illite (10 A) plotted against kaolinite (7.15 A). These peaks were chosen as representative of the amount of and crystallinity of these particular clays. Lines were drawn for the three lithologies which seem to best fit the data. An attempt was made to formally regress the data but the results seemed relatively less meaningful than an educated guess at best fit. Also, the degree of precision of the data did not warrant formal mathematical treatment. Contours were drawn to represent the field of variation of each lithology after the method of Esquivin (1969).

This plot suggests that kaolinite and illite may have existed together as a detrital mixture in the mudstones. Later solutions transported kaolinite from these mudstones or another source into the sandstones.

Illites exist as three common polymorphs. The 1Md form develops during weathering and transport. A 1M illite is formed under varying conditions. A 2M illite is found in micas of the metamorphic zones or in detrital illites from continents where the cold and dry climate was not favourable to hydrolysis.

No attempt to determine the polymorphic type was made as it is difficult in the presence of other minerals. The above indicates it should be 1Md.

SMECTITES

The presence of smectites on the diffractograms is indicated by peaks at 12.0 A (7) and 4.5 A (19.8). The 12.0 A peak expands on glycolation to approximately 17.8 A (5.2) in a very similar manner to an example of a random mixed layer 14 A montmorillonite - illite investigated by Thorez (1975). Heating to 375 C. for 30 minutes collapses the peak back to close to 10 A.

Figure 8 shows that smectite is associated with illite (low kaolinite/illite ratio) in the mudstones and is absent in the sandstones.

Dunoyer de Segonzac (1970) gives the following table describing the evolution of smectite into illite during burial diagenesis in Logbaba boreholes:

Table 4:Smectite-->Mixed layers-->Illite

Depth (m)	Type	d(001) no tr.	d(001) E.G.	d(001) Heated
915	M	14	17	10
1350	I-M	11.5	17	10
1497	I-M	12	14	10
2041	I-M	11	12.5	10
3423	I-M	10.5	12	10
3586	I-M	10.5	12 broad	10
4019	I	10	10	10

There is a similarity in the behavior of the test run at 1350 meters (4050 feet) and the behavior of the smectites from the mudstones at Santa Rosa.

The environmental significance of I-M mixed layer clays lies in the fact that they represent the fixation of K+ by smectites in a potassium-rich environment of early diagenesis.

The work of several authors indicates that the zone of stability of mixed layers to be between 80-200 degrees C.

CHLORITE

The presence of small peaks at 14.1 A (6.2) and 4.7 A (18.7) indicate that chlorite may be present in small quantities. Chlorite is difficult to distinguish in the presence of kaolinite because its very strong 7 A peak is obscured by that of kaolinite (001).

The chlorite may be detrital or it may be a result of diagenetic aggradation and reordering of illites. Chlorites are unstable in highly leached environments.

CORRENSITE

The presence of corrensite in a sandstone from the Santa Rosa was reported by Glass et al (1973). The corrensite of Lippman (1954) has peaks at 14.2-A, (VS) 10-A (M), 7.08 (W), 4.72 (M), and 3.34-A (VS). These peaks coincide well with the peaks observed on an untreated diffractogram of the mudstone. However, the diagnostic 30.8-A (2.9) peak is missing.

Corrensite represents an intermediate step in the evolution of illites towards chlorite by fixation of magnesium (Dunoyer de Segonzac, 1970). It is generally associated with evaporites in Permian and Triassic rocks of Europe.

ANALYSIS BY SEM

Scanning electron microscope photographs indicate well crystallized books of kaolinite in the sandstones and a layering of illite-montmorillonite flakes in the mudstones. Kaolinite may exist as a poorly crystallized variety which may be hidden by the "leaves" of illite and mixed layer clays.

Figure 9 shows quartz qrains in the sandstone which was sawed. The water associated with sawing may have washed out the kaolinite. Visible is a 100 micron (.1 mm) wide muscovite flake.

Figure 10 shows quartz grains surrounded by stacks of kaolinite flakes 6-10 microns in diameter and 10-20 microns long.

Figure 11 of mudstone shows mixed layer illite-smectite flakes 2-15 microns in size. Ordered kaolinite is conspicuously absent.

Figure 12 shows a closer view of I-M mixed layer clay.

SEM study (Kotelnikov (1965) suggests that detrital illite may occur as isometric flakes and diagenetic illite may appear as elongated flakes in the form of slabs. Based on this, the illite in the mudstone as shown in SEM micrographs is detrital.

Considerable microporosity exists between the kaolinite books in the sandstone. The kaolinite in general shows the structure described by Keller (1976). Loose packing of the stacks of plates differentiates this kaolinite from one produced in a hydrothermal environment which would have a tighter packing.

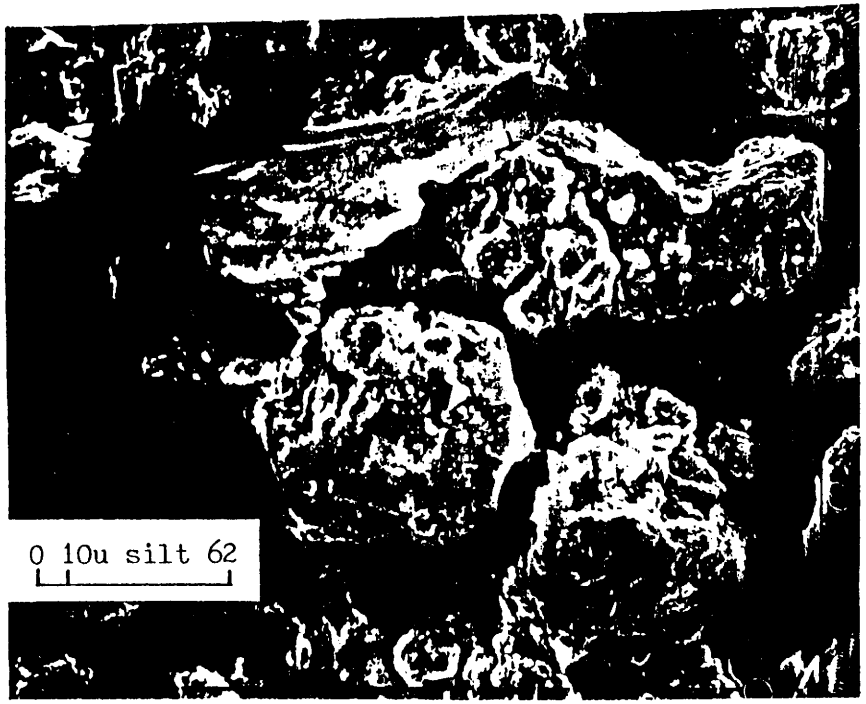

ST8-396
X410

FIG. 9

ST8-396
X2000

FIG. 10

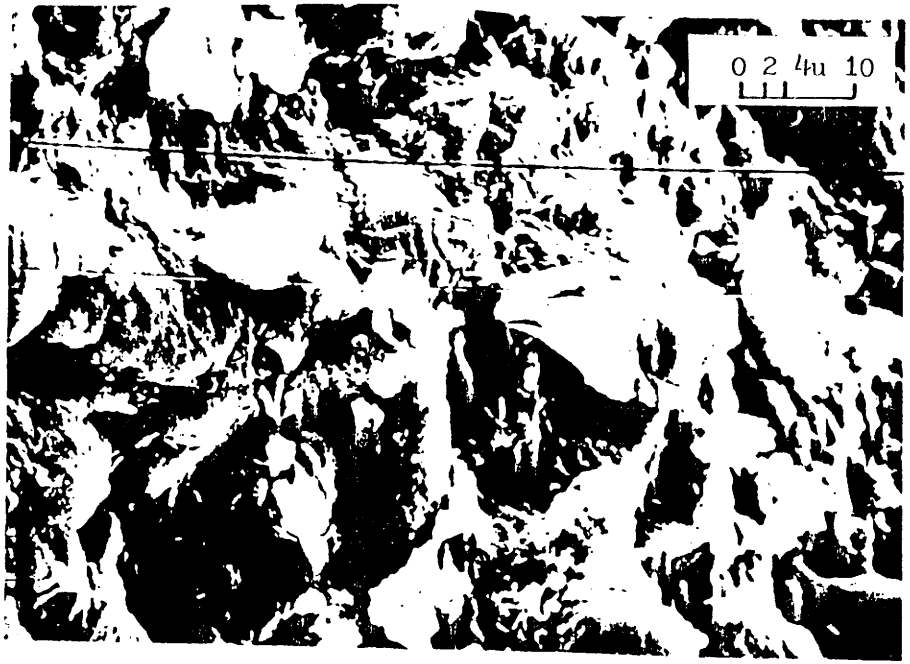

SAI-396
X1500

FIG. 11

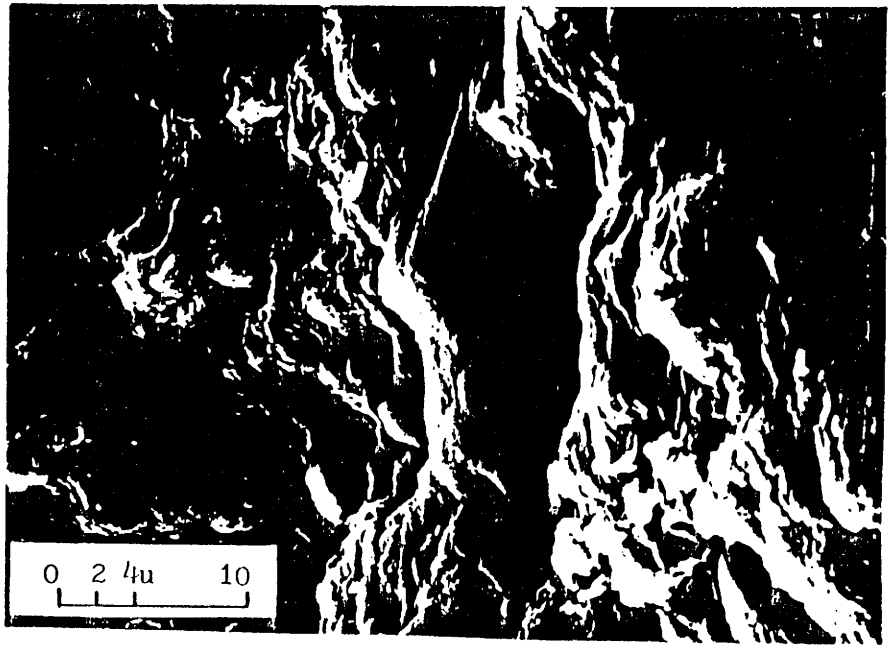

SAI-396
X 2500

FIG. 12

CORE LABS also made and analyzed SEM micrographs of the cores. Their analysis was similar to the above. They noted abraded kaolinite (possibly detrital?) in the sandstone and a clay coating on some of the grains of undetermined composition.

In general, kaolinites are easy to identify by SEM because of their platelet morphology. Illites and smectites exhibit a soggy cornflake-like morphology but their diffentiation and percentage determination is very difficult.

ANALYSIS BY THIN SECTION

The sandstones were composed of well-sorted silt size (.05 mm) - med. sand size (.3 mm) quartz (80%), feldspar (5%), chert (5%), with traces of dolomite, muscovite, hematite, and clays. Grain contacts are tangential and concavo-convex. Cement occurs in the form of quartz overgrowths and dolomite.

The clays were difficult to identify in thin section. Identification was made even more difficult be the presence of oil which masks the true features of the clays. Since prior identification was made by X-Ray this was not a cause for concern.

The clays exist as intergranular matrix. Little primary (except for the previously described microporosity) porosity is evident. Secondary porosity seems absent as well. Visual estimates of the blue epoxy impregnated slides gave an effective porosity of 10-12%.

Several photographs of Triassic sandstone thin sections are used as examples in AAPG Memoir 22:A Color Guide to Sandstone Petrology (1979) and show visible kaolinite stacks. Other clays are described as well.

GENESIS OF THE CLAYS

The Santa Rosa sandstone was deposited in a humid to semi-humid climate by a terrestrial fluvial system which flowed over Permian carbonates, shales, and evaporites (McGowen, 1983). Flow was to the southeast towards a lake basin at the Texas border. Deposited with the sandstone were numerous plant fragments which were later coalified. Their presence along with pyrite indicates an acidic reducing environment similar to that of coal swamps The area was later subjected to sufficient chemical and physical diagenesis to produce coalification. A rough estimate of maximum burial based on personal observation of the remnant mesas capped by rocks as young as the Cretaceous age would be 3000-5000 feet. These depths are sufficient to produce a temperature of 150 degrees farenheit.

The almost complete absence of feldspars in the rock indicate either their absence in the source rocks or their complete alteration. The few grains which were found were altered so as to be almost unrecognizable.

The probable sequence of genesis probably included these steps:

1. Overbank muds of mixed kaolinite, smectite, and illite from the Permian formations were deposited by the river system.

2. The system was later covered by sediments. Ion concentration in the pore water began to increase as temperature increased solubilities. Conversion of smectites to illites began after the model of Hower et al (1976).

3. The area began to be eroded and water began to circulate through the formation. Kaolinite was precipitated in the pore space of the sandstone.

STEAMFLOOD PERFORMANCE

Water temperature, ion content of the water, and type of clay are major factors affecting steamflood performance.

The approximate composition of the injection water currently used at the site is shown below in Table 3:

Table 3: Water Analyses (Martin, 1983)

	Injected Steam Water	
pH	8.6	
Alkalinity as HCO3	524	mg/liter
Chlorides as Cl	57	mg/liter
Sulfates as SO4	510	mg/liter
Hardness as CaCO3	0	
Calcium as Ca	0	
Magnesium as Mg	0	

Steam is being injected at the rate of 60 barrels of water/day at a temperature of 310 degrees F. (333°C) and under a pressure of 250 psi (Martin, 1983). Average porosity of the formation is 20% and average air permeability is 200 md.

To demonstrate the sensitivity of clays to different solutions Mungan (1963) tested cores of St. Peter sandstone consisting of very pure silica sand and 0.4% kaolinite with a 30,000 ppm NaCl solution and a 0.5 N NaOH solution. The brine reduced permeability by about a third while the NaOH solution reduced it by half (Fig. 13).

Mungan (1963) also investigated the effects of flooding with a 30,000 ppm NaCl solution followed by distilled water on a core of Berea sandstone containing illite, chlorite, kaolinite, and interlayered illite. The permeability dropped from 190 md to 0.9 md. almost immediately upon introduction of distilled water to the core. Clays were also produced in the effluent indicating dispersal of grains was occurring (Fig. 14).

These effects can be alleviated by eliminating the 'shock' effect of fresh water and reducing the salinity very gradually as was shown in another experiment.

Experiments with NaOH solutions at 180 degrees F. produced a permeability reduction from 240 md. to 180 md. in an oil-wet core. Following the caustic flood with distilled water at 180 deg. F. produced a further reduction of permeability to 55 md. (Mungan, 1963) Fig. 14.

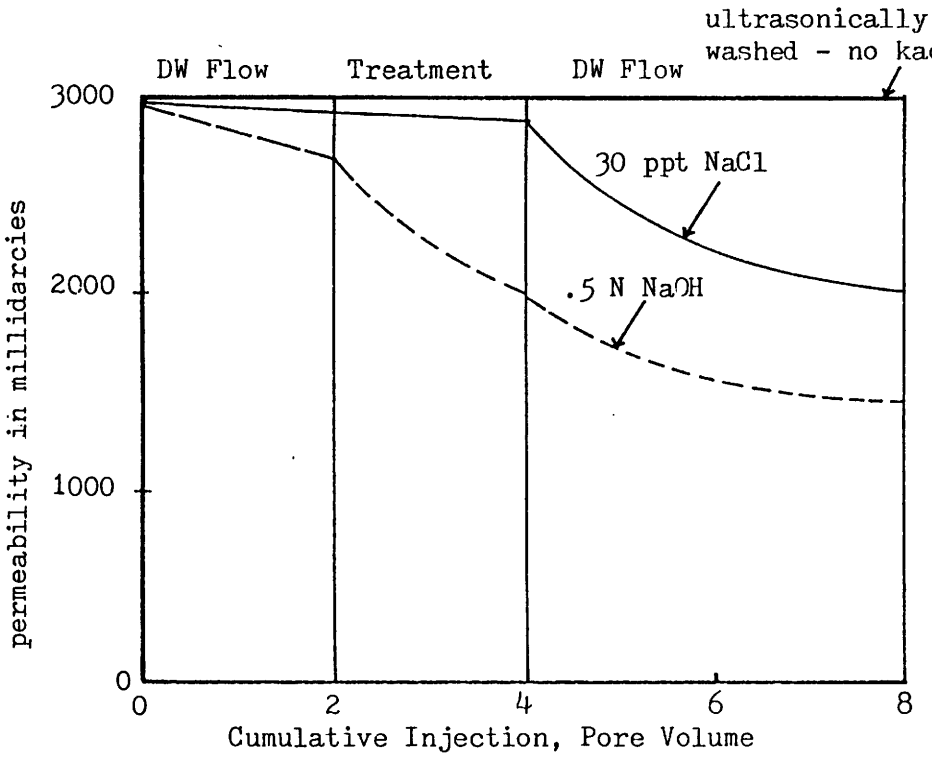

The Effect of Small Quantity of Indigenous Kaolinite on the Permeability of Unconsolidated St. Peter Sand Cores (approx. 0.4% kaolinite)

FIG. 13

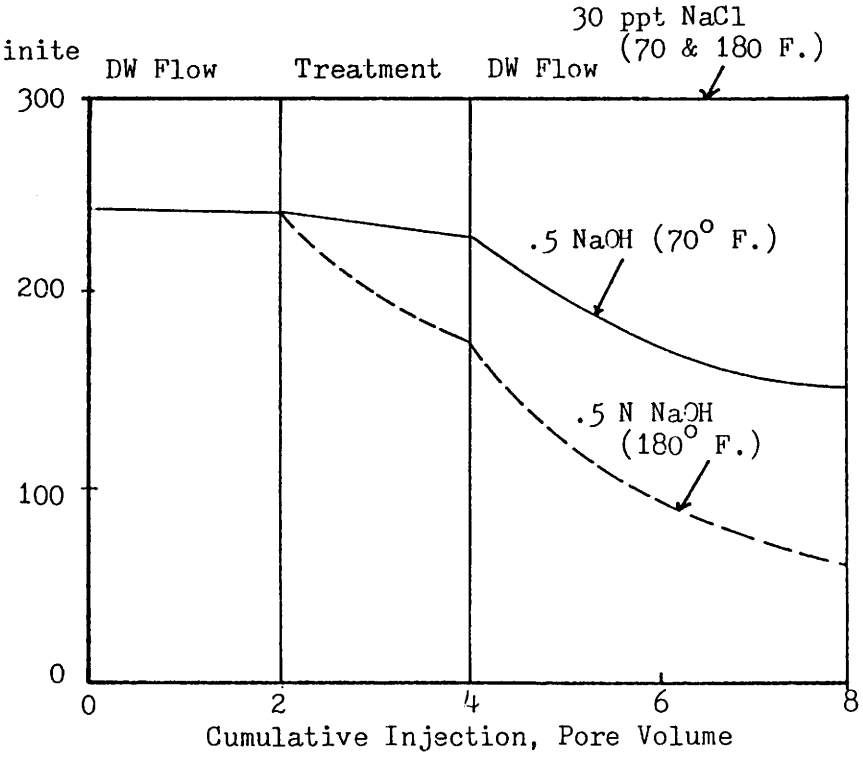

The Effect of Temperature on Sensitivity of Nonextracted Cores from Formation A. (approx. 1% kaolinite)

FIG. 14

(after Mungan, 1963)

NEWKIRK FIELD CORES

FIG. 15

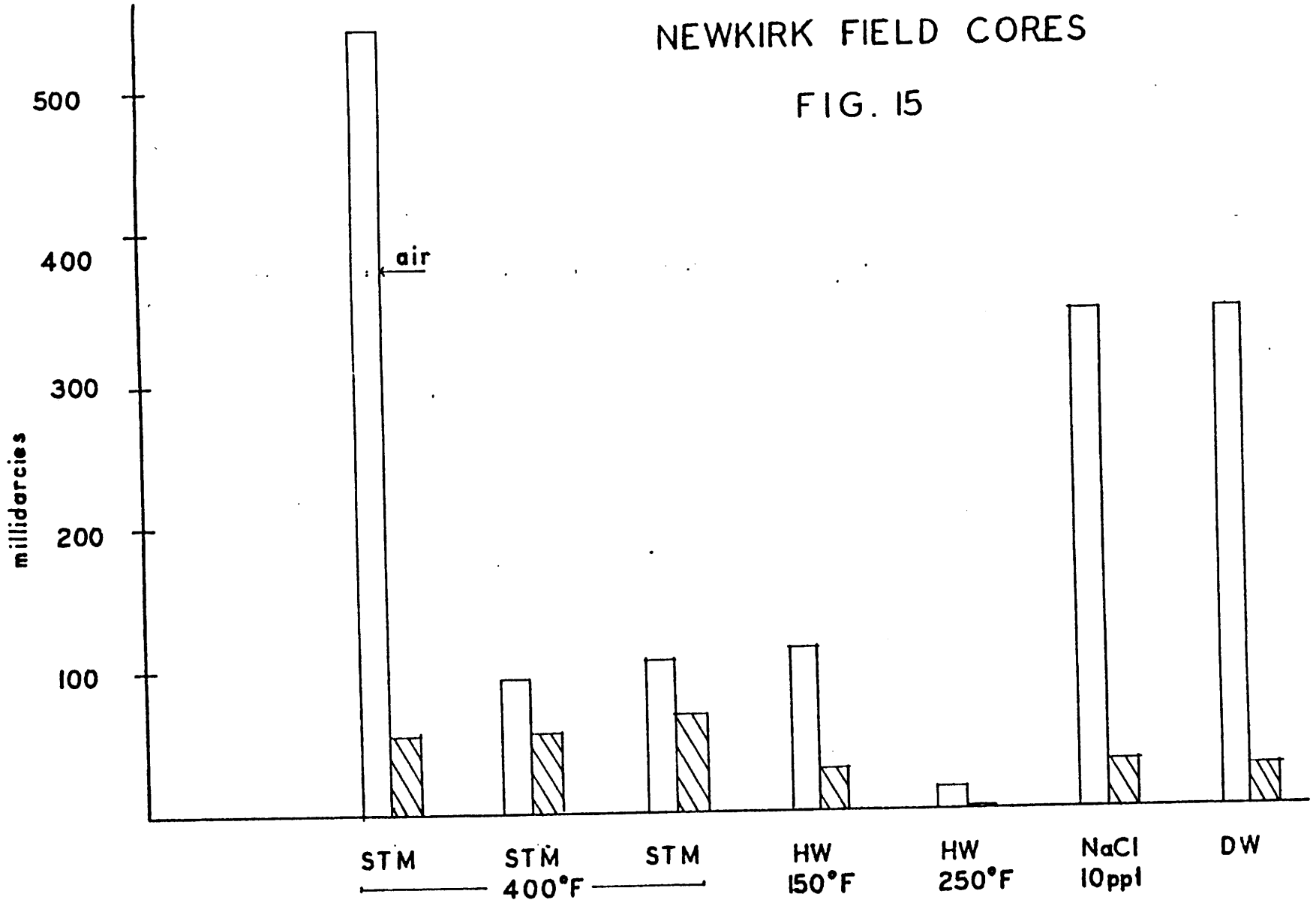

AIR PERMEABILITY V. WATER PERMEABILITY (after CORE LABS)

The conclusions of these experiments are:

1. The primary cause of permeability reduction is blocking of the pore passages by dispersed particles.

2. Permeability reduction due to salinity changes occurs regardless of the type of clay.

3. NaOH generally caused more damage than brine solutions because it dissolves matrix material, disperses clays, and dislodges fine material which then block pore throats.

Little work has been done on the long term (1-15 years) effects of steamflooding on clays. The similarity to hydrothermal systems is evident with the main difference being the vast difference in time. Potential exists for illitization of kaolins and destruction of permeability, in effect, creating a shale where a sandstone once was. Theoretically, this condition would show as a pressure buildup in injection pressure. This has not been the case at the steamflood project.

CORE LABS ran several tests on oil saturated cores from the Newkirk Field to determine steamflood viability. The tests included steamflood (400 degrees F.) sensitivity, Hot water (150 & 250 degrees F.), and water sensitivity for 10,000 ppm NaCl and distilled water. The results are summarized in Fig. 15.

The tests indicated that steam was effective at removing most of the oil while hot water was not.

According to these tests, permeability to steam was actually twice that of distilled water. Permeability was not affected by 150 degree F. hot water or a brine solution. Only the 250 degree F. hot water reduced permeability significantly (to < 2 md.). Also, air permeabilites were a poor guide to fluid permeabilities due in part to the clays in the pores.

CONCLUSION

Kaolinites, illites, and mixed layer clays in the fluvial fine grained Santa Rosa sandstone constitute the major impediment to fluid flow in the formation. Steamflooding in progress may be further aggravating the situation by:

1. Increasing the temperature
2. Introducing water of lower ion content which disperses the clays.
3. Introducing water of higher OH- content which also aids dispersal of the clays.
4. Potentially creating illites from kaolinites which have a greater potential for blocking pores.

The state of current work is insufficient to construct models which might predict trends of reduced kaolinite and greater permeability.

More study on the long term effects of steam would be helpful in determining effects on clays and potential permeability reduction.

BIBLIOGRAPHY

Budding, A.J., (1979) Geology and oil characteristics of the Santa Rosa tar sands, Guadalupe County, N.M.. Prepared under grant number 78-3316, N.M. Energy Institute at NMIMT, Socorro, N.M.

Chepilov, K.R., Ermolova, E.P. and Orlova, N.A. (1959) Epigenetic minerals as indicators of time arrival of petroleum into commercial sand reservoirs. Dokl. Akad. Nauk S.S.S.R. 125:1097-1099.

CORE LABS (1980) Screening tests for thermal oil recovery for Public Lands Exploration, INC., report to George Scott, consulting geologist, Roswell, N.M..

Donoyer de Segonzac, G. (1970) Clay-minerals diagenesis and low grade metamorphism. Sedimentology, V. 15, p. 281-346.

Esquivan, J., (1969) Influence de la composition chimique des illites sur leur cristallinite. Bull. Centre Rech. Pau-SNPA, 3:147-632.

Hemingway, J.E. and Brindley, G.W. (1948) The occurrence of dickite in some sedimentary rocks. Intern. Geol. Congr., 18th, London, 1948, Rept.,13:308.

Hower, J., Eslinger, E., Hower, C., Perry, H. (1976) Mechanism of burial metamorphism of argillaceous sediment: 1. Mineralogical and chemical evidence. GSA Bull. v. 87, p. 725-737.

Keller, W.D., (1976) Scan electron micrographs of kaolins collected from diverse environments of origin (parts I and II). Clays and Clay Min., Vol 24.

Keplinger and associates, Inc. (1980) An appraisal of estimated heavy oil recovery via steamflood from the Newkirk East and Newkirk West Prospects, Guadalupe County, NM, submitted to Public Lands Exploration Co., Dallas, Tx.

Kelley, Vincent C. (1972) Triassic Rocks of the Santa Rosa Country. N.M.Geol. Soc. Guidebook, 23 Fld. conf., E-Central NM.

Kotelnikov, D.D. (1965) Sur les caracteres morphologiques des illites dans les roches sedimentaires. Mineral. Sb., 19:26-35.

Lippman, Friedrich (1954) Uber einen Keuperton von Zaisersweiher bei Maulbronn. Heidelberg Geitr. Min., v. 4, p. 130-134.

Lindquist, Sandra J. (1983) Nugget Formation Reservoir Characteristics Affecting Production in the Overthrust Belt of Southwestern Wyoming., J. Pet. Tech., July, 1983.

Martin, Dave (1983) Steamflood pilot in the O'Connell Ranch Field. PRRC Report 83-9, Socorro, NM.

Mcgowen, J.H., Granata, G.E., Seni, S.J.. (1983) Depositional Setting of the Triassic Dockum Group, Texas Panhandle and Eastern New Mexico. Mesozoic Paleogeography of west-central U.S. (Reynolds, M.W. and Dolly, E.D. eds.), Denver, Colorado.

Mungan, Necmettin (1963) Permeability Reduction through changes in pH and Salinity. J. Pet. Tech., Dec. 1963.

Scott, Andy (1983) personal communication (CORE LABS).

Thorez, J. (1975) Phyllosilicates and clay minerals. Editions G. Lelotte, Dison, Belgium.

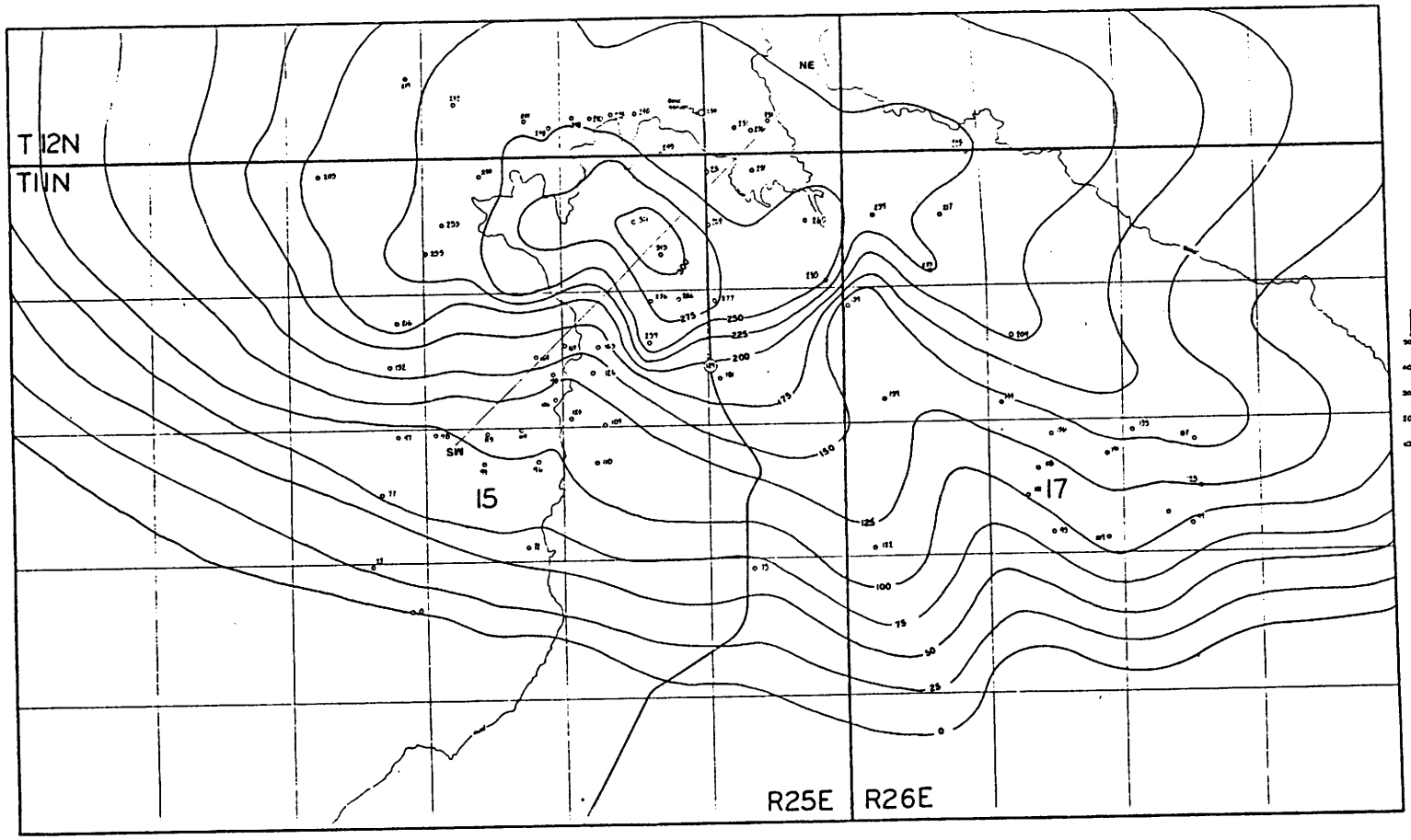

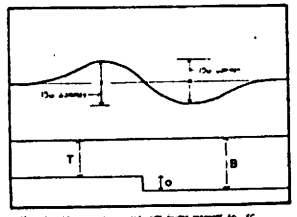

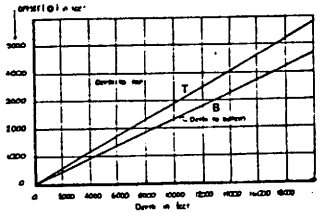

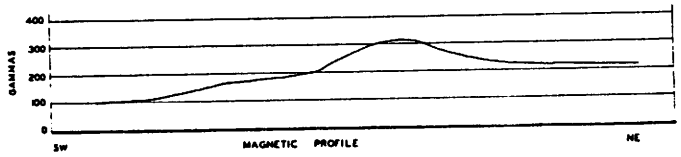

MAGNETIC ANOMALIES MAP

CONTOUR INTERVAL: 25 GAMMAS

COUNTY: GUADALUPE
STATE: NEW MEXICO
BY: J. Curtis McKallip Jr.

0 1 mi

PLATE 1

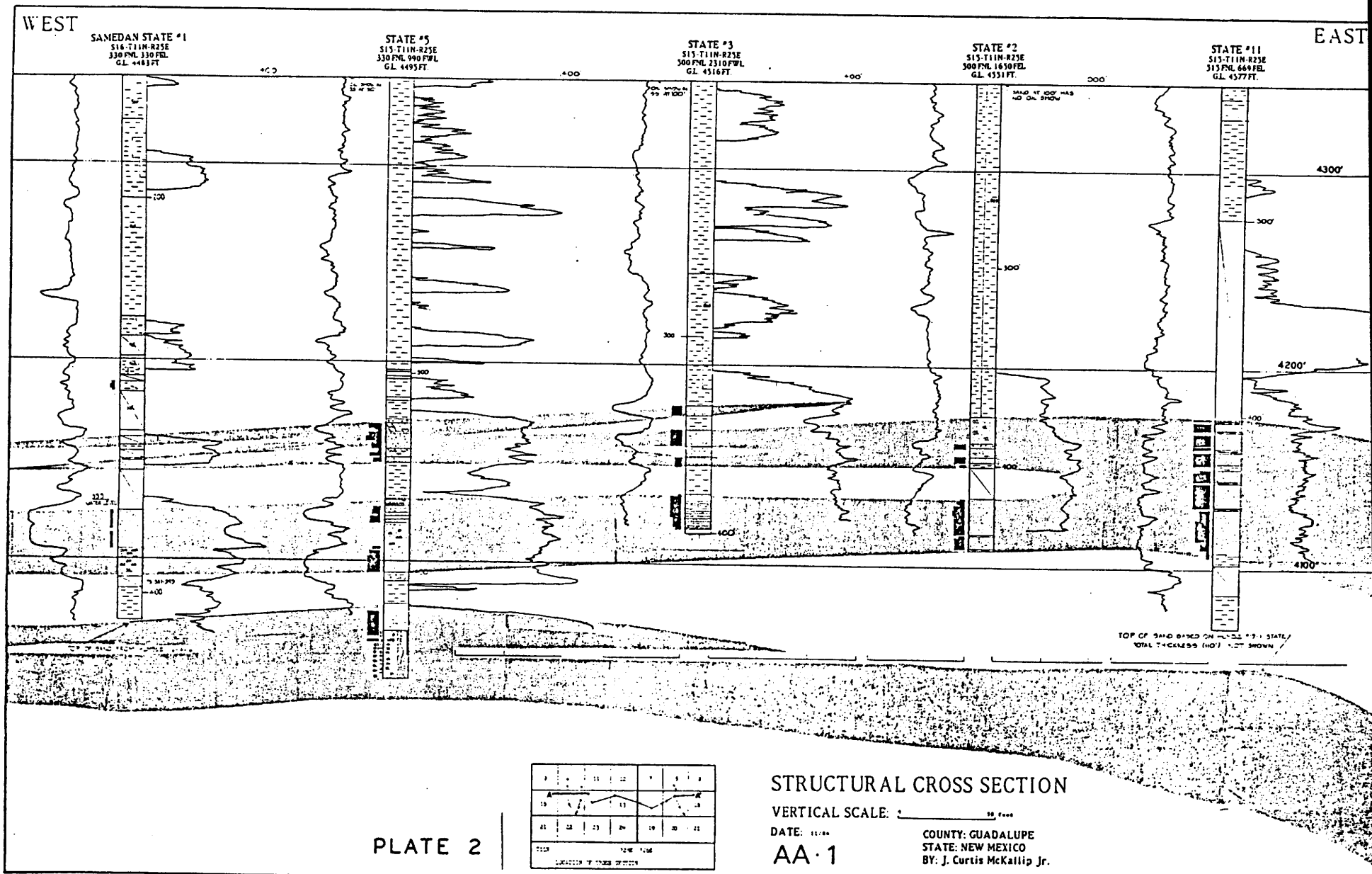

PLATE 2

STRUCTURAL CROSS SECTION

VERTICAL SCALE:

DATE:

AA·1

COUNTY: GUADALUPE
STATE: NEW MEXICO
BY: J. Curtis McKallip Jr.

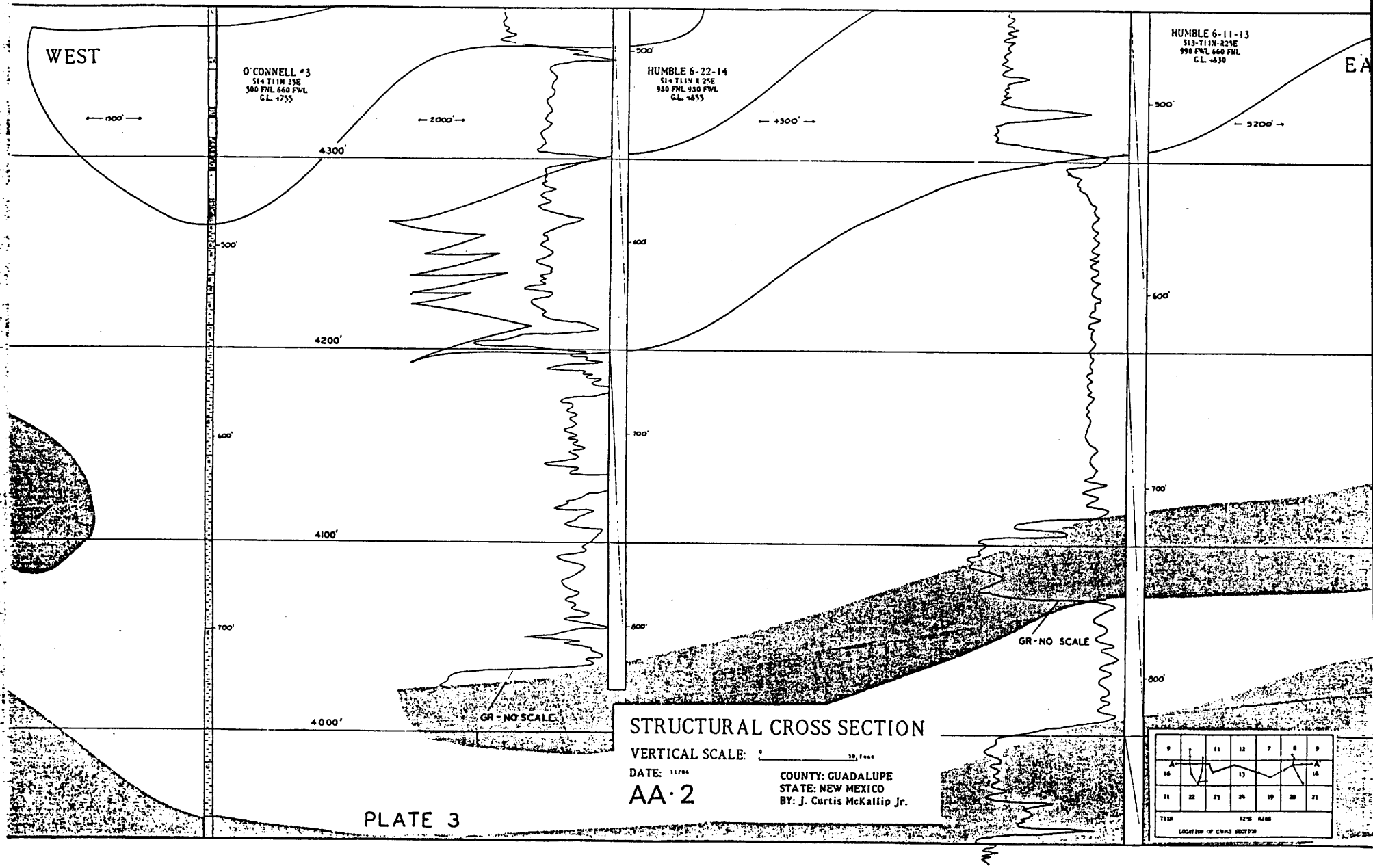
WEST
O'CONNELL #3
S14 T11N 25E
500 FNL 660 FWL
G.L. 4755
HUMBLE 6-22-14
S14 T11N R 25E
980 FNL 950 FWL
G.L. 4835
HUMBLE 6-11-13
S13-T11N-R25E
990 FWL 660 FNL
G.L. 4830
EA
1500'
2000'
4300'
3200'
4300'
4200'
4100'
4000'
500'
600'
700'
800'
GR - NO SCALE
GR-NO SCALE
STRUCTURAL CROSS SECTION
VERTICAL SCALE:
DATE:
AA·2
COUNTY: GUADALUPE
STATE: NEW MEXICO
BY: J. Curtis McKallip Jr.
PLATE 3

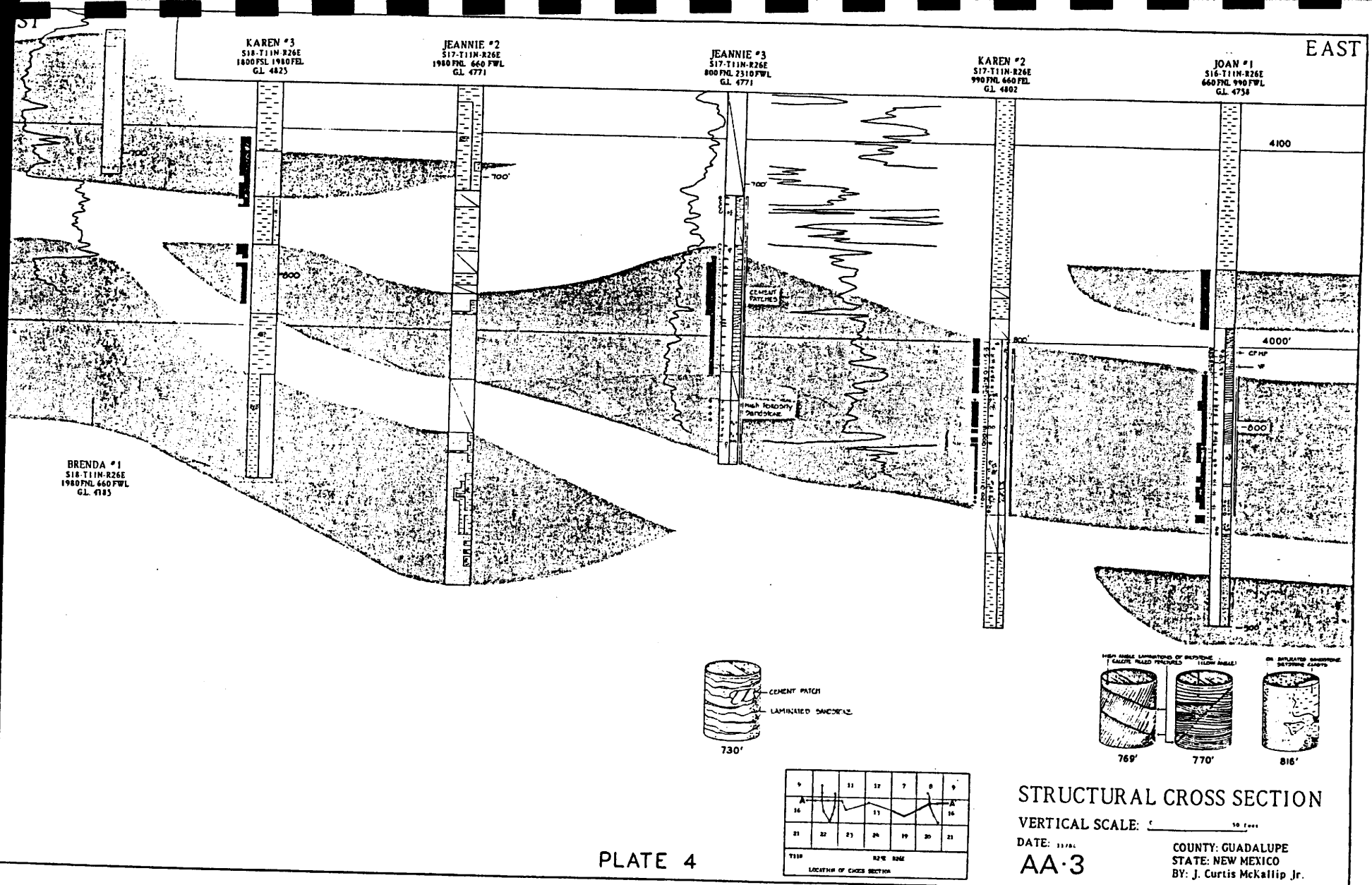

PLATE 4

STRUCTURAL CROSS SECTION

VERTICAL SCALE: 1" = 50 Feet

DATE: 11/84

AA·3

COUNTY: GUADALUPE
STATE: NEW MEXICO
BY: J. Curtis McKallip Jr.

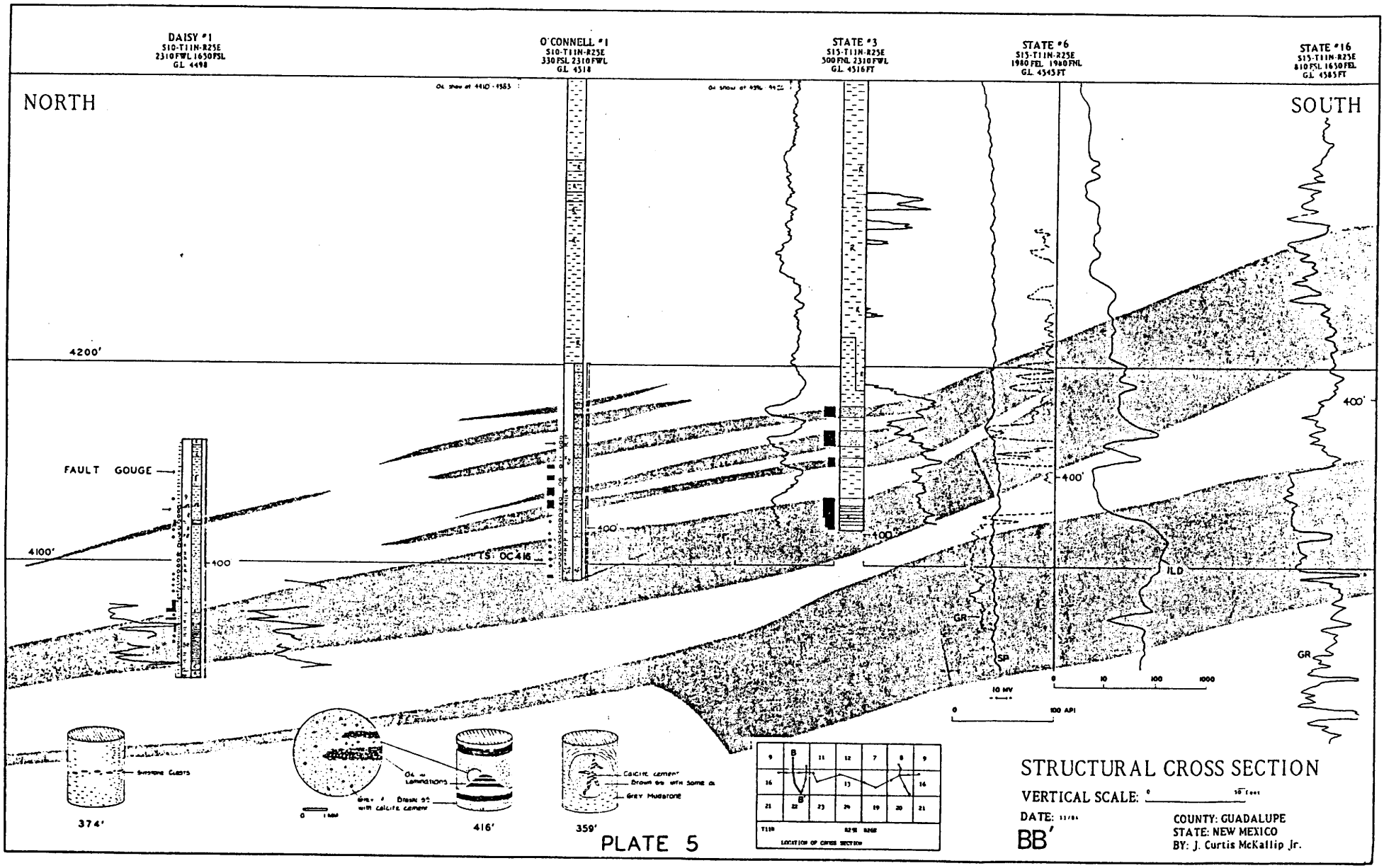
DAISY #1
S10-T11N-R25E
2310FWL 1650FSL
GL 4498
O'CONNELL #1
S10-T11N-R25E
330FSL 2310FWL
GL 4518
STATE #3
S15-T11N-R25E
500FNL 2310FWL
GL 4516FT
STATE #6
S15-T11N-R25E
1980 FEL 1980 FNL
GL 4545FT
STATE #16
S15-T11N-R25E
810FSL 1650FEL
GL 4585FT
NORTH
SOUTH
4200'
4100'
400'
FAULT GOUGE
TS OC416
GR
SP
ILD
10 MV
100 API
Siltstone Clasts
Oil in Laminations
Grey & Brown ss with calcite cement
Calcite cement
Brown ss with some oil
Grey Mudstone
374'
416'
359'
PLATE 5
STRUCTURAL CROSS SECTION
VERTICAL SCALE:
DATE:
BB'
COUNTY: GUADALUPE
STATE: NEW MEXICO
BY: J. Curtis McKallip Jr.

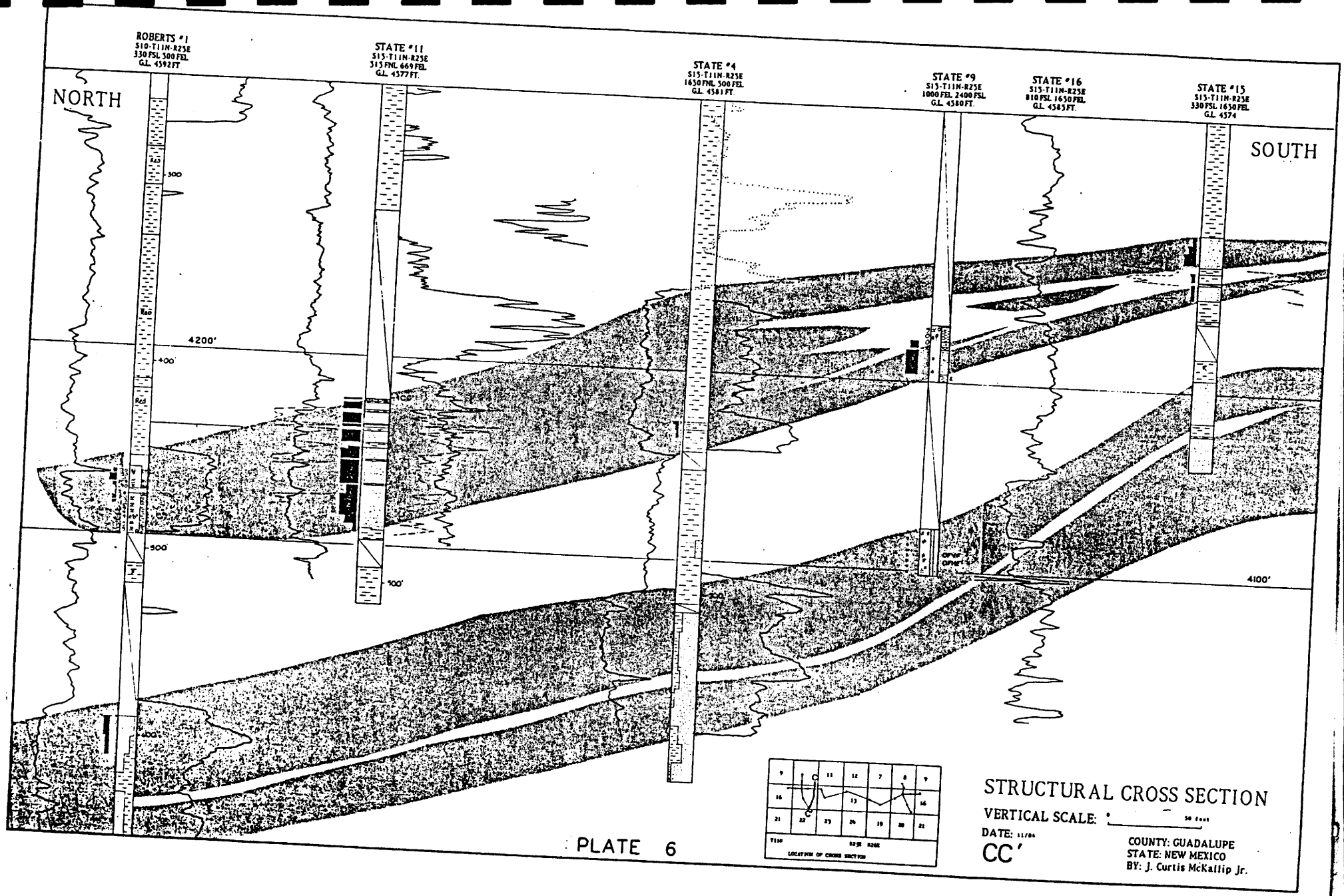

PLATE 6

STRUCTURAL CROSS SECTION

VERTICAL SCALE: 1" = 50 Feet

DATE: 11/84

CC'

COUNTY: GUADALUPE
STATE: NEW MEXICO
BY: J. Curtis McKallip Jr.

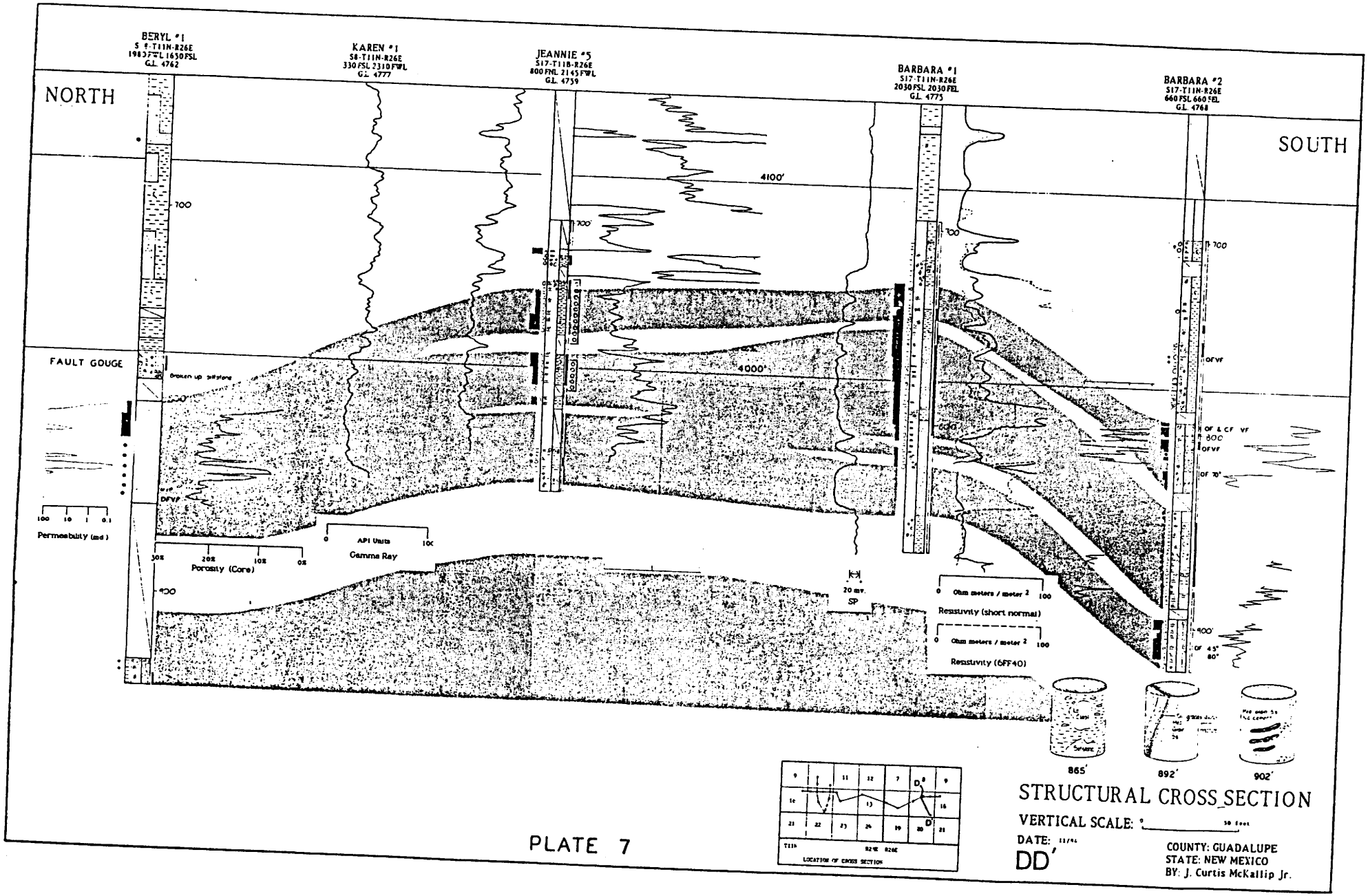
BERYL #1
S 8-T11N-R26E
1983 FEL 1650 FSL
G.L. 4762
KAREN #1
S8-T11N-R26E
330 FSL 2310 FWL
G.L. 4777
JEANNIE #5
S17-T11S-R26E
800 FNL 2145 FWL
G.L. 4759
BARBARA #1
S17-T11N-R26E
2030 FSL 2030 FEL
G.L. 4775
BARBARA #2
S17-T11N-R26E
660 FSL 660 FEL
G.L. 4768
NORTH
SOUTH
FAULT GOUGE
4100'
4000'
700
800
900
Permeability (md)
Porosity (Core)
Gamma Ray
API Units
SP
20 mv.
Resistivity (short normal)
Resistivity (6FF40)
Ohm meters / meter 2
865'
892'
902'
STRUCTURAL CROSS SECTION
VERTICAL SCALE:
DATE:
DD'
COUNTY: GUADALUPE
STATE: NEW MEXICO
BY: J. Curtis McKallip Jr.
LOCATION OF CROSS SECTION

PLATE 7

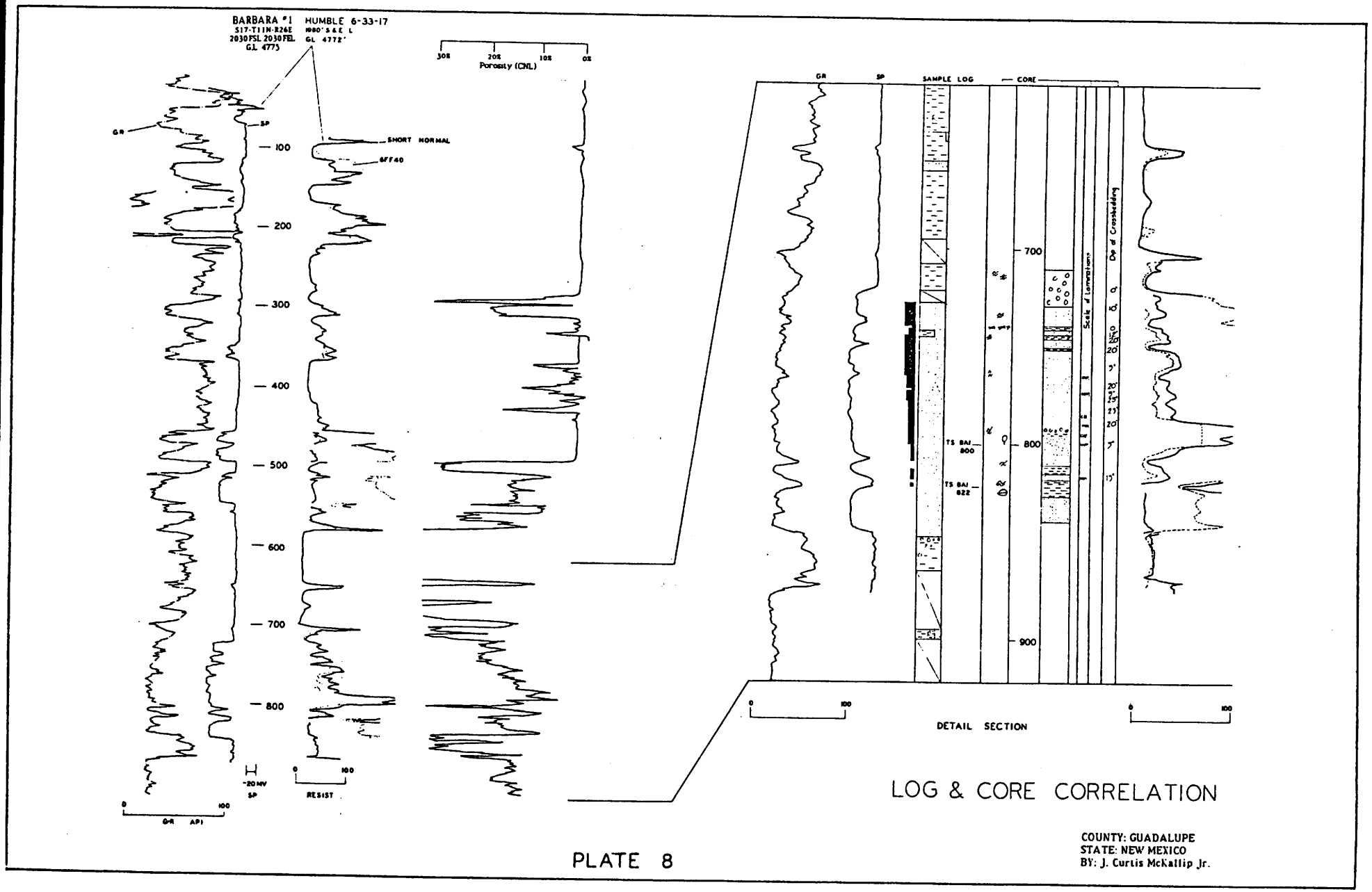
BARBARA #1
S17-T11N-R26E
2030FSL 2030FEL
GL 4775
HUMBLE 6-33-17
1980' S & E L
GL 4772'
30% 20% 10% 0%
Porosity (CNL)
GR
SP
SHORT NORMAL
6FF40
100
200
300
400
500
600
700
800
-20 MV
SP
0
100
RESIST
0
100
GR API
GR
SP
SAMPLE LOG
CORE
700
800
900
TS BAI 800
TS BAI 822
Scale of Lamination
Dip of Crossbedding
0
100
0
100
DETAIL SECTION
LOG & CORE CORRELATION
COUNTY: GUADALUPE
STATE: NEW MEXICO
BY: J. Curtis McKallip Jr.

PLATE 8

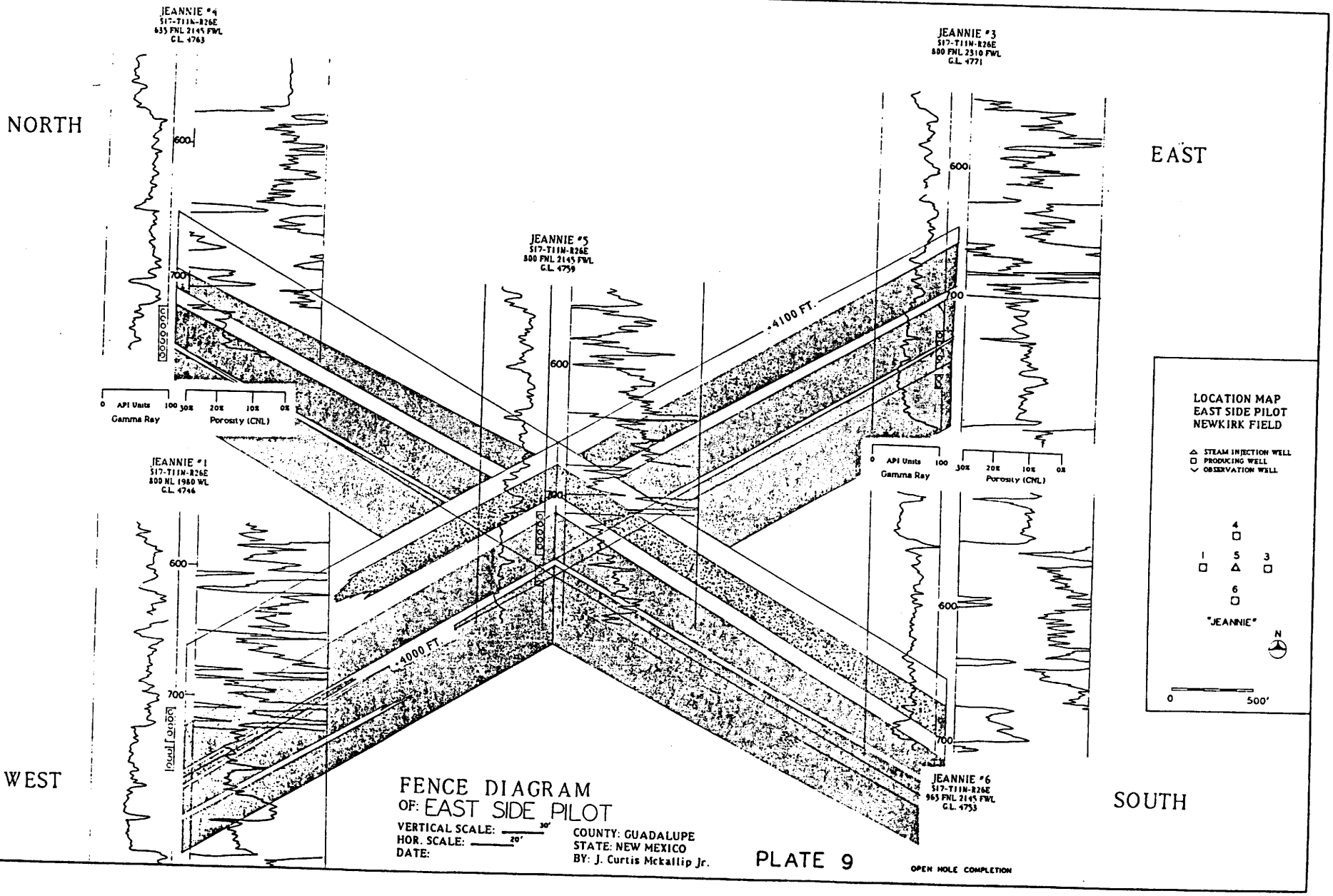
NORTH
EAST
WEST
SOUTH
JEANNIE #4
S17-T11N-R26E
635 FNL 2145 FWL
G.L. 4763
JEANNIE #3
S17-T11N-R26E
800 FNL 2510 FWL
G.L. 4771
JEANNIE #5
S17-T11N-R26E
800 FNL 2145 FWL
G.L. 4759
JEANNIE #1
S17-T11N-R26E
800 NL 1980 WL
G.L. 4746
JEANNIE #6
S17-T11N-R26E
965 FNL 2145 FWL
G.L. 4753
4100 FT.
4000 FT.
600
700
API Units
Gamma Ray
Porosity (CNL)
LOCATION MAP
EAST SIDE PILOT
NEWKIRK FIELD
STEAM INJECTION WELL
PRODUCING WELL
OBSERVATION WELL
"JEANNIE"
0
500'
FENCE DIAGRAM
OF: EAST SIDE PILOT
VERTICAL SCALE: 30'
HOR. SCALE: 20'
DATE:
COUNTY: GUADALUPE
STATE: NEW MEXICO
BY: J. Curtis Mckallip Jr.
PLATE 9
OPEN HOLE COMPLETION

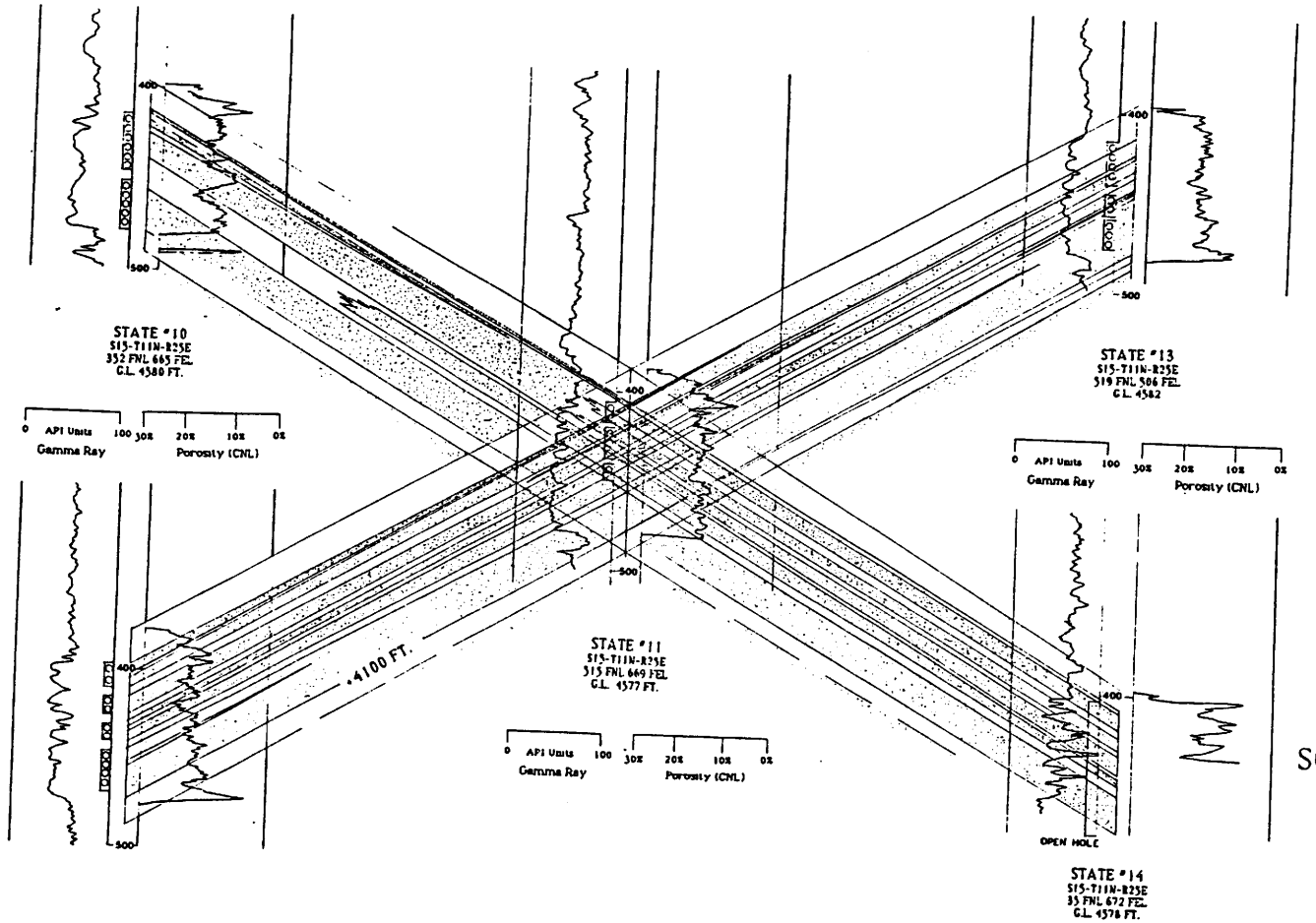

FENCE DIAGRAM
OF: WEST PILOT

VERTICAL SCALE: 30'
HOR. SCALE: 20'
DATE: 7-84

COUNTY: GUADALUPE
STATE: NEW MEXICO
BY: J. Curtis Mckallip Jr.

LEGEND:
- SANDSTONE
- MUDSTONE
- PERFORATIONS

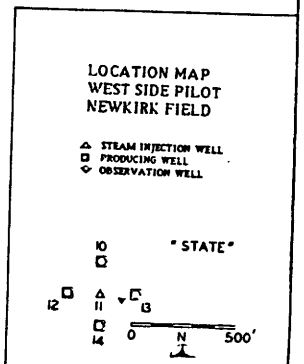

PLATE 10

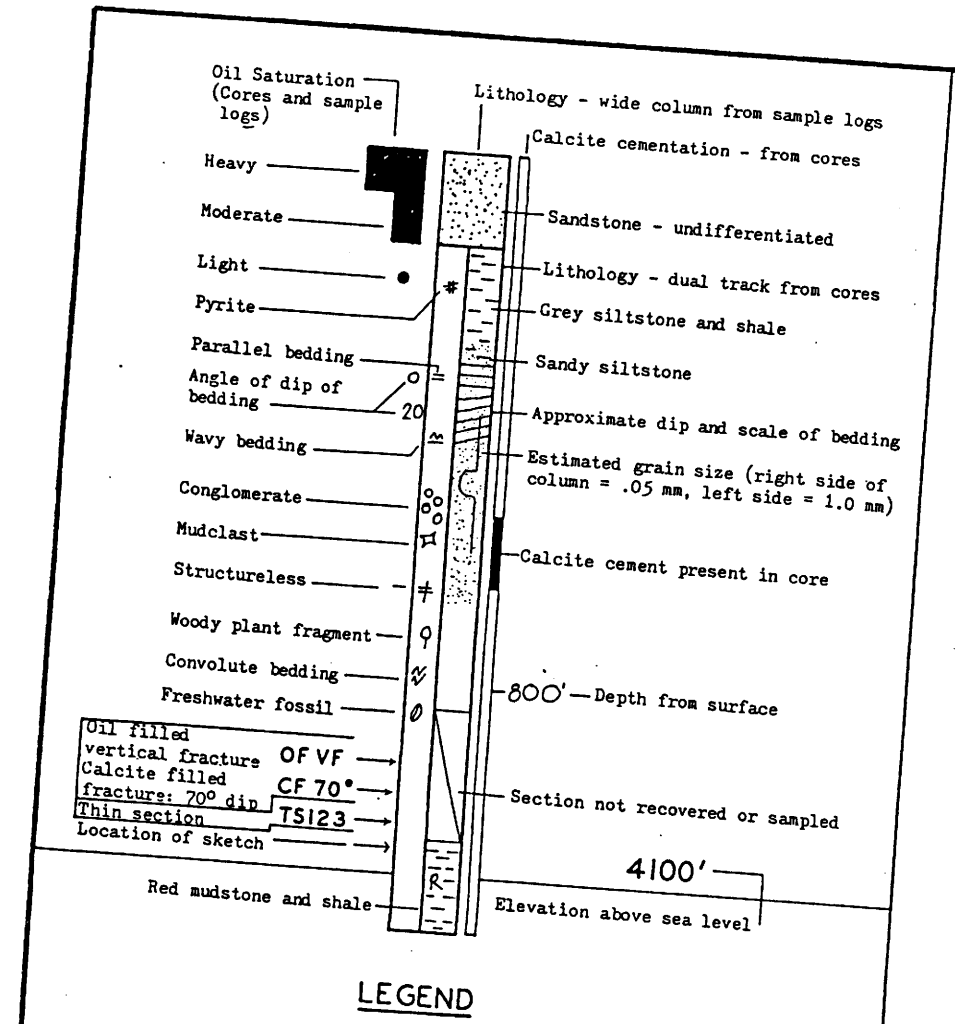

LEGEND

PLATE II

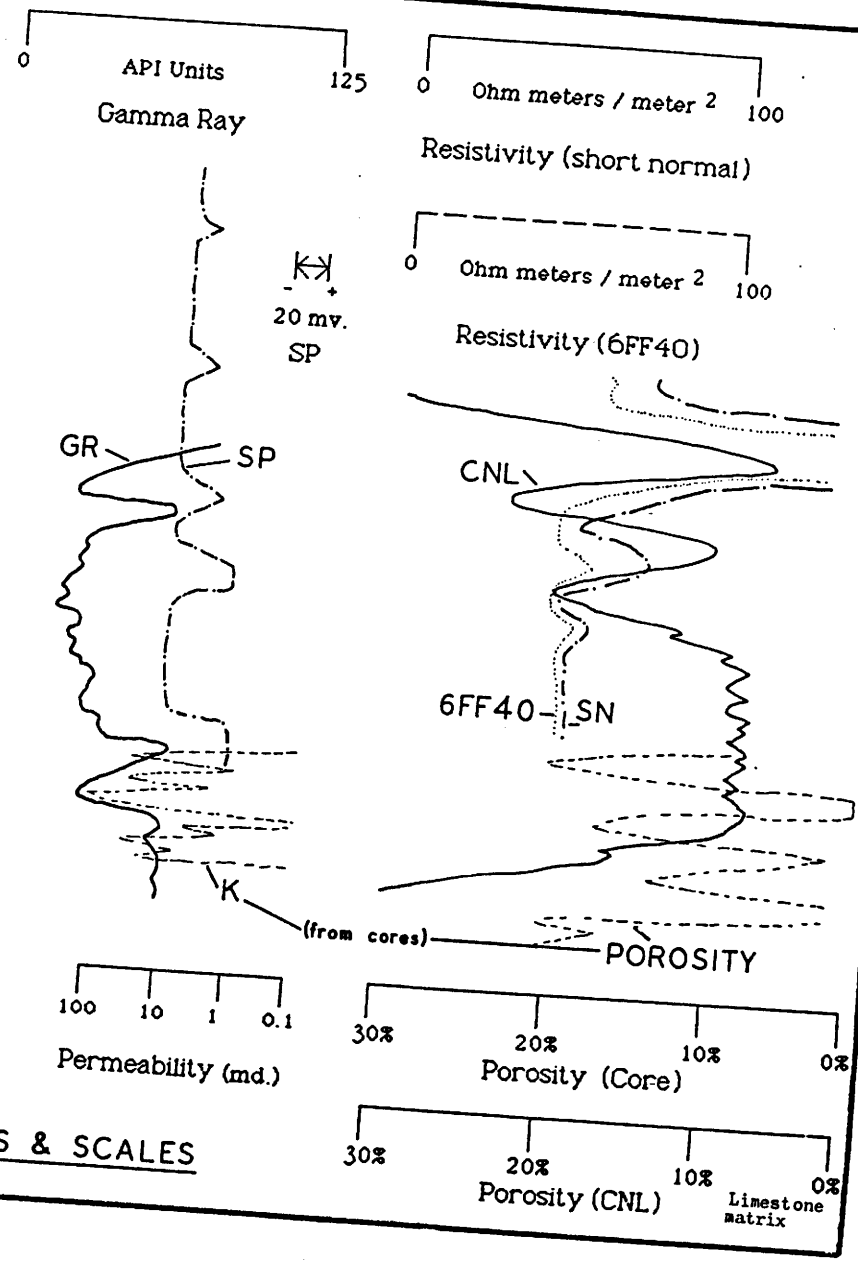

LOGS & SCALES

T 12N

T 11N

R25E

R26E

NE

SW

15

17

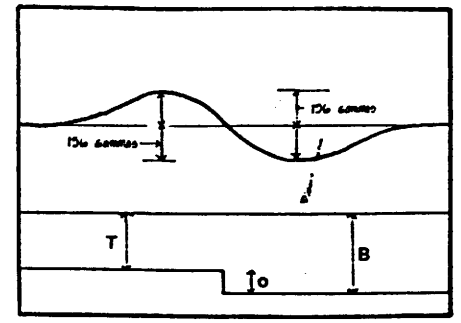

Magnetic anomaly associated with faulted basement key to relationships shown below

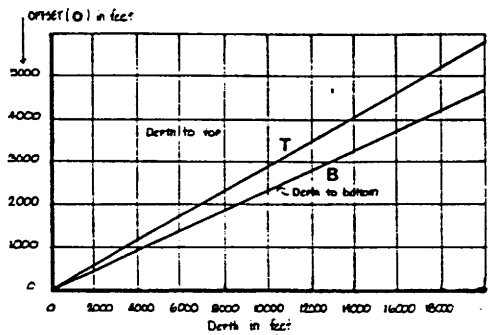

Possible combinations of effect and depths for an anomaly of 150 gammas

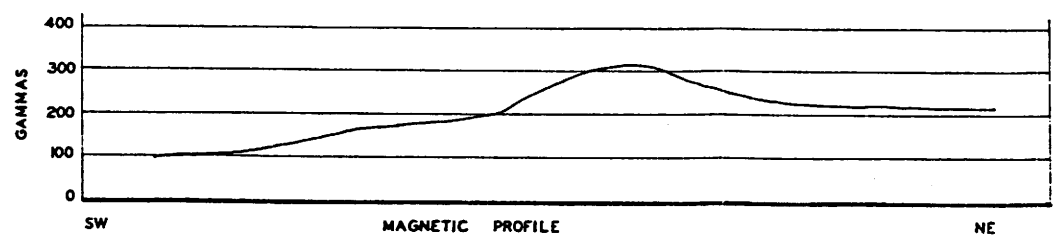

MAGNETIC ANOMALIES MAP

CONTOUR INTERVAL: 25 GAMMAS

0 1 mi

COUNTY: GUADALUPE
STATE: NEW MEXICO
BY: J. Curtis McKallip Jr.

PLATE 1

WEST

SAMEDAN STATE #1
S16-T11N-R25E
330 FNL 330 FEL
G.L. 4483 FT.

STATE #5
S15-T11N-R25E
330 FNL 990 FWL
G.L. 4495 FT.

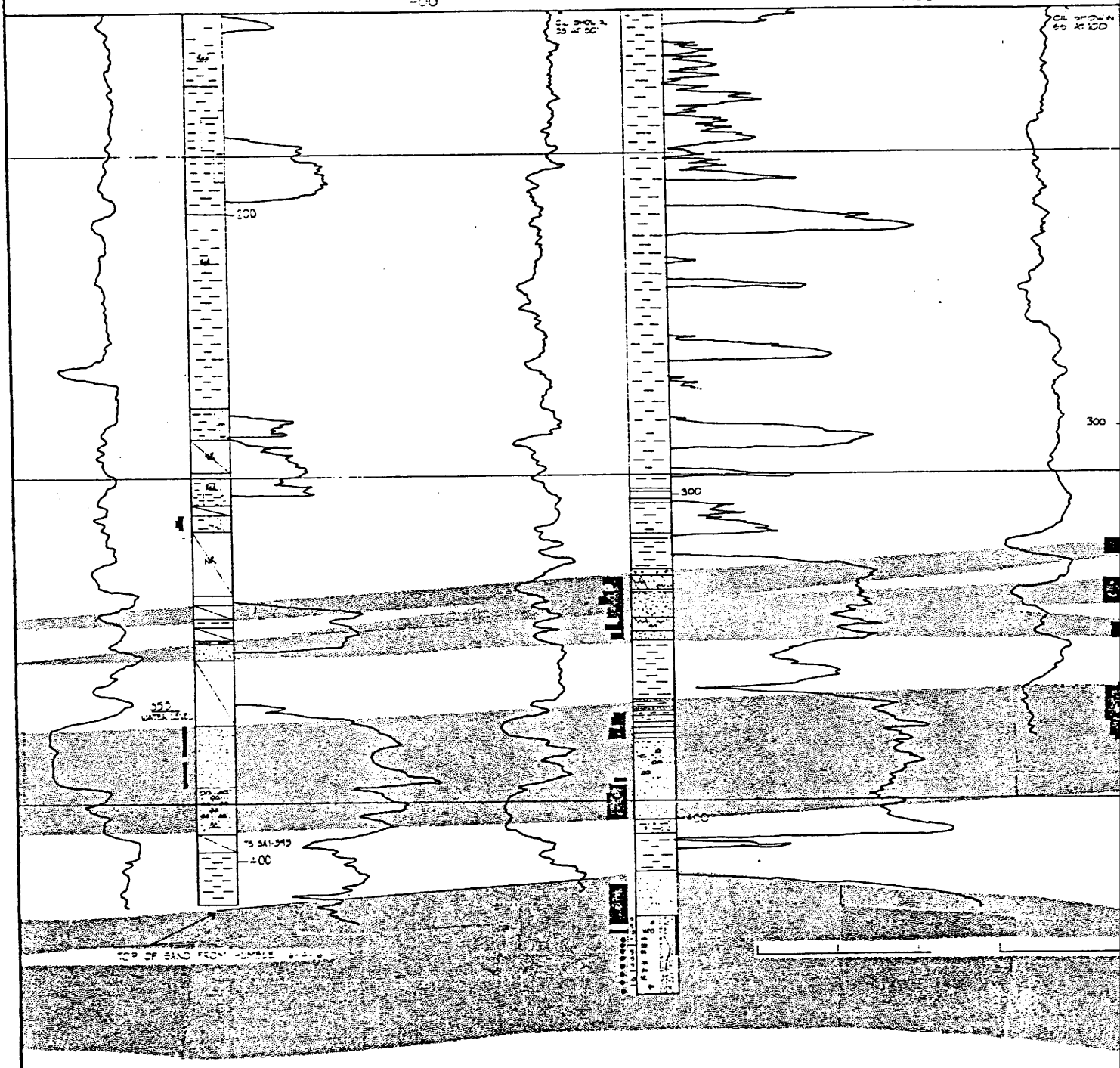

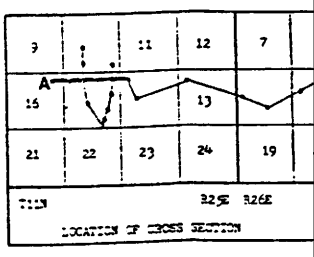

PLATE 2

WEST

O'CONNELL #3
S14 T11N 25E
500 FNL 660 FWL
G.L. 4755

HUMBLE 6-22-14
S14 T11N R 25E
980 FNL 980 FWL
G.L. 4855

HUMBLE 6-11-13
S13-T11N-R25E
990 FWL 660 FNL
G.L. 4830

EAST

1500'

2000'

4300'

500'

4300'

500'

600'

4200'

600'

700'

4100'

700'

800'

700'

800'

4000'

GR-NO SCALE

GR-NO SCALE

STRUCTURAL CROSS SECTION

VERTICAL SCALE: 1" = 50 feet

DATE: 11/84

AA·2

COUNTY: GUADALUPE
STATE: NEW MEXICO
BY: J. Curtis McKallip Jr.

PLATE 3

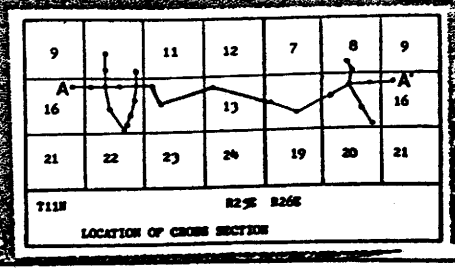

WEST

EAST

KAREN #3
S18-T11N-R26E
1800FSL 1980FEL
G.L. 4825

JEANNIE #2
S17-T11N-R26E
1980FNL 660FWL
G.L. 4771

JEANNIE #3
S17-T11N-R26E
800FNL 2310FWL
G.L. 4771

KAREN #2
S17-T11N-R26E
990FNL 660FEL
G.L. 4802

JOAN #1
S16-T11N-R26E
660FNL 990FWL
G.L. 4758

BRENDA #1
S18-T11N-R26E
1980FNL 660FWL
G.L. 4785

700'

600

700'

700'

CEMENT PATCHES

High Porosity Sandstone

800'

4'100

4000'

GR

VF

600'

500'

CEMENT PATCH

LAMINATED SANDSTONE

730'

HIGH ANGLE LAMINATIONS OF SILTSTONE
CALCITE FILLED FRACTURES

(LOW ANGLE)

OIL-SATURATED SANDSTONE
SILTSTONE CLASTS

769'

770'

816'

9		11	12	7	8	9
A 16			13			A' 16
21	22	23	24	19	20	21

T11N R25E R26E

LOCATION OF CROSS SECTION

STRUCTURAL CROSS SECTION

VERTICAL SCALE: 0 50 feet

DATE: 11/84

AA·3

COUNTY: GUADALUPE
STATE: NEW MEXICO
BY: J. Curtis McKallip Jr.

PLATE 4

DAISY #1
S10-T11N-R25E
2310FWL 1650FSL
G.L. 4498

O'CONNELL #1
S10-T11N-R25E
330FSL 2310FWL
G.L. 4518

STATE #3
S15-T11N-R25E
500FNL 2310FWL
G.L. 4516FT.

STATE #6
S15-T11N-R25E
1980FEL 1980FNL
G.L. 4545FT.

STATE #16
S15-T11N-R25E
810FSL 1650FEL
G.L. 4585FT.

NORTH

SOUTH

Oil show at 4410'-4555'

Oil show at 4516'-4625'

4200'

4100'

400'

FAULT GOUGE

TS OC416

ILD

GR

SP

10 MV

0 100 API

0 10 100 1000

Siltstone Clasts

374'

Oil in Laminations

Grey & Brown SS with calcite cement

0 1MM

416'

Calcite cement

Brown SS with some oil

Grey Mudstone

359'

9	B	11	12	7	8	9
16			13			16
21	22	B' 23	24	19	20	21

T11N R25E R26E

LOCATION OF CROSS SECTION

STRUCTURAL CROSS SECTION

VERTICAL SCALE: 0 50 feet

DATE: 11/84

BB'

COUNTY: GUADALUPE
STATE: NEW MEXICO
BY: J. Curtis McKallip Jr.

PLATE 5

ROBERTS #1
S10-T11N-R25E
330 FSL 500 FEL
G.L. 4592 FT.

STATE #11
S15-T11N-R25E
515 FNL 669 FEL
G.L. 4577 FT.

STATE #4
S15-T11N-R25E
1650 FNL 500 FEL
G.L. 4581 FT.

STATE #9
S15-T11N-R25E
1000 FEL 2400 FSL
G.L. 4580 FT.

STATE #16
S15-T11N-R25E
810 FSL 1650 FEL
G.L. 4585 FT.

STATE #15
S15-T11N-R25E
330 FSL 1650 FEL
G.L. 4574

NORTH

SOUTH

300'

4200'

400'

500'

500'

300'

4100'

600'

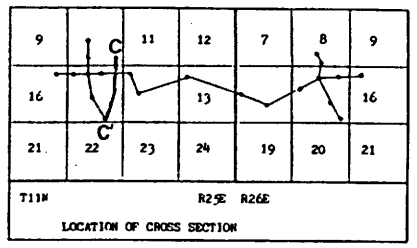

STRUCTURAL CROSS SECTION

VERTICAL SCALE: 0 50 feet

DATE: 11/84

CC'

COUNTY: GUADALUPE
STATE: NEW MEXICO
BY: J. Curtis McKallip Jr.

PLATE 6

BERYL #1
S 2-T11N-R26E
1980 FWL 1650 FSL
G.L. 4762

KAREN #1
S8-T11N-R26E
330 FSL 2310 FWL
G.L. 4777

JEANNIE #5
S17-T11B-R26E
800 FNL 2145 FWL
G.L. 4759

BARBARA #1
S17-T11N-R26E
2030 FSL 2030 FEL
G.L. 4775

BARBARA #2
S17-T11N-R26E
660 FSL 660 FEL
G.L. 4768

NORTH

SOUTH

4100'

4000'

700'

800'

900'

FAULT GOUGE

Broken up siltstone

OF VF

OF & CF VF

OF 70°

OF 45°
80°

100 10 1 0.1
Permeability (md.)

0 API Units 100
Gamma Ray

30% 20% 10% 0%
Porosity (Core)

20 mv.
SP

0 Ohm meters / meter² 100
Resistivity (short normal)

0 Ohm meters / meter² 100
Resistivity (6FF40)

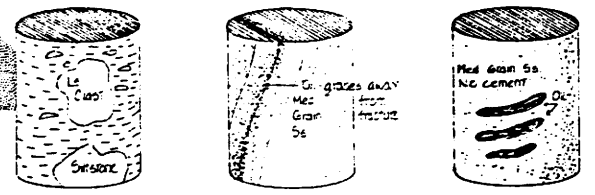

865' 892' 902'

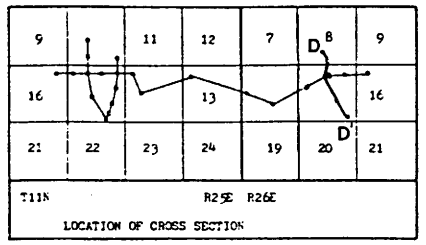

STRUCTURAL CROSS SECTION

VERTICAL SCALE: 0 50 feet

DATE: 11/84

DD'

COUNTY: GUADALUPE
STATE: NEW MEXICO
BY: J. Curtis McKallip Jr.

PLATE 7

BARBARA #1
S17-T11N-R26E
2030 FSL 2030 FEL
G.L. 4775

HUMBLE 6-33-17
1980' S & E L
GL 4772'

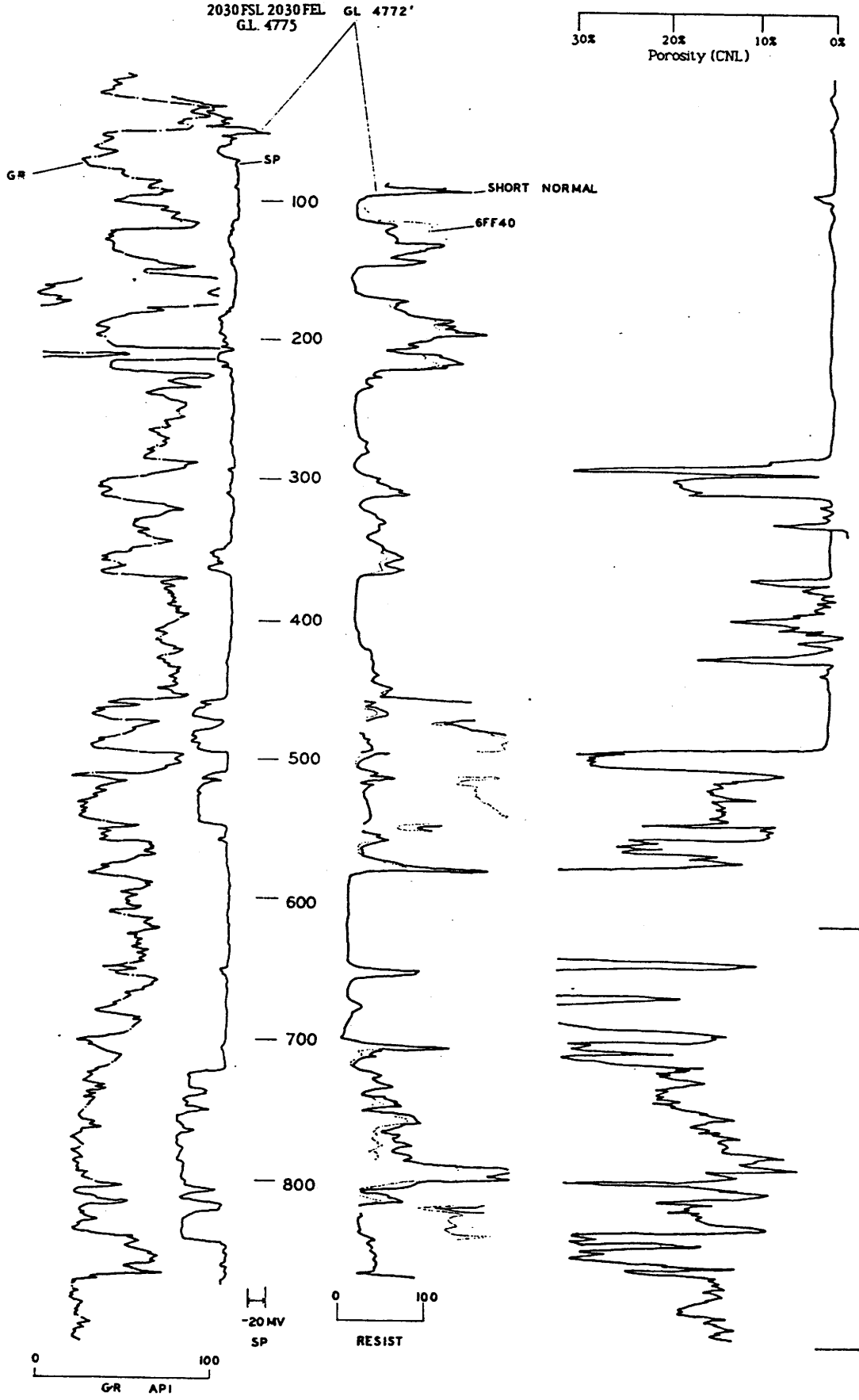

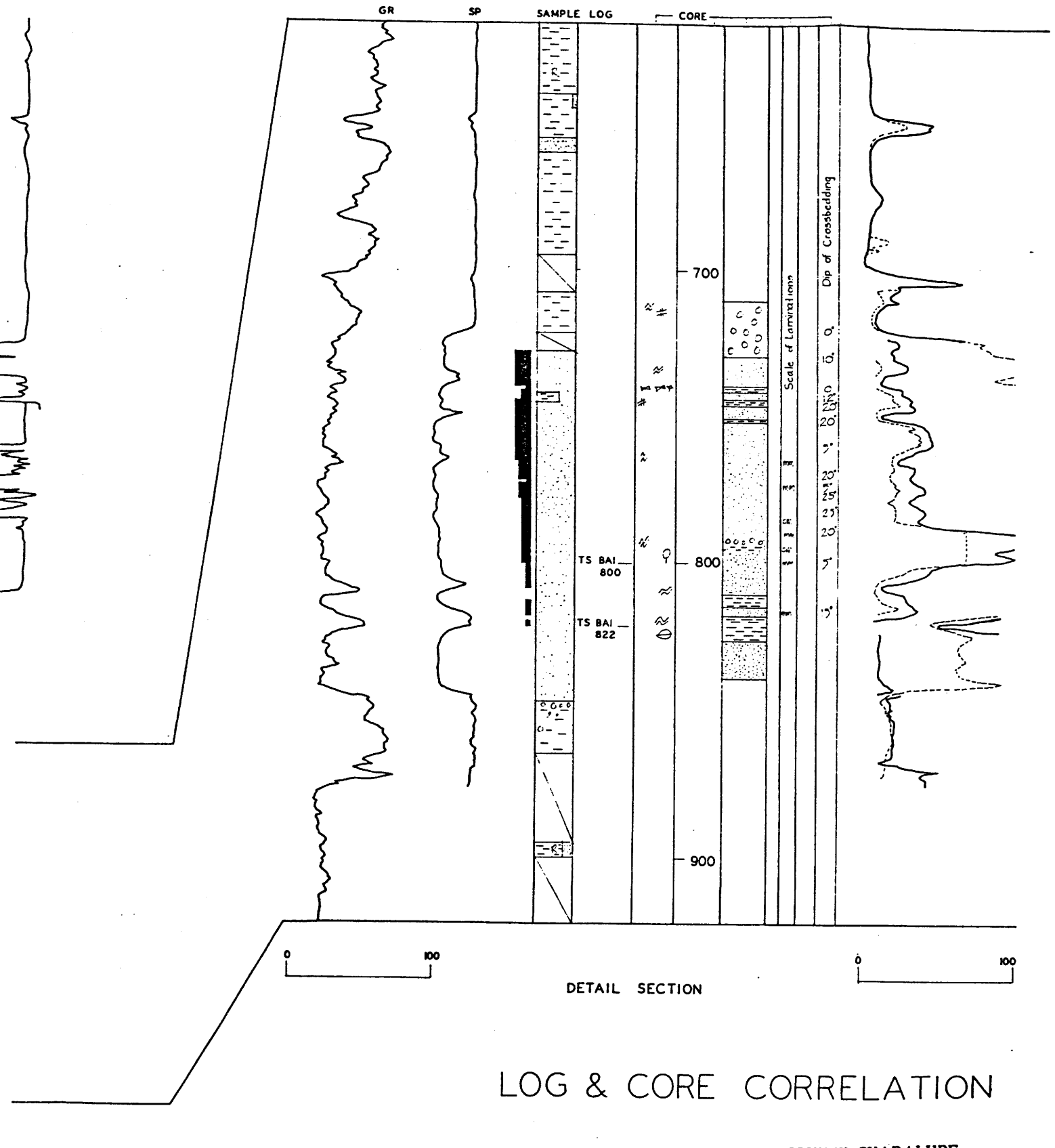

LOG & CORE CORRELATION

COUNTY: GUADALUPE
STATE: NEW MEXICO
BY: J. Curtis McKallip Jr.

PLATE 8

NORTH

EAST

WEST

SOUTH

JEANNIE #4
S17-T11N-R26E
635 FNL 2145 FWL
G.L. 4763

JEANNIE #3
S17-T11N-R26E
800 FNL 2310 FWL
G.L. 4771

JEANNIE #5
S17-T11N-R26E
800 FNL 2145 FWL
G.L. 4759

JEANNIE #1
S17-T11N-R26E
800 NL 1980 WL
G.L. 4746

JEANNIE #6
S17-T11N-R26E
965 FNL 2145 FWL
G.L. 4753

600

700

0 API Units 100
Gamma Ray

30% 20% 10% 0%
Porosity (CNL)

+4100 FT.

+4000 FT.

LOCATION MAP
EAST SIDE PILOT
NEWKIRK FIELD

△ STEAM INJECTION WELL
□ PRODUCING WELL
◇ OBSERVATION WELL

4 □
1 □ 5 △ 3 □
6 □

"JEANNIE"

N

0 500'

FENCE DIAGRAM
OF: EAST SIDE PILOT

VERTICAL SCALE: 30'
HOR. SCALE: 20'
DATE:

COUNTY: GUADALUPE
STATE: NEW MEXICO
BY: J. Curtis Mckallip Jr.

PLATE 9

OPEN HOLE COMPLETION

NORTH

EAST

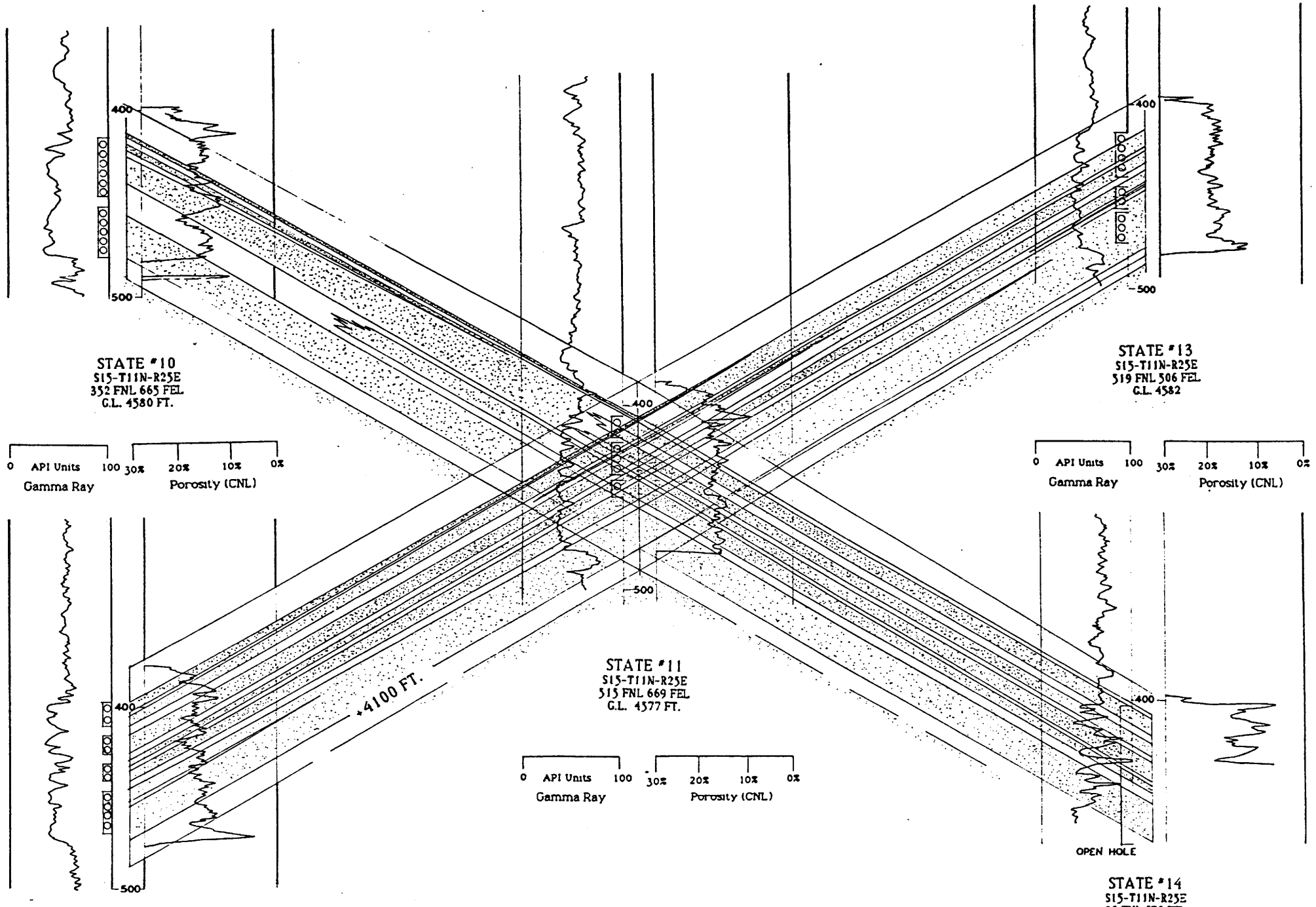

SOUTH

WEST

FENCE DIAGRAM
OF: WEST PILOT

VERTICAL SCALE: 30'
HOR. SCALE: 20'
DATE: 7-84

COUNTY: GUADALUPE
STATE: NEW MEXICO
BY: J. Curtis Mckallip Jr.

LEGEND:
- SANDSTONE
- MUDSTONE
- PERFORATIONS

LOCATION MAP
WEST SIDE PILOT
NEWKIRK FIELD

- STEAM INJECTION WELL
- PRODUCING WELL
- OBSERVATION WELL

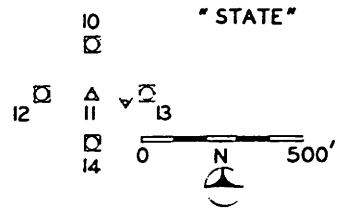

PLATE 10

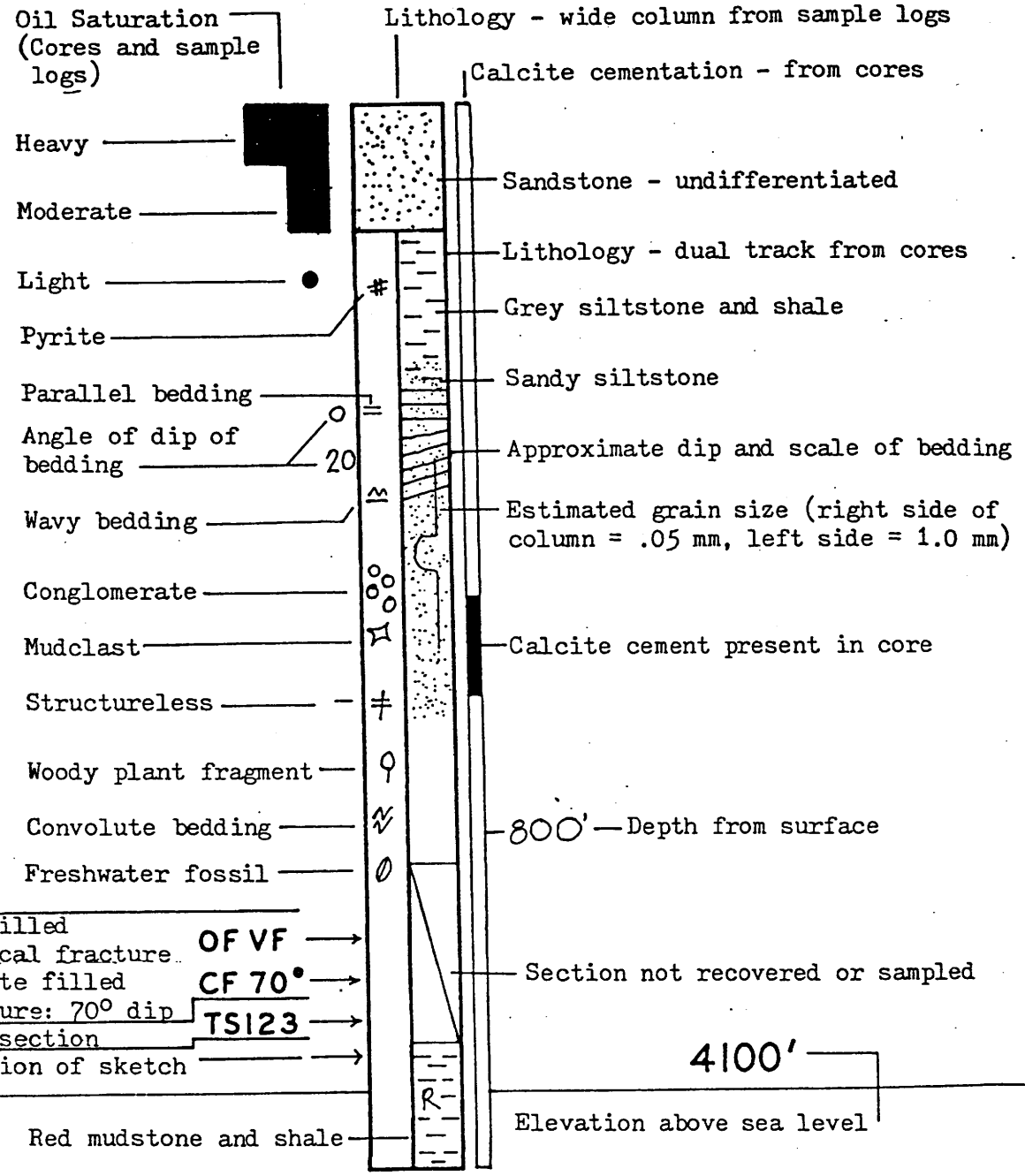

LEGEND

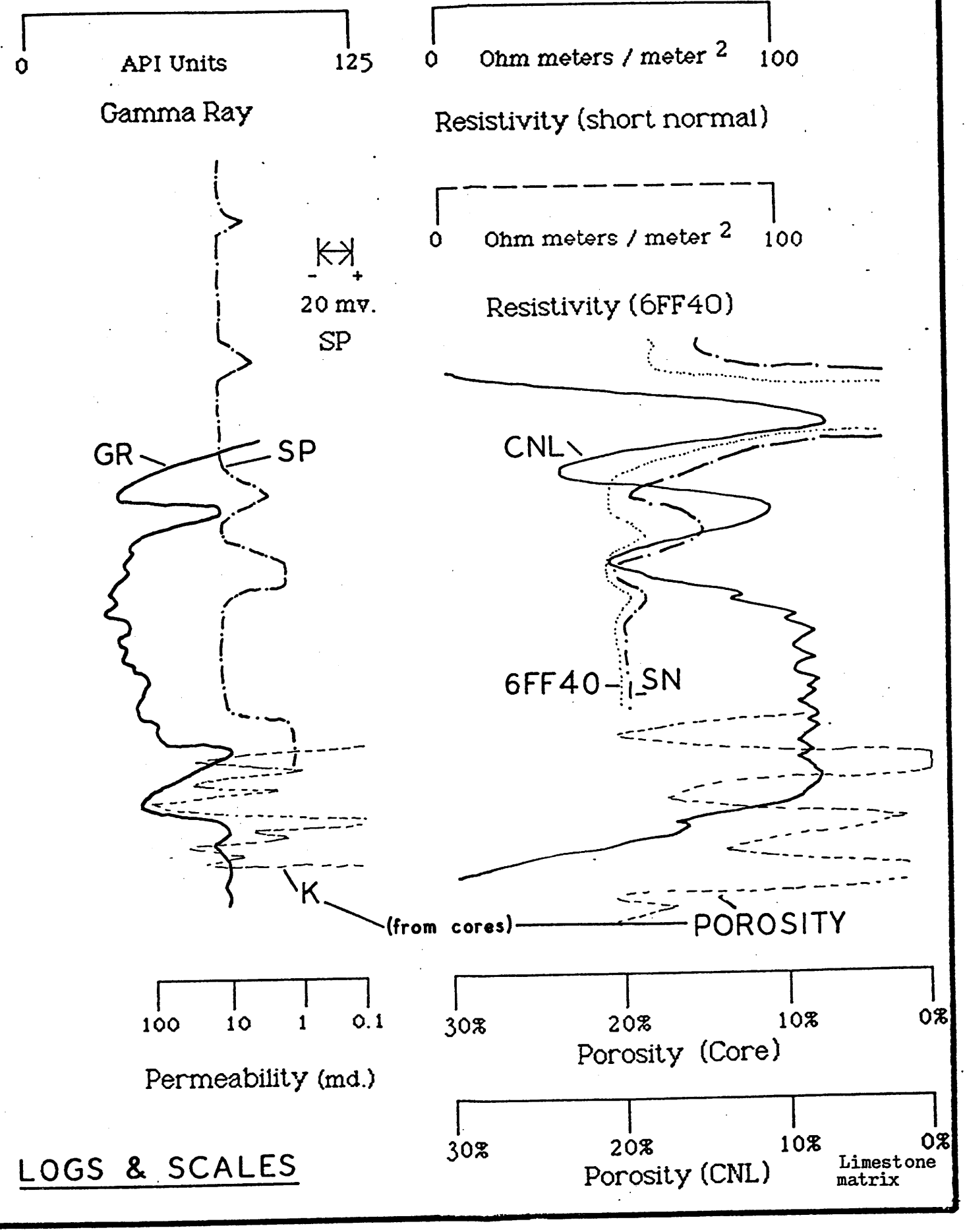

LOGS & SCALES

PLATE II